LIPOCALIN-2 (LCN-2) IS A NOVEL MYOKINE THAT REDUCES LIPID ACCUMULATION AND INDUCES LIPOLYSIS IN ADIPOCYTES

By

Areej Minwar Alsolami

Thesis submitted to the university of Nottingham for the degree of

Doctor of Philosophy

August 30th, 2023

Supervisors

Associate Professor Andrew J Bennett. Associate Professor of Molecular Biology/Biochemistry. University of Nottingham

Professor Dr. Kostas Tsintzas. Professor of Human Physiology, Faculty of Medicine & Health Sciences, University of Nottingham

Keywords

Adipose tissue; EPS; Exercise; Lipid accumulation; Lipid metabolism; Lipoalin-2 (LCN-2); Lipolysis; Muscle contraction; Myokines; Skeletal muscle.

Abstract

Introduction

LCN-2 is an acute phase protein, first identified as an adipokine secreted by adipose tissue. Contradictory experimental results show that LCN-2 is involved in pro- and anti-inflammatory states and can both increase and decrease insulin resistance. However, whilst the Lipocalin-2 protein is widely expressed in several tissues/cells, its expression has been poorly studied in skeletal muscle. Experiments in FRAME lab have demonstrated that the mRNA expression of LCN-2 is increased after exercise post 3-hr *in vivo* in *3* partipiants out of *6*, and therefore its role in skeletal muscle following exercise needs to be investigated. We hypothesise that LCN-2 is a novel potential myokine, acting post exercise in an endocrine fashion that affects lipid metabolism.

Methods

Primary human myotubes were isolated from healthy volunteers and cultured to study LCN-2 expression and secretion in response to EPS stimulation and AICAR treatment. The lentiviral inducible vector pINDUCER20 was used to enable inducible overexpression of LCN-2 in human primary myotubes. Lastly, adipocytes were exposed to conditioned media (CM) derived from human myotubes that overexpress LCN-2 to study the crosstalk between muscle and adipose tissue.

Results

We found that LCN-2 mRNA expression was significantly upregulated in a time-dependant manner (2 h, 4 h, 16 h) by EPS ($p<0.0001$; 6-fold post-16 hr) and protein

was secreted by human myotubes in response to 16 h of EPS ($p<0.0001$; 43% increase). Moreover, the level of LCN-2 secretion by myotubes increased in response to AICAR treatment for 48 h ($p<0.0001$; 3-fold increae). Lipid accumulation in adipocytes (3T3L-1) reduced significantly post-48 h when adipocytes (3T3L-1) were exposed to 50% CM derived from human myotubes that overexpress LCN-2 ($p<0.0001$; 3-fold). Moreover, a significant increase in release of glycerol (nmol/mg of cell protein) post48 h occurred when exposed to human myotube CM ($p<0.001$; 2-fold). Additionally, we found that ATGL protein was upregulated in response to LCN-2 containing conditioned medium ($p<0.0001$; ~ 4-fold).

Conclusion

We conclude that LCN-2 is a novel exercise-induced myokine that appears to induce lipolysis and decrease lipid accumulation in adipocytes.

Table of Contents

List of Figures

List of Tables

List of Abbreviations

AMPK	Adenosine Monophosphate-Activated Protein Kinase
AICAR	5-Aminoimidazole-4-carboxamide ribonucleotide
AKt	Protein Kinase B
ANOVA	Analysis of Variance
ATGL	Adipocyte Triglyceride Lipase
BAT	Brown Adipose Tissue
BCA	Bicinchoninic Acid Assay
BMI	Body Mass Index
BSA	Bovine Serum Albumin

cAMP	cyclic AMP
cDNA	Complimentary DNA
CM	Cell Media / Conditioned Media
DAG	Diacylglycerol
DMSO	Dimethyl Sulfoxide
dNTP	Deoxyribonucleotide Triphosphate
DOX.	Doxycycline
E.coli	Escherichia coli
EDTA	Ethylenediaminetetraacetic Acid
EPS	Electrical Pulse Stimulation

ERK	Extracellular Signal-Regulated Kinase 1/2
FA	Fatty Acid
HS	Horse Serum
HSL	Hormone Sensitive Lipase
Hu.	Human species
IBMX	3-isobutyl-1-methylxanthine
IL-6	Interleukin 6
LCN-2	Lipocalin-2
LD	Lipid Droplet
LV	Lentiviral Vector
MAG	Monoacylglycerol

MGL	Monoacylglycerol Lipase
mRNA	Messenger Ribose Nucleic Acid
ms.	Mouse species
Myokines	Proteins secreted by skeletal muscle
NF-κB	Nuclear Factor Kappa-Light-Chain-Enhancer of Activated B Cells
PGC1-a	Peroxisome Proliferator-Activated Receptor Gamma Coactivator 1-Alpha (PGC-1α)
PLIN1	Perilipin 1
PPAR	Peroxisome Proliferator-Activated Receptor
q.RT-PCR	Quantitative Real Time Polymerase Chain Reaction
qPCR	Real-Time Polymerase Chain Reaction

RIPA	Radioimmunoprecipitation Assay Buffer
RNA	Ribose Nucleic Acid
SkM	Skeletal Muscle
STATs	Single Transducer and Activator of Transcription
T2DM	Type 2 Diabetes
TAG	Triacylglycerol
TNF	Tumour Necrosis Factor
TNF-a	Tumour Nuclear Factor
UCP1	Uncoupling Protein 1
WAT	White Adipose Tissue

β-ARs	β-Adrenergic Receptors

Declaration

The work contained in this thesis has not been previously submitted to meet requirements for any award at this institution or another. To the best of my knowledge, the thesis contains no material previously published or written by another person except where due reference is made; everything was performed by me.

Signature: Areej Alsolami

Date: 30.08.2023

Presentations

Oral Presentations

1. Studying the expression of Lipocalin-2 in human skeletal muscle in response to various stimuli. A. M. Alsolami, A. J. Bennett, K. Tsintzas. O. Postgraduate Oral Presentation, University of Nottingham Life science school, Queen's Medical Centre, 16th July 2021

Poster Presentation

1. LCN-2 is a potential novel myokine with powerful effects on lipolysis and lipid accumulation. A. M. Alsolami, A. J. Bennett, K. Tsintzas. The adipocyte across biological scales hybrid meeting, university of Edinburgh, 9th-10th December 2021
2. Modeling the expression and secretion of lipocalin-2 in human skeletal myokines using an inducible lentiviral vector. A. M. Alsolami, A. J. Bennett, K. Tsintzas. Postgraduate poster presentation, University of Nottingham, 20th July 2019

Publication and Licensing Rights (Bio-Render)

1. Confirmation of publication, 31.08.2022
2. Agreement number WC24L7UT9U

Acknowledgements

First and foremost, I would like to express my gratitude to my supervisors, Dr. Andrew Bennett for his expert guidance and encouragement during my studies, and Professor Kostas Tsintzas for his additional support and guidance.

I thank Andrew, a PhD student at the University of Nottingham for enabling me to obtain extra samples from participants for my studies, particularly during the times of the COVID19 pandemic. I also want to thank the laboratory technicians, Monika Own and Nicola Di Vivo, for their technical support at the lab bench. Thank you for all FRAME Lab doctoral students for many laughs and their kindness throughout my studies.

This endeavour would not have been possible without the support and love of my family before, during and after my studies. Specifically, to my beloved husband, Sultan, thank you for being there with me all the time and facing challenges together. To my lovely daughters, Sumoo, Tanal, and Areej. Feeling your love and your presence every day brings me such joy and inspires me to do more.

This thesis was funded by Jouf University at Saudi Arabia. My sincerest thanks for your financial support.

Chapter 1: General Introduction

1.1 SKELETAL MUSCLE

Skeletal muscle is considered to be the largest tissue of the entire body, representing approximately 40% of the body mass of humans (around 35 to 40% in rats) (Shi *et al.*, 2007) and it has the property of cell contraction, which is important for energy homeostasis (Abdul-Ghani & DeFronzo, 2010) (Figure 1.1). Skeletal muscle is formed of several types of muscle fibres, which can generally be divided into type I (oxidative, slow-twitch) and type II (fast-twitch) fibres based on their metabolic and contractile characteristics. Type II muscle fibres may be further divided into type IIa, IIx and IIb fibres, which have greater glycolytic energy metabolisms (Shi *et al.*, 2007). Type I muscle fibre is important for long periods it can function without fatiguing usually helpfual to maintane body position (Posture) and stabilise the bone and joint, this type of muscle fibre do not require a lrage amounts of energy (Lexell *et al.*, 2010). However, type II muscle fibre is oxidative and used for fast movement that requires more energy, such as when walking or running, and so this fibre takes longer to fatigue. A condition known as sarcopenia occurs due to a decrease in the total muscle mass, mainly from both type I and type II fibers and secondarily from a preferential atrophy of type II fibers. A decline of muscle mass resulting from aging is related to loss of size of muscle fibre type II, but it is unclear how the decrease in these muscle fibre types may be specifically linked to the sarcopeni condition rather than simply being due to aging in general. In addition, there is significant difference between men and women in this regard (Kramer *et al.*, 2017)

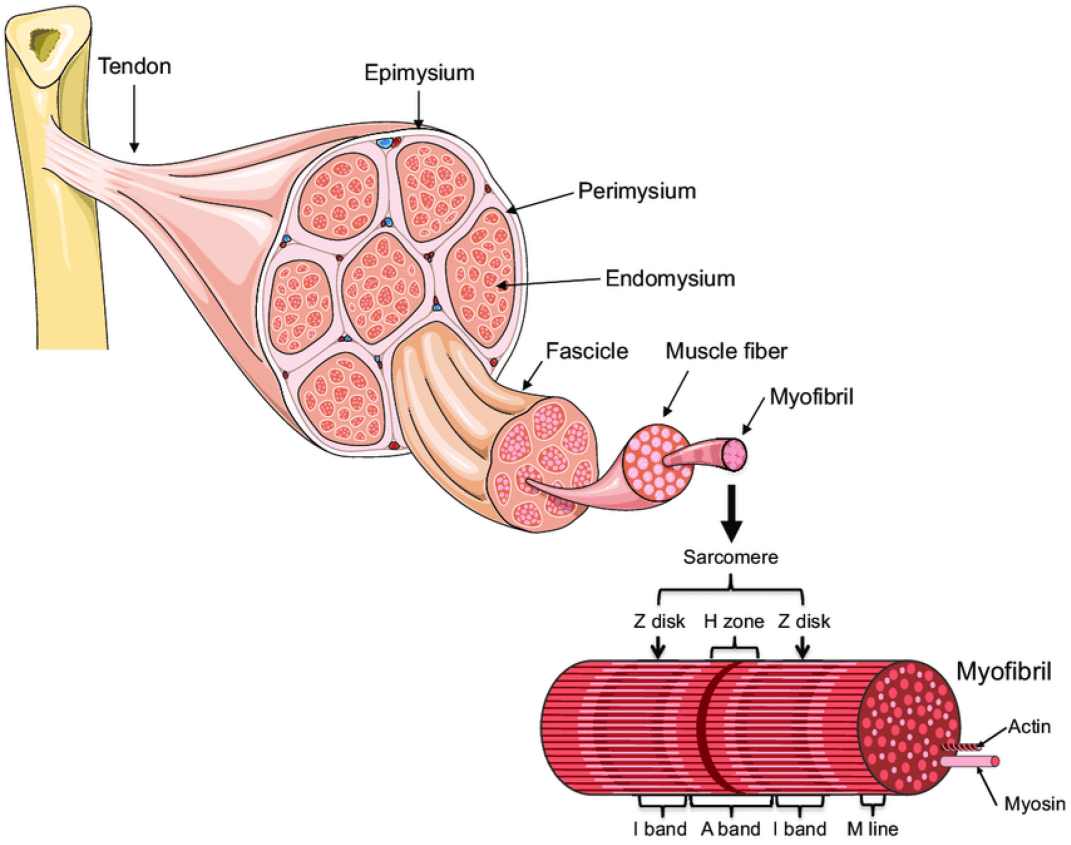

Figure 1.1. Structure of skeletal muscle and its organisation. Skeletal muscles are comprised of many fascicles, each formed of many individual muscle fibres which contain many myofibrils (Adapted from servier medical art https://smart.servier.com/smart_image/tendon-anatomy/).

According to recent research, contracting muscle cells produce and secrete a variety of humoral factors (or cytokines), which have been proven to be crucial to metabolism. Due to its capacity to release hormone-like substances or myokines, such as interleukin (IL)-6, IL-8, and IL-15, that may affect the metabolism of other tissues and organs, skeletal muscle can be thought of as an endocrine organ (Pedersen, 2011b). Researchers have been attempting to link the muscle contraction that occurs in response of exercise and alterations in other nearby tissues that are prompted by the release of proteins known as myokines. These proteins modulate various exercise-induced metabolic changes in other organs, including the liver and

adipose tissue (Pedersen, 2011b), and it has been found that skeletal muscle expresses a number of myokines, including interleukin (IL)-6, IL-8, and IL-15 (Pedersen *et al.*, 2007). Research has also demonstrated that concentric muscle contractions regulate the expression of IL-6, IL-8, and IL-15, and that IL-15 mRNA is upregulated in human skeletal muscle after strength training (Febbraio & Pedersen, 2002; 2005; Pedersen, Steensberg, Fischer *et al.*, 2003; Pedersen, Steensberg, Keller *et al.*, 2003; Nielsen *et al.*, 2007).

In reaction to exercise or muscular contraction, the main source of IL-6 in the bloodstream is skeletal muscle. The levels of IL-6 mRNA in skeletal muscle are extremely low while the muscle is at rest; however, type I fibres may contain trace quantities of IL-6 protein that have been shown as possibly utilising sensitive immunohistochemistry techniques (Plomgaard, Penkowa, & Pedersen, 2005). Exercise causes the amount of circulating IL-6 to increase exponentially (up to 100 times), peaking at the end or just after activity and then rapidly declining to its level before exercise (Pedersen & Fischer, 2007). Skeletal muscle and immune cells – particularly macrophages – can both generate IL-6. However, IL-6 that is generated and manufactured by muscle cells does not activate traditional pro-inflammatory pathways, whereas IL-6 that is produced and synthesised by macrophages causes an inflammatory response (Pedersen & Febbraio, 2008).

Additionally, it is proposed that IL-6 is linked with AMP-activated protein kinase (AMPK). According to Kahn, Alquier, Carling, and Hardie (2005), IL-6 boosts AMPK activity in skeletal muscle and adipose tissue, and fatty acid oxidation and glucose uptake are both enhanced when AMPK is activated (Kelly *et al.*, 2004). Data generated using healthy humans models demonstrates that human IL-6 stimulates lipolysis and its role is inhibited in response to insulin treatment, which is

logical since IL-6 has been identified as a lipolytic factor (Lyngso, Simonsen, & Bulow, 2002; van Hall *et al.*, 2003). As such, understanding the regulation of these myokines secreted by skeletal muscle is important in developing targeted interventions for metabolic diseases.

1.2 ADIPOSE TISSUE

Implications of metabolic diseases include reduced life expectancy, shorter lifespan, and greater financial burden (Wang *et al.*, 2007; Seidell & Halberstadt, 2015). In addition, any disorder of the functioning of adipose tissue associated with obesity has been strongly associated with alterations in the development of metabolic diseases and whole-body metabolism (Crewe, An, & Scherer, 2017). Adipose tissue is a connective tissue and consists of adipocyte cells (fat cells), fibroblasts, some immune cells (macrophages, neutrophils and eosinophils, and lymphoid), and epithelial cells (Birbrair *et al.*, 2013). There are two types of adipose tissue: WAT (white adipose tissue) and BAT (brown adipose tissue), with adipose genes controlling the regulation of these tissues (Rosen & Spiegelman, 2014). Adipose tissue is derived from pre-adipocytes, their main function being to store any excess free fatty acid (FFA) and glucose in the form of TGA WAT, which is either a visceral or subcutaneous deposit. However, subcutaneous deposits are known to be more metabolically active than visceral. Importantly, fat or lipid accumulation in the cytoplasm is associated with the development of T2DM and metabolic diseases (Wang, Rimm, Stampfer, Willett, & Hu, 2005).

During fasting, adipose tissue hormone sensitive lipase (HSL), adipose triglyceride lipase (ATGL), and monoglyceride lipase (MGL) are upregulated as a result of the increased level of catecholamine (Young & Zechner, 2013). These lipases normally break down triglycerides into FFAs and glycerol, and therefore are

meant to be sent to other tissues to provide energy. Due to the capacity of adipose tissue to store lipids for energy, they are considered a regulator of whole-body metabolism and as an endocrine organ. In addition, adipose tissue can secrete certain cytokines and adipokines (Young & Zechner, 2013). These released adipokines have a role in the crosstalk between adipose tissue and other distant tissues. Adipose tissue also has an influence on other tissues in endocrine, paracrine and autocrine fashions. Examples of adipokines include Leptin, RBP-4 (retinol binding protein 4), and Lipocalin-2 (LCN-2), all of which play different roles such as the regulation of insulin sensitivity, lipid homeostasis and inflammatory responses, and the balancing of energy (Rodríguez, Ezquerro, Méndez-Giménez, Becerril, & Frühbeck, 2015). Any dysregulation of factors secreted by adipocytes will result in the development of certain metabolic disorders (Smith & Kahn, 2016).

1.3 PHYSICAL ACTIVITY *VS* INACTIVITY ON HEALTH

Regular physical activity (exercise) has not only been proven to be a factor in preventing certain health implications, such as T2DM and other metabolic diseases (Hansen *et al.*, 2016; Bhati *et al.*, 2018), it has also been shown to reduce adiposity (Grøntved, 2013) and improve mental health (Klenger, 2016). Physical activity can be defined as movement of any body parts by skeletal muscle fibre, a process which requires energy. By physical activity, here we mean any form of physical exercise at varying forms of intensity and duration. On the other hand, physical inactivity is defined as any form of inactivity that does not meet the global recommendations of physical activity for health (WHO recommendations, 2010).

It is important to note that a major factor in global mortality is inactivity (Lee *et al.*, 2012), and predications suggest that five million deaths per year could be prevented if the population were more active (Strain *et al.*, 2020). Interestingly,

Gleeson *et al.,* in studies conducted using mice models, revealed that the effects of anti-inflammatory factors following physical exercise rely on other mechanisms such as the infiltration of macrophage into adipose tissue (Gleeson *et al.*, 2011). Finally, the beneficial effects of regular physical activity against certain metabolic diseases, such as cardiovascular disease, cancer and T2DM, are well documented and established (Pedersen & Febbraio, 2008).

1.4 MYOKINES MEDIATE CROSSTALK BETWEEN SKELETAL MUSCLE AND OTHER TISSUES IN PARACRINE, AUTOCRINE AND ENDOCRINE FASHIONS

Skeletal muscle is an endocrine organ – as is adipose tissue – that synthesises and secretes humoral factors or cytokines via myotubes, the latter of which have been found to play a role in muscle metabolism and exert either endocrine or paracrine effects on other tissues (Pedersen, 2011). During physical activity, skeletal muscle expresses many of these cytokines, but not all of them are released into circulation. Conversely, some cytokines in circulation are not expressed in skeletal muscle in response to physical activity (Pedersen, 2006).

The release of cytokines depends on the mode, intensity, and duration of exercise (Pedersen, 2007). Recently, research has suggested that cytokines are produced from myocytes that express and release following physical activity. These factors are known as myokines (Duzova, 2012; Pedersen, 2007), which are cytokines produced, expressed and released by skeletal muscle. It is well established that myokines have endocrine, autocrine and paracrine signals (Huh, 2017). Indeed, researchers have tried to understand the relationship between muscle contraction and changes in other organs (e.g., liver and adipose tissue) due to myokine release, which can mediate several exercise-induced metabolic changes (Pedersen, 2011). It has also been noted that regular exercise promotes a better functioning of the human body via

stimulation of anti-inflammatory processes, improvement of energy efficiency and an increase in insulin sensitivity (Pedersen *et al.*, 2007). The discovery of these myokines has increased our understanding of how muscles communicate with other organs (Raschke & Eckel *et al.*, 2013; Carson *et al.*, 2017).

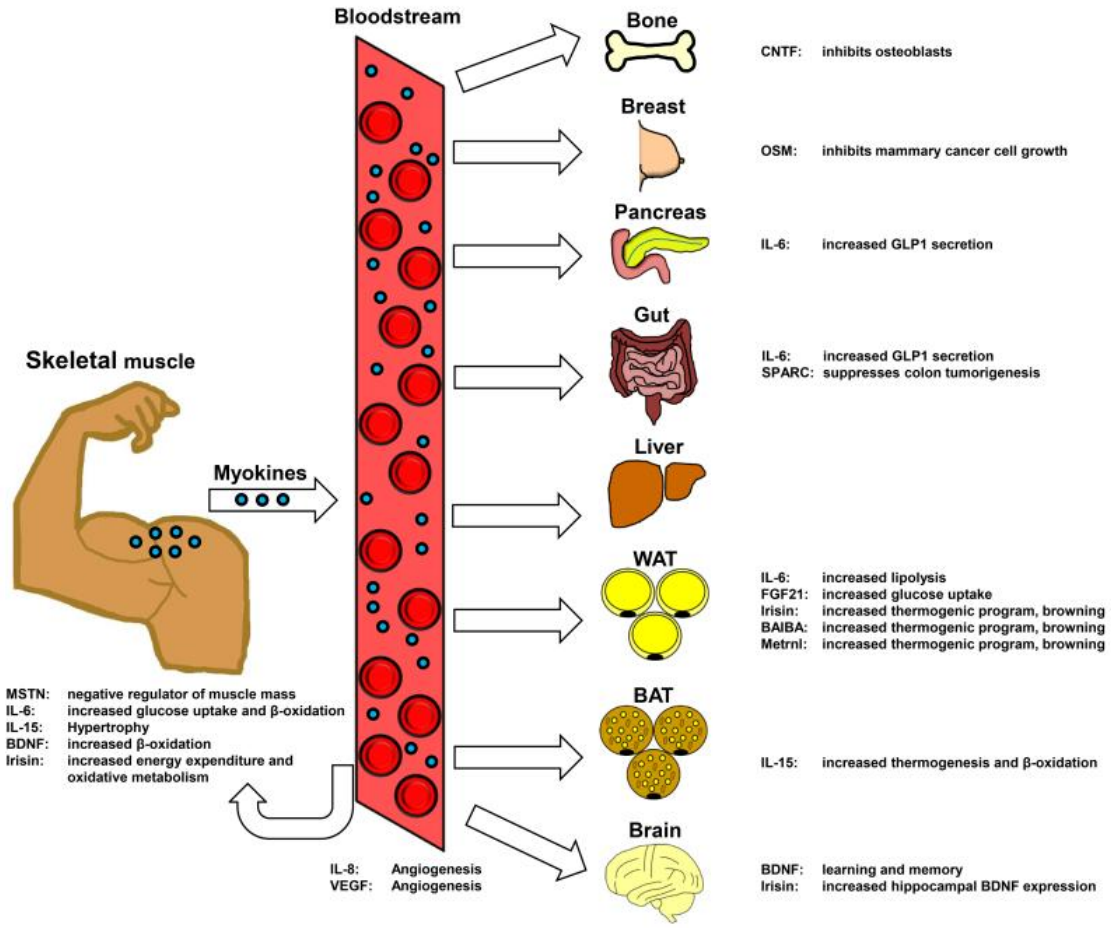

Figure 1.2. Myokines and their effects in autocrine, paracrine and endocrine fashions (Schnyder & Handschin, 2015).

1.5 LIPOCALIN-2 (LCN-2)

1.5.1 Overview

Lipocalin-2 (LCN-2) is a member of the lipocalin family, which comprises small, secreted proteins that transport molecules (hydrophobic, large or small) such as fatty acids, steroids, hormones and retinoids. The *LCN-2* gene is located on chromosome 9 and has various functions in the cell that all encode for a 198 a.a-secreted LCN-2 protein (Flower, 1994). Two known receptors have been found to bind to LCN-2 when secreted and internalised through an endocytotic mechanism: GP330/megalin, which binds to the protein; and SLC22A17/24p3R. GP330/megalin is a low-density lipoprotein cell receptor, known to bind to LCN-2 in epithelial cells during inflammation (Hvidberg *et al.*, 2004). Adipocyte, liver, kidney and spleen cells – amongst others – can uptake LCN-2 via the mechanism of endocytosis to transport the ligand binding of LCN-2 into cells. A variety of ligands can bind to LCN-2 and shape its effect inside cells (Cowland & Borregaard, 1997). Turning to the other receptor, SLC22A17, this has been reported to bind to LCN-2 with high affinity, but its identification and mechanism remain unclear (Devireddy *et al.*, 2005). It is known, however, that this receptor is important for transporting iron and for homeostasis. SLC22A17 can distinguish between holo-LCN-2 and apo-LCN-2, binding to the former and internalising it into cells to release iron. In this manner, the concentration of iron in cells is increased, preventing apoptosis and playing a role in protecting against infection, injury, and inflammation (Cabedo Martinez *et al.*, 2016). It has also been suggested that LCN-2 plays a role in homeostasis and lipid metabolism, but its mechanism for modulating homeostasis and lipid metabolism is not fully understood. In terms of research that has been conducted into this, a study by Jin (2011) showed that using a mouse model in which the mice lacked LCN-2 revealed that LCN-2 increased body mass, hypertrophy and levels of fat in the liver.

In addition, the level of PPARγ decreased, suggesting the role of LCN-2 in haemostasis and lipid metabolism is mediated by PPARγ (Guo *et al.*, 2010; Jin *et al.*, 2011).

1.5.2 Structure of LCN-2

Lipocalin 2 (LCN-2), also known as neutrophil gelatinase-associated lipocalin, has been identified as a 25-kDa acute secreted protein. It was first discovered to be secreted from human neutrophils (Kjeldsen *et al.*, 1994). LCN-2, as with other members of the family of lipocalins, shares the same three-dimensional structure, consisting of a single eight-stranded sheet with an enclosing cavity similar to fatty acid-binding proteins (FABPs). The cavity has an increased ability to bind to a wide variety of hydrophobic molecules such as retinol, fatty acids, steroids and thyroid hormone as LCN-2 has more polar and positively charged amino acids than other proteins in the same lipocalin family (Kjeldsen *et al.*, 2000) (Figure 1.2).

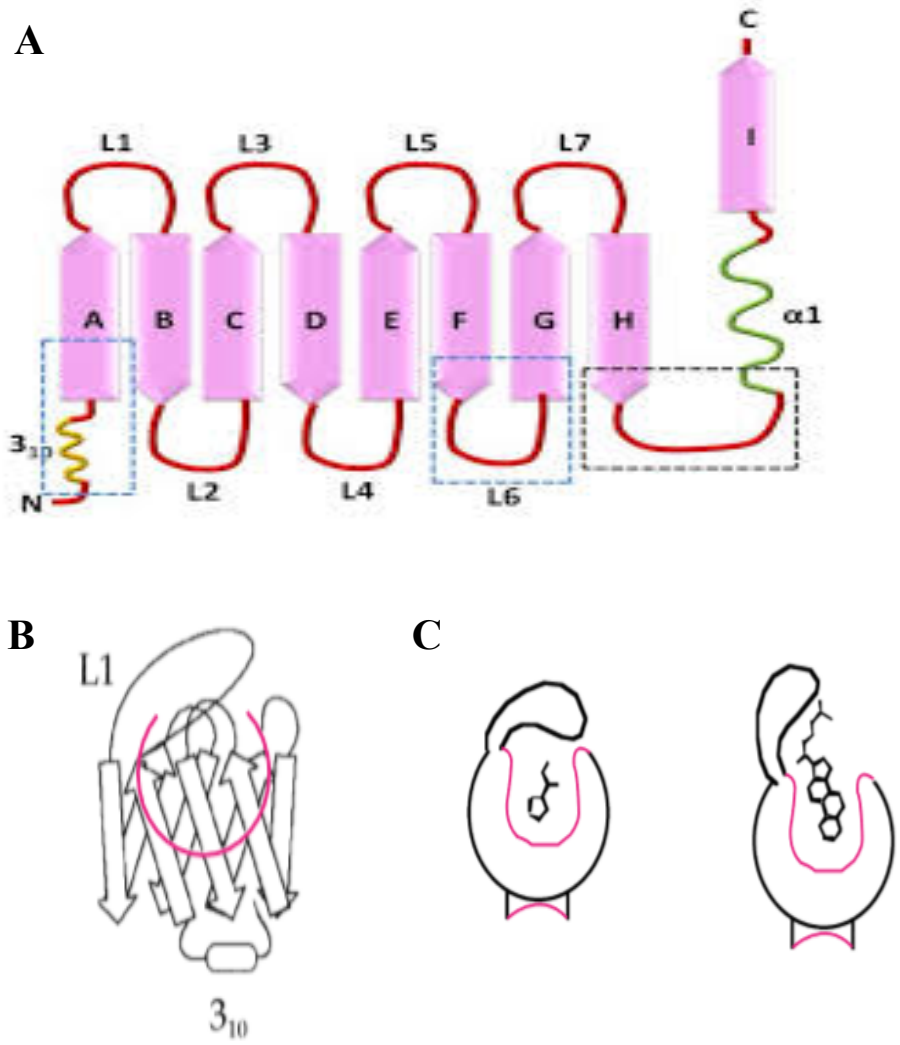

Figure 1.3. A schematic representation of the LCN-2 fold and structure. **A**. The lipocalin fold and its structure consists of eight-stranded beta sheets that are connected by loops. The N-terminal and C-terminal helices are connected to the beta sheets. **B**. The three-dimensional structure of LCN-2 with the binding pocket. **C**. Illustration of how hydrophobic ligands bind with different sizes and shapes (Flower, 1996).

The promoter region of LCN-2 comprises binding sites for the key inflammatory transcription factors NF-κB, C/EBP, STATs and ERK, suggesting that regulation of LCN-2 by these transcription factors is associated with metabolic syndrome and inflammation. The signalling pathway by which these transcription factors regulate the expression and secretion of LCN-2 is illustrated in Figure 1.4 (Kjeldsen *et al.*, 1993; Flower *et al.* 1996; Jaberi *et al.*, 2021).

A

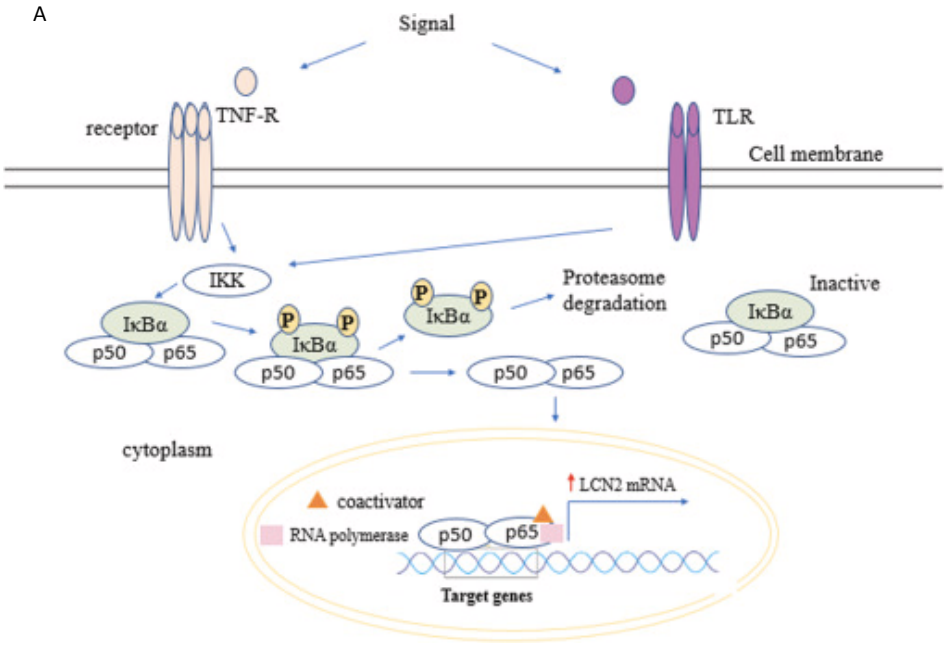
Signal
receptor
TNF-R
TLR
Cell membrane
IKK
IκBα
p50
p65
P
Proteasome degradation
Inactive
cytoplasm
coactivator
RNA polymerase
LCN2 mRNA
Target genes

B

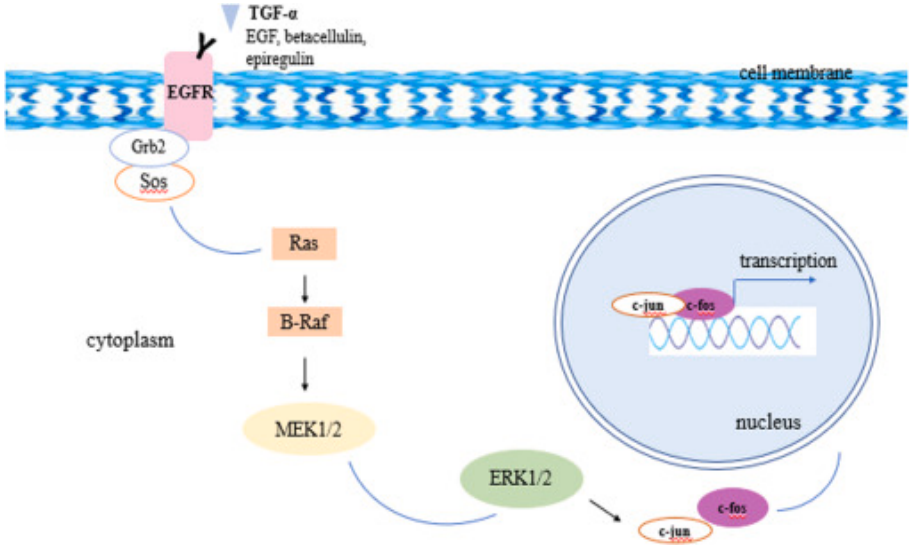
TGF-α
EGF, betacellulin, epiregulin
EGFR
cell membrane
Grb2
Sos
Ras
B-Raf
MEK1/2
ERK1/2
cytoplasm
transcription
c-jun
c-fos
nucleus

C

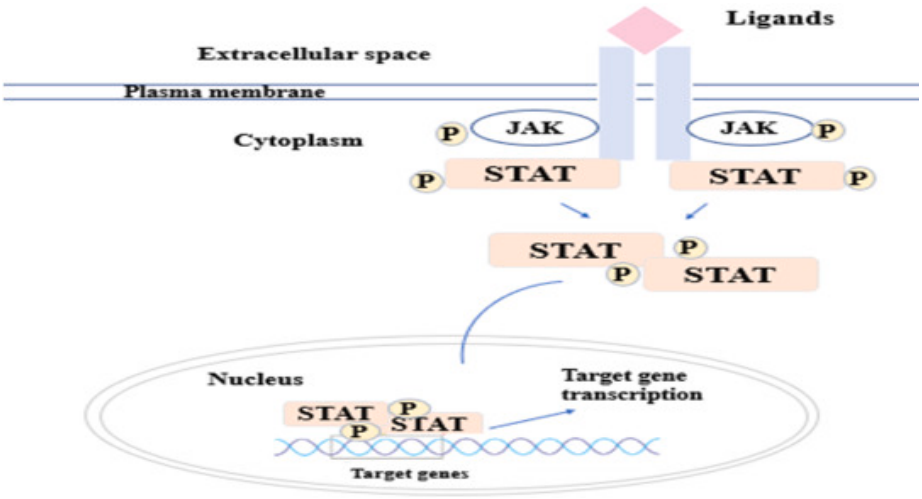

Figure 1.4. The regulation of LCN-2 gene expression by key transcription factors in response to inflammatory markers. The most common transcription factors of LCN-2 are (A) NF-κB, (B) ERK, and (C) STATs. Pro-inflammatory and anti-inflammatory markers, such as TNF-α, IL-1β, IL-3, IL-6, IL-17, and IFN-γ, can induce the expression and secretion of LCN2 under inflammatory responses (Kjeldsen *et al.*, 1993; Flower *et al.*, 1996; Jaberi *et al.*, 2021).

1.5.3 Gene Regulation of LCN-2

In general, LCN-2 mRNA expression has been shown to be upregulated by several factors such as environmental stress, metabolic diseases and infection (Li & Chan, 2011). Moreover, gene expression of LCN-2 has been upregulated in response to pro-inflammatory cytokines such as TNF-a, IL-17, IL-1 β and LPS (lipopolysaccharide) (Pawluczyk, Furness, & Harris, 2003; Yan *et al.*, 2007; Bu *et al.*, 2006).

Other factors that affect the expression of LCN-2 have been found. For example, the serum level in an obese group compared to lean was elevated in 229 participants, with the results showing that LCN-2 serum concentration was higher in the obese group in 32 of the participants ($P < 0.001$). The same study also showed that LCN-2 is correlated well with BMI, suggesting that obesity is a factor that

induces LCN-2 (Wang *et al.*, 2007). Another study found that level of LCN-2 was higher in those who smoked than in non-smokers by an average of 48% in terms of mRNA expression. Moreover, the circulating level of adipocyte-derived LCN-2 was shown to be higher in human subjects with type 2 diabetes and obese animals (Yan *et al.*, 2007). In another study, LCN-2 has been shown to be higher in men in terms of mRNA expression than women (Kamble, Pereira, Almby & Eriksson, 2019). In terms of obesity, it has been shown that LCN-2 is correlated well with BMI, suggesting that obesity is a factor that induces LCN-2 (Wang *et al.*, 2007). In a prior study, the level of LCN-2 was measured using three different methods: western blot analysis, immunoassay and immune-precipitation. All methods showed that the level of LCN-2 in plasma increased in obese subjects compared to lean. The same results have been shown in a murine model (Wang *et al.*, 2007). In terms of mRNA expression, LCN-2 was also found to be upregulated in obese (ob/ob) mice (Yan *et al.*, 2007).

1.5.4 LCN-2 in Various Tissues

LCN-2 is expressed in several tissues, including the kidneys, liver, lungs, bone marrow, adipose tissue, and macrophages (Cowland *et al.*, 1997). However, the expression of LCN-2 is absent in skeletal muscle without any stimulation (Rebalka *et al.*, 2018). In 2005, it was discovered that LCN-2 is secreted from adipocytes. Since then, it has been widely described as an adipokine that appears to affect glucose metabolism and insulin sensitivity, and the role of LCN-2 as a new adipokine in metabolism has been well examined (Chen *et al.*, 2005; Yan *et al.*, 2007).

i. In liver

Over the past few years, Lipocalin-2 (LCN-2) has been known to express in liver under pathophysiological changes. The alteration of expression and the functions of LCN-2 have been reported in many hepatic conditions such as hepatic inflammation, and acute and chronic liver injury. It was noted that the hepatocytes of LCN-2 knockout mice showed the accumulation of lipid droplets and increased apoptosis, which suggests that LCN-2 activity may be involved in the regulation of lipid metabolism. In the same study, it was revealed that patients with chronic liver disease / fibrosis showed significantly higher concentrations of LCN-2 compared to healthy volunteers, suggesting that LCN-2 levels positively correlate with inflammation **(**Fierbinteanu-Braticevici, 2010).

ii. In adipose tissue

Studies have shown that LCN-2 can be expressed and released from adipocytes. The expression of LCN-2 is also increased during the process of adipogenesis, with data indicating that LCN-2 has a specific role in High Fat Diet-induced adipose tissue remodelling (Guo *et al.*, 2013). Previous studies have investigated certain inducers of insulin resistance which upregulate the expression of LCN-2 such as IL-IB, LPS and glucocorticoids (Yan *et al.*, 2007). As regards agents or drugs, insulin-sensitiser thiazolidinedione has been shown to inhibit the expression of LCN-2. Additionally, the circulating level of adipocyte-deriver LCN-2 increased in human subjects with type 2 diabetes and obese animals (Yan *et al.*, 2007). It should be noted that the mechanism and function of LCN-2 in modulating insulin resistance remain unknown. However, a study has indicated that exogenous LCN-2 promotes insulin resistance in cultured hepatocytes, and the authors concluded that LCN-2 is an adipokine, highlighting its importance in insulin resistance and obesity

(Yan *et al.*, 2007). However, several papers have shown that mice lacking LCN-2 developed insulin resistance and gained more weight with HFD compared to wild-type mice (Law *et al.*, 2010; Guo *et al.*, 2013; Zhang *et al.*, 2014). Thus, LCN-2 could either cause insulin resistance to occur or inhibit insulin resistance in adipocytes.

In further studies on the function of LCN-2 on metabolism, it has been reported that LCN-2 is upregulated and acts as a pro-inflammatory agent. It has also been shown that the adipose tissue of LCN-2 knockout mice accumulates less macrophages, and the level of TNF- α is lower in comparison to the wild type (Law *et al.*, 2010). A recent study revealed contradictory evidence related to the involvement of LCN-2 adipokine in the development of the anti-inflammatory response, specifically as an anti-inflammatory regulator of macrophage polarisation and the activation of pathway (NF-κB/STAT3) (Guo *et al.*, 2014). They showed an increase in the activation of target genes of NF-κB, c-Jun, and STAT3 signalling pathway such as IL-1β, IL-6, and MCP-1 in an LCN-2−/− bone marrow-derived macrophage treated with LPS compared with the control sample (wild-type). A recent study using a mouse model also investigated the regulation of LCN-2 expression in adipose tissue in response to metabolic stress on the expression and the secretion of LCN-2 by various cytokines and nutrients in 3T3-L1 adipocytes. In mice, the mRNA expression of LCN-2 was shown to be upregulated in white /brown adipose tissues both in fasting and cold stress. In 3T3-L1 adipocytes, TNFα, IL-1β, and IL-6, IL-1β (among other cytokines) affected LCN-2 expression and secretion. Insulin stimulated the expression and secretion of LCN-2 in a dose-dependent manner; significantly, the effect of insulin in the presence of a low concentration of glucose was cancelled. Moreover, insulin affected the expression and secretion of

LCN-2, which was attenuated by blocking the activation of the NF-κB pathway (Zhang *et al.*, 2014). All these data suggest the role of LCN-2 in inflammation and metabolic diseases.

iii. In skeletal muscle

Investigations have recently revealed that LCN-2 is induced by exercise in serum, but whether Lipocalin-2 is released by skeletal muscle or other cells such as macrophages remains unclear. That said, a few studies have indicated upregulation of LCN-2 in serum when measured by ELISA, such as those by Damirchi, Rahmani-Nia and Mehrabani (2011) and Ponzetti *et al.* (2021). In our lab, a previous PhD student has shown that rat mRNA expression of LCN-2 was upregulated *in vitro* post-electrical pulse stimulation using 12 V, 1 Hz and 1 ms for 24 hr, but not the protein content and its secretion level into cell media. However, human mRNA, protein, and secretion of LCN-2 have not been investigated, and thus form the focus of this present thesis. In previous studies, LCN-2 was measured higher in serum when performing exercise, but no investigation has been done to measure the protein content in human skeletal muscle and the level of secretin by skeletal muscle. The evidence that does exist highlights the actions of LCN-2 cytokine, indicating that LCN-2 may act on the whole body as an exercise-induced myokine. In general, myokines, when secreted in response to physical activity, have been shown to mediate the beneficial effects of exercise in whole-body metabolism (Pedersen & Febbraio, 2008). However, the previously determined endocrine effects of LCN-2 when originating from adipose tissue contradict this hypothesis. So far, very few investigations have aimed to determine the ligand bound to LCN-2 when it is secreted into the plasma. Given that both osteoblast- and adipocyte-derived LCN-2 are the same protein (Mosialou *et al.*, 2017), the difference in their endocrine actions

may indicate that the ligand that is bound to LCN-2 determines its action within the body when derived from different tissues.

1.6 HYPOTHESIS AND AIMS

The regulation, synthesis and secretion of the human LCN-2 gene in skeletal muscle and in response to exercise remains poorly understood. As growing evidence reveals the diversity of tissue specific secretion of LCN-2 into the plasma, the metabolic action of LCN-2 in the body appears increasingly complex. However, despite the established role of ligand binding and transport for members of the calycin protein superfamily, little research has been carried out to identify what is bound to LCN-2 in the plasma when derived from different tissues. With new evidence revealing LCN-2 secretion from skeletal muscle in response to exercise, the interest of this present investigation is to show mRNA, protein content and secretion level of LCN-2 in response to exercise and to gain an insight into the function of LCN-2 as a myokine on other tissues (e.g., adipose tissue) in an endocrine fashion. We have shown in our lab that the mRNA expression of LCN-2 is upregulated by rat skeletal muscle post exercise and in response to a lipid-free medium. Preliminary work has also been done in the FRAME laboratory indicating that LCN-2 was upregulated in response to eccentric exercise in two participants out of four in human skeletal muscle biopsies only three hours post exercise, which then dramatically decreased 48 hours post exercise.

Expression of LCN-2 is induced by various types of pro inflammatory stimuli, such as TNF, IL-1b and IL-17, in various tissues (Pawluczyk, Furness and Harris, 2003; Bu *et al.*, 2006; Yan *et al.*, 2007). Given the idea that the promoter region of LCN-2 comprises binding sites for key inflammatory transcription factors, NF-κB, C/EBP, STAT-1 and STAT-3, it is probable that the expression of LCN-2 is regulated in inflammatory and metabolic conditions. In addition, contradicting evidence has shown the involvement of LCN-2 in both pro- and anti-inflammatory

states in a variety of experimental models (Ferreira *et al.*, 2015). LCN-2 has also been shown to be involved in causing and reducing insulin resistance (Yan *et al.*, 2007; Law *et al.*, 2010). The role of LCN-2 is thus not clear and needs further investigation. On this basis, we decided to investigate the potential role of LCN-2 as a novel myokine *in vitro*. To produce more conclusive and verifiable results, we set aims to determine the validity of our hypothesis that LCN-2 is a novel exercise-induced myokine that exerts potential effects as an endocrine on other tissues; particularly adipose tissue.

Therefore, the aims of this thesis are as follows:

1. To develop an *in vitro* exercise model of human and murine skeletal muscle myotubes using the parameters 1 Hz, 20 V, 2 ms for 16 h (Chapter 3).
2. To investigate the effects of an *in vitro* exercise model on the mRNA expression, protein content in the lysate, and secretion level into cell media (CM) of human and murine skeletal muscle to further consider LCN-2 as a novel myokine (Chapter 4).
3. To examine the effects AICAR treatment on the protein expression and secretion of AMPKa^{Thr172} and LCn-2 *in vitro* in skeletal muscle (Chapter 4).
4. Overexpress LCN-2 in cells (and therefore its secretion level into cell media of LCN-2 and PGC1-a) using a lentiviral inducible vector. Overexpress PGC1-a in cells, and therefore examine the secretion level of LCN-2 into cell media (Chapter 5).

5. To examine the endocrine role of LCN-2 as a novel myokine on lipolysis and lipid accumulation in cultured adipocytes (3T3L-1) *in vitro* (Chapter 6).

Chapter 2: Materials and Methods

2.1 ETHICAL APPROVAL AND VOLUNTEER RECRUITMENT

Volunteers were recruited to undergo a skeletal muscle biopsy procedure for the generation of human primary myotubes cultures used in Andrew Whilhelmsen's PhD study, and extra tissues were donated for this research to generate primary human skeletal muscle culture. Approval has given by the Medical School Ethics Committee at the University of Nottingham (REC #143-1811). Participants were recruited based on an advertisement disseminated using social media platforms and notice boards at the University of Nottingham (https://www.callforparticipants.com). All volunteers were provided with a participant information sheet that explained the details of the study and their expected commitments. Inclusion/exclusion-criteria were determined and screening done. Following this, emails were sent to all participants before the initial visit at the David Greenfield Human Physiology Unit at the University of Nottingham Medical School, Queen's Medical Centre.

2.2 CONSENT AND PARTICIPANT HEALTH SCREENING

If participants met any of the following exclusion criteria, they were excluded from the study:

- Aged < 18 or > 70.
- Body mass index (BMI) < 18.5 kg/m^2 or > 40.0 kg/m^2.
- Any metabolic (e.g., diabetes), endocrine (e.g., hyperthyroidism) or cardiovascular (e.g., coronary artery disease) diseases or abnormalities.
- Hypertension (blood pressure exceeding 140/90).

- Taking regular medication that is known to alter skeletal muscle regulation or cardiovascular function.
- High alcohol consumption (routinely > 4 units per day).
- Clinically significant abnormalities in full blood count, clotting factors, or urea and electrolyte screening.
- Regular smoking.

At any time and at any stage, participants were provided the option to withdraw from their involvement in the study, without any justification needing to be made. Additionally, participants had the opportunity to ask any questions at any time. Participants who were happy to proceed completed a written informed consent form that included a routine health screening. Medical screening results were reviewed by a clinician before participants were invited to undertake any further visits to the laboratory. This screening comprised standard anthropometric measures (height, body mass, waist, and hip circumference), blood pressure, 12-lead electrocardiogram, venous blood samples for routine laboratory screening (including a full blood count, clotting factors, urea analysis and electrolyte concentrations), and a short International Physical Activity Questionnaire (IPAQ). Participant information used in this thesis is described in the table below.

Table 2.1

Characteristics of participants in studies

Participant Code	Sex	Age (y)	Mass (Kg)	Height (m)	BMI	Biopsy yield (mg)
1	Female	19	62.5	1.756	20.268938	~150mg
2	Male	22	81.2	1.75	26.51428571	~100mg
3	Female	22	60.5	1.695	21.05794415	~100mg
4	Female	21	53.5	1.533	22.8	~100mg
5	Male	23	75.5	1.785	23.7	~150mg

2.3 PARTICIPANT LABORATORY VISITS

Upon arrival to the laboratory in the morning (typically ~9:00 am), participants were asked to provide more detail about their physical activity within the last 48 h and to confirm if they had followed the fasting protocol. If their answers were satisfactory, body mass was measured and then individuals rested semi-supine on a hospital bed prior to blood and muscle sampling. Upon completion of the laboratory visit, a light breakfast/lunch was provided, and participants were briefly monitored to ensure they were in a fit state to leave the laboratory.

2.4 HUMAN MUSCLE TISSUE COLLECTION

A practising clinician acquired samples from *vastus lateralis* muscle tissue using the suction-modified percutaneous needle biopsy (Bergström) technique (Bergström, 1975; Shanely *et al.*, 2014). The incision site was cleansed with an iodine solution before 1% lignocaine was administered: first to the skin and then into the muscular belly. The Bergström needle was advanced into the muscular belly via a small incision created with a scalpel. At the same time, suction was administered to the inner trocar using a 50 ml syringe. To guarantee sufficient tissue for culturing, the outer trocar was retracted to draw muscle into the aperture. This was followed by quick closure to cut a tiny sample of tissue; a process that was repeated numerous times while rotating the needle assembly. Muscle tissue was ejected into an ice-cold petri dish, where any significant connective tissue, adipose tissue, or blood was dissected out before being transferred to a universal tube containing ice cold 1x PBS. It was then maintained on ice until processing later that morning. Following this, human skeletal muscle tissue samples were subjected to primary skeletal muscle cell culture, as detailed in the next section.

2.5 PRIMARY HUMAN SKELETAL MUSCLE CELL CULTURE

The fresh skeletal muscle samples were immersed in ice-cold 1x phosphate-buffered saline (PBS) to wash out the residual blood. The muscles were placed on a petri dish and homogenised using a scalpel blade. The tissues were transferred into a universal tube and 5 ml of trypsin/EDTA (0.5 g/l porcine trypsin and 0.2 g/l EDTA) was added. An autoclaved stirrer magnet was then placed next to the tube, and the sample was gently mixed for 30 min at 37°C. The supernatant was then transferred to a fresh falcon tube, and an equal volume of Ham F-10 medium (Sigma-Aldrich, USA) was added and centrifuged for 5 min at 1700 rpm. The supernatant layer was removed, and the cell pellet (satellite cells) was resuspended in Ham's F10 (Sigma-Aldrich, USA) growth medium and pre-plated on an uncoated flask for 10 min at 37°C to purify the satellite cells from existing fibroblasts in the extract. The non-adherent cells were then transferred to 6-well plates coated with 0.2% (W/V) gelatin. The standard growth medium volumes for myoblast culture are provided in Table 2.2 below. The satellite cells were then grown to confluence as myoblasts and differentiated into myotubes in growth medium, as detailed in Table 2.3. After 48 h, the cells were fed with fresh medium, and the medium changed every subsequent 48 h until the cells were ready. The cells were fed with 20% (V/V) FBS (fetal bovine serum) in the fresh medium for approximately one week. This was changed to 6% horse serum (Gibco, Life Technologies, USA) for the subsequent week until the cells fused to form mature myotubes. Horse serum contains a lower level of growth factors and thus promotes the process of cell differentiation. The progress of cell growth is shown in Figure 2.1.

Table 2.2

Standard Growth Medium Volumes for Myoblast Culture

Culture Vessel	Surface Area (cm^2)	Growth Medium Volume (ml per well/flask)
6-well plate	9.0	2.0
12-well plate	4.0	1.0
24-well plate	2.0	0.5
48-well plate	1.0	0.3
96-well plate	0.3	0.2
T25 flask	25.0	5.0
T75 flask	75.0	15.0

Table 2.3

Growth Medium Compositions

Growth Phase	Base Medium	Sera	Antibiotics
Proliferation	Ham's F10* (500ml)	(20%) FBS (100ml)	Pen/Strep (5ml)
Differentiation	Ham's F10* (500ml)	(6%) HS (30ml)	Pen/Strep (5ml)

**20% (V/V) fetal bovine serum (FBS) (Thermo Scientific, USA) and 5 ml antibiotics (10,000 units Penicillin and 10 mg streptomycin/ml in 0.9% NaCl) (Sigma-Aldrich, USA) were added to the Ham's F10 medium.*

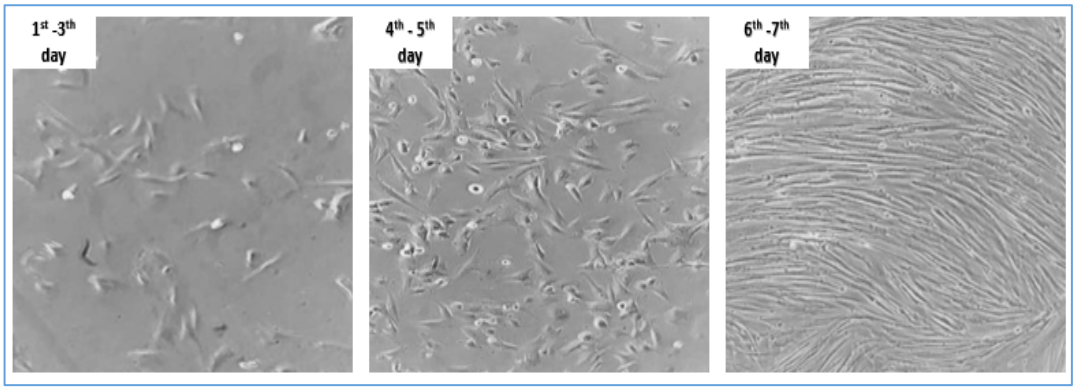

Figure 2.1. Myogenic differentiation (myoblasts towards mature myotubes). Primary human myoblasts were induced to differentiate towards myotubes by culture for the indicated dates in Ham's F-10 cell media with 6% HS were both examined by phase-contrast microscopy at 10x magnification.

2.6 CELL CULTURE

C_2C_{12} myoblast cell line (CRL-1772™), 3T3L-1 fibroblast cell line (CL-173-ATCC) and MDA-MB-468 breast cancer cells (ATCC® HTB- 132™) were purchased from the American Type Culture Collection (ATCC, Manassas, VA, USA). Commercial human skeletal myoblasts cells (HSkM-S) (Cat. No. A12555) were purchased from Thermo-fisher (Gibco). A human embryonic kidney (HEK) 293FT cell line was purchased from ATCC. All cell culture procedures were performed in a microbiological safety cabinet using aseptic techniques for sterility. Mycoplasma contamination testing was performed after cell thawing and before cryopreservation of the cells. The cell lines and media used in the studies are listed in Table 2.4.

Table 2.4

Cell Lines and Media Used in the Studies Describes in this Thesis

Cell lines	Organism	Tissue	Media
HSkM (ATCC® HTB-22) 5%CO_2	Human	Normal skeletal myoblasts from single donor, female.	Ham's F-10 (Gibco, Cat. 11550043) Growth medium supplemented with 20% FBS, 100 U/ml penicillin, 100 µg/ml streptomycin sulphate and 2 mM L-glutamine Differentiation medium supplemented with 6% horse serum, 100 U/ml penicillin, 100 µg/ml streptomycin sulphate and 2 mM L-glutamine
MDA-MB468 (ATCC® HTB-132) 5%CO_2	Human	Mammary gland, breast;	Dulbecco's Modified Eagle Medium (DMEM) (D6046; Sigma-Aldrich, St Louise, MO, USA) supplemented with 10% FBS
Human embryonic kidney (HEK) 293FT 5%CO_2	Human	Embryonic kidney cells	DMEM (D5671; high glucose Sigma-Aldrich, St Louise, MO, USA) supplemented with 10% FBS, 2 mM L-glutamine and 5 mM Sodium Pyruvate
C_2C_{12} 5%CO_2	Mouse	Myoblasts	DMEM (D5671; high glucose Sigma-Aldrich, St Louise, MO, USA) Growth medium supplemented with 10% FBS, 100 U/ml penicillin, 100 µg/ml streptomycin sulphate and 2 mM L-glutamine Differentiation medium supplemented with 2% horse serum, 100 U/ml penicillin, 100 µg/ml streptomycin sulphate and 2 mM L-glutamine
3T3L-1 10%CO_2	Mouse	Fibroblasts	DMEM high glucose (Sigma D5671 sigma-Aldrich) supplemented with 10% calf serum, 100 U/ml penicillin, 100 µg/ml streptomycin sulphate and 2 mM L-glutamine for maintenance.

2.7 CELL LINE MAINTENANCE AND SUB-CULTURING

At 37°C, the cells were incubated in a humidified environment containing either 5% CO_2 or 10% CO_2 depending on cell type as the table illustrated. Every 2-3 days, the media was replaced with new media and cells were passaged when they reached around 70-80% confluence. Cell culture medium was taken from the flask, and the cells were washed twice with 1x phosphate-buffered saline (PBS) solution for sub-culturing (BR0014G; Oxoid, Cheshire, UK). Sufficient trypsin ethylenediaminetetraacetic acid (EDTA) solution (T3924; Sigma-Aldrich, St Louis, MO, USA) was added to cover the full surface area of the flask (3 ml for the T75 flask and 5 ml for the T175 flask). The cells were incubated at 37°C until they completely detached (5-7 min). Culture medium with serum (at least double the volume of trypsin) was added to inactivate the trypsin. Cells were aspirated via gently pipetting and then transferred into a sterile tube. The cell suspension was centrifuged at 125 g for 5 min. Thereafter, the supernatant was discarded, and the cell pellet was resuspended in an appropriate amount of fresh culture medium. The appropriate aliquot of the cell suspension was transferred to a new cell culture flask containing fresh media. Sub-cultivation ratios for MDA-MB468, HEK293FT, human skeletal muscle and C_2C_{12} cells were 1:10, 1:10, 1:3 and 1:10 respectively.

2.8 CELL COUNTING

Cell concentration and viability was important to ensure reproducibility in the experiment, and sub-culturing was important to monitor growth rates and for cryopreservation. We determined cell concentration by cell counting using a haemocytometer. To exclude dead cells, we used Trypan Blue, which stained cells a blue colour. 10 µl of cell suspension sample was diluted with 10 µl of Trypan Blue and mixed well. 10 µl of the mixture was then loaded onto the haemocytometer under

a coverslip. The cells inside the four large corner squares of the haemocytometer were counted under an inverted light microscope at 10x magnification. To calculate cell concentration, we followed this formula:

$$Total\ cells\ (cells/ml) = \frac{(Total\ cell\ count \times Dilution\ factor) \times 10^4}{Number\ of\ squares\ counted}$$

2.9 CRYOPRESERVATION OF CELLS

During the exponential phase, we harvested cells using trypsin, as described previously. After centrifugation, cells were resuspended in cryopreservation medium consisting of 5% dimethyl sulfoxide (DMSO) in complete growth medium to a concentration of approximately 3 x10^6 viable cells/ml. 1 ml of cell suspension was dispensed into a 1 ml-labelled cryopreservation vial. Filled cryopreservation vials were then placed into an insulated freezing container and cooled overnight at -80 °C before being transferring to a liquid nitrogen container for long-term storage in vapour-phase liquid nitrogen (between -140 °C and -180 °C).

2.10 DIFFERENTIATING 3T3L-1 TOWARDS ADIPOCYTE-LIKE CELLS

Cultures were incubated at 37°C in a suitable incubator with 10% CO_2. Cell cultures were regularly checked for attachment and health, and media was changed every 48 h until the cells were ready. Differentiation of fibroblast cells towards adipocyte-like cells was validated in the FRAME lab using four different growth media (M1, M2, M3 and M4). For sufficient differentiation of these cells to adipocyte like-cells, 6-well or 12-well culture plates were used (Table 2.5). M1 is the maintenance media that was only included the DMEM media with high glucose and calf serum media. This was then left to grow to confluence (70%-80%) and was

ready for M2 on the next day (M1, day#1). M2 was used to start the differentiation process, whereby we added an IBMX (Isobutylmethylxanthine, 1-Methyl-3-Isobutylxanthine) mix to reduce lipolysis for fast conversion to accumulate more lipids. Dexamethasone was also added to reduce inflammatory effects. In M3, Insulin was added to the growth media to facilitate the uptake of glucose and activate the downstream pathway of PPR-gamma for fast conversion of glucose into lipid molecules. M4, the last media, was used to maintain the lipid accumulation inside cells. The differentiation course was done over seven days, and at day six or seven, cells were ready for imaging or treatment (Figure 2.2)

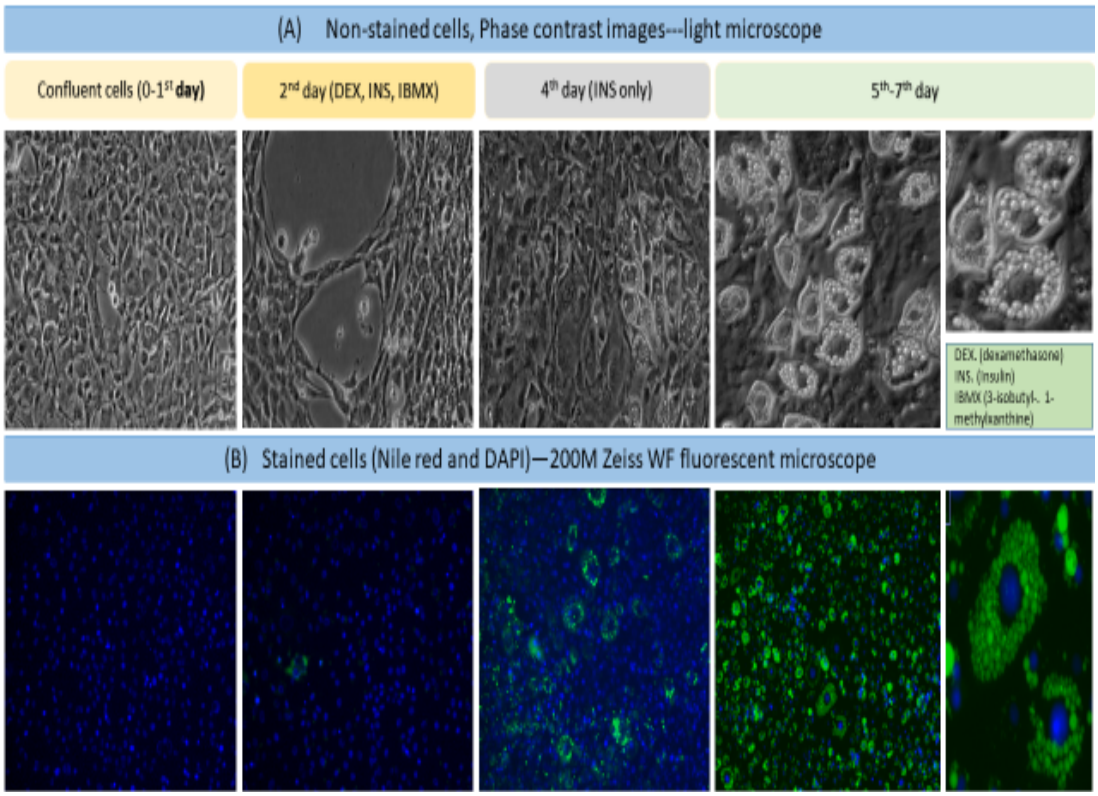

Figure 2.2. Differentiation process of 3T3L1 cells towards adipocyte-like cells. **(A)** Phase contrast images of 3T3-L1 cells from day zero to day seven post-induction. Cells initially display a fibroblast phenotype. Over the course of differentiation, cell morphology changes and accumulate more lipids internally. **(B)** Nile Red and DAPI staining, scale bar 105um. All images in **(A)** were taken with an inverted light microscope and in **(B)** with a fluorescent microscope (200M Zeiss WF).

Table 2.5

Growth Media Compositions of Differentiation of the 3T3-L1 Cells

Growth Phase	Base Medium	Sera	Supplements	Antibiotics
(M1) 3T3-L1 maintenance medium	DMEM high glucose (Sigma D5671 (500 ml) +Glutamine	10% calf serum	----	Pen/Strep (5 ml) and 200 mM gentamicin
(M2) Differentiation medium-starting	DMEM high glucose (Sigma D5671) (500 ml) with Glutamine	10% FBS	1 ml IBMX +1 ml Dexamethasone (125 uM stock) +166nM insulin	Pen/Strep (5 ml) and 200 mM gentamicin
(M3) Differentiation medium	DMEM high glucose (Sigma D5671) (500 ml) with Glutamine	10%FBS	166 nM insulin	Pen/Strep (5 ml) and 200 mM gentamicin
(M4) Adipocyte maintenance medium	DMEM high glucose (Sigma D5671) (500 ml) with Glutamine	10%FBS		Pen/Strep (5 ml) and 200 mM gentamicin

2.11 AICAR (AMPK ACTIVATOR 5-AMINOIMIDAZOLE-4-CARBOXAMIDE-1--D-RIBONUCLEOSIDE) TREATMENT

C_2C_{12} myoblasts and human skeletal myoblasts were maintained at 37°C in a 5% CO_2 atmosphere. AICAR was diluted in sterile distilled water at 10 mM as a stock concentration. Five days after the initiation of myoblasts differentiation, myotubes were incubated with AICAR (AICAR; Sigma, St. Louis, MO). To investigate AMPK activation (phosphorylation level of AMPK Th172) and Lipocalin-2 (LCN-2) expression and secretion, myotube cells were incubated with AICAR at 2mM to measure time-dependent effects of AICAR. Cells were incubated with or without AICAR (2 mM) for 15 min, 30 min, 60 min, 24 h and 48 h. Cells without AICAR served as a negative control. Subsequently, human/murine myotube cells were harvested for downstream analysis (protein analysis).

2.12 STOCK PALMITATE PREPARATION

Because palmitate is insoluble in water, we employed bovine serum albumin (BSA) as a carrier. Fatty acid free BSA encourages palmitate to dissolve into palmitate conjugated to BSA, which allows cells to then absorb and utilise palmitate. BSA was then added to equal 80% of the goal volume – the amount of BSA required to generate a 2 mM solution contributes significantly to the final volume. To dissolve BSA, the BSA solution was stored in a fridge an overnight at 4°C. The BSA solution was then filter-sterilised in a culture hood the following day and kept at 4°C, away from light. 20 mM solution was the final product.

Following this, using a volume of 0.01 M NaOH and sodium palmitate powder, 20 mM sodium palmitate was created. The Na-palmitate was then dissolved in NaOH and kept in the water bath at 80°C. To pair Na-palmitate with BSA, the following procedure was followed:

- Two water baths were prepared: one at 70°C for the Na-palmitate, and the other at 50°C for the other components (BSA and coupling).
- Stock were dissolved (20 mM stock of Na-palmitate) in the water bath at 70°C, and 250 mM of Na-palmitate was promptly withdrawn into 12mM BSA, which was incubated at 50°C.
- Samples were carefully pipetted up and down numerous times, then the tube was sealed and gently vortexed for a few seconds.
- Conjugate of Palmitate and BSA were created by incubating the mixture for at least 1 h, with gentle vortexing every 10-15 min.
- Conjugate of the palmitate-BSA solution was then aliquoted and kept at -20°C for future use.

2.13 PALMITATE TREATMENT OF HUMAN MYOTUBES

On day six, myotube cells were treated with 300 uM Palmitate or Vehicle for 24 h. Post-24 h, cells were lysed in RIPA buffer for protein analysis. Protein levels were measured using a BCA protein assay kit (Thermo Scientific™ Cat. 23225).

Preparation of RIPA lysis buffer:

- 10mM of Tris-HCl, pH 8.0
- 1mM of EDTA
- 0.5mM of EGTA
- 1% of Triton X-100
- 0.1% of Sodium Deoxycholate
- 0.1% of SDS and 140mM of NaCl
- Dilute the stock with ddH2O
- Add 1mM of protease and phosphotease inhibitor immediately before use.

2.14 INSULIN TREATMENT OF HUMAN MYOTUBES

On day seven, myotube cells were treated with 100 nM Insulin (Sigma-Aldrich I9278-5ML) or vehicle for 15 min. Post-15 min, cells were lysed in RIPA buffer for protein analysis. Protein were measures by BCA protein assay kit (Thermo Scientific™ Cat. 23225).

2.15 ELECTRICAL PULSE STIMULATION (EPS): AN IN VITRO EXERCISE MODEL

Fully differentiated human (HSkM) and murine (C_2C_{12}) myotubes were induced to contract by EPS. On day six, myotubes were stimulated at 2 ms, delivering 20 V at a frequency of 1 Hz for 16 h (2-ms, 20-V at 1Hz) (see Figure 2.2)

using a C-Dish Culture Dish Electrode System combined with a C-Pace EP Pulse Generator (IonOptix, Milton, MA, USA) (see Figure 2.3). The myotubes were then placed into the cell culture medium in a 6-well plate. Post-16 h, the cell media (CM) were stored, and the cells were collected both in TRI Reagent (Sigma-Aldrich, USA) for mRNA analysis and in RIPA buffer for protein analysis.

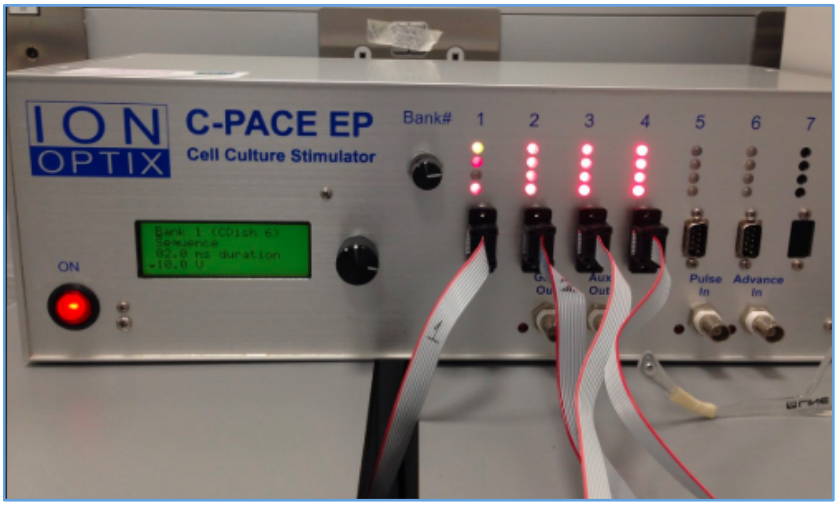

Figure 2.3. Cell culture stimulator (C-Pace EP) used in the study.

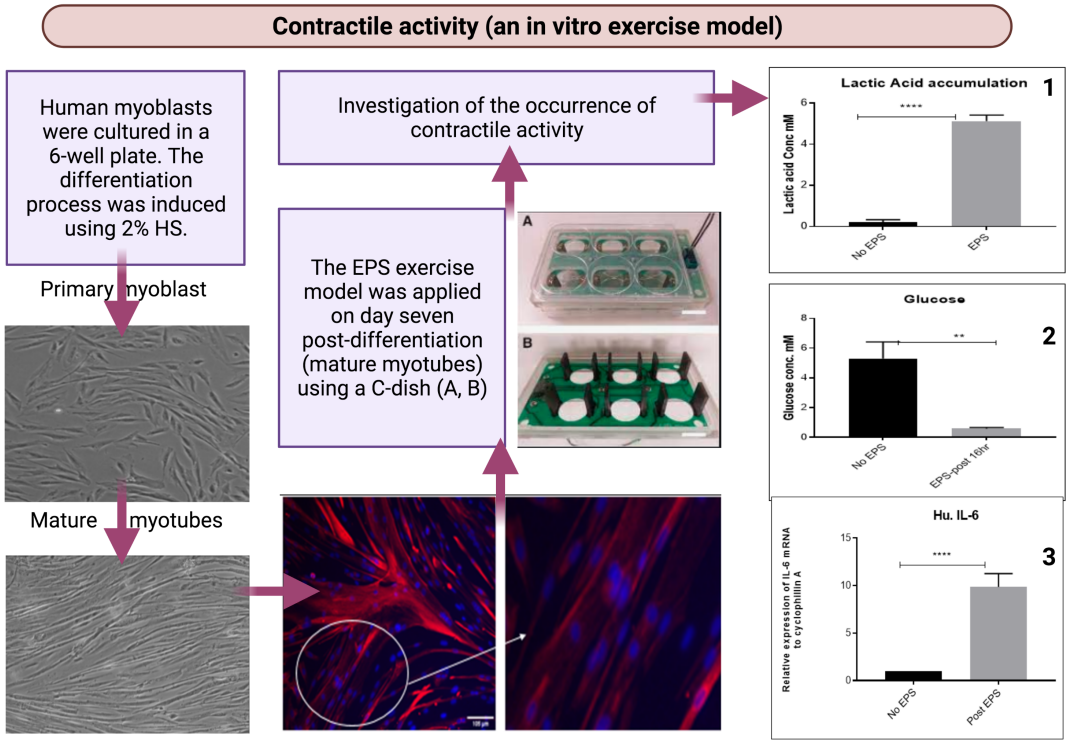

Figure 2.4. Representative figure of experimental methods used to investigate the potential role of LCN-2 as a novel myokine. The figure represents the EPS model used in vitro to induce muscle contraction and therefore mimic acute physical activity. A C-Dish™ electrode board was used to induce contractions of human- (HSkM) and murine- (C2C12) cultured skeletal muscle cells. **A.** 6-well plate with a pin to connect to an external generator with a single chamber stimulation. **B.** The board has a carbon electrode pair for each cell chamber and underlying circuit pathways. Created using Bio-render website (https://biorender.com/)

2.16 LACTIC ACID ASSAY

The lactate determination method relied on the conversion of LDH-mediated lactate to pyruvate, which also converted NAD+ to NADH. The rise in NADH at 340 nm was used to calculate the enzyme rate. In 20 ml aqueous glycine-EDTA-hydrazine buffer pH 9.0, 20 u/ml L-Lactate Dehydrogenase from rabbit muscle (Sigma Aldrich, USA) and 3 mM -Nicotinamide adenine dinucleotide sodium salt (Sigma Aldrich, USA) were added (200 mM glycine, 2 mM EDTA, 250 mM hydrazine hydrate). Standards were made in Ham's F-10 culture medium using a 1:2 serial dilution of 5 mM lactic acid (Fisher Scientific, USA). Assays were carried out by assaying a set of standards, samples (diluted and not diluted), and blanks into a

96-well plate in triplicates. A reaction mix of 100 µL was added to each well, and the absorbance was measured at 340 nM immediately (t0) and after 30 min (t30) using a FLUOstar Omega Spectrometer-Based microplate reader (BMG Labtech, Germany). Readings were taken and lactic acid concentration (lactate accumulation) was determined by reference to the standard curve (t30-t0).

2.17 GLUCOSE ASSAY

The oxidation of glucose by glucose oxidase (GOD) to glucoronic acid and hydrogen peroxide was the basis of this glucose measurement test. The hydrogen peroxide was then measured stoichiometrically using a chromogen and a horseradish peroxide-linked acceptor (tetra-amino benzidine to a blue-yellow product measured at 450 nm or dianisidine to a pink product measured at 540 nm). The reagent mix was made by combining 0.4 mg glucose oxidase (Sigma-Aldrich, USA) and 1 mg horseradish peroxidase (Sigma-Aldrich, USA) in 10 ml TrisHCl 1M, pH 7.4, and then adding 0.1 tetramethylbenzidine (Sigma-Aldrich, USA). The standards were made using a 1:2 serial dilution of Ham's F-10 Culture Medium (Sigma-Aldrich, USA) (6.1 mM glucose concentration). The assay was carried out by putting 10 µL of standards and samples into a 96-well plate and then adding 100 µL of reaction mix to each well. After 10 min, the reaction in each well was stopped with 0.2 M sulphuric acid, and the absorbance was measured at 450 nm using a FLUOstar Omega Spectrometer-Based microplate reader (BMG Labtech, Germany). The standard curve was prepared by curve fit ‘single site binding’ using PRISM 5, and the samples’ concentrations were derived from the standard curve.

2.18 OVEREXPRESSION OF LCN-2 AND PGC1-A

Generally, the overexpression of LCN-2 is a two-step process. First, plasmid DNA containing the gene of interest is transduced into the genome of the host cell

using the lentiviral vector system (as shown in Figure 2.4). Second, an antibiotic is applied selectively for successfully transduced cells. Once the cells are adequately selected, colonies are chosen, and the cells are expanded.

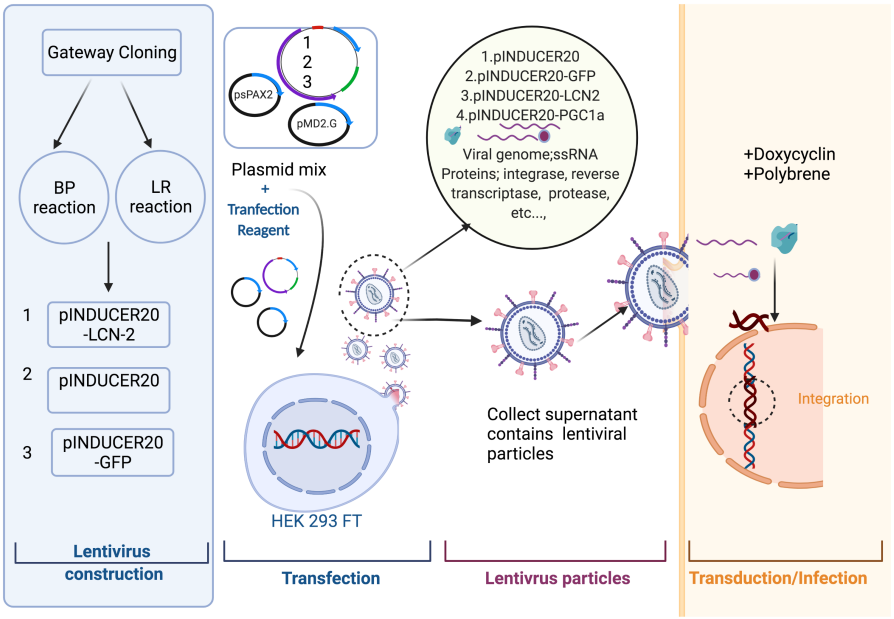

Figure 2.5. Representative figure of experimental method used to study the endocrine effects of LCN-2 as a novel myokine on adipose tissue using the lentiviral vector system. Created with Bio-render (https://biorender.com)

2.19 CONSTRUCTION OF INDUCIBLE LCN-2 AND PGC1-A EXPRESSION PLASMID VECTOR

Gateway® Technology with Clonase® II (11789-020 and 11791-020; Thermo Fisher Scientific, Waltham, MA, USA) was used to clone *LCN-2* and *PGC1-a* genes into pINDUCER20 plasmids. Gateway cloning consists of the BP recombination reaction to create the entry clone containing gene-specific sequences. This is followed by the LR recombination reaction, which transfers gene-specific sequences from the entry clone into a destination vector (pINDUCER20), thereby creating an expression clone. Recombination occurs between specific attachment (*att*) sites on the interacting vector by switching the DNA segment.

2.20 DESIGNING ATTB-POLYMERASE CHAIN REACTION (PCR) PRIMERS

LCN-2 and PGC1-alpha DNA sequences were acquired from the National Center for Biotechnology Information (NCBI) database. Forward and reverse primers were designed using the Primer-BLAST open-source program (https://www.ncbi.nlm.nih.gov/tools/primer-blast). To enable efficient Gateway® cloning, four guanine bases at the 5' end followed by 25 base pairs *att*B1 site and Kozak sequence were inserted in front of the *LCN-2 and PGC1-a* gene sequence (at least 18-25 base pairs) to construct the forward primer. Four guanine bases at the 5' end followed by 25 base pairs *att*B2 site were inserted as a reverse primer (Table 2.6). Primers were purchased from Eurofins Scientific (Luxembourg). Sterile DNase- and RNase-free was added to reconstitute the primers and create 100 µM of stock concentration based on the manufacturer's guidance. The stock was diluted 1:10 to a concentration of 10 µM before use.

Table 2.6

Lipocalin-2 Primer Sequences for Gateway® Cloning

Primer	Sequence (5' - 3')
LCN-2 forward primer	GGGGACAAGTTTGTACAAAAAAGCAGGCT TCGCCACC**TCAACGGGAGAGAAGGAAGTGGCT**
LCN-2 reverse primer	GGGG**ACCACTTTGTACAAGAAAGCTGGGT T AGGGCCCCAGGATCGACATGA**
PGC1-a forward primer	GGGGACAAGTTTGTACAAAAAAGCAGGCT TCGCC ACC **GGACTCAAGTGGTGCAGTGAC**
PGC1-a reverse primer	GGGGACCACTTTGTACAAGAAAGCTGGGT**CCTAC TCAGACAATGCGATGCA**

**Underlined sequences are attB sites. Bold sequences are LCN-2 and PGC1-a gene.*

2.21 PRODUCING *ATT*B-PCR PRODUCTS

DNA templates used for amplification were cDNA-synthesised from a human liver tissue sample provided by FRAME lab. LCN-2 and DNA Plasmid (pcDNA4

myc/his PGC-1 alpha-Plasmid #10974) for PGC1-a Phusion® High Fidelity DNA polymerase (M0530L; New England Biolabs, Ipswich, MA, USA) were purchased and used for PCR to produce *att*B-PCR products. The PCR was performed using a thermal cycler (T100™ Thermal Cycler; Bio-Rad, Hercules, CA, USA). Reaction conditions and thermocycling conditions are shown in Tables 2.7 and 2.8 respectively. 10 µl of *att*B-PCR products were then mixed with loading buffer and separated via 1% agarose gel electrophoresis. The *att*B-PCR products were visualised using ultraviolet light (GeneGenius Imaging System; Syngene, India).

Table 2.7

Reaction Conditions for Producing attB PCR Products

Component	Volume (µl)
5x Phusion HF Buffer	10
10 mM dNTPs	2
10 µM forward primer	2
10 µM reverse primer	2
Template DNA	3
Phusion DNA Polymerase	0.5
Nuclease-free water	(Final volume up to 50 µl)

Table 2.8

Thermocycling Conditions for PCR

Step	Temperature	Time	Cycle(s)
Initial denaturation	98 °C	1 min	1
Denaturation	98 °C	30sec	30
Annealing	60 °C	30 sec	
Extension	72 °C	2 min	
Final extension	72 °C	5 min	1
Hold	4 °C	∞	-

2.22 AGAROSE GEL ELECTROPHORESIS

Agarose gel electrophoresis was used to verify the quality and quantity of PCR products. By applying an electrical field, negatively charged DNA is moved though an agarose matrix toward a positive electrode. Short DNA fragments migrate though the gel faster than long fragments; thus, DNA fragments are separated by length. To prepare 1% agarose gel, 1 g of agarose powder (A9539; Sigma-Aldrich, St Louise, MO, USA) was dispersed in 100 ml of 1x TAE buffer (pH 8.3). The agarose was heated in an oven using medium power for 2-3 min until completely dissolved. The melted agarose was then cooled to 50 °C. Ethidium bromide (46067; Sigma-Aldrich, St Louise, MO, USA) was added to the agarose to a final concentration of 1 µg/ml, then it was slowly pouring it into a gel tray with a comb in place to create wells for loading samples. The agarose was left at RT for 15 min until completely solidified. Once solidified, the agarose gel was placed in a gel tank. 1x TAE buffer was added until the agarose gel was covered and the comb then removed. 10 µl of PCR product was mixed with 2 µl of 6x loading buffer (B7024S; New England Biolabs, Ipswich, MA, USA) before loading. The gel was run at 100 V for 1.5 h. PCR products were visualised under ultraviolet light (GeneGenius Imaging System; Syngene, India).

2.23 PURIFYING *ATT*B-PCR PRODUCTS

Purification of *att*B-PCR products is recommended to eliminate *att*B primers and any *att*B primer-dimers. Primers and primer-dimers can recombine with the donor vectors in the BP reaction and increase the number of background colonies after transformation into *Escherichia coli*. 150 µl of Tris-ethylene-diamine-tetraacetic acid (TE; 10 mM Tris-HCl, 1 mM EDTA, pH 8.0) buffer was added to 50 µl of amplification reaction containing *att*B-PCR products. This was followed by 100 µl of 30% polyethylene glycol (PEG) 8000/30 mM $MgCl_2$. The mixture was vortexed

thoroughly and centrifuged immediately at 10,000 g for 15 min at RT. Supernatant was removed and the pellet was dissolved in 50 µl of TE buffer (pH 8.0) to a concentration of more than 10 ng/µl. The concentration of purified products was determined using a spectrophotometer (FLUOstar Omega microplate reader; BMG Labtech, Offenburg, Germany). 5 µl of purified *att*B-PCR product was mixed with loading buffer and separated via 1% agarose gel electrophoresis to evaluate the quality.

2.24 CREATING ENTRY CLONES USING THE BP RECOMBINATION REACTION

By using the BP clonase II enzyme, the BP recombination reaction facilitates the insertion of the *att*B-PCR product into the *att*P-containing donor vector (pDONR^{TM}221 [35- 1687; Invitrogen, Carlsbad, CA, USA]) to create an entry clone (see Figure 2.6). The reaction mixture is transformed into a suitable *E. coli* host (One Shot Top10 Chemically Competent *E. coli* (44-0301; Invitrogen, Carlsbad, CA, USA)). Entry clones were then selected using appropriate antibiotics.

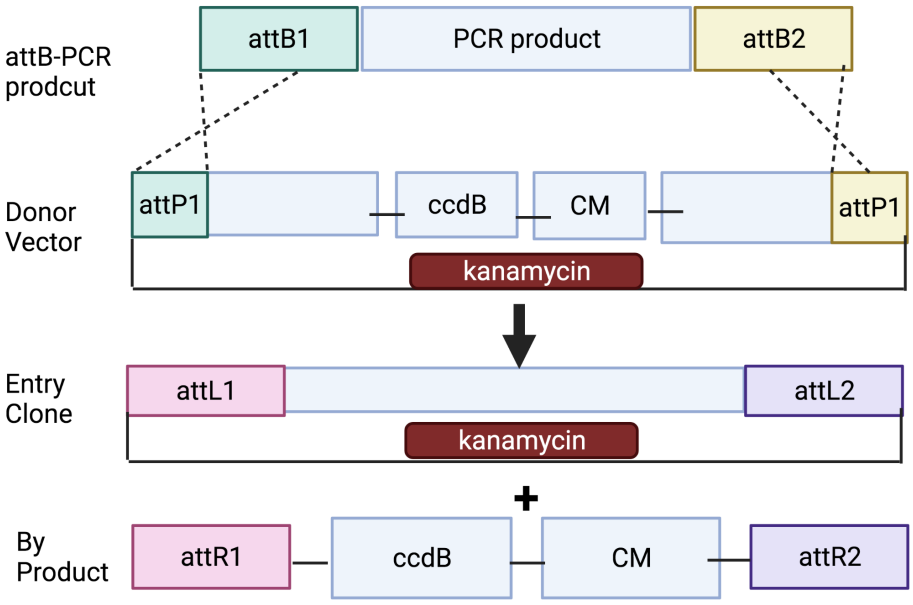

Figure 2.6. BP recombination reaction. The diagram depicts a BP recombination reaction between an attB-PCR product and a donor vector to create an entry clone and a by-product. The PCR product is transferred from the attB-PCR product into the entry clone following recombination. Created with Bio-render (https://biorender.com/)

2.25 PERFORMING THE BP RECOMBINATION REACTION

Fifty femtomoles (fmol) of *att*B-PCR products were mixed with 150 ng of pDONR^{TM}221 at RT. TE buffer (pH 8.0) was added to a final volume of 8 µl. Gateway® BP clonase® II enzyme mix was thawed on ice for 2 min then vortexed twice for 2 s each time. 2 µl of the enzyme mix was added to the sample and mixed thoroughly via vortexing twice for 2 s each time. 100 ng of pEXP7-tet vector was used as a positive control. A negative control was set up by omitting the enzyme mix. The reactions were incubated at 25°C overnight. 1 µl of proteinase K solution was added to each sample to terminate the reaction before incubating the resulting samples at 37°C for 10 min.

2.26 TRANSFORMING COMPETENT *E. COLI* AND SELECTING ENTRY CLONES

A vial of One Shot Top10 Chemically Competent *E. coli* was thawed on ice for each transformation. 1 µl of BP recombination reaction was added to a vial of Top10

E. coli and mixed gently. 10 pg (Picogram) of pUC19 was used as a positive control for transformation. The vials were incubated on ice for 30 min. Heat-shock was then performed at 42°C for 30 s followed by incubation on ice for 2 min. 250 µl of S.O.C medium (0.5% Yeast Extract, 2% tryptone, 10 mM NaCl, 2.5 mM KCl, 10 mM $MgCl_2$, 10 mM $MgSO_4$, 20 mM glucose) was added to each vial. The vials were incubated at 37°C for 1 h on a horizontal shaker running at 225 rpm. After the transformation mixture was diluted 1:10 in lysogeny broth (LB) medium (1% trypton, 0.5% yeast extract and 1% NaCl, pH 7.0), 50 µl was spread on the pre-warm agar plate (1.5% agar in LB medium) with appropriate antibiotic and incubated at 37°C overnight.

2.27 COLONY PCR

To verify that the *LCN-2* or *PGC1-alpha* gene presented as an entry clone, a colony PCR was performed using M13 sequencing primers (see Table 2.9). A reaction mixture was prepared using BIOTAQ^{TM} DNA Polymerase (BIO-21040; Bioline, London, UK) (see Table 2.6). The colony was labelled, and half was scraped using a pipette tip and then resuspended in the reaction mixture. The PCR was performed with a thermal cycler (see Table 2.7). After PCR was complete, the PCR product was separated via 1% agarose gel electrophoresis at 120 V for 15-20 min and then visualised under ultraviolet light.

Table 2.9

M13 Sequencing Primers

Primer	Sequence (5' - 3')
M13 forward primer	GTAAAACGACGGCCAGT
M13 reverse primer	GGAAACAGCTATGACCATG

Table 2.10

Reaction Conditions for Colony PCR

Component	Volume (µl)
10x NH4 Reaction Buffer	2
50 mM MgCl2 Solution	0.6
10 mM dNTPs	0.4
10 µM forward primer	1
10 µM reverse primer	1
BIOTAQ DNA Polymerase	0.25
Nuclease-free water	14.75 (Final volume up to 20 µl)

Table 2.11

Thermocycling conditions for colony PCR

Step	Temperature (°C)	Time	Cycle(s)
Initial denaturation	96 °C	5 min	1
Denaturation	96 °C	15 sec	30
Annealing	50 °C	20 sec	
Extension	72 °C	70 sec	
Final extension	72 °C	5 min	1
Hold	4 °C	∞	-

The single colony demonstrating *LCN-2* and *PGC1-alpha* gene insertion was selected and transferred into a tube containing 5 ml LB medium with kanamycin 50 µg/ml. The bacterial culture was incubated at 37°C overnight in a horizontal shaker at 225 rpm. 500 µl of bacterial culture was mixed with 500 µl of 50% glycerol to create bacterial glycerol stock stored at -80 °C. The entry clone was recovered from 4 ml of bacterial culture using a QIAprep Spin Miniprep Kit (27104; Qiagen, Hilden, Germany) according to the manufacturer's instructions. The entry clone was quantified using a spectrophotometer FLUOstar Omega microplate reader (BMG

Labtech, Offenburg, Germany) and submitted for Sanger sequencing (Source Bioscience, Nottingham, UK) to verify the insertion sequence. Sequences were analysed using A plasmid Editor (ApE) software.

2.28 CREATING EXPRESSION CLONES USING THE LR RECOMBINATION

The LR recombination reaction was performed after the BP recombination reaction to transfer the gene of interest from the entry clone into an *att*R-containing destination vector (pINDUCER20 [44012; Addgene, Watertown, MA, USA]) (see Figure 2.6), creating an *att*B-containing expression clone (Figure 2.7). The reaction mixture was then transformed into a suitable *E. coli* host (One Shot Stbl3 Chemically Competent *E. coli* [C7373-03; Invitrogen, Carlsbad, CA, USA]). Finally, entry clones were selected using appropriate antibiotics.

2.29 PERFORMING THE LR RECOMBINATION REACTION

The reaction was set up at RT by mixing 150 nanogram (ng) of entry clone with 150 ng of pINDUCER20. TE buffer, pH 8.0, was added to a final volume of 8 µl. Gateway® LR clonase® II enzyme mix was thawed on ice for 2 min, then vortexed twice for 2 s each time. 2 µl of the enzyme mix was then added to the sample and mixed well by vortexing twice for 2 s each time. 100 ng of pENTR-gus vector was used as a positive control. A negative control was set up by omitting the enzyme mix. The reactions were incubated at 25°C overnight. 1 µl of proteinase K solution was added to each sample to terminate the reaction before the samples were incubated at 37 °C for 10 min.

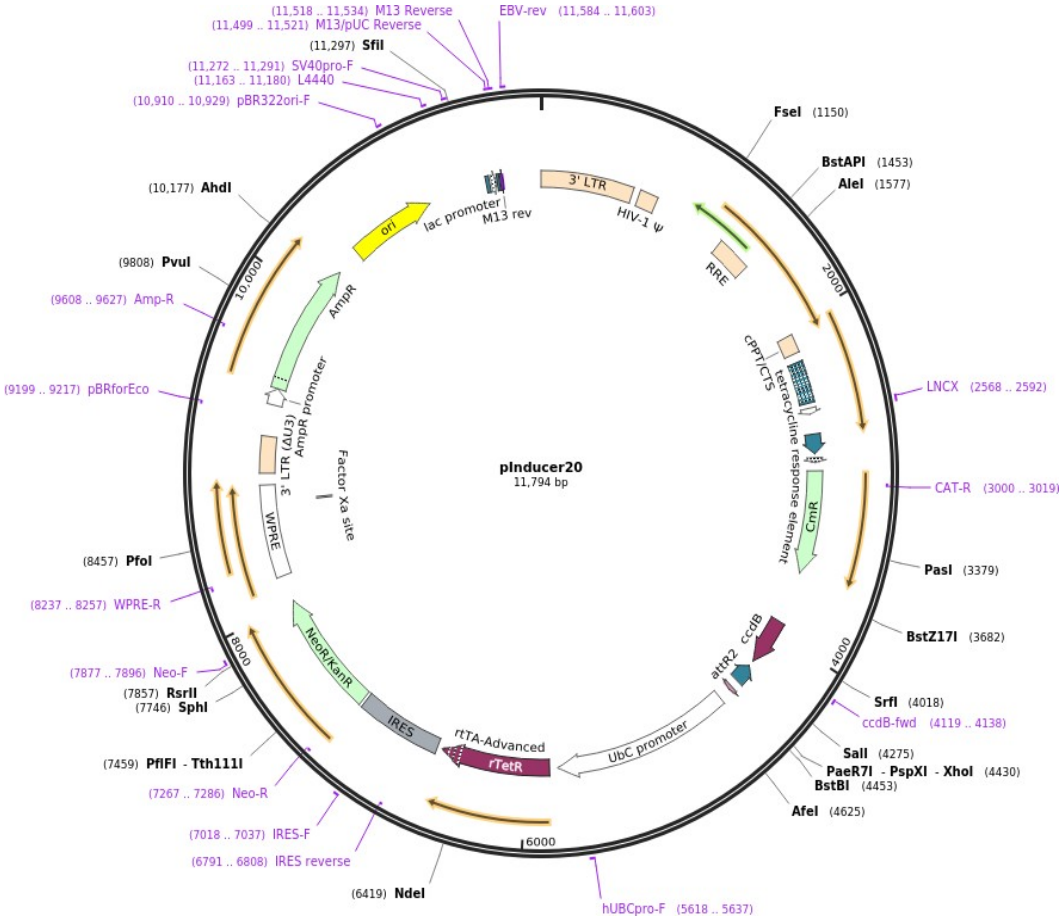

Figure 2.7. Full sequence map of pINDUCER20. Image generated by SnapGene software.

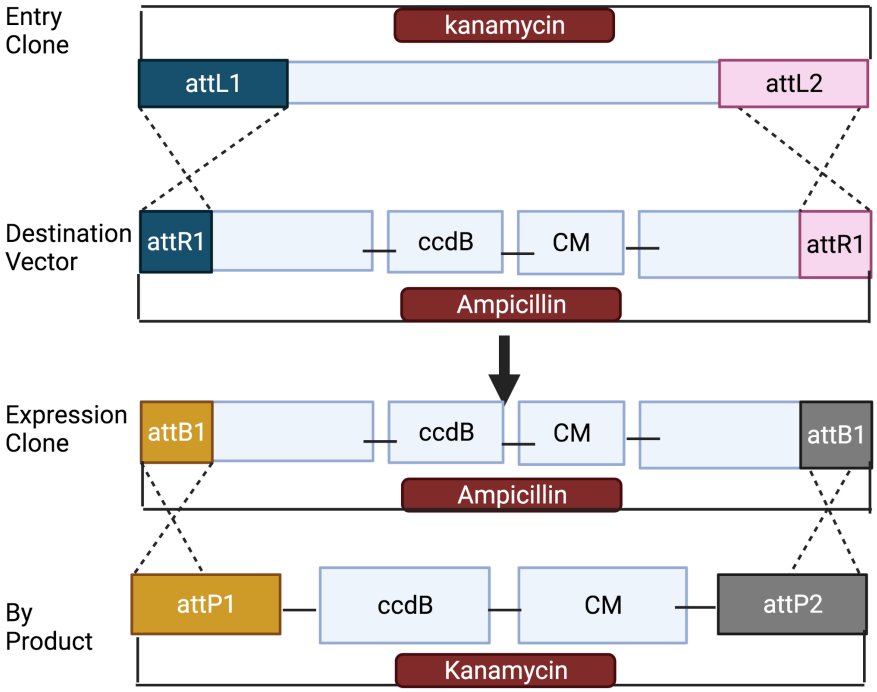

Figure 2.8. LR recombination reaction. The diagram depicts an LR recombination reaction between an entry clone and the destination vector to create an expression clone and a by-product. The gene of interest is transferred from the entry clone into the expression clone following recombination. Created with Bio-render (https://biorender.com/).

2.30 TRANSFORMING COMPETENT *E. COLI* AND SELECTING EXPRESSION CLONES

The LR recombination reaction mixture was transformed into One Shot Stbl3 Chemically Competent *E. coli* using the protocol described previously, and pUC19 was used as a positive control for transformation. The heat-shock step was performed at 42°C for 45 s.

2.31 COLONY PCR

To select the expression clones, a colony PCR was performed, as described previously. LNCX and PIND20 were used as forward and reverse primers respectively (Table 2.12). The annealing temperature in the thermocycling condition was 55°C.

Table 2.12

LNCX and PIND20 Primers

Primer	Sequence (5' - 3')
LNCX forward primer	AGCTCGTTTAGTGAACCGTCAGATC
PIND20 reverse primer	GGTTACTCCAGACTGCCTTGG

The colony carrying the *LCN-2* and *PGC1-a* gene was selected and inoculated into a 5 ml LB medium containing ampicillin 50 µg/ml. The bacterial culture was incubated at 37°C for ~ 8 h in a horizontal shaker at 225 rpm. 400 µl of bacterial culture was then mixed with 200 ml LB medium containing ampicillin 50 µg/ml and incubated at 37°C overnight on the horizontal shaker at 225 rpm. Bacterial glycerol stock was created and stored at -80°C. The expression clone was recovered from bacterial culture using NucleoBond Xtra Midi (740410.50; Macherey-Nagel GmbH & Co. KG, Düren, Germany) according to the manufacturer's instructions. The expression clone was quantified using a spectrophotometer (FLUOstar Omega microplate reader; BMG Labtech, Offenburg, Germany) and submitted for Sanger sequencing (Source Bioscience, Nottingham, UK) to verify the insertion sequence. Sequences were analysed using ApE (A plasmid Editor) Version 2.0 software (available at https://jorgensen.biology.utah.edu/wayned/ape/). After finishing construction of the human LCN-2 and PGC1-a expression plasmid vector (pINDUCER20-LCN-2) and (pINDUCER20-PGC1-a) – lentivirus containing pINDUCER20-LCN-2 and pINDUCER20-PGC1-a plasmid respectively – the lentiviruses were produced and prepared to be transduced into myotubes cells.

2.32 PRODUCTION OF LENTIVIRAL VECTOR

Lentivirus is a genus of retroviruses commonly used in research due to its ability to introduce gene products. Lentiviruses used in research are based on the human immunodeficiency virus (HIV) -1 and classified as Biosafety Level 2 (BSL-2) organisms. The components for viral production are separated into multiple plasmids to increase the safety of working with this virus. Moreover, many HIV proteins are deleted, which prevents the generation of replication-capable virus. All steps involved with lentivirus were performed in a biological safety cabinet class 2. Lentivirus particles were transported or stored out of the safety cabinet using double containment. All equipment was decontaminated with 10% Chemgene or 2% Distel for 24 h prior to disposal. HEK 293FT cells were used to generate the lentiviral vector because they are fast growing and highly transfectable. HEK 293FT cells were plated at a density of $2x10^6$ cells on a 10 cm culture dish containing 10 ml DMEM supplemented with 10% non-heat inactivated FBS and 0.292 g/L L-Glutamine (2 mM). The cells were incubated at 37°C in a 5% CO_2 humidified atmosphere overnight to reach confluency of approximately 80% before transfection. The next day, 2 µg of lentiviral transfer plasmid (expression clone [pINDUCER20-LCN-2] or [pINDUCER20-PGC1a] or pINDUCER20- green fluorescent protein [pINDUCER20-GFP] used as positive control and for optimisation), 2 µg of packaging plasmid (psPAX2 [12260; Addgene, Watertown, MA, USA]) and 2 µg of envelope plasmid (pMD2.G [12259; Addgene, Watertown, MA, USA]) were diluted in 600 µl of Opti-MEM™ I media (11058021; Thermo Fisher Scientific, Waltham, MA, USA). 18 µl of the X-tremeGENE HP DNA Transfection Reagent (06366236001; Roche, Penzberg, Germany) was added directly to the diluted plasmid (3:1 ratio of transfection reagent [µl] to plasmid [µg]). The transfection complex was

mixed gently by pipetting and then incubated at RT for 30 min. HEK 293FT cell media was gently removed and replaced with 7 ml Opti-MEM^{TM} I media. After 30 min of incubation, the transfection complex was added to the cells in a dropwise manner. The culture dish was swirled gently to distribute the transfection complex over the entire plate, before it was incubated at 37°C in a 5% CO_2 humidified atmosphere for 6 h. After this, Opti-MEM^{TM} I media was removed and replaced with 12 ml fresh complete EMEM medium. Transfected cells were then incubated at 37°C in a 5% CO_2 humidified atmosphere for 48 h. After incubation was complete, virus-containing supernatant was harvested using sterile syringes and filtered through a 0.45 µm syringe filter. The filtered lentiviral supernatant could be stored at 4°C for up to 14 days. The morphology of HEK293FT cells during the viral production process is demonstrated in Figure 2.9. The media containing the virus was collected using a snap-freeze with liquid nitrogen inside the safety cabinet and then aliquoted into screw cap tubes and stored at -80°C.

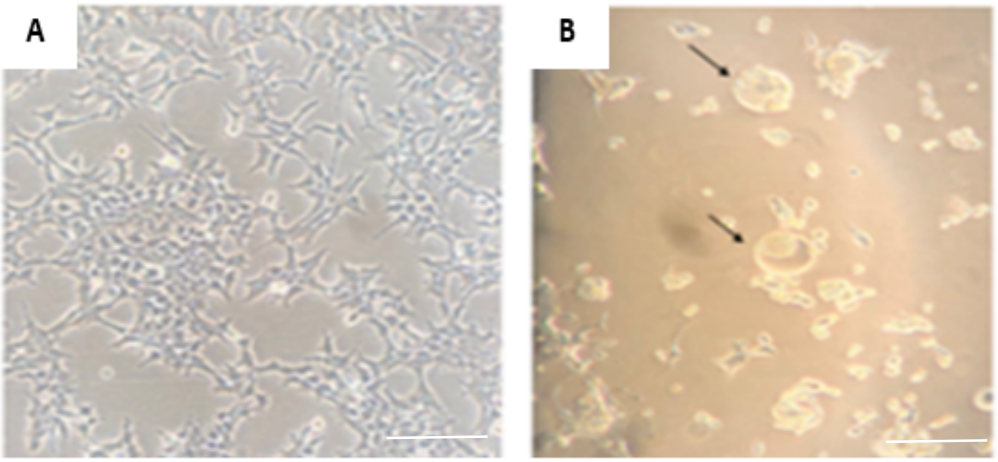

Figure 2.9. Morphology of HEK 293 FT cell line during the production of Lentivirus. HEK293FT cells were transfected with lentivirus plasmids at a 1:1 ratio. **A:** HEK293 FT cells prior to the transfection process. **B:** After 48 h of transfection, many cells had died, showing cytoplasmic inclusion bodies and cellular swelling (B, arrows) - cell Lysis/death post-48 h caused the release of lentiviruses into the HEK293FT cell media. The images were collected with an inverted light microscope. Scale bar is 100 µm.

2.33 LENTIVIRAL TRANSDUCTION

Human myotubes and C_2C_{12} myotube cells were plated at a density of $1x10^5$ cells/well in 6-well cell culture plates containing 2 ml medium in each well. The cells were incubated at 37°C in a 5% CO2 humidified atmosphere overnight to reach confluency of approximately 60%. The cell culture media was gently removed and replaced with 1 ml fresh media containing 10 µg/ml hexadimethine bromide (polybrene [9268; Sigma-Aldrich, St Louise, MO, USA). Hexadimethine bromide is a polycation which neutralises a charge repulsion between the virus and target cell surface and thus helps viral integration into the cell. Concentration was optimised in FRAME lab previously. Lentiviral aliquot was thawed on ice and then 600 µl (optimised) was added to the cells in a dropwise manner. Two wells were left without viral additions to serve as non-transduction controls. The cell culture plate was swirled gently to ensure even distribution of virus over the entire plate before incubation at 37°C in a 5% CO_2 humidified atmosphere for 4 h. The culture media was then changed to fresh medium and incubated for a further 48 h. Lentiviral transduction conditions varied greatly across cell types and needed to be optimised prior to the experiments to ensure the success of transduction.

2.34 RNA ISOLATION AND QUANTIFICATION

Total RNA was isolated from the cells using TRI Reagent® (T9424; Sigma-Aldrich, St Louise, MO, USA) (1 ml per 10 cm^2 of culture surface area). The cells were lysed using cold TRI Reagent®. The samples were then placed at RT for 5 min to permit complete dissociation of nucleoprotein complexes. 200 µl of 1-bromo-3-chloropropane (BCP) per 1 ml of TRI Reagent® lysate was added. Samples were vortexed for 10 s and placed at RT for 15 min. Centrifugation of the samples at 12,000 g for 15 min at 4°C was performed to separate the lysate into three phases.

The clear upper aqueous phase was transferred to a sterile nuclease-free micro-centrifuge tube and mixed with 500 µl of 2-propanol per 1 ml of TRI Reagent® lysate to precipitate the RNA. Samples were incubated at RT for 10 min and then at -20°C overnight. The samples were then centrifuged at 12,000 g for 10 min at 4°C, followed by 21,130 g for 10 min at 4°C. The supernatant was aspirated and discarded. The RNA pellets were washed twice in 0.5 ml of 70% ethanol per 1 ml of TRI Reagent® lysate and centrifuged at 21,130 g for 10 min at 4°C. This was followed by removal of the ethanol and brief air-drying of the RNA pellet for 5 min. It was important to ensure that the RNA pellet was not completely dry, otherwise its solubility would have decreased. Diethyl pyro-carbonate (DEPC)-treated high-performance liquid chomatography (HPLC) grade water, 87.5 µl, was added to the samples before heating at 65°C for 5 min. Deoxy-ribonuclease I (DNase I) 2.5 µl and RDD buffer 10 µl (79254; Qiagen, Hilden, Germany) were added to each sample for DNA digestion and RNA purification. Samples were kept at RT for 10 min. 300 µl of DEPC-treated HPLC-grade water and 400 µl of phenol/chloroform/iso-amyl alcohol were added and mixed with each sample. The samples were then separated into two phases by centrifugation at 10,000 g for 10 min at 4°C. The upper aqueous phase was transferred to a sterile nuclease-free micro-centrifuge tube. 40 µl of 3M sodium acetate (pH 5.2) and 800 µl of absolute alcohol were added and mixed with each sample to precipitate the pure RNA. The samples were then incubated at -20°C overnight. The RNA was pelleted by centrifugation at 21,130 g for 10 min at 4°C. The supernatant was removed, and the RNA pellets were washed twice in 0.5 ml of 70% ethanol per 1 ml of TRI Reagent® lysate and centrifuged at 21,130 g for 10 min at 4°C. The ethanol was removed, and the RNA pellets were briefly air-dried for 5 min. The RNA was dissolved in 50 µl of DEPC-treated HPLC-grade water. The

concentration and purity of the RNA were estimated by measuring the absorbance at 260 and 280 nm. The 260/280 ratio of 1.9-2.2 was indicative that the RNA was free from contamination.

2.35 CDNA SYNTHESIS VIA REVERSE TRANSCRIPTION

An Affinity-Script Multiple Temperature cDNA Synthesis Kit (200436; Agilent Technologies, Santa Clara, CA, USA) was used for the first-strand cDNA synthesis using 500 ng of total RNA. DEPC-treated HPLC-grade water was added to the calculated RNA volume for a total volume of 10.7 µl, followed by 3 µl (0.1 µg/µl) random primers. The samples were incubated at 65°C for 5 min and then cooled to RT for 10 min to allow the primers to anneal to the RNA. The following components were added: 2 µl of 10x Affinity-Script RT Buffer, 2 µl of 100 mM dithiotheitol (DTT), 0.5 µl of dNTP mix (25 mM each dNTP), 0.5 µl of RNase Block Ribonuclease Inhibitor (40 U/µl), and 1 µl of Affinity-Script Multiple Temperature RT. The samples were placed in a temperature-controlled thermal block at 25°C for 10 min to extend the primers. The temperature was then increased to 50°C for 60 min to synthesise cDNA. The reaction was terminated by incubating the sample at 70°C for 15 min. Samples were stored at -20°C for real-time qPCR. Non-template and non-enzyme controls were included in the experiment.

2.36 REAL-TIME QUANTITATIVE POLYMERASE CHAIN REACTION (REAL-TIME QPCR)

Real-time qPCR was performed to measure a cDNA target during each amplification cycle of the PCR. The gene expression was quantified using a relative standard curve method. Primers and probes sequences were designed using Primer Express® Software Version 3.0 (Applied Biosystems Inc., Foster City, CA USA) (see Tables 2.13 and 2.14). Primers and probes were purchased from Eurofins Scientific

(Luxembourg). Sterile DNase Rnase-free water was added according to manufacturer's instruction to reconstitute the primers and create 100 µM stock concentration. The stock was diluted 1:10 to a concentration of 10 µM before use.

Table 2.13

Primer and Probe Sequences for Real-Time qPCR (Human Gene)

Human Gene	Sequence (5'-3')
Cyclophilin A TaqMan	Forward: CAAATGCTGGACCCAACACA
	Reverse: TGCCATCCAACCACTCAGTCT
	Probe: TGGTTCCCAGTTTTTCATCTGCACTGC
RPLP0 (60s acidic ribosomal protein P0) TaqMan	Forward: TCGTGGAAGTGACATCGTCTTT
	Reverse: CTGTCTTCCCTGGGCATCA
	Probe: CGTGGCAATCCCTGACGCACC
PGC1-a (Peroxisome proliferator-activated receptor gamma coactivator 1-alpha) TaqMan	Forward:5′-CAAGCCAAACCAACAACTTTATCTCT-3′
	Reverse: 5′-CACACTTAAGGTGCGTTCAATAGTC-3′
	probe:5′-AGTCACCAAATGACCCCAAGGGTTCC-3′
IL-6 (Interleukin -6) TaqMan	Forward: 5′-TTACAGGGAGAGGGAGCGAT-3′
	Reverse: 5′-TCAGACATCTCCAGTCCTCTT-3′
	Probe: 5′-TGCAAGATGCCACAAGGTCCTCC-3′
IL-1b (Interleukin-1 beta) TaqMan	Forward 5'-CCCTAAACAGATGAAGTGCTCCTT-3'
	Reverse 5'-GGTGGTCGGAGATTCGTAGCT-3'
	Probe 5'-CTGGACCTCTGCCCTCTGGATGGC-3'
TNF-a (Tumor Nuclear factor a) TaqMan	Forward: CCCAGGGACCTCTCTCTAATCA
	Reverse: GGTTTGCTACAACATGGGCTACA
	Probe: CTCTGGCCCAGGCAGTCAGATCATCT
Lipocalin-2 (LCN-2) SYBR-GREEN	Forward: ACGGGAGAACCAAGGAGCTG
	Reverse: CACTGGTCGATTGGGACAGG

Table 2.14

Primer and Probe Sequences for Real-Time qPCR (Mouse Gene)

Human Gene	Sequence (5'-3')
Ms-Beta actin	Forward: GCTTCTTTGCAGCTCCTTCGT
	Reverse: GCGCAGCGATATCGTCATC
	Probe: CACCCGCCACCAGTTCGCCAT
Ms-PGC1-a	Forward: ACAATGAATGCAGCGGTCTTAG
	Reverse: CCATGAATTCTCGGTCTTAACAATG
	Probe: CAGAACCATGCAGCAAACCACACCC
Ms-LCN-2	Forward: GCCTCAAGGACGACAACATCA
	Reverse: GCATCCCAGTCAGCCACACT
	Probe: CTCTGTCCCCACCGACCAATGCATT
Ms-IL-6	Forward: CCACGGCCTTCCCTACTTC
	Reverse: TGCACAACTCTTTTCTCATTTCCA
	Probe: TCACAGAGGATACCACTCCCAACAGACCTG

An undiluted standard sample was produced by pooling an equal amount of each sample together. For a standard curve, two-fold serial dilutions of the neat standard sample were performed at specific dilution ranges: 1:2, 1:4, 1:8, 1:16 and 1:32. Each sample was diluted with DEPC-treated HPLC-grade water to 1:8. The reaction mixture for each sample was prepared, as shown in Table 2.15. 10 µl of the reaction mixture was transferred into each well of a 96-well PCR plate, and 3 µl of the diluted neat standard sample or first-strand cDNA sample were added and gently mixed without creating bubbles. The plate was sealed with transparent film and centrifuged for 30 s before being placed into the real-time qPCR machine (G8830A [AriaMx Real-Time PCR instrument]; Agilent Technologies, Santa Clara, CA, USA]). The real-time qPCR cycling programme was set up as recommended by the qPCR master mix manufacturer (see Table 2.16). Each sample was examined in triplicate including non- template and non-enzyme control samples. A standard curve

was included in each plate cycle. The target gene expressions were normalised to the reference gene expression. Cyclophillin A and *β-actin* were used as reference genes for human and mouse genes respectively.

Table 2.15

Reaction Mixture for Real-Time qPCR- Taqman Assay

Component	Volume (µl)
Precision® FAST qPCR Master Mix (Z-PFAST-LR; Primerdesign, Camberley, UK)	6.5
10 µM forward primer	0.4
10 µM reverse primer	0.4
10 µM probe	0.25
DEPC-treated HPLC-grade water	2.45

Table 2.16

Thermocycling Conditions for Real-Time qPCR

Step	Temperature	Time	Cycle(s)
Enzyme Activation - Hot Start	95 °C	2 min	1
Denaturation	95 °C	5 sec	40
Data collection	60 °C	20 sec	

2.37 PROTEIN ISOLATION

After careful removal of cell culture media, cells were gently washed with ice-cold 1x PBS three times. Approximately 120-150 µl/10 cm^2 culture surface area of cold radioimmunoprecipitation assay (RIPA) buffer was added to the cells. Culture plates were stored on ice for 30 min, and then cell lysate was gathered to one side by scraping the cells with a scraper. The lysate was transferred to a clean microcentrifuge tube and sonicated on ice using the following setting: amplitude 3%, process time 30 s, pulse on 10 s, pulse off 15 s. The sonicated sample was incubated

in a cold room at 4 °C on an end-over-end rotator for 45 min. Centrifugation at 21,130 g for 15 min at 4°C was performed to pellet the debris. The supernatant was collected and stored at -20°C for further analysis.

2.38 DETERMINATION OF PROTEIN CONCENTRATION

Protein was quantified using a Pierce™ BCA Protein Assay Kit (23227; Thermo Fisher Scientific, Waltham, MA, USA) according to the manufacturer's instructions. The standard curve was prepared using serial dilutions of the albumin standard (bovine serum albumin [BSA]) in a concentration range of 2,000 µg/ml to 25 µg/ml as a dilution scheme for standard test tube protocol and microplate procedure. Samples were diluted in HPLC water at 1:10. Bicinchoninic acid (BCA) working reagent was prepared by mixing 50 parts BCA Reagent A with one part BCA Reagent B (50:1, Reagent A:B). 10 µl of each standard or diluted sample was pipetted into each well of a 96-well plate in triplicate. 200 µl of BCA working reagent was added to each well. The plate was placed on a plate shaker for 30 s for mixing and incubated at 37°C for 30 min. The plate was then cooled at RT for 10 min before measuring the absorbance at 562 nm using a spectrophotometer (FLUOstar Omega microplate reader;BMG Labtech, Offenburg, Germany).

2.39 WESTERN BLOTTING

Western blotting is an analytical technique to identify target proteins in a complex sample. A target protein can be identified using antibody-based probes after electrophoretic separation of the protein in the sample. The protein sample was mixed with Laemmli buffer and heated at 95°C for 5 min for denaturation. The denatured protein samples were separated on either 10% or 12% poly-acrylamide gel depending on the MW of protein submerged in running buffer. The gel was run at 100 V though a stacking gel for approximately 15 min, followed by 200 V though a resolving gel for

approximately 45 min. The gel was removed from the electrophoresis tank and the stacking gel was cut off. A cassette sandwich was used for transferring the protein on to the nitrocellulose membrane by placing the membrane next to the gel and sandwiching it between the sponges and filter papers. The cassette was placed in a transfer tank filled with transfer buffer and an ice pack. The transfer cassette was run at 200 milliampere (mA) for 90 min for one gel or 300 mA for 120 min for two gels. After completing the protein transfer, the membrane was stained with diluted Ponceau S solution (P7170; Sigma-Aldrich, St Louise, MO, USA) to demonstrate the protein bands on the membrane and successful transfer of proteins. The membrane was destained by rinsing with deionised water and washing in Tris-buffered saline and 0.1% Tween 20 (TBST) on an orbital shaker. The membrane was blocked to prevent non-specific background binding of primary and secondary antibodies by incubating with blocking buffer (5% skimmed milk in TBST or 5% BSA in TBST) on an orbital shaker for 60 min at RT. The primary antibody was prepared in a 50 ml Falcon tube by dilution with blocking buffer according to the antibody datasheet (see Table 2.17). The membrane was incubated with the primary antibody in a Falcon tube overnight on a roller in a cold room. The next day, the blot was washed three times with TBST for 10 min each and incubated with IRDye secondary antibodies (LI-COR) (1:5000) for 60 min on a roller. The membrane was washed with TBST three times for 5 min per wash on an orbital shaker. The target protein was visualised using an Odyssey® Infrared Image system (LICOR Biosystems, USA) at 700 nm or 800 nm.

Table 2.17

Primary Antibodies Used for Western Blotting

Primary antibodies	Dilution (Concentration)	Product code; Supplier
Rabbit anti-human Desmin antibody	1:600	ab15200; abcam
Rabbit anti-actin	1:1000 (unless otherwise specified)	A2066, Sigma-Aldrich
Rabbit anti-human LCN-2 antibody		ab206427, abcam
Rabbit Anti-PGC1 alpha + beta antibody		ab188102, abcam
Rabbit Anti-AMPK-alpha antibody		#2603S Cell Signaling
Rabbit Anti-Phospho-AMPK (Th172)-(40H9) antibody		#2535, cell signalling
Rabbit Anti-Akt antibody		#9272, Cell Signalling
Mouse Anti-Phospho-Akt (Ser473) antibody		#4051, cell signalling
Rabbit Anti-HSL antibody		#4107, cell signaling
Rabbit Anti-Phospho HSL (Ser 563) antibody		#4139, cell signalling
Rabbit ant ATGL antibody		#2139, cell signalling
Mouse anti-beta actin antibody		A5441, Sigma-Aldrich

2.40 QUANTIFICATION OF WESTERN BLOT BANDS USING IMAGE J

Image J software was used to quantify the intensities of proteins bands. A protocol that allows calculation of the relative amounts of each protein as a ratio to the loading control's bands was explained by Hossein Davarinejad (see http://www.yorku.ca/yisheng/Internal/Protocols/ImageJ.pdf). The data was represented as a graph using GraphPad prism to compare results to control samples. The proteins were detected using a near infra-red Licor system. This scanner was used to scan blots using the same exposure time and intensity. High resolution images were exported as TIFF file formats.

2.41 CONDITIONED MEDIUM (CM) PREPARATION

Cell media (CM) were collected from cultured cells containing secreted protein. These cells comprised growth factors, cytokines and hormones. CM was prepared following the three experiments. In the first preparation, for overexpression of LCN-2 and PGC1-a by an inducible vector system or EPS stimulation in human myotubes or C_2C_{12} experiments, cells were plated in 6-well culture plates at a density of $1x10^5$ cells/dish in 2 ml medium (reduced serum). On day five, myotubes were infected (transduced) with 600 ul lentivirus – either the (pINDUCER20-LCN-2) or the (pINDUCER20-PGC1-a) – and incubated in a humidified atmosphere containing 5% CO_2 at 37°C for 4 h with 10ug/ml polybrene. Doxycycline 1000 ng/ml was then applied to obtain inducible overexpression and left for a further 48 h before cell culture media collection. Cells without doxycycline were prepared for CM comparison. The cells were then further incubated for 48 h. CM was filtered though a 0.22 μm syringe filter and stored at -20°C until used for western blot analysis.

The second preparation was used for studying the crosstalk between muscle and adipose tissue by the inducible vector system. For this, human myotube cells were plated in three units of 60 mm cell culture dishes at a density of $2x10^5$ cells/dish in 5 ml medium. On day five, myotubes were infected (transduced) with 600 ul lentivirus of (pINDUCER20-LCN-2) and incubated in a humidified atmosphere containing 5% CO_2 at 37°C for 4 h with 10 ug/ml polybrene. Doxycycline 1000 ng/ml was applied to obtain inducible overexpression and left for a further 48 h before cell culture media collection. Cell culture dishes without doxycycline were prepared for CM comparison. The cells were then further incubated for 48 h. 15 ml of CM was filtered though a 0.45 µm syringe filter, collected in a 50 ml falcon tube and stored at -80 °C until used for the treatment on adipose tissue.

2.42 CONCENTRATION OF PROTEIN IN CELL CULTURE MEDIA

LCN-2 and PGC1-a protein was concentrated in cell culture media for western blot analysis. Cell culture media was collected into a clean 15 ml conical tube and centrifuged at 10,000 rpm for 5 min to remove cell debris. The supernatant was then transferred to a clean tube. 2 ml of the supernatant was filled into a Vivaspin® 2, 10,000 molecular weight cutoff (MWCO), polyethersulfone (PES) membrane (VS0201; Sartorius, Göttingen, Germany) and centrifuged in a swing bucket at 3,901 g at 20°C for approximately 10 min each time until the concentrated sample was less than 500 µl. Finally, 60 ul of concentrated CM was loaded on SDS-PAGE for western blot analysis.

2.43 ENZYME-LINKED IMMUNOSORBENT (ELISA)

Human Lipocalin-2 (LCN-2) protein levels in culture media (CM) were quantified using a Quantikine ELISA kit (cat. no. DLCN-20, R&D Systems, USA) and assayed according to the manufacturer's instructions. The ELISA plate was read

using a FLUOstar Omega multi-mode microplate reader (BMG LABTECH, Germany) set to 450 nm and using wavelength correction set at 570 nm. Quantification and analysis of Lipocalin-2 in the samples was carried out using MARS Data Analysis Software (BMG LABTECH, Germany). Data was presented using GraphPad prism.

2.44 DESMIN STAINING OF MYOTUBE CELLS (ICC)

Myotubes cells were grown on a coated 6-well plate culture with (0.2% (w/v) gelatine). On day seven, cells were fixed with 4% paraformaldehyde in PBS, pH 7.4 for 15 min at room temperature. The cells were then washed twice with ice cold PBS. Cells were permeabilised via incubation of the samples in PBS containing 0.3% Triton-100 (Tx-100) in PBS, and cells were then washed in PBS three times for 5 min. To block unspecific binding of the antibodies, cells were incubated for 2 h at room temperature on a plate shaker in Blocking Buffer (5% Bovine Serum Albumin (BSA) + 0.1% Tx-100). Primary (1°) Antibody (Ab) was incubated with cells overnight at 4°C in a cold room on a plate shaker. Secondary (2°) antibodies were added after 1 h at room temperature on a plate shaker in the dark. The cells were then washed three times with PBS for 5 min each in the dark. Before mounting the cover slip on a slide, the nuclei were stained with DAPI (1µg/mL) for 1 min using a 200 M wide-field fluorescent microscope (Carl Zeiss, Germany). Phase contrast images were taken from the same fields and adjusted to obtain fluorescence images at 10x magnification). Primary and secondary antibodies used in this study are shown in the table below.

Table 2.18

Primary and Secondary Antibodies Used in Immunocytochemistry Experiments

Primary antibody	Dilution (Concentration)	Secondary antibody	Dilution (Concentration)
Anti-Desmin Antibody - Cytoskeleton Marker (ab15200)	1:1000 in primary dilution buffer (1% BSA + 0.1% Tx-100 in PBS) (Unless otherwise specified)	Donkey Anti-Rabbit IgG H&L (Alexa Fluor® 647) (ab150075)	1:000 in dilution buffer (1% BSA + 0.1% Tx-100 in PBS) (Unless otherwise specified)

2.45 NILE-RED FLUORESCENT DYE STAINING OF NEUTRAL LIPIDS

Two approaches were used to assess the accumulation of neutral lipid inside adipocytes using Nile Red fluorescent dye. Adipocytes were washed twice with 1x phosphate-buffered saline (PBS) containing Ca2+ and Mg2+ and then fixed with 4% Paraformaldehyde (PFA) for 20 min and subsequently washed twice with PBS. Stock (15.8mg in 50ml DMSO) of Nile red (Sigma N-3013) was diluted in HBSS to 30 uM before use. Cells were stained and incubated at room temperature on a rocking incubator for 15 min and covered with aluminium foil to protect cells from the light.

In the first approach, stained cells were quantified by measuring absorbance at 480 nm excitation and 520 nm emission to measure the accumulation of neutral lipid using a BMG LABTECH's FLUOstar Omega plate reader. For the second approach, adipocytes cells were stained with Nile Red and images quantified using a 200 M wide-field fluorescent microscope (Carl Zeiss, Germany). Before fluorescence imaging, the nuclei were stained with DAPI (1µg/mL) for 1 min. The phase contrast images were taken from the same fields and adjusted to obtain fluorescence images at 10x magnification (480 nm excitation and 520 nm emission) (see Figure 2.2).

2.46 QUANTIFICATION OF STAINED NEUTRAL LIPID DROPLETS USING IMAGE J

Five field images per well were randomly acquired, and the whole area intensity of all stained cells in the field (green channel-480 nm excitation and 520 nm emission) was automatically quantified under similar conditions via Image J analyse/measure functions. Average readings were calculated and presented using Graph Pad PRISM 7.

2.47 TREATMENT OF 3T3-L1 ADIPOCYTES WITH HUMAN MYOTUBE CM THAT OVEREXPRESSES LCN-2 (MYO.LCN-2+DOX)

3T3-L1 fibroblasts were differentiated over the course of seven days (as explained in section 2.4). A mixture of 1:1 adipocyte differentiation medium and human myotube CM was added for 6 h, 24 h and 48 h. Adipocytes treated with myotube CM that overexpresses LCN-2 using an inducible vector were defined as Myotubes CM (LCN-2+DOX.). These and the control samples for this treatment were as follows:

- Adipocyte cells treated with myotube CM that overexpresses LCN-2 but with no induction of Doxycycline (DOX.) were defined as Myotubes CM (LCN-2-DOX.)
- Adipocyte cells treated with myotube CM only were defined as a control and defined as (Myotubes CM)
- Adipocyte cells treated with adipocyte CM only were set as another control and defined as (No treatment).
- Post-6 h, 24 h and 48 h treatment, all myotube CM cells were lysed and CM were collected for further analysis.

2.48 BASAL AND STIMULATED LIPOLYSIS MODEL IN CULTURED ADIPOCYTES

Differentiated adipocytes (3T3-L1) in growth media #1 (see Table 2.4) were incubated with isoproterenol in the presence or absence of triacsin C (5 μM) for 1 min at 37°C in a 10% CO_2 atmosphere (stimulated lipolysis) with Triacsin-C being used as an inhibitory component for acyl-CoA synthetases. Unstimulated cells were left as a control for lipolysis (basal). Media were replaced by identical fresh media containing 2% FA-free BSA and incubated for 1 h. Following this, media were collected, and cells were washed and collected in RIPA buffer. The protein content of the cell lysate was determined using a BCA protein assay kit. Free glycerol content of the cell culture media was measured using free glycerol reagent and the appropriate standard solutions (Sigma).

2.49 LIPOLYSIS ASSAY

Post-differentiation, 6 h, 24 h and 48 h following the last treatment, glycerol released in the cell culture media was measured via colourimetry using the free glycerol reagent (Sigma) according to the manufacturer's instructions. Calculation of the lipolysis of adipocytes was presented as nmol glycerol per mg cell protein and hour.

2.50 STATISTICAL ANALYSES

All data reported in the present thesis represent means ± SEM. Statistical analyses were performed with the Graph Pad Prism version 7 for Windows, GraphPad Software (San Diego, CA, USA). An unpaired t-test was used to compare the data between two groups, and one-way analysis of variance (ANOVA) was used to compare three or more groups to allow post-hoc comparisons. A probability value (p value) of less than 0.05 ($p < 0.05$) was considered statistically significant.

Chapter 3: Development of an In Vitro Exercise Model Using EPS

3.1 INTRODUCTION

Generally, muscle contraction – either voluntary or involuntary – is beneficial for health and wellbeing. To simulate this, electrical pulse stimulation (EPS) is often used as an *in vitro* model of exercise. The EPS model was first used in the 1970s by Shainberg and Burstein (1976) to study the regulation of acetylcholine (Ach) receptor during muscle contraction. To date, numerous studies have been conducted involving the use of the EPS model on cultured skeletal muscle cells generated from rat, mouse, and primary human skeletal muscle, mostly used on murine C_2C_{12}.

EPS can be used in an *in vitro* model to mimic exercise by inducing contraction in skeletal muscle cells (myotubes) and thus allow evaluation of exercise-like effects (Bakke *et al.*, 2012). In Bakke *et al.*'s (2012) study, EPS was applied to myotubes for 24 h and demonstrated exercise-like effects, including the activation of the two common signalling pathways in response to exercise – AMPK and MAPK. In another study, the levels of insulin sensitivity and glucose uptake were evaluated post EPS, focusing on their level of increase (Fujita *et al.*, 2008), confirming the use of electrical stimulation (EPS) as a model to mimic exercise *in vitro* by understanding physical exercise and its beneficial effects on our health. Table 3.1 provides an overview of most recent studies of this nature, including details regarding their EPS parameters, the upregulation of genes, and the signalling pathways activated post-exercise.

Table 3.1

Summary of Recent EPS Application and its Effects (Compiled by the Author)

Cell type	Duration	parameters	Sample size	Effect of EPS			Outcome	Reference
				Expression	Signalling	Metabolic Effect		
Murine C2C12 myotubes	3 h	35 V, 15–20 mA at 1 Hz for 25 ms at 975 ms intervals	n= 3-6	IL-6 and IL-15 secretion ↔ 1:1 mixture of 3T3-L1 differentiation medium and muscle conditioned medium EPS-CM (on day 10,)– adiponectin protein expression and its release is increased ↑ mRNA of PPARγ2, FAS, LPL, and aP2 ↑ UCP-1 and TNF-a (non significant increased) mRNA HSL and ATGL. Lipolysis induced ↑	phosphorylation of AMPK (Thr172) ↑	-Lactate dehydrogenase ↔ -Lactic acid concentration ↑ -glucose concentration ↓	EPS-CM promoted adipogenesis, EPS-CM enhanced adiponectin secretion Stimulated lipolysis and lipid droplet formation in mature adipocytes in vitro model for investigating the physiological functions of myokines, directly acting on distant organs	(Tamura et al., 2020)
Human myotubes	8 h	2 ms pulses at 12 V, with a frequency of 1 Hz.	human muscle biopsies (*n* = 5)	mRNA MSTN ↓ IL-6 secretion-(EPS+4 h) ↑	phosphorylated mTOR. P = 0.03 (EPS+0 h). 4E-BP1. (P=0.01), (EPS+0 h). pAMPK ↑	lactate dehydrogenase ↔	-EPS-based cell culture model induces hypertrophy (*) -a resting period of 8 h after EPS is a crucial of *	(Tarum et al., 2017) **Cited by 5 articles**
Human myotubes either obliquus internus abdominis or vastus Lateralis	24 h 1-6 h	(1 Hz, 2 ms, 11.5 V) after 5 days of Differentiation. (1 Hz, 2 ms, 11.5 V) after 6 days of Differentiation.	Male donors age from (33-62) n=3	mRNA MSTN, ↓ mRNA L6 , IL1B, CXCL1, CXCL2, CXCL3, CXCL8, CCL2, and CCL8, post 2hr ↑ mRNA CSF1- post 2hr ↑	Were Not studied	Were Not studied	Used Simple EPS protocol. Identified CSF1 as a novel myokine, which was increased after acute and long-term exercise in vivo and secreted in vitro in both	(Pourteymour et al., 2017) **Cited by 24 articles**
Cell type	**Duration**	**parameters**	**Sample size**	**Effect of EPS**			**Outcome**	**Reference**
				Expression	**Signalling**	**Metabolic effect**		
Hybrid myotubes comprised of human myotubes and murine C2C12 myotubes	16 hr	1 Hz, 4-ms, 20 V	n=3	mRNA of IL-6/ CXCL1, post 3hr. ↑ Secretion of IL-6, IL-8, IL-10, IL16,CXCL1, CXCL2, CXCL5,CXCL6,CXCL10, CCL1, CCL2, CCL7, CCL8, CCL11, CCL13,CCL16, CCL17, CCL19, CCL20, CCL21, CCL22, CCL25, CCL27), and IFN-γ ↑	Were Not studied	GLUT-4 Translocation ↑	Alternative tool for analysing contractility using hybrid myotubes	(Chen et al., 2019) **Cited by 4 articles**
human myotubes	3hr 24hr	Acute intense exercise model (24-ms pulses at 10 V, with a frequency of 0.5 Hz) Chronic moderate exercise (2-ms pulses at 10 V, with a frequency of 0.1 Hz)	n=8	**EPS 3hr**; mRNA of IL-6, IL-15, and FGF21 ↑ -Lactic acid concentration ↑ -glucose concentration ↔ glycogen depletion ↔ glucose oxidation rate ↔ **EPS 24hr** glycogen content ↑ glucose and lipid oxidation rate ↑ IL-6 mRNA level (~3-fold, $P < 0.01$), slightly induced MSTN ↑ FNDC5 and BDNF mRNA ↓ CM from EPS3h, basal Lipolysis-(~1.3-fold, $P < 0.001$ ↑ CM from EPS24h, basal lipolysis (~3-fold, $P < 0.001$) as well as NEFA release (1.7-fold, $P < 0.05$) ↑	CaMKII, pAMPK ↑	Not studied	exercise-mediated skeletal muscle contraction produces secreted factors able to activate lipolysis in adipocytes in vitro.	(Laurens et al., 2020) **Cited by 10 articles**

Cell type	Duration	parameters	Sample size	Effect of EPS			aim	Outcome	Reference
				Expression	Signalling	Metabolic effect			
Human myotubes	48 h	2 ms, 30 V and 1 Hz-	n= 4–5	mRNA expression of NKAα1–3 and NKAβ1 ↔ NKAβ2 and NKAβ3, (P = 0.07) ↑ mRNA expression of SERCA1 ↑ mRNA expression SERCA2 ↔ The abundance of FXYD5 ↑ The abundance of FXYD1 ↓	Were not studies		Test whether electrically-stimulated contractions modulate expression of NKA subunits and FXYDs.		(Jan et al., 2021)

There are several approaches and parameters used for development of the EPS protocol, including frequency, the pulse being trains or single, and duration of EPS. The classification of EPS is defined as acute or chonic; however, its definitions vary among research papers. For instance, there is no common agreement of the exact definitions of exercise, such as resistance exercise vs. endurance exercise or acute exercise vs. regular exercise. As a result, conducting further research in determining the effects of the EPS protocol to various forms of exercise is needed. Moreover, well-known biomarkers or factors of exercise would aid in the development of suitable EPS methods *in vitro*. PGC-1a and IL-6 are obvious biomarkers or factors since they are well-known to be stimulated by exercise. However, the expression levels of these two proteins in human skeletal muscle cells may vary significantly between donors.

IL-6 is expressed and secreted by skeletal muscle cells, and therefore it is a "myokine" (Kanzleiter *et al.*, 2014). The term of myokine is defined as cytokines or other peptides that are produced, expressed, and released by myotubes and exert effect on other tissues in a paracrine, an autocrine or an endocrine fashion. Despite various attempts over the last decade to describe and characterise skeletal muscle myokines, our understanding of myokines and their synthesis and release – either during or after muscle contraction – remains limited. One of the most difficult tasks

has been to show that skeletal muscle cells are the source of particular myokines (Nikolić *et al.*, 2012). The EPS method, when combined with the analysis of the transcriptome or secrotome, could offer a unique platform for identifying new contraction-regulated myokines. However, these methods do pose limitations regarding the detection of myokines: myokines are measured in pg/ml, amounts that are difficult to detect in plasma or cell culture media (Nikolić *et al.*, 2012; 2016).

Recently, the focus in the field has been to examine proteins or factors that are released by skeletal muscle post EPS, allowing the study of crosstalk effects on nearby tissues by generating a cell media (CM) of the muscle (Evers-van Gogh *et al.*, 2015; Miyatake *et al.*, 2016), primary human myotubes (Chistensen *et al.*, 2015) or C_2C_{12} (Tamura *et al.*, 2020). Results are varied, potentially caused by the differences in EPS protocols that were used.

3.2 AIMS OF THIS CHAPTER

In general, we aimed to develop an *in vitro* model of exercise (acute short-term exercise) of both cultured C_2C_{12} and human skeletal muscle cells (myotubes) suitable for investigating an exercise-induced myokine. We examined several factors and biomarkers that are well-known to be activated or regulated by exercise. To validate the results, measurements were taken – as detailed below – following the EPS protocol described in Chapter 2. First, we examined biochemical changes following 16 h of muscle contraction, such as lactic acid accumulation (Lactate) and level of glucose in cell culture media (CM), in the stimulated and unstimulated C_2C_{12} and human myotubes. We then compared the mRNA of mitochondrial biogenesis marker, PGC1-αlpha, in both stimulated and unstimulated C_2C_{12} and human myotubes. PGC1-αlpha is the peroxisome proliferator-activated receptor γ (PPARγ) co-activator 1α which has been known to be a central regulator of physical exercise adaptation in skeletal muscle. PGC-1α upregulates some genes that are involved in the mitochondrial biogenesis and the contractile apparatus to enable a higher endurance capacity by activating some of the transcription factors. This process is still poorly understood (Furrer *et al.*, 2016). Another parameter we tested was the activation of AMPK; therefore, we examined the phosphorylation level of $pAMPK^{T172}$ following EPS contractile stimulation. Lastly, we studied the level of mRNA expression of the well-known myokine, IL-6, in stimulated and unstimulated C_2C_{12} and human myotubes following the EPS protocol.

3.3 RESULTS

3.3.1 Myotubes Culture and Their Donors

Myotubes cultures were established from a total of n = 2 individual, male healthy adults for all experiments in this chapter. Descriptive donor data is presented in Table 3.2. The experiments performed in independent donor repeats was determined principally by the number of myoblasts were passaged, since cultures were restricted to no more than three passages to best preserve any effects of donor phenotype (an independent experiments n=3 based on a single biopsy derived from a healthy male human donor passaged three times). Within an independent experiment, multiple treatment replicates were performed (e.g., the use of 3 treatment replicates meant 3 wells of cells from each independent experiment were exposed to each treatment condition). All reported n values are the number of independent experiments n=3.

Table 3.2

Characteristic Data for Skeletal Muscle Biopsy Donor from Whom Myotube Cultures Were Derived

Sex	Age (y)	Mass (Kg)	Height (m)	BMI	Fasting Glucose (mmol/L)	Biopsy yield (mg)
Male	**22**	81.2	1.75	26.514	3.73	~150mg
Male	**23**	75.5	1.785	23.7	4.35	~150mg

3.3.2 Cell Morphology of Differentiated C_2C_{12} and Human Myotubes Pre- and Post-Electrical Pulse Stimulation (EPS) *In Vitro*

The morphology of human and mouse C_2C_{12} myotubes cells was demonstrated using microscopic images shown in Figures 3.1 and 3.2. Electrical pulse stimulation, as an *in vitro* exercise model, did not affect the morphology of the cells: myotube cells had long, consistent-diameter, parallel myotubes, and good shape and arrangement.

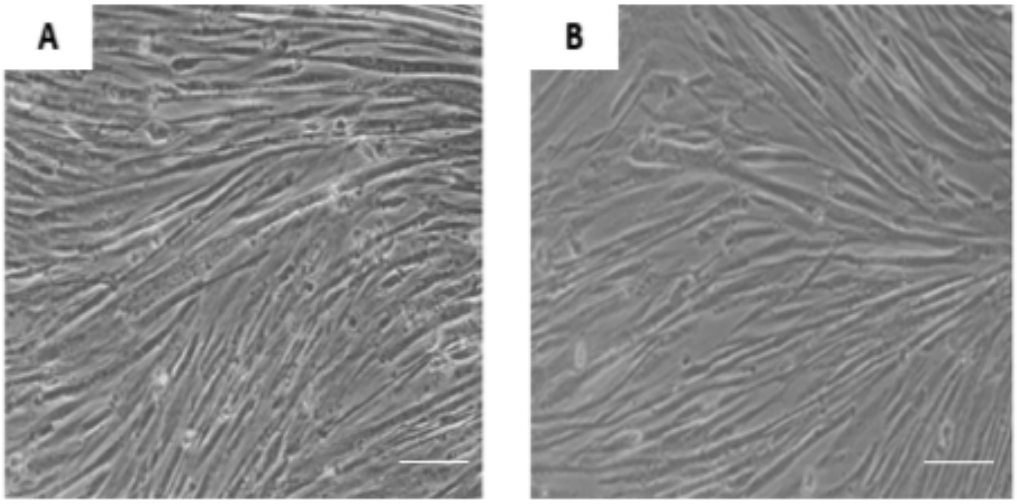

Figure 3.1. Morphology of differentiated C_2C_{12} myotubes pre- and post-EPS *in vitro*. C_2C_{12} cells were cultured in complete DMEM (high glucose, 4500 mg/L) and 4% horse serum. **A**. Pre EPS. **B**. Post EPS. The images were acquired using an inverted light microscope. Scale bar is 50 **µ**m at 20x magnification.

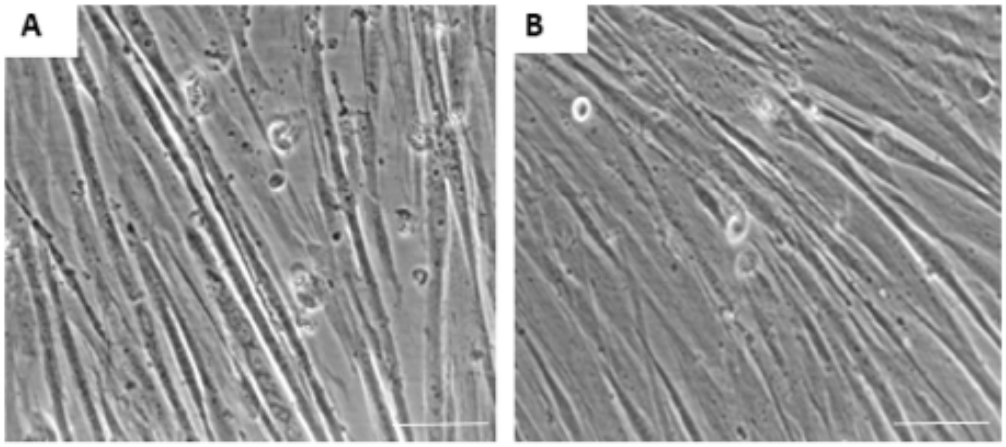

Figure 3.2. Morphology of differentiated human myotubes pre- and post-EPS *in vitro*. Human cells were cultured in Ham's F-10 growth media with 6% horse serum. **A**. Pre EPS. **B**. Post EPS. The images were acquired using an inverted light microscope. Scale bar is 50 **µ**m at 20x magnification.

3.3.3 Immunocytochemistry Staining of Desmin Expression in C_2C_{12} and Human Myotubes

Immunocytochemistry experiments were used to determine the differentiation progress of $C_2C_{12}$and human myotubes. Desmin was used as a valid marker for mature myotubes that is known to be highly expressed in mature myotubes compared to myoblasts (pre-differentiated cells) (Lacham-Kaplan, Camera & Hawley, 2020). C_2C_{12} and human myotubes were treated overnight with rabbit anti-Desmin antibody at concentrations of 1:600. Desmin stained the positive myotubes (as shown in Figures 3.3 and 3.4) on day seven of the differentiation progress, confirming the success of myotube development.

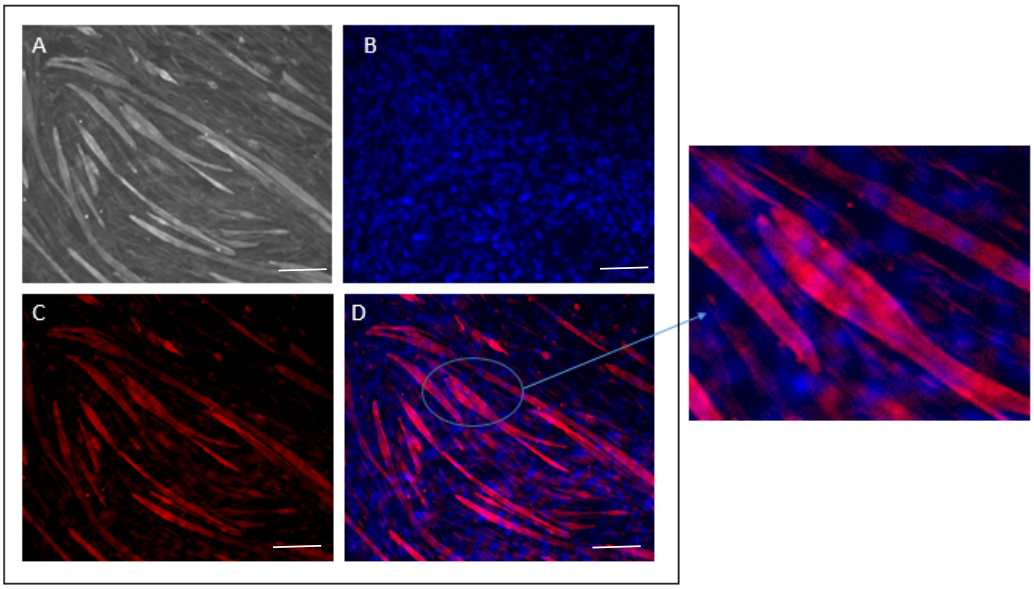

Figure 3.3. Immunocytochemistry staining of Desmin expression in C2C12 myotubes. A. Bright field (grey). B. DAPI staining (blue). C. Desmin-stained positive myotubes (red). D. Merged channel. Images were acquired at 10x magnification using a wide-field system fluorescence microscope-Zeiss 200M. Scale bar is 100 μm.

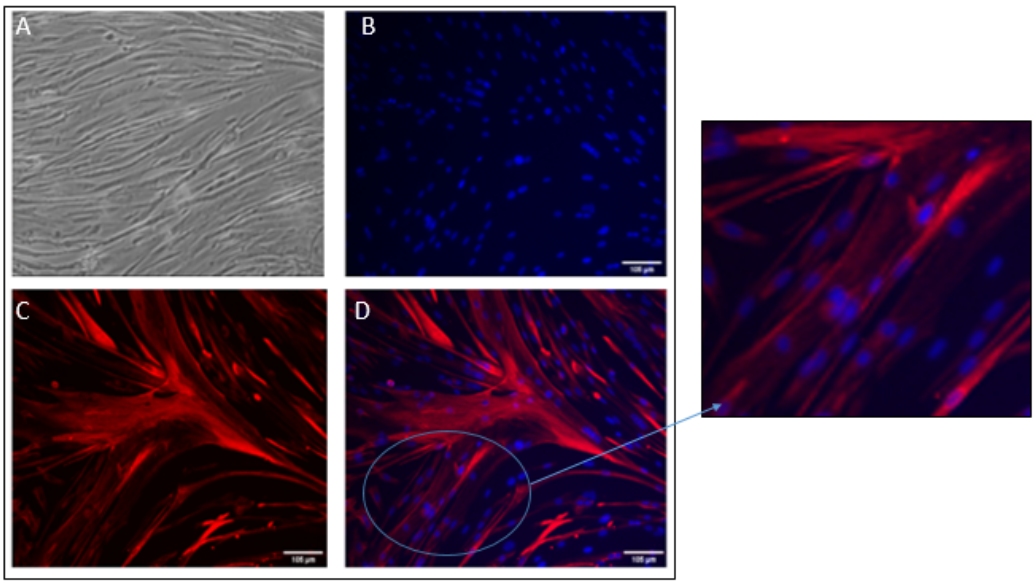

Figure 3.4. Immunocytochemistry staining of Desmin expression in human myotubes. A. Bright field (grey). B. DAPI staining (blue). C. Desmin-stained positive myotubes (red). D. Merged channel. Images were acquired at 10x magnification using a wide-field system fluorescence microscope-Zeiss 200M. Scale bar is 100 μm.

3.3.4 Glucose Concentration in Cell Media (CM) of C_2C_{12} Mouse and Human Myotubes Post-16 h EPS

Glucose concentrations were measured in the cell media of both C_2C_{12} and human myotubes. Glucose concentration in the cell media of C_2C_{12} decreased significantly post-16 h EPS in stimulated myotubes by ~2 fold (EPS 16 h) over unstimulated myotubes (No EPS 16 h). In addition, a significant reduction of glucose concentration by ~4 fold in human myotubes was seen in the cell media post-16 h EPS compared to unstimulated myotubes ($p<0.0008$, $n=3$, independent experiments) (see Figure 3.5).

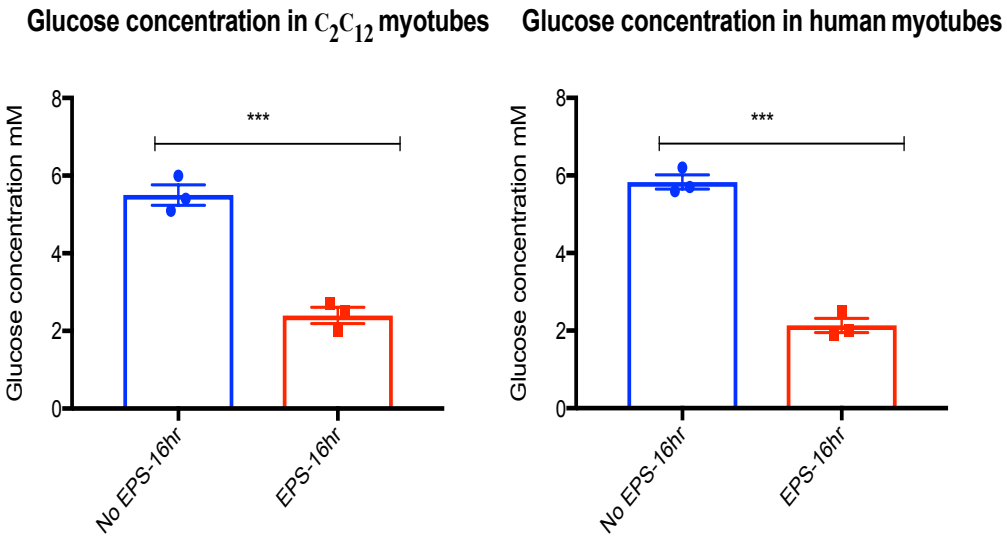

Figure 3.5. The concentration of glucose in the cell media of human and mouse (C2C12) myotubes post EPS. Cells were exposed to either stimulated cell media (EPS 16 h) or unstimulated standard growth cell media (No EPS 16 h) for 16 h (1 Hz, 2 ms pulses, 20 V). Glucose concentration decreased in response to EPS, confirming the occurrence of muscle contraction in vitro n=3 independent experiments (see section 3.3.1. for details). Data is significantly different from unstimulated cell media (No EPS 16 h). An unpaired t-test (two-tailed) was used to analyse data, *** p< 0.0008. Data are presented as mean ± SEM.

3.3.5 Lactate Concentration in the Cell Media of C_2C_{12} Mouse and Human Myotubes Post-16 h EPS

Lactic acid concentrations in the C_2C_{12} cell media increased post-16 h EPS in stimulated myotubes (EPS 16 h) by ~4 fold over unstimulated myotubes (No EPS 16 h). A significant increase (by ~3 fold) was seen in the lactate concentration of the human cell media post-16 h EPS over unstimulated myotubes (No EPS 16 h) ($p<0.0003$, n=3, independent experiments) (see Figure 3.6).

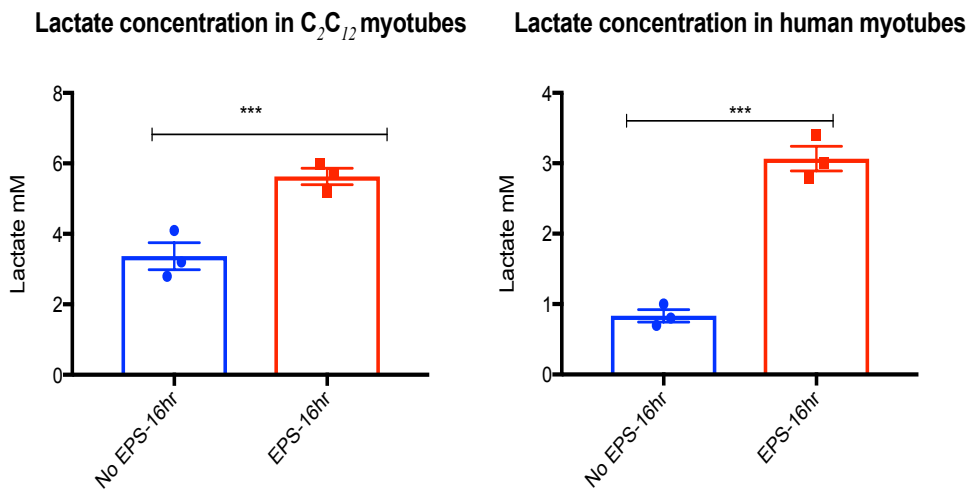

Figure 3.6. The concentration of lactate in the cell media of human and murine (C_2C_{12}) myotubes post EPS. Cells were exposed to either stimulated cell media (EPS 16 h) or standard unstimulated growth cell media (No EPS 16 h) for 16 h (1 Hz, 2 ms pulses, 20 V). Lactate accumulation increased in response to EPS, confirming the occurrence of muscle contraction in vitro. Data are significantly different from unstimulated cell media (No EPS 16 h). n=3 independent experiments (see section 3.3.1. for details). An unpaired t-test (two-tailed) was used to analyse data, *** p< 0.0003. Data are presented as mean ± SEM.

3.3.6 Gene Expression (mRNA) of PGC1-alpha in C_2C_{12} Mouse and Human Myotubes Post-16 h EPS

The mRNA expression of ms.PGC1-alpha (murine PGC1-a) in C_2C_{12} myotubes increased in EPS-stimulated myotubes (EPS 16 h) by ~3-fold compared to the unstimulated myotubes (No EPS 16 h) ($p<0.0007$, n=3 independent experiments) (see Figure 3.7). However, the mRNA expression of hu.PGC1-alpha (human PGC1-a) in human myotubes increased in EPS-stimulated myotubes (EPS 16 h) by ~2-fold over unstimulated myotubes (No EPS 16 h) ($p<0.0052$, n=3 independent experiments) (see Figure 3.7).

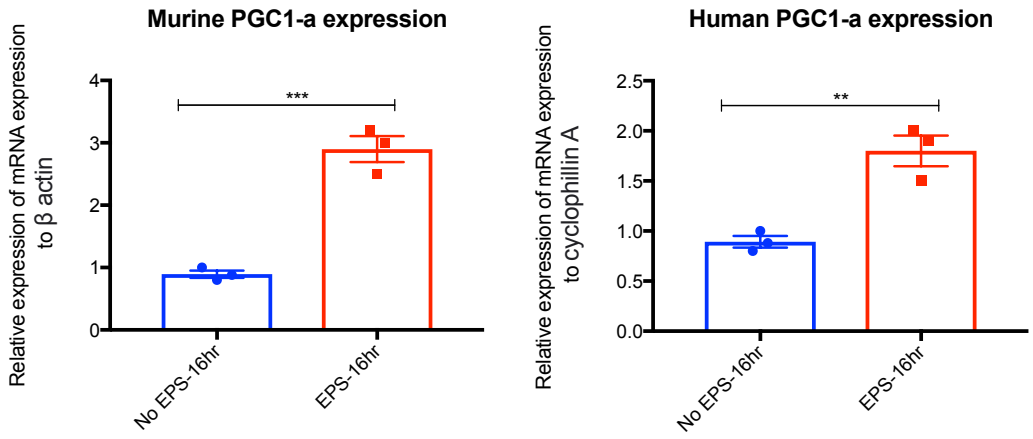

Figure 3.7. PGC1-α alpha mRNA gene expression in both C_2C_{12} mouse and human myotubes post-16 h EPS. An unpaired t-test (two-tailed) was used to analyse data, *** $p< 0.0007$ and ** $p<0.0052$. n=3 independent experiments (see section 3.3.1. for details). Data are presented as mean ± SEM.

3.3.7 Gene Expression (mRNA) of IL-6 in C_2C_{12} Mouse and Human Myotubes Post-16 h EPS

The mRNA expression of ms.IL-6 in C_2C_{12} mouse myotubes was significantly increased in EPS-stimulated myotubes (EPS-16 h) by 60-fold over unstimulated myotubes (No EPS 16 h) ($p<0.0001$, n=3, independent experiments) (Figure 3.8). However, the mRNA expression of hu.IL-6 in human myotubes increased in EPS-stimulated myotubes (EPS 16 h) ~6 fold over unstimulated myotubes (No EPS 16h) ($p<0.0007$, n=3, independent experiments) (Figure 3.8).

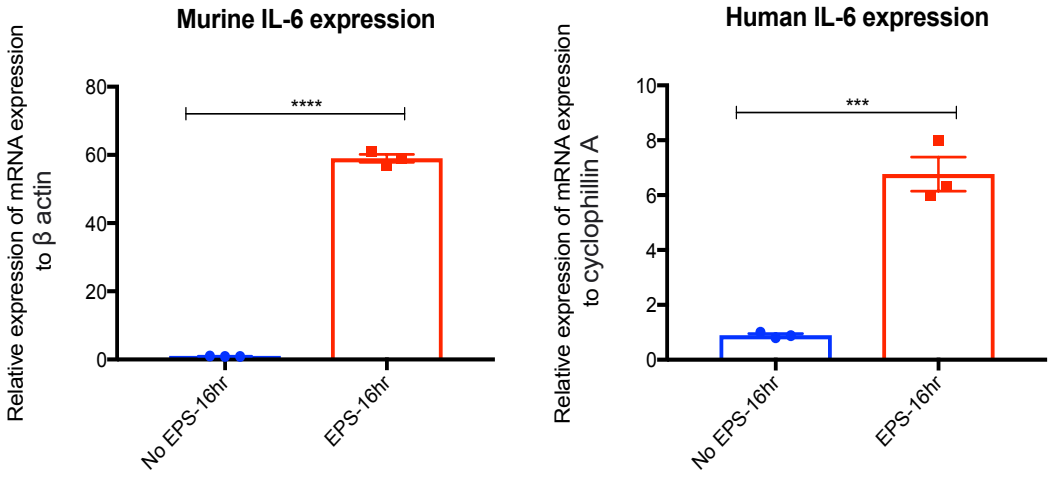

Figure 3.8. IL-6 mRNA gene expression in both C_2C_{12} mouse and human myotubes post-16 h EPS. An unpaired t-test (two-tailed) was used to analyse data, ***** $p<0.0001$ and *** $p< 0.0007$. n=3 independent experiments (see section 3.3.1. for details). Data are presented as mean ± SEM.

3.3.8 Activation of AMPK-a (Th172) Protein Post-16 h EPS

To confirm the accuracy of muscle contraction using EPS as an *in vitro* exercise model, we analysed the activation of p.AMPK^{T172} post-16 h EPS. AMPK-a activation was measured via protein phosphorylation of AMPK-a^{T172} post-16 h of EPS in C_2C_{12} mouse myotubes. Protein was measured by BCA and 30 ug of the protein samples (unstimulated and stimulated myotubes) loaded on 10% SDS-PAGE gel. 16 h of EPS increased p.AMPK phosphorylation in stimulated myotubes (EPS 16 h) by ~0.83-fold over the unstimulated myotubes (No EPS 16 h) (Figure 3.9). Protein bands of p.AMPK-a^{T172} were strong post-16 h EPS; however, faint bands appeared in unstimulated myotubes. Total AMPK-a detected but did not show any change in terms of its level of expression post-16 h EPS (Figure 3.9). The ratio of the data was calculated based on the p.AMPK-a^{T172} bands and their backgrounds, as was Total AMPK-a (loading control) bands and their backgrounds. The final relative

quantification values were essentially the ratio of the net sample band to the net loading control band.

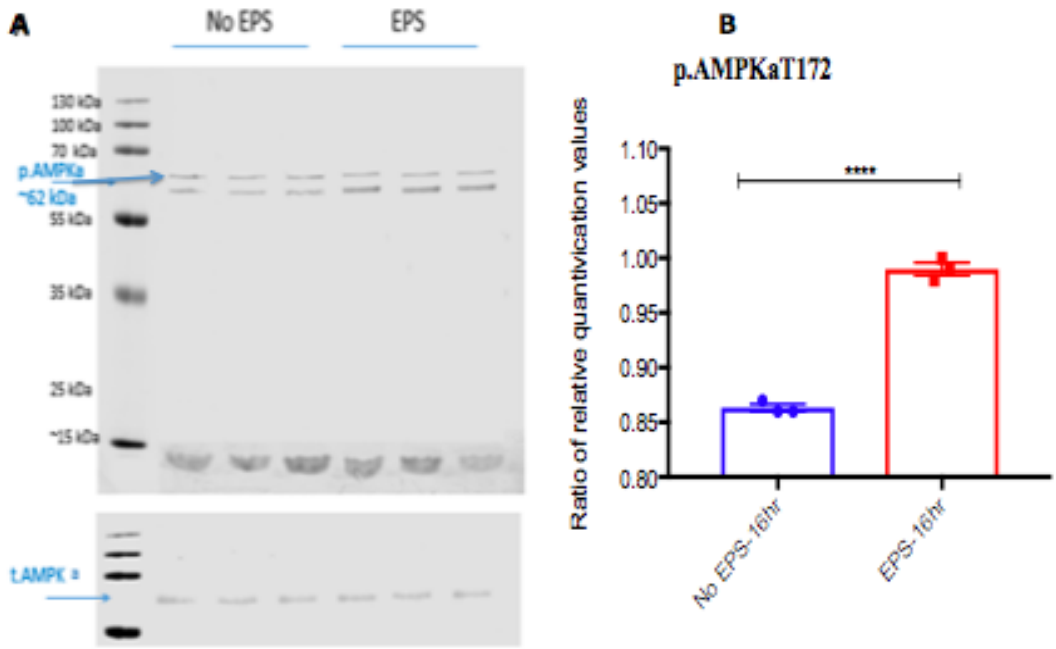

Figure 3.9. Western blot analysis of 16 h EPS on p.AMPKaT172. Cultured C_2C_{12} myotubes were electrically stimulated (1 Hz, 2 ms, 20 V) for 16 h of the differentiation period (on day seven). The results of western blot show an increase of p.AMPKa protein level post EPS. Cells were collected and lysed in RIPA buffer with protease/phosphatase inhibitors. 30 ug of protein was loaded per lane. Cell extracts were separated by 10% SDS-PAGE and transferred onto nitrocellulose membranes. Each membrane was reacted with anti-p.AMPKa antibody and total AMPKa antibody with 10 mM NaF. t.AMPKa total protein was used in this experiment as a loading control. MW of the p.AMPKa ~62kDa (top) and t.AMPKa ~60 kDa (bottom). A. Representative blots of the activation of p.AMPKa. B. Ratio of relative quantification value of protein of interest (n=3 independent experiments (see section 3.3.1. for details)

3.4 DISCUSSION

In this chapter, we have described the evaluation of the concentration of lactate and glucose in cell media (CM) of C_2C_{12} and human myotubes. We observed an increase of lactate level in CM; on the other hand, the glucose concentration was significantly reduced. Lactate accumulation in C_2C_{12} myotubes was significantly increased by 1.5-fold, and this was even more pronounced in human myotubes by 2-fold compared to the no EPS samples (unstimulated myotubes) post-16 h EPS. Using our EPS protocol, we observed a 1.7-fold reduction in the glucose concentration in C_2C_{12} cell media, and in human myotubes, glucose concentration was reduced 3-fold compared to unstimulated myotubes (No EPS 16 h). These results following EPS suggest that contractile activities occurred for the *in vitro* model of EPS.

When the body performs aerobic exercise (acute exercise), either *in vivo* or *in vitro*, more O_2 is transported to the working muscle to generate its energy. In some cases, when the body performs chronic resistance exercise (e.g., lifting heavy weights that requires more rapid energy production than normal), the energy is generated anaerobically. Glucose undergoes glycolysis, a process in which it is broken down or converted into pyruvate though a sequence of processes. When there is adequate oxygen in the body, pyruvate is transferred to an aerobic pathway and further broken down for energy. When there is a lack of oxygen, the body converts pyruvate to lactate, allowing glucose breakdown, and consequently, energy generation to continue, resulting in oxidation of $NADH/H^+$ to NAD^+ (Baker, McCormick, & Robergs, 2010).

PGC1α alpha is an important positive parameter of contractile activities (e.g., following exercise) as many critical elements of skeletal muscle biology are regulated by PGC1α, such as the stimulation of cellular respiration, biogenesis of

mitochondria, metabolism, FA oxidation, and muscle fibre-type transitions (Liang & Ward, 2006; Supruniuk, Mikłosz, & Chabowski, 2017). We tended to observe that PGC1α alpha mRNA expression increased significantly post-16 h EPS; it was upregulated by ~3-fold in both C_2C_{12} and human myotubes compared to unstimulated myotubes, indicating the occurrence of muscle contraction in cultured myotubes. These results are in line with those of similar studies (see Norrbom *et al.*, 2004; Silvennoinen *et al.*, 2015; Tripp *et al.*, 2022). Furthermore, mRNA expression of IL-6 was measured, showing an increase of its expression by 60-fold post-16 h EPS compared to unstimulated myotubes; however, in human myotubes this was upregulated by 7-fold. *In vivo*, interleukin-6 is known to be secreted by skeletal muscle following exercise, and this result is consistent with a study by Tantiwong *et al.* (2010) showing an increased level of IL-6 mRNA in healthy and T2D participants following EPS treatment.

AMP-activated protein kinase was observed post-16 h of EPS in cultured myotubes. The western blotting study of phosphorylation on AMPK (p.AMPK^{T172}) revealed an increase in protein phosphorylation of AMPK in C_2C_{12}-cultured myotubes compared to unstimulated myotubes. This indicates the EPS protocol used in this study was able to stimulate an increase in p.AMPK^{T172} protein expression, which may mimic similar physiological effects that occur post exercise *in vivo*. AMPK is mainly activated when a decrease in intracellular ATP level is detected. As highlighted in a recent study, AMPK plays an important role in metabolic reprogramming and regulation of cell proliferation and possesses an important ability to be a pathway used in cellular processes such as autophagy and cell polarity (Wang *et al.*, 2021). Moreover, the activation of AMPK in skeletal muscle post-exercise has been recorded as intensity-dependant (Hardie, Ross, & Hawley, 2012; Friedrichsen,

Mortensen, Pehmøller, Birk, & Wojtaszewski, 2013). However, due to its important role in skeletal muscle post-exercise, there is the distinct possibility that it could regulate glucose uptake following exercise.

The application of EPS has been widely used on cultured myotubes and described in various studies, including those focusing on murine C_2C_{12} cells (see Fujita, Nedachi, & Kanzaki, 2007; Nedachi *et al.*, 2008; Burch *et al.*, 2010), L6 cells (see Yano *et al.*, 2011), primary rat skeletal muscle cells (see Silveira, Pilegaard, Kusuhara, Curi, & Hellsten, 2006) and human myotubes (see Aas *et al.*, 2002; Lambernd *et al.*, 2012; Nikolic *et al.*, 2012). In addition, the frequency of 1 Hz used in the studies described here has been applied to C_2C_{12} and human myotubes since it has been shown to be the optimum frequency level for skeletal muscle culture to produce maximum peak twitch force (Ito *et al.*, 2014). In relation to this, our EPS performed similarly to the protocol established by Chen *et al.* (2019) – 1 Hz, 2 ms and 20 V for 16 h – for identifying contraction-regulated myokines.

To our knowledge, this is first time that the PGC1-a (PGC1-alpha) mRNA expression, IL-6 mRNA expression, AMPK protein were all measured using this EPS protocol in both C_2C_{12} and human cultured myotubes. The results of the EPS model all suggest that the protocol resembles trained muscle. In conclusion, by applying acute low-frequency EPS to myotubes, several important aspects of *in vivo* effects of exercise were observed. We were able to demonstrate lactate accumulation and a decrease in glucose concentration in the myotube cell media for both cultured C_2C_{12} and human myotubes: a significant rise of PGC1-a mRNA expression, up-regulation of IL-6 mRNA expression, AMPK activation, and recruitment of GLUT-4 via immunocytochemistry. Thus, we can conclude that this model of EPS in

myotubes represents a physiologically relevant *in vitro* model of exercise that can be used for future studies relating to contraction-regulated myokines.

Chapter 4: Regulation of LCN-2 Expression with Exercise-Like Treatments (EPS and AICAR) in Cultured C_2C_{12} and Human Myotubes

4.1 INTRODUCTION

Obesity, dyslipidemia, hypertension, hyperglycemia, hyperinsulinemia, and insulin resistance are among the metabolic disorders that can arise from metabolic syndrome. Obesity and low-grade chonic inflammation, which are thought to induce abnormalities associated with metabolic syndrome, have been linked in studies examining the molecular processes behind metabolic syndrome (Gregor & Hotamisligil, 2011). During both normal and pathological situations, skeletal muscle is an important component for whole-body glucose metabolism. In fact, skeletal muscles are increasingly being shown to produce myokines, which exert effects in autocrine, paracrine, or endocrine fashions. Several myokines are known, including interleukin-6 (IL-6) (Steensberg *et al.*, 2000), FGF 21 (Izumiya *et al.*, 2008), follistatin-like 1 (Ouchi *et al.*, 2008), insulin-like 6 factor (Zeng *et al.*, 2010), and irisin (Boström *et al.*, 2012). As a result, skeletal muscle may be the body's largest endocrine organ, and myokine release is likely to be important for understanding the crosstalk between skeletal muscle and other tissues (Table 4.1).

Table 4.1

Myokines and their effects on metabolism

Name	Action	Signaling Pathway	Reference
Interleukin-6 (IL-6)	Regulating muscle growth Inhibiting the production of pro-inflammatory cytokine Regulating the metabolism of lipid/glucose Enhancing the expression GLUT-4 and insulin sensitivity	AMPK, PI3K, STAT3	(Huh, 2018)
Irisin/FNDC5	Stimulating white adipocyte to switch to browning Regulating glucose/lipid metabolism Suppressing the expression of myostatin	AMPK, cAMP-PKA-perilipin/HSL	(Huh, 2018)
Interleukin-15 (IL-15)	Stimulating muscle growth Increasing glucose uptake in muscle cells Enhancing the activity of mitochondria Protecting against oxidative stress Reducing the mass of white adipocyte and the accumulation of lipids	AMPK-PPARδ, JAK3-STAT3	(Huh, 2018)
Myonectin	Increasing the recruitment of GLUT-4 Enhancing glucose uptake Stimulating fatty acid oxidation Promoting fatty acid uptake	AMPK, FA transport	(Raschke & Eckel, 2013)

The most studied myokine is IL-6, which is known to be released by skeletal muscle, exerting autocrine effects and promoting certain signaling proteins involved in fat/glycogen metabolism (Keller *et al.*, 2001; Brandt *et al.*, 2012), glucose uptake (Carey *et al.*, 2006) and hypertrophy (Serrano *et al.*, 2008). Although extensive research on IL-6 has been conducted, its specific molecular role inside skeletal muscle remains unclear. More specifically, IL-6 protein was not detected inside the myotubes of humans or mice (Hiscock *et al.*, 2004) unless in inflammation conditions (Garibotto *et al.*, 2006; Raj *et al.*, 2005) or when damage had occurred in muscle (Serrano *et al.*, 2008).

It has also been found that, two days post-cardiotoxin damage in skeletal muscle, LCN-2 production is dramatically stimulated post intense exercise (Rebalka, 2018). In preliminary data, LCN-2 was secreted by rats but not by human skeletal muscle cells (myotubes) *in vivo*. Its expression was not detected at rest (0 h); however, LCN-2 expression was found to increase over time (3 h) post-eccentric exercise and declined post-48 h in two participants out of six. Moreover, the study investigated the effect of LCN-2 deletion on repair of skeletal muscle following an injury, with results showing that the deletion severely affects the regeneration of skeletal muscle (Rebalka *et al.*, 2018). Overall, new research on LCN-2 expression in skeletal muscle, as well as earlier data indicating issues in LCN-2 cytokine effects within the body, point to the need for more research into LCN-2's ability to operate as a contraction-regulated myokine.

Exercise induces the secretion of myokines and increases the activity of AMP-activated protein kinase (AMPK) in skeletal muscle, and AMPK signalling pathways have been postulated to mediate a variety of metabolic consequences (Fujii *et al.*, 2006). AMPK regulates anabolic and catabolic pathways to maintain energy storage as an intracellular energy, and the role of AMPK as an energy sensor is important in tissues with a high rate of energy turnover. Skeletal muscle is one of these tissues due to the dramatic variations in energy demand that occur pre and post exercise. However, despite a relationship between the activation of AMPK and the secretion of various myokines by muscle not yet having been observed, exercise-stimulated activity of AMPK has been linked to an increase of IL-6 post-exercise in muscle. (MacDonald *et al.*, 2013; Steensberg *et al.*, 2013) The activation of AMPK has also been shown to affect the expression level of IL-6, although mixed evidence is available from different studies. For example, incubating C_2C_{12} muscle cells with the

AICAR for 24 h increased the mRNA level of IL-6 (Weigert *et al.*, 2016). However, another study found that incubating with AICAR for 2-4 h reduced the mRNA level of IL-6 in muscle (Lihn *et al.*, 2008; Glund *et al.*, 2009). As a result, the exact involvement of AMPK in the regulation of IL-6 in skeletal muscle remains unknown.

That said, the activation level of AMPK has been shown to be linked to whole-body insulin sensitivity improvement. Several investigations have found that the AMPK activator, AICAR, is able to mimic the benefits of regular exercise, reducing the risk of diabetes-related skeletal muscle insulin resistance (Hardie *et al.*, 2012). AICAR has also been widely used as an activator to metabolic pathways linked with activation of AMPK in a range of tissues and cells (Valero-Breton *et al.*, 2020). Thus, AICAR treatment represents a good strategy for improving insulin sensitivity and has been demonstrated to have anti-inflammatory effects in various cell types, including skeletal muscle cell and adipose tissue in various models (Hardie *et al.*, 2012; Valero-Breton *et al.*, 2020). Based on other findings of pre-exercise and exercise-induced activation of AMPK in skeletal muscle of patients with type 2 diabetes (Musi *et al.*, 2001; Højlund *et al.*, 2004; Kjøbsted *et al.*, 2016), AMPK in skeletal muscle may have a potential role in the prevention and treatment of inflammation and insulin resistance.

In the current chapter, we determine whether both human skeletal muscle and murine express LCN-2 under muscle contraction compared to resting conditions using our well-developed exercise model that is fully explained in Chapter 3, an *in vitro* model of exercise. In addition, we examine if exercise using the EPS model and AICAR treatment regulates LCN-2 secretion *in vitro* and whether phosphorylation of AMPKa^{Th172} has a role in mediating the secretion of LCN-2 post-exercise (EPS) and post-AICAR treatment.

4.2 AIMS OF THIS CHAPTER

In this chapter, we hypothesise that EPS, as an *in vitro* model of exercise, increases the expression and secretion of LCN-2 in human skeletal muscle cell (myotubes) as a primary endpoint. Additionally, we investigated whether AICAR could also induce the expression and secretion of LCN-2. Three studies were carried out (#2, 3 and 4) to investigate these hypotheses.

Initially, we investigated LCN-2 levels of protein expression under normal physiological states in human hepatocytes, adipocytes (3T3L-1), C_2C_{12} myotubes, human myotubes and human liver tissue.

Then, we examined mRNA expression and secretion of LCN-2 in both cultured C_2C_{12} and human skeletal muscle cells (myotubes) post EPS to validate its role in skeletal muscle post-exercise.

Finally, we used another exercise-like stimulus, AICAR, to investigate the effects of AICAR treatments on the expression and secretion of LCN-2 in C_2C_{12} skeletal muscle cell (myotubes), therefore determining the relationship between the activation of AMPK and LCN-2 in response to exercise.

4.3 RESULTS

4.3.1 Myotubes cultures and their donors

Myotubes cultures were established from a total of n = 2 individual, female healthy adults for all experiments in this chapter. Descriptive donor data is presented in Table 4.1. The experiments performed in an independent donor repeats was determined principally by the number of myoblasts were passaged, since cultures were restricted to no more than three passages to best preserve any effects of donor phenotype (an independent experiments n=3 based on a single biopsy derived from a human donor passaged three times). Within an independent experiment, multiple treatment replicates were performed (e.g., the use of 3 treatment replicates meant 3 wells of cells from each independent experiment were exposed to each treatment condition). All reported n values are the number of independent experiments n=3.

Table 4.2

Characteristic Data for Skeletal Muscle Biopsy Donor from Whom Myotube Cultures Were Derived

Sex	Age (y)	Mass (Kg)	Height (m)	BMI	Fasting Glucose (mmol/L)	Biopsy yield (mg)
Female	**22**	60.5	1.695	21.0579	3.6	~150mg
Female	**21**	53.5	1.533	22.8	4.8	~150mg

4.3.2 LCN-2 Protein is Highly Expressed in Human Liver Tissue without Stimulation or Treatment

Examining the relative expression level of LCN-2 across different cells and tissue under normal conditions and without any stimuli was the aim of Study 2. Human hepatocytes (healthy donor-L139/11/N, see appendix-1), human liver tissue (healthy donor- L325/18/N, see appendix-1), mouse adipocytes (3T3L-1), mouse and human myotubes (the latter from a young, healthy, male donor), and cellular lysates were prepared from each cell and tissue to study protein expression of LCN-2 under normal conditions and without any stimulation. 50 μg of protein was loaded into a single lane of the SDS-PAGE gel for each cell and tissue. After running the gel and transferal of all blots into membranes, the blots were incubated with anti-Lipocalin-2 antibodies. We used anti-β. actin antibody as a loading control since it is essential for the reliability of Lipocalin-2 data. The loading control had an equal intensity band across all samples.

Lipocalin-2 is expressed in human hepatocytes, adipocytes (3T3L-1) and in C_2C_{12} mouse myotube cells with different band intensity. However, human LCN-2 in human liver tissue (see Figure 4.1, Lane 2) has the strongest band under normal conditions, suggesting human liver tissue as a suitable positive control for LCN-2 under normal conditions. We also examined the expression of LCN-2 in human myotubes. Human myotube cells did not express LCN-2 under normal conditions, suggesting that Lipocalin-2 expression is absent without stimulation or treatment (normal conditions).

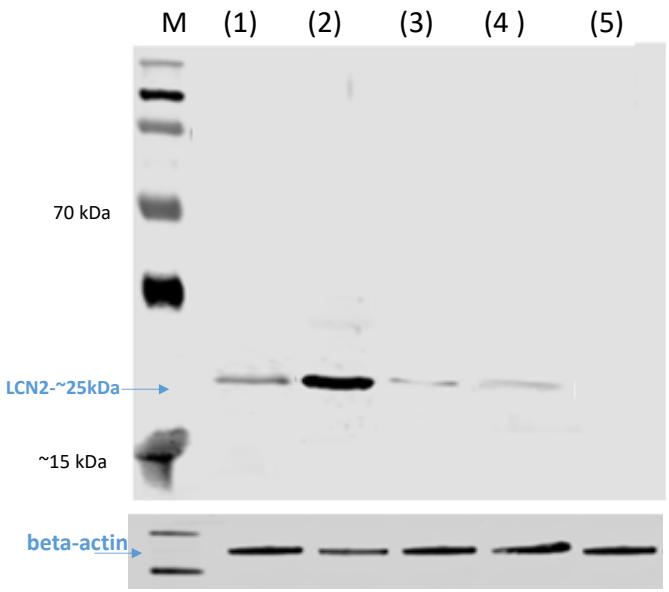

Figure 4.1. Western blot of Lipocalin-2 (LCN-2) protein expression in various cells and tissue (n=1). **(1)** Human hepatocytes; **(2)** Human liver tissue; **(3)** 3T3L1 adipocytes; **(4)** C_2C_{12} myotubes; **(5)** Human myotubes. All lanes express the level of LCN-2 inside cells in normal conditions. Tissues were homogenised in 1 ml tri reagent, and protein was extracted and denatured in 7 M urea. Cells were collected and lysed in RIPA buffer. 50 µg protein was loaded per lane. Cell/tissues extracts were separated using 12% SDS-PAGE and transferred onto a nitrocellulose membrane. The membrane was reacted with anti-Lipocalin-2 antibody and antibody β. Actin, the latter being used as a loading control. **M** denotes the protein ladder.

4.3.3 Lipocalin-2 (LCN-2) mRNA Expression is Upregulated in C_2C_{12} Mouse Myotubes Post-16 h EPS Stimulation (Acute Exercise-Like Stimuli)

After determining that LCN-2 protein is expressed under normal conditions in C_2C_{12}, we investigated the effects of acute exercise (16 hr) of EPS stimulation on the expression of LCN-2. Myotubes stimulated with 16 h EPS (EPS 16 h) (see Figure 4.2) showed a significant increase of LCN-2 mRNA expression by ~50 fold over unstimulated myotubes (No EPS 16 h). An unpaired t-test (two-tailed) was used ($p<0.0001$, n=3, independent experiments).

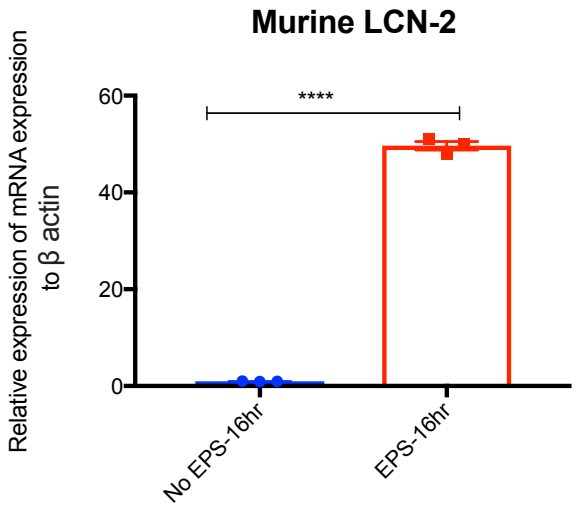

Figure 4.2. Effects of 16 h EPS (acute exercise) on Lipocalin-2 (LCN-2) mRNA expression in C_2C_{12} mouse myotubes. Cultured murine myoblasts (C_2C_{12}) were differentiated towards mature myotubes in 4% horse serum. On day seven, cells were electrically stimulated (1 Hz, 2 ms pulses, 20 V), for 16 h. Samples were collected in 1 ml Tri-Reagent and processed for qPCR analysis. qPCR results showed a significant increase in the mRNA expression of LCN-2 in stimulated myotubes (EPS 16 h) over unstimulated myotubes cells (No EPS 16 h). mRNA expression was normalised to beta-actin. An unpaired t-test (two-tailed) was used. Statistically significant differences were: **** $p < 0.0001$ (n=3, independent experiments, x3 passage with 3 wells replicates). Data are represented as mean ± SEM.

4.3.4 LCN-2 Protein is Expressed and Secreted by C_2C_{12} Mouse Myotubes Post-16 h EPS (Acute Exercise-Like Stimuli)

The mRNA expression of LCN-2 in C_2C_{12} myotubes is upregulated post-16 h EPS, indicating that LCN-2 could be an exercise-induced myokine. We followed this finding by measuring the level of its expression and secretion post-16 h EPS. Protein levels in the cell lysate of C_2C_{12} increased by 20% post-16 h EPS compared to unstimulated myotubes. All band intensities were calculated based on the band intensity of the loading control (beta-actin). Despite LCN-2 protein having been expressed in cell lysate by both stimulated and unstimulated myotubes, it was only secreted into C_2C_{12} myotube cell media in response to 16 h of EPS, as shown in Figure 4.3. An unpaired t-test (two-tailed) was used ($p<0.0001$, n=3, independent experiments).

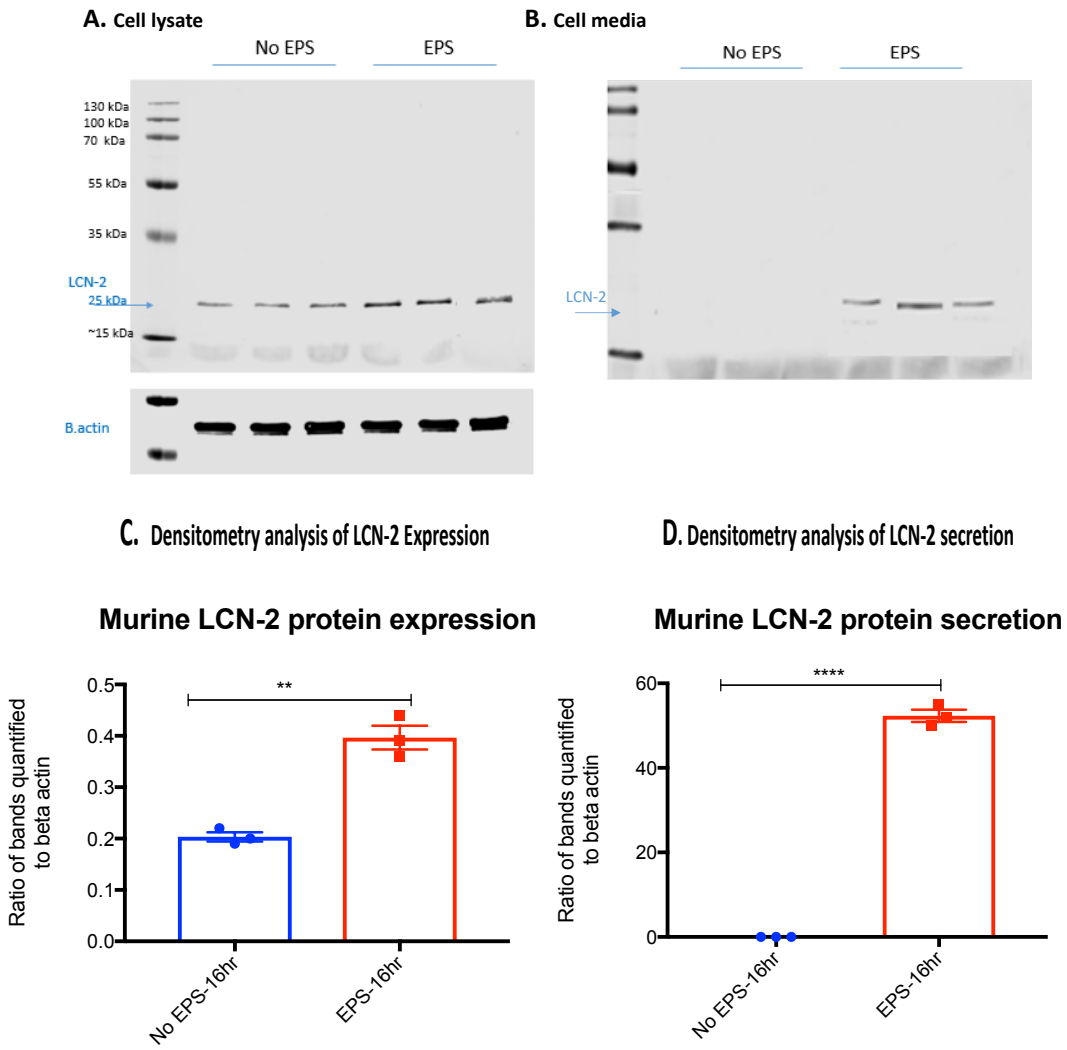

Figure 4.3. Effects of 16 h EPS (acute exercise) on the expression and secretion of Lipocalin-2 (LCN-2). Cultured C_2C_{12} myotubes were electrically stimulated (1 Hz, 2 ms pulses, 20 V), for 16 h (on day seven). **A.** Protein in cell lysate. **B.** Protein in cell culture media. A and B are representative western blots showing an increase of LCN-2 expression and secretion post-16 h EPS. Cells were collected and lysed in RIPA buffer with protease/phosphotease inhibitors, and cell media were collected and concentrated using a VIVAspin column (MWCO 10k). 50 µg protein was loaded per lane and cell extract separated using 12% SDS-PAGE. Each membrane was reacted with anti-Lipocalin-2 antibody and beta-actin antibody. Beta-actin was used as a loading control. **C and D.** Densitometry analysis of western blot band intensities (n=3, independent experiments, x3 cell passage with 3 wells replicates).

4.3.5 LCN-2 mRNA Expression is Upregulated in Human Myotubes Post-16 h EPS Stimulation (Acute Exercise-Like Stimuli)

We observed a significant increase of LCN-2 mRNA and protein expression post-16 h EPS (acute exercise) in C_2C_{12} myotube cells. To compare murine versus human LCN-2 expression we used human myotube cells isolated from a healthy female donor (n=3, independent experiments) (donor information in Table 4.2). A

significant increase by 6-fold of mRNA expression in stimulated human myotube cells (EPS 16 h) was seen over unstimulated myotubes cells (No EPS 16 h) (see Figure 4.4).

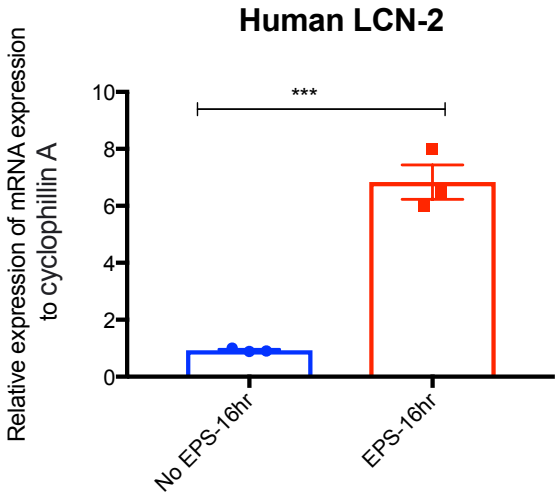

Figure 4.4. Effects of acute exercise (EPS) on Lipocalin-2 (LCN-2) mRNA expression. Cultured human myoblasts were differentiated towards mature myotubes in 6% horse serum (H.S). On day seven, cells were electrically stimulated (1 Hz, 2 ms pulses, 20 V) for 16 h. Samples were collected in 1 ml Tri-Reagent and processed for qPCR analysis, qPCR result shows an increase in the mRNA expression of Lipocalin-2. It is significantly different from unstimulated cells (No EPS). The mRNA expression was normalised to cyclophillin A. An unpaired t-test (two-tailed) was used. Statistically significant differences were: **** $p < 0.0001$ (n=3, independent experiments-single biobsy derived from a healthy female donor with 22.8 BMI passaged three times - see table 4.2 for descriptive data). Data are represented as mean ± SEM.

4.3.6 LCN-2 Protein Expression and its Secretion in Human Myotubes Post-16 h EPS (Acute Exercise-Like Stimuli) (Study 3)

Since we observed the significant up-regulation of LCN-2 mRNA, we next evaluated whether this correlates well with its protein level. We did not detect LCN-2 in human cell lysate but did detect proteins intended to be secreted by human myotubes cells. The secretion level of LCN-2 increased in response to EPS stimulation (EPS 16 h) by 43% over unstimulated myotubes (No EPS 16 h), indicating that LCN-2 is an exercise-induced myokine (Figure 4.5). These results suggest an important role of LCN-2 as an exercise-induced myokine in human skeletal muscle cells (myotubes).

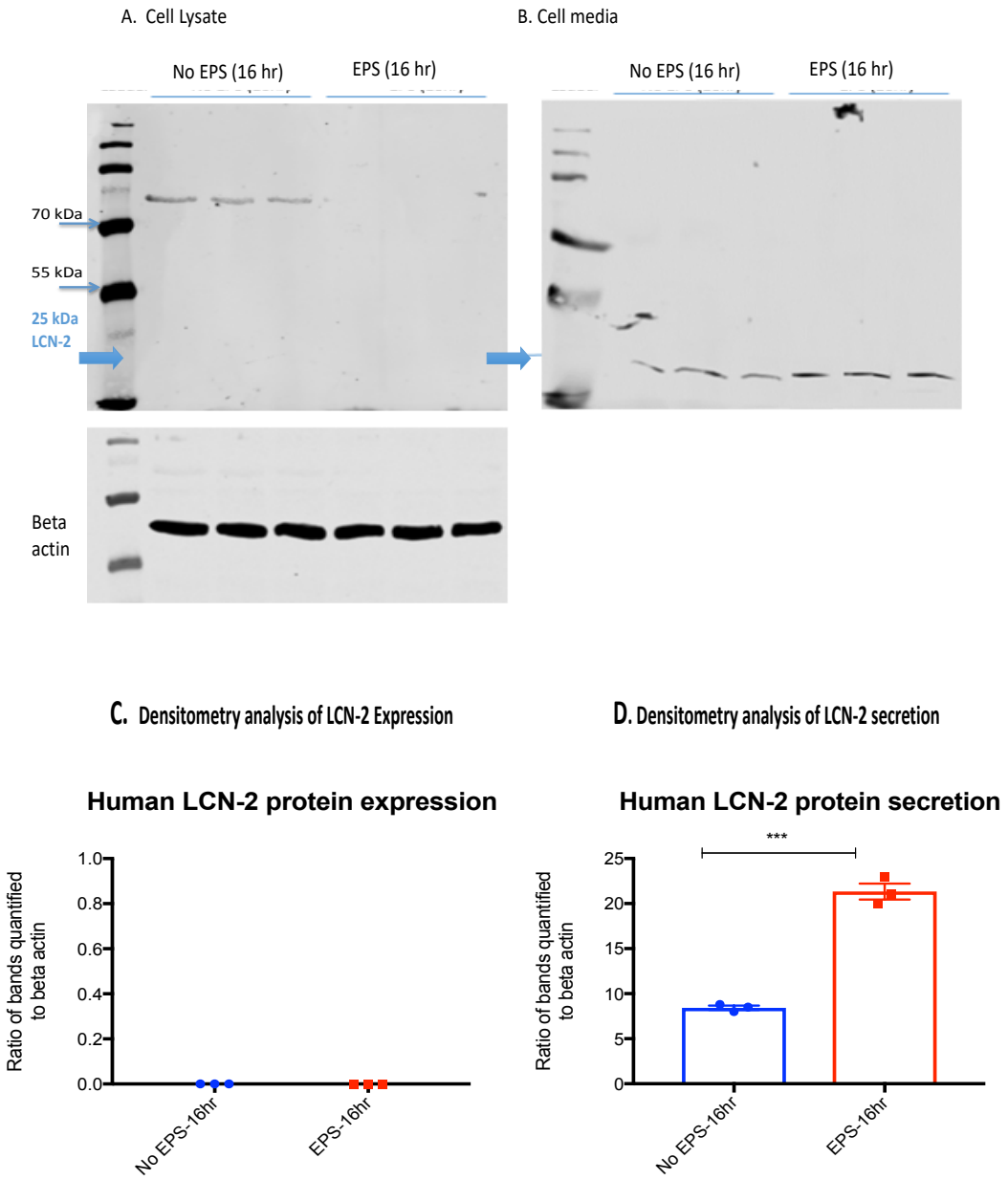

Figure 4.5. Effects of 16 h EPS (acute exercise) on the protein expression and secretion of Lipocalin-2 (LCN-2). Cultured human myotubes were electrically stimulated (1 Hz, 2 ms pulses, 20 V), for 16 h (on day seven). **A.** Protein in cell lysate **B.** Protein in cell culture media. A and B are representative western blots showing an increase of LCN-2 secretion into cell media post-16 h EPS. However, no LCN-2 protein is present in the cell lysate. Cells were collected and lysed in RIPA buffer with protease/phosphotease inhibitors, and cell media were collected and concentrated using VIVAspin column (MWCO 10k). 50 µg of protein was loaded per lane, and the cell extract was separated using 12% SDS-PAGE. Each membrane was reacted with anti-Lipocalin-2 antibody and beta-actin antibody, the latter being used as a loading control. **C and D.** Densitometry analysis of band intensity (n=3, independent experiments-single biobsy derived from a healthy female donor with 22.8 BMI passaged three times - see table 4.2 for descriptive data).

4.3.7 LCN-2 mRNA Expression in Human Myotubes Post-2 h and -4h EPS (Acute Exercise-Like Stimuli)

Based on results obtained from C_2C_{12} and human myotubes post-16h EPS stimulation (the longer time period), we evaluated the mRNA and protein expression of LCN-2, as well as its secretion in stimulated human myotubes post-2 h and -4 h (shorter time periods). LCN-2 mRNA expression upregulated gradually, and post-4 h EPS showed a significant 30-fold increase. Altogether, regulation of mRNA expression post EPS stimulation in human myotubes indicates that LCN-2 gradually increased from 2 h to 4 h by approx 3-fold (2 h EPS vs. 4 h EPS), and then LCN-2 mRNA expression gradually declined until 16 h post-EPS stimulation. This reveals that mRNA, at the 16 h point, was translated into protein (*** p< 0.0001, n=2, independent experiments). Data are represented as mean with SEM (Figure 4.6).

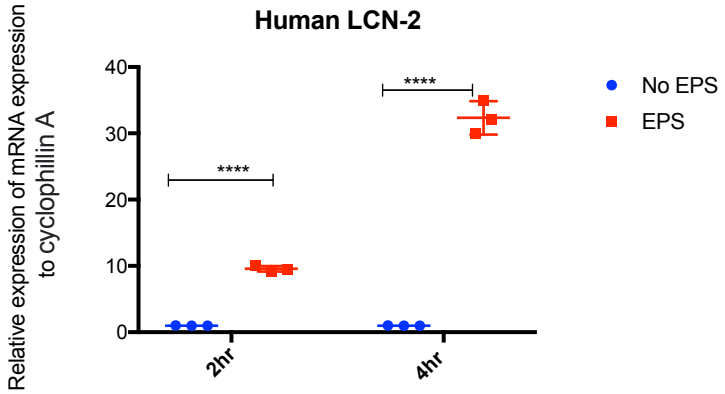

Figure 4.6. Effects of 2 h and 4 h acute exercise (EPS) on Lipocalin-2 (LCN-2) mRNA expression. Cultured human myoblasts were differentiated towards mature myotubes in 6% horse serum (H.S). On day seven, cells were electrically stimulated (1 Hz, 2 ms pulses, 20 V) for 2 h and 4 h. Samples were collected in 1 ml Tri-Reagent and processed for qPCR analysis. qPCR results show a significant increase in mRNA expression of LCN-2 post-4 h from unstimulated cells (No EPS). mRNA expression was normalised to Cyclophillin A. An unpaired t-test (two-tailed) was used. Statistically significant differences were: **** p< 0.0001 (n=2, independent experiments - single biobsy derived from a healthy female donor with 21.05 BMI, myotubes were passaged two times and 3 well treatment conditions were used within each cell passage - see table 4.2 for descriptive data). Data are represented as mean ± SEM.

4.3.8 LCN-2 Protein Expression and its Secretion into Human Myotubes Post-2 h and -4 h EPS (Acute Exercise-Like Stimuli)

We next assessed whether LCN-2 was expressed in cell lysate and secreted into human cell media post-2 h and -4 h EPS stimulation, finding no bands in either cell lysate or cell media (see Figure 4.7).

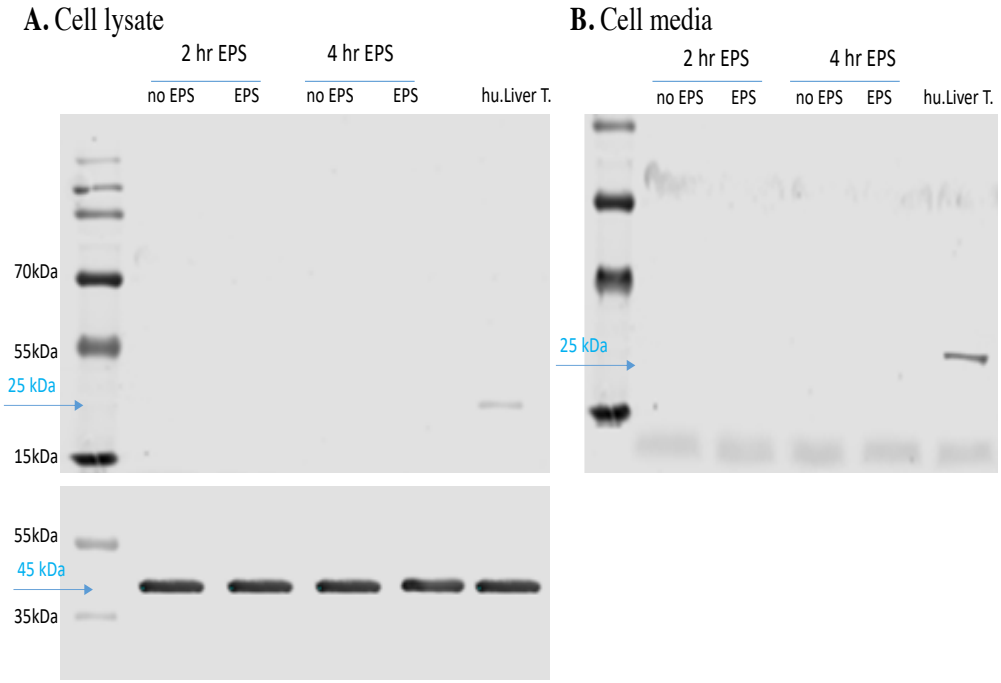

Figure 4.7. Effects of both 2 h and 4 h post EPS stimulation (acute exercise) on the expression and secretion of human Lipocalin-2 (LCN-2). Cultured human myotubes were electrically stimulated (1 Hz, 2 ms pulses, 20 V), for 2 h and 4 h (on day seven). **A.** Cell lysate. **B.** Cell media. Representative western blot analysis did not show Lipocalin-2 expression and secretion post-2 h and -4 h EPS (n=2, independent experiments). Cells were collected and lysed in RIPA buffer with protease/phosphotease inhibitors. Cell culture media were collected and centrifuged to remove cell debris. Cell culture media was then concentrated using a VIVAspin column (MWCO 10k) in equal amounts. 50 µg of protein was loaded per lane, and the cell extract was separated using 12% SDS-PAGE. 30 µl of concentrated cell culture media was loaded and separated using 12% SDS-PAGE. Each membrane was reacted with anti-Lipocalin-2 antibody and β.actin antibody, the latter being used as a loading control (n=2, independent experiments - single biobsy derived from a healthy female donor with 21.05 BMI, myotubes were passaged two times and 3 well treatment conditions were used within each cell passage - see table 4.2 for descriptive data). MW of LCN-2 is 25 ka and β.actin is 45 kDa.

4.3.9 Effect of AICAR on pAMPKT172 in C_2C_{12} Myotubes

We have seen in a previous chapter that EPS activates the pathway of AMPK-a (specifically $pAMPK^{T172}$) post-16 h EPS, and therefore, we further investigated whether AICAR treatment activates $pAMPK^{T172}$. To examine LCN-2 protein expression and secretion in response to AICAR treatment, the $pAMPK^{T172}$ activation was first confirmed. C_2C_{12} myotubes cells were treated with 2 mM AICAR treatment for 15 min, 30 min and 60 min. Untreated cells served as a control. Phosphorylated protein was evaluated using western blotting. Findings indicate 2 mM of AICAR in C_2C_{12} myotubes phosphorylates $pAMPK^{T172}$ at all time points (15 min, 30 min and 60 min), and its expression increased after 60 min of AICAR treatment (see Figure 4.8), indicating that acute exercise (EPS) and 2 mM AICAR activates $pAMPK^{T172}$ in parallel effects.

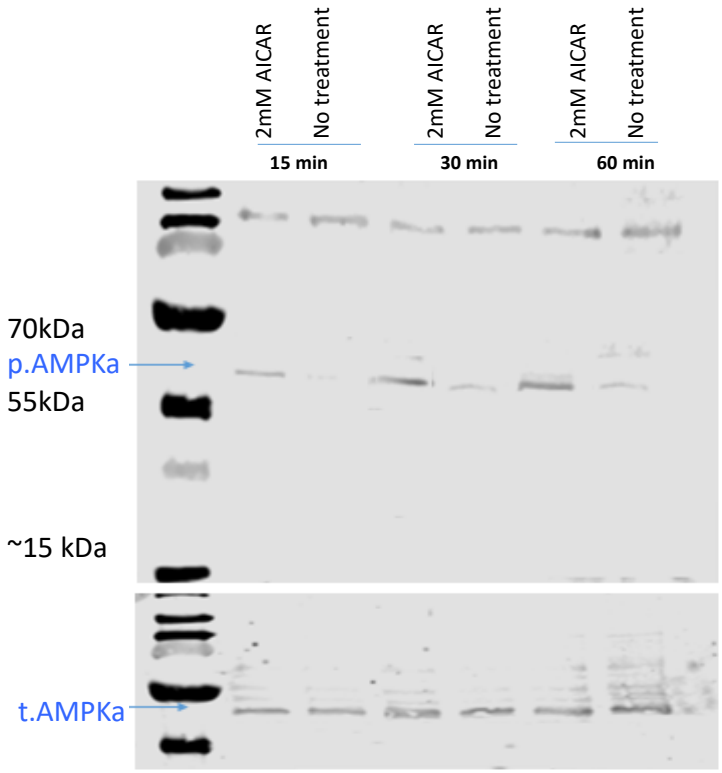

Figure 4.8. Effects of AICAR treatment on the phosphorylation of pAMPKT172 (n=1). Cultured C_2C_{12} myotubes were treated with 2 mM AICAR for 15 min, 30 min and 60 min. The results of western blot anaylsis shows an increase of $pAMPK^{T172}$ protein levels post-AICAR treatment at all time points indicated. Cells were collected and lysed in RIPA buffer with protease/phosphotease inhibitors. 30 µg of protein was loaded on the SDS-PAGE gels per lane. The cell extract was separated using 10 % SDS-PAGE and transferred onto nitrocellulose membranes. Each membrane was reacted with anti-$pAMPKa^{T172}$ antibody and total AMPKa antibody in the presence of 1M NaF. t.AMPKa (total protein) was used as a loading control.

4.3.10 LCN-2 Protein is upregulated by AICAR Treatment for 24 h in C_2C_{12} Myotubes

The effect of AICAR on LCN-2 protein expression in cell lysate was investigated by western blotting. After differentiating C_2C_{12} myoblasts towards C_2C_{12} mature myotubes cells, the cells were treated with 2 mM AICAR for 24 h and 48 h (see Figure 4.10). We chose these longer durations (24 h and 48 h) to investigate effects of AICAR on the transcriptional level of LCN-2 protein. AICAR treatment for 24 h significantly increased the protein expression of LCN-2 in the cell lysate. However, treatment for 48 h did not prompt expression of LCN-2 protein in

the cell lysate of C_2C_{12} myotubes. We subsequently assessed the cell media of LCN-2 because the protein in the cell lysate may have all been secreted following the AICAR treatment for 48 h, which could explain the undetectable protein expression of LCN-2 in the cell lysate (see Figure 4.9).

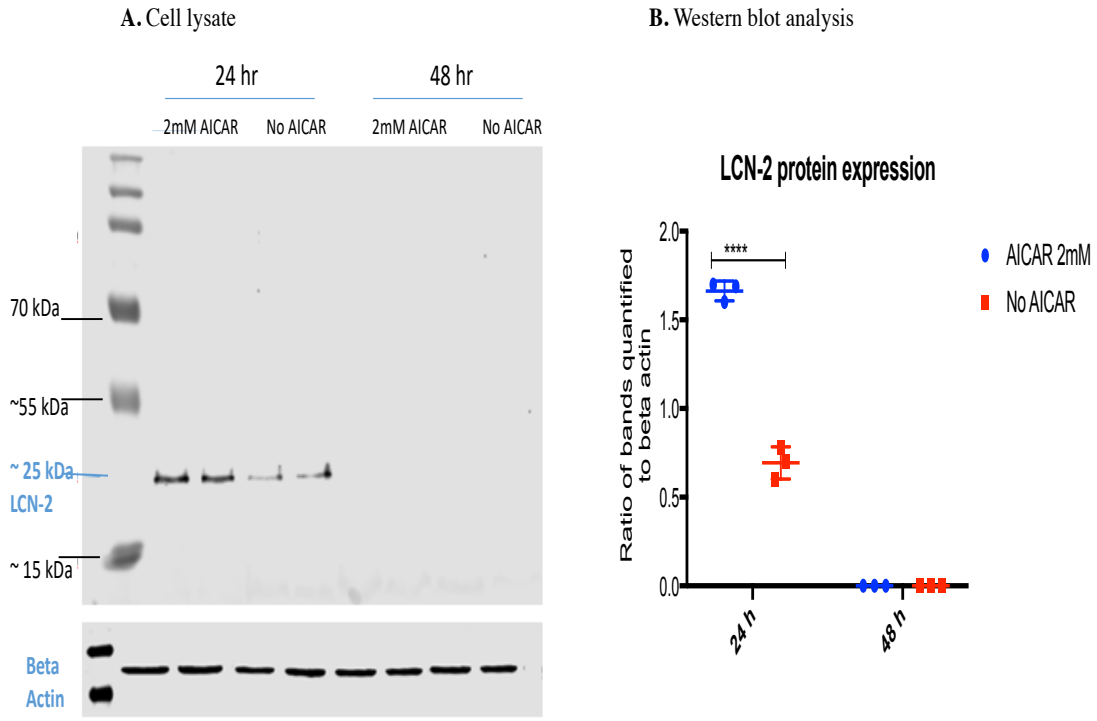

Figure 4.9. The effects of 2 mM AICAR on protein expression of LCN-2 in C_2C_{12} myotubes. Cultured C_2C_{12} myotubes were treated with 2 mM AICAR for 24 h and 48 h. **A.** Representative western blot showing an increase of protein expression of LCN-2 post-24 h AICAR treatment in cell lysate. **B.** Western blot analysis of two independent experiments in C_2C_{12} myotubes. Cells were collected and lysed in RIPA buffer with protease/phosphotease inhibitors. 50 µg of protein was loaded per lane. Cell extract was separated using 12% SDS-PAGE and transferred onto nitrocellulose membranes. Each membrane was reacted with Lipocalin-2 antibody and β.actin antibody, with the latter being used as a loading control. Statistically significant differences were: **** $p < 0.0001$ (n=2, independent experiments - single biobsy derived from a healthy female donor with 21.05 BMI, myotubes were passaged two times and 3 well treatment conditions were used within each cell passage - see table 4.2 for descriptive data). Data are represented as mean ± SEM.

4.3.11 LCN-2 Protein Secretion is increased by AICAR Treatment for 48 h in C_2C_{12} Myotubes

The assessment of protein expression of LCN-2 in cell lysate following AICAR (2 mM) was investigated, showing that LCN-2 was only expressed after 24 h AICAR treatment. We also observed the LCN-2 secretion level in the C_2C_{12}

myotubes cell media. Western blot results showed that AICAR treatment (2 mM) for 24 h caused secretion of LCN-2 protein in the cell media without any significant difference between treated and untreated cells (AICAR). However, AICAR treatment for 48 h did cause stronger bands in treated cells compared to untreated cells (No AICAR) (see Figure 4.10).

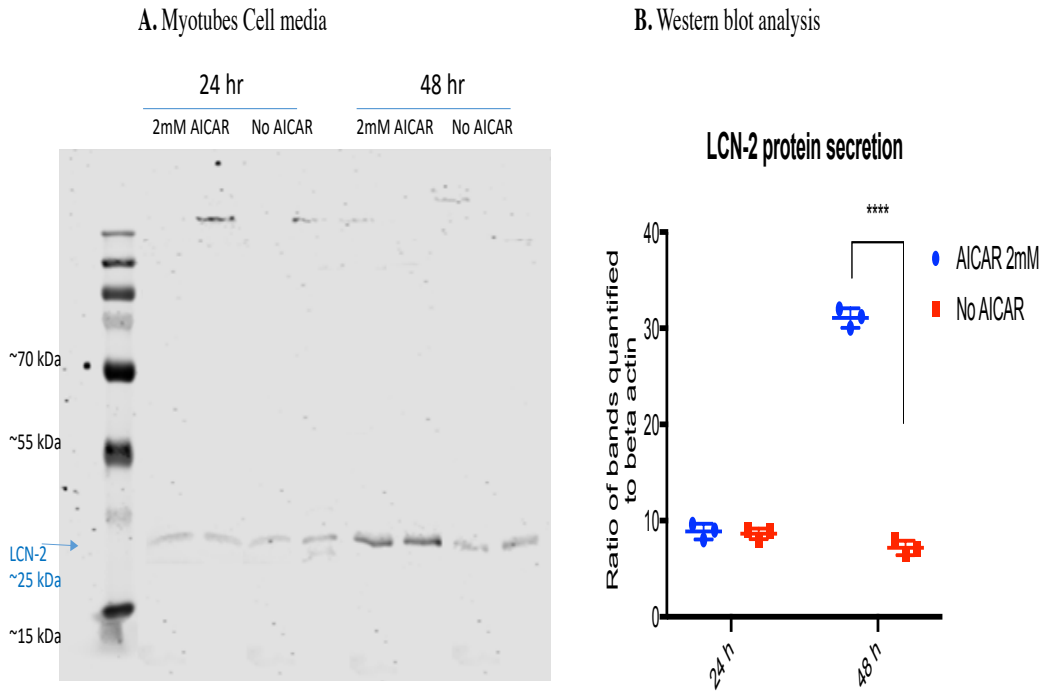

Figure 4.10. The effects of 2 mM AICAR on protein secretion of LCN-2 in C_2C_{12} myotubes. Cultured C_2C_{12} myotubes were treated with 2 mM AICAR for 24 h and 48 h. **A.** Representative western blot showing an increase of protein expression of LCN-2 post-24 h AICAR treatment in cell media. **B.** Western blot analysis of two independent experiments in C_2C_{12} myotubes. Cell media were collected and concentrated using a VIVA-spin column (MWCO 10k). Concentrated cell media were separated using 12% SDS-PAGE and transferred onto nitrocellulose membranes. Each membrane was reacted with Lipocalin-2 antibody and β.actin antibody, with the latter being used as a loading control. Statistically significant differences were: **** $p < 0.0001$ ((n=2, independent experiments - single biobsy derived from a healthy female donor with 21.05 BMI, myotubes were passaged two times and 3 well treatment conditions were used within each cell passage - see table 4.2 for descriptive data). Data are represented as mean ± SEM.

4.4 DISCUSSION

Exercise improves the performance of skeletal muscle in terms of insulin sensitivity, but its mechanisms remain unclear (Cartee *et al.*, 2015; 2016). Evidence from previous studies indicates that the activation of 5′ AMP-activated protein kinase (AMPK) might be exercise-induced, enhancing insulin sensitivity in skeletal muscle (Kjøbsted *et al.*, 2015; Cartee *et al.*, 2016; Kjøbsted *et al.*, 2016; 2017). It has also been proposed that both EPS and AICAR mimic the effect of muscle contraction on the AMPK pathway and, in turn, glucose transport (Merrill, Kurth, Hardie & Winder, 1997). Whilst AICAR does not stimulate muscle contraction directly, it has been shown that AICAR does affect glucose and lipid metabolism (Chen *et al.*, 2002; Spangenburg, Jackson, & Schuh, 2013; Brown, Jones, Walker, & Newton, 2015), and the secretion/regulation of myokines (Seldin, Peterson, Byerly, Wei, & Wong, 2012; Sánchez, Nozhenko, Palou, & Rodríguez, 2013; Paula *et al.*, 2015).

The focus of this chapter has been to use AICAR and EPS as an exercise-like treatments *in vitro* to explore the effects of EPS and AICAR on LCN-2 mRNA and protein expression, and therefore, their secretion levels by human skeletal muscle cells (myotubes). Firstly, we examined the expression and secretion of LCN-2 and the possibility of muscle contraction (EPS) post-2 h, -4 h and -16 h *in vitro* to stimulate LCN-2 expression. Our results indicate that LCN-2 is secreted into human myotube cell media with no detection of its protein presence inside myotube cell lysate post-16 h EPS. This suggests that LCN-2 has a potential exercise-induced effect and could also induce crosstalk effects on other metabolically active cells as other secreted factors do in response to exercise. On the other hand, the treatment of AICAR in skeletal muscle activates AMPK-a, specifically on Th172 ($pAMPK^{T172}$), as EPS does. Similarly, LCN-2 is secreted by C_2C_{12} myotubes in response to AICAR

treatment for 48 h. These findings highlight important aspects of LCN-2 expression in the two models used and show their effect on LCN-2 secretion into myotube cell media post-exercise-like treatments (EPS and AICAR).

LCN-2 was first noted in previous studies to be secreted by adipocytes, and since then, the role of LCN-2 as a new adipokine has been widely discussed (Aigner *et al.*, 2007; Mosialou *et al.*, 2018; Jaberi *et al.*, 2021). However, despite Lipocalin-2 protein being widely expressed in several tissues, its role has not been fully investigated in skeletal muscle (Rebalka *et al.*, 2018; Jaberi *et al.*, 2021). In Study 2, presented in this chapter, we investigated the protein expression of Lipocalin-2 in human hepatocytes, human liver tissue, adipocytes cells (3T3L1- cell), and C_2C_{12} and human myotubes cells without treatment or stimulation. Primary human skeletal muscles are a well-known model to study skeletal muscle *in vitro* and reflect human health (Turner *et al.*, 2020). We also used cell lines that are commonly used for *in vitro* studies focused on exercise and metabolism research.

The C_2C_{12} myoblast cell line represents the phenotypic disparities of myotubes, as established by Yaffe and Saxel (C_2C_{12} | ATCC, 2022). Compared to primary human myoblasts, C_2C_{12} myoblasts differentiate rapidly and produce characteristic muscle proteins (C_2C_{12} | ATCC, 2022). 3T3L-1 cells represent an *in vitro* model of white adipocytes to study adipocyte differentiation and metabolism (Morrison & McGee, 2015). This cell line can be used to learn more about the basic molecular pathways that cause diabetes, obesity, and other disorders. These cells were used to investigate the level of LCN-2 in cell lysates without stimulation or treatment (normal physiological conditions).

In our study, we examined LCN-2 protein expression in cells (adipocyte, hepatocytes, human/mouse myotubes) and human liver tissue demonstrated by

western blotting using cell lysates. We used 50 μg of total protein to load the same amount from all cell lysates along with 1:1000 concentration of LCN-2 primary antibody. The protein expression of LCN-2 differs with different band intensities among cells and tissue, perhaps relating to the tissue-specific role of LCN-2. However, the level of LCN-2 protein expression was demonstrated to be higher in human liver tissue. This higher level indicates that liver tissue is a potential main source of LCN-2 under normal physiological conditions. This result is in agreement with a study showing that LCN-2 is expressed in liver tissue and hepatocytes, but 40-50-fold increases of expression were analysed in this study post-bacterial infection (Xu *et al.*, 2015).

We also found that LCN-2 protein is expressed in adipocytes (3T3L-1) in a faint band, showing that adipocyte cells are similar to hepatocyte cells in this regard. A similar study has shown that LCN-2 expression is upregulated in diabetic and obese mice, with its concentrations positively correlated to adiposity and waist-to-hip ratio. This suggests a role for LCN-2 in obesity (Yan *et al.*, 2007). Importantly, in our western blotting results, we demonstrated the absence of LCN-2 protein levels in human myotubes, a finding which parallels the findings that were recorded previously in the Human Protein Atlas. Another study by Rebalka *et al.* (2018) confirms the absence of LCN-2; however, its expression was unregulated two days following injury in mouse skeletal muscle cells. The findings from this present study demonstrate different levels of LCN-2 expression in different cells and tissue, suggesting that human liver tissue is the main source and must be used as a positive control in all experimental setups in this thesis. The absence of LCN-2 expression in human myotubes could be related to the sensitivity of western blot. It may also suggest that LCN-2 regulates under stimulation or treatment in human skeletal

muscle since its role has not been fully investigated and is still unclear. Interestingly, in a study conducted by Ponzetti *et al.* (2021), the diaphragm, quadriceps and soleus were shown to be the most abundant sources of LCN-2 in mouse muscle but not EDL muscle, suggesting that the expression of LCN-2 in muscle may differ depending on the section of muscle.

Studies 2 and 3 in this chapter examined the expression of LCN-2 under exercise-like treatments/stimulations in skeletal muscle; EPS and AICAR. In Chapter 3, the study aimed to validate an exercise model *in vitro* using EPS in human/mouse skeletal muscle cells (myotubes), showing a significant increase in concentration of lactate in cell media, a reduction of glucose concentration in cell media, and up-regulation of PGC1-a and IL-6 mRNA expression. In addition, $AMPKa^{Th172}$ protein was phosphorylated post-16 h EPS.

Results showed that the up-regulation level of LCN-2 mRNA in C_2C_{12} mouse myotube cells post-16 h (EPS 16 h) in stimulated myotubes increased 50-fold compared to unstimulated cells (No EPS 16-h). As regards the up-regulation level of LCN-2 mRNA in C_2C_{12} mouse myotube cells after EPS stimulation (an *in vitro* exercise-like stimulus), it is possible that EPS upregulates the mRNA expression of LCN-2 in human myotubes. Therefore, the effect of an *in vitro* exercise model (EPS) on LCN-2 expression in human myotubes was evaluated. LCN-2 mRNA expression in human myotubes upregulated compared to unstimulated cells post EPS; its expression differing based on time. Human myotubes showed a 10-fold increase in synthesis of LCN-2 post-2 h EPS and 30-fold post-4 h compared to unstimulated myotubes. However, its expression declined 7-fold post-16 h.

The protein and secretion level of LCN-2 in and by skeletal muscle (myotubes) was also observed post EPS. In C_2C_{12} myotubes, cells expressed LCN-2 2-fold more

compared to unstimulated cells post-16 h EPS. However, its level of secretion significantly increased 50-fold. On the other hand, human myotubes did not express LCN-2 post-2 h, -4 h and -16 h EPS. The undetectable level of protein expression of LCN-2 in cell lysate of human myotubes post-2 h and -4 h EPS was due to the rise in mRNA level of expression not being high enough to be translated into protein. Once LCN-2 mRNA forms, synthesises and accumulates, it is transported outside the nucleus to cytoplasm and translated into LCN-2 protein, at which point it is secreted by skeletal muscle cell to perform a specific function. Thus, all LCN-2 protein secreted by human myotube cells post-16 h increased 3-fold compared to unstimulated human myotubes, explaining the decline in mRNA expression of LCN-2 post-16 h of EPS but not post-2 h or 4 h. Another possibilities of the undetectable level of protein expression of LCN-2 in cell lysate of human myotubes post-2 h and -4 h EPS could be that LCN-2 levels were very low in the cell lysate and thus western blot was not able to detect it.

This is the first time that the mRNA and protein expression of LCN-2 in skeletal muscle cells has been investigated and described post EPS stimulation. The outcomes evidenced are similar to those of other myokines, such as IL- 6, IL-8 and IL-15, which are known to be upregulated post-exercise. To be specific, the level of IL-6 in circulation has been shown to rise a 100-fold in response to acute exercise (Pedersen & Fischer, 2007). Our findings are also in line with studies by Damirchi, Rahmani-Nia and Mehabani (2011) and Ponzetti *et al.* (2021), which have shown the increased level of LCN-2 in circulation post acute exercise training in obese participants compared to normal participants. Another study by Nakai *et al.* (2021) demonstrated that LCN-2 circulation level did not change with long-term endurance exercise or diet, indicating its stability over 12 weeks of exercise and adherence to

the NASH diet. These results suggest that LCN-2 expression in circulation is related to the intensity and duration of exercise since papers have shown increases post short duration exercise, not long duration exercise. Lines of evidence indicate the role of LCN-2 in inflammation and energy homeostasis since its expression increases after LPS, TNFa and IL-1b treatment in a variety of tissues (Aigner *et al.*, 2007; Chen *et al.*, 2007; Yan *et al.*, 2007). This finding suggests the increased level of LCN-2 post exercise could be related to reduced instances of health disorders in nearby tissues. In sum, the EPS effects on LCN-2, and the up-regulation level of mRNA and protein post-exercise-like stimulus (EPS) suggest that LCN-2 is a novel myokine secreted by skeletal muscle in a time-dependant manner.

Phosphorylated AMPK was studied in Chapter 3 post-16 h EPS, and in this chapter, we showed that AMPK was activated by AICAR at time points of 15 min, 30 min and 60 min. That said, its expression only increased slightly after 60 min of AICAR treatment in C_2C_{12}. On this basis, skeletal muscle EPS-phosphorylated AMPK, synthesised and secreted LCN-2, and the relation between the AMPK pathway and LCN-2 should be further explored.

The role of AMPK in stimulating the expression and secretion of myokine, as well as identifying novel myokine, is supported by the literature. First, the production of myokine IL-15 decreased in mouse models (KO, a β1 and β2 AMPK sub-units) in skeletal muscle (Marcinko & Steinberg, 2014). AMPK agonist has also been shown to activate several metabolic genes in skeletal muscle and induce change post-endurance exercise by ~ 2-fold as compared to a control (Narkar *et al.*, 2008). Additionally, activation of AMPK in human models has been shown to trigger fibre-type switching post-exercise in skeletal muscle (Lee-Young, Canny, Myers, & McConell, 2009; Magnoni, Palstra, & Planas, 2014). However, despite researchers

having noted a possible relationship between the AMPK pathway and myokine secretion or production, we should mention that a study by Marcinko and Steinberg (2014) found that IL-d does not change in KO mice of AMPK sub-units.

In our study, we questioned whether AMPK activation following AICAR treatment induces LCN-2 expression and secretion. To answer this question, 2 mM of AICAR was used to treat C_2C_{12} myotubes. We found that LCN-2 protein expression in C_2C_{12} cell lysate was undetectable after 48 h of AICAR treatment; however, its expression was detected after 24 h. In cell media of C_2C_{12} myotubes, LCN-2 did not secrete after 24 h AICAR treatment, but was all secreted after 48 h, despite its secretion level being 4-fold higher than untreated cells (No AICAR). Even though we were able to show synthesis and secretion of LCN-2 by skeletal muscle in response to exercise-like stimuli (EPS, AICAR), its effects on other tissues, such as adipose, need to be investigated to be able to characterise LCN-2 as a novel myokine.

Identification of novel myokines secreted by skeletal muscle is essential to understand the communication between muscle and other tissues such as liver and adipose. Therefore, in Chapters 4 and 5, we focused on modelling the expression of Lipocalin-2 (a novel exercise-induced myokine) using a doxycycline-inducible vector system to understand its contribution in an endocrine fashion, specifically between muscle and adipose.

Chapter 5: Overexpression of LCN-2 and PGC1-a and the Effect of PGC1-a Overexpression on LCN-2 Secretion

5.1 INTRODUCTION

With the rising risk of metabolic syndrome and related comorbidities, it is more critical than ever to fully understand the endocrine signals that traverse metabolically active tissues, such as adipose tissue and skeletal muscle, and how this crosstalk could affect metabolism. The metabolic function of LCN-2 in the body is being understood to be increasingly complex as evidence is found, revealing the diversity of tissue-specific secretion of LCN-2 into plasma. Myokines, when secreted in response to exercise, are hypothesised to exert anti-inflammatory effects and mediate beneficial effects of exercise (Pedersen & Febbraio, 2008). With evidence pointing towards LCN-2 as an exercise-induced myokine in human skeletal muscle, the goal of this research is to prompt overexpression of LCN-2 from human skeletal muscle *in vitro* to aid an understanding of the role of LCN-2 as a new myokine in crosstalk with adipose tissue; specifically on lipolysis and lipid accumulation.

The gateway cloning method is a universal approach that permits efficient transfer of DNA sequences into various types of vector systems using a doxycycline-inducible lentiviral vector to facilitate either LCN-2 or PGC1-a expression (Landy, 1987). It is now appreciated that skeletal muscle secretes a variety of proteins that influence various metabolic parameters – including proteins that are also known to be secreted from adipose tissue – and that modulate adipocytokine effects within the

body (Guo *et al.*, 2010; Huh, 2018). These include factors that have been found to promote insulin sensitivity, as well as others that induce insulin resistance.

In this study, an inducible lentiviral vector allowing LCN-2 and PGC1-a overexpression was constructed to model their expression and secretion *in vitro* in skeletal muscle. The structure of LCN-2 comprises one N-glycosylation and one intra-chain disulfide link (Bandaranayake *et al.*, 2011). It was important for this study to mimic the expression of LCN-2 in human myotubes to retain the LCN-2 protein in its native structure, with accurate post-translational modifications that are necessary for its release by myotubes cells. Since myotube cells are non-proliferative, the lentiviral vector gene delivery method was chosen for this study due to its ability to infect both dividing and non-dividing cells. We previously observed the secretion of endogenous LCN-2 by skeletal muscle into cell media from cultured rat myotubes. In line with this, our pilot study revealed the up-regulation of LCN-2 post-eccentric exercise in human skeletal muscle tissue *in vivo* (pilot study), suggesting a role of this protein as an exercise-induced myokine.

PGC1-a expression and post-translational modification have previously been shown to be upregulated by the major signalling pathways that are activated in response to muscle fibre contractions (Schnyder & Handschin, 2015). Though studies have indicated that myokines are primarily regulated by contractile activity (Kostrominova, 2016), the mechanism that regulates the secretion level of myokines and their effects on whole body metabolism are not fully understood. A useful method to investigate the regulation of myokines in response to exercise is to model the phenotype of trained muscle cells in an exercise model *in vitro*. PGC1-a is responsible for coordinating the programming of gene expression, resulting in an endurance-trained muscle phenotype. The mouse genome has also been shown to

recruit PGC1-a to over 7500 distinct sites in muscle cells, inducing 984 and inhibiting 727 genes (Lin *et al.*, 2004). In transgenic mice, when PGC1a is overexpressed in muscle, a trained phenotype is observed (Wu *et al.*, 2002). However, when PGC1a is knocked out, mouse models show reduced capacity for endurance exercise (Handschini *et al.*, 2007). Additionally, numerous research papers indicate the upregulation and activation of PGC1-a in response to acute and regular exercise in skeletal muscle, considered to be vital to prompt exercise-induced effects (Ruth, 2012; Roberts *et al.*, 2014). Additionally, mitogen-activated protein kinase (MAPK) p38 and adenosine monophosphate-activated protein kinase (AMPK) are known to induce PGC-1α expression during exercise (Jäger *et al.*, 2007), and there is evidence to suggest that the PGC1a transcription factor and AMPK mediate the secretion of myokines by skeletal muscle in response to contractile activity (Karlsson *et al.*, 2020).

5.2 AIMS OF THIS CHAPTER

This chapter describes our attempts to model the expression of LCN-2 in the cel lysate and its secretion to characterise the role of LCN-2 as a novel myokine, with evidence highlighting the release of LCN-2 into cell media of both cultured C_2C_{12} and human skeletal muscle *in vitro*. On the other hand, we examined the secretion of LCN-2 into skeletal muscle cell media following PGC1-a overexpression since it has been shown that mRNA expression of LCN-2 is upregulated in C_2C_{12} myotube cells (Deis *et al.*, 2019). Our objectives of this chapter were to model and assess the construction and overexpression of the protein, and the specific aims are as follows:

- Validate the successful cloning and construction of LCN-2 and PGC1-a into pINDUCR20 lentiviral-inducible vector using Agarose Gel Electrophoresis.
- Investigate the expression of green fluorescence protein (GFP) following lentiviral transduction of cells including MDA-MB-468, C_2C_{12} and human myotubes using a fluorescence microscope.
- Investigate LCN-2 overexpression and secretion following lentiviral transduction in MDA-MB-468 as an initial transduction of the lentiviral using western blotting.
- Investigate the overexpression of LCN-2 in both cultured C_2C_{12} and human myotubes using western blotting.
- Investigate PGC1a overexpression in C_2C_{12} myotubes.
- Investigate LCN-2 secretion into myotubes cell media in response to PGC1-a overexpression.

Several controls were used for our qPCR and western blot experiments, as described below:

1. pINDUCER20, an empty vector.
2. Either pINDUCER20-LCN-2 or pINDUCER20-PGC1a No.DOX; non-inducible genes.
3. Untransduced cells as a negative control for the transduction.

5.3 RESULTS

5.3.1 Myotubes Cell Cultures and Their Donor

Myotube cultures were established from a total of n = 1 individual, female, healthy adult. Descriptive donor data is presented in Table 5.1. The experiments performed in an independent donor, and repeats was determined principally by the number of myoblasts passaged, since cultures were restricted to no more than three passages to best preserve any effects of donor phenotype (independent experiments n=3 based on a single biopsy derived from a human donor. Cells were passaged three times or two times, as shown in Figure 5.12). Within an independent experiment, multiple treatment replicates were performed (i.e., the use of 3 treatment replicates meant 3 wells of cells from each independent experiment were exposed to each treatment condition). All reported n values are the number of independent experiments n=3.

Table 5.1

Characteristic Data for Skeletal Muscle Biopsy Donor from Whom Myotube Cultures Were Derived.

Sex	Age (y)	Mass (Kg)	Height (m)	BMI	Fasting Glucose (mmol/L)	Biopsy yield (mg)
Female	19	62.5	1.756	20.268938	4.63	~150mg

5.3.2 Successful Cloning, Construction, and Insertion of LCN-2 into an Inducible Lentiviral Vector (pINDUCER20-LCN-2)

PCR products were generated to create entry clones with the *LCN-2* gene using *att*B primers flanked by LCN-2. Sites of *att*B were incorporated into the LCN-2 PCR product to enable the recombination with the *att*P site that contained donor vector pDONR221. The *LCN-2* gene is approximately 700 bp in length, and electrophoretic analysis of PCR products successfully displayed a band at approximately 750 bp, which corresponds to the length of *att*B-LCN-2 (Figure 5.1 **A**). Transformation of pDONR221-LCN-2 into a suitable *rec*A *E. coli* strain was performed to allow selection of entry clones. *Rec*A negative *E. coli* strains were used for transformation to prevent vector instability due to recombinational repair of long repeats within the plasmid sequence. Colony PCR amplification of entry clone inserts u M13 primers (see Chapter 2, section 2.27) was carried out to ensure the correct LCN-2 sequence was inserted into the vector (Figure 5.1 **B**).

We chose pINDUCER20 as our destination vector for the overexpression of LCN-2 in skeletal muscle cell (myotubes) as it provides a rapid and doxycycline-inducible overexpression vector system. Following my successful generation of entry clones and destination vector (see Chapter 2, section 2.28), the expression clone of pINDUCER20-LCN-2 was then transformed into a suitable *rec*A *E. coli* strain, and the fragment of LCN-2 was amplified using colony PCR (Figure 5.1 **C**) with LNCX and PIND20 primers, as explained in Chapter 2, Section 2.31.

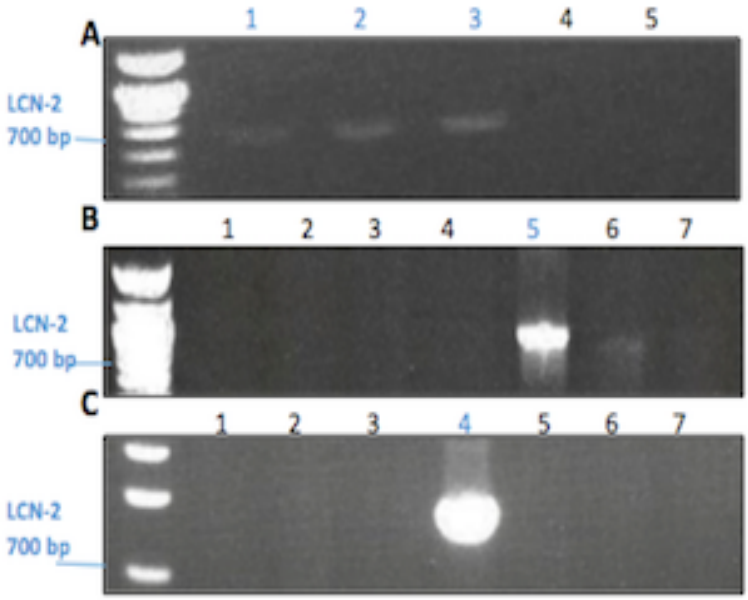

Figure 5.1. Electrophoresis analysis of lentivirus vector construct (pINDUCER20-LCN-2). **A.** Agarose gel (1%) showing PCR amplification of the Lipocalin-2 (LCN-2) gene at approximately 750 bp using attB-primers (Lanes 1-3). **Lane 4:** No template cDNA control PCR reaction. **Lane 5:** No DNA polymerase enzyme control PCR reaction. **B.** Agarose gel (1%) showing colony PCR products resulting from transformation of TOP10 E. coli with entry clone generated from the BP reaction (lanes 1-7). pDONR221-LCN-2 was successfully transformed into colonies represented in lane 5. **C.** Agarose gel (1%) showing colony PCR products resulting from transformation of Stbl3 E. coli with pINDUCER20-LCN-2 generated from the LR reaction (lanes 1-7). pINDUCER20-LCN-2 was successfully transformed into the colony represented in lane 4, as explained in Chapter 2, Section 2.31.

5.3.3 Validating the Optimal Transduction of GFP Overexpression in the MDA-MB-468 Cell Line (pINDUCER20-GFP)

The efficiency of GFP transduction was first tested in the MDA-MB-468 cell-line as a preliminary experiment to overexpress GFP in cells. The results from this experiment were used to determine the optimal amount of lentivirus to be used, whereby more than 85% of the cells expressed the target protein. Cells were infected with pINDUCER20-eGFP and imaged. GFP in the cytoplasm was observed in almost all cells using a fluorescence microscope. These served as a positive control for the transduction of lentiviral post-48 h. The optimal amount of lentivirus was 700 µL for the MDA-MB-468 cell-line, which was used later for transduction of the

pINDUCER20-LCN-2 lentiviral vectors to overexpress LCN-2 protein and therefore secrete LCN-2 into MDA-MB-468.

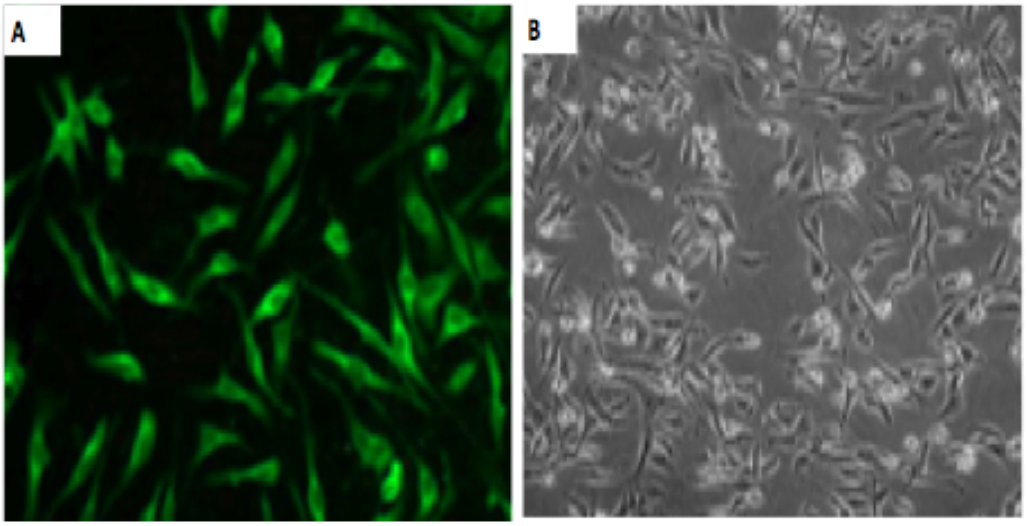

Figure 5.2. Overexpression of GFP (eGFP) in the MDA-MB-468 cell-line. Monitoring of the transduction efficiency in MDA-MB-468 cells using light and fluorescence microscopy. **A.** GFP fluorescent protein expressing in MDA-MB-468 cell-line using 700 µL of lentivirus checked post-48 h. **B.** Bright field of MDA-MB-468 post-48 h of transduction. Fluorescence images were acquired using a wide-field Zeiss 200M florescence microscope (scale bar is 100 **µ**m).

5.3.4 LCN-2 is Overexpressed and Secreted by the MDA-MB-468 Cell Line

Transduction was carried out in MDA-MB-468 cells with 700 µL of the lentiviral stock containing pINDUCER20-LCN-2 growth medium. After 48 hr of treatment with doxycycline, cells were lysed and media were collected for western blot analysis, which was performed to test for the presence of LCN-2 (see Figure 5.3). A band is present at approximately 25 kDa in cell lysates infected with pINDUCER20-LCN-2, and a faint band from samples infected with lentivirus containing control plasmids, confirming that the lentiviral construct can be used to successfully transduce the *LCN-2* gene and induce overexpression of LCN-2 protein (Figure 5.3 **A**). The presence of a band for LCN-2 in samples containing the

corresponding cell medium also confirms that the protein is secreted from MDA-MB-468 cells (Figure 5.3 **C**).

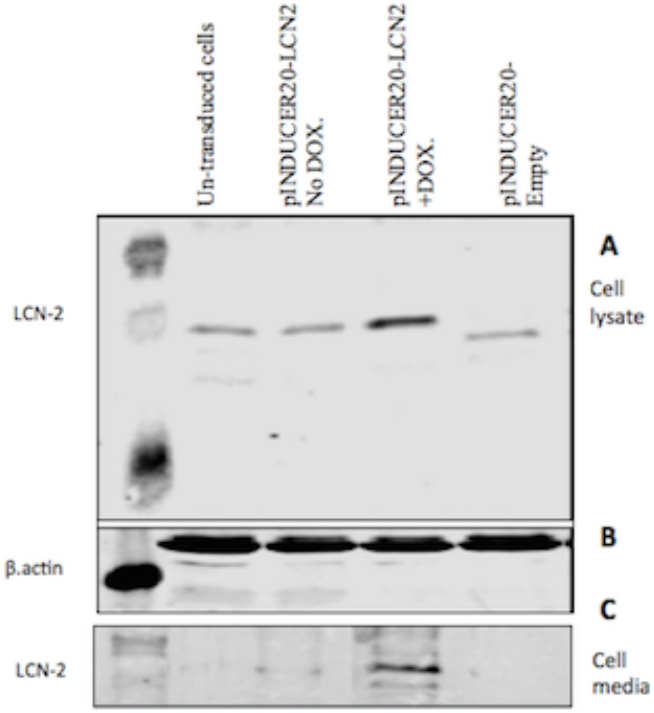

Figure 5.3. Representative western blot shows successful expression and secretion of Lipocalin-2 (LCN-2) in the MDA-MB-468 cell-line. Samples are pINDUCER20-LCN-2+Dox (Doxycycline, 1ug/ml); pINDUCER20-LCN-2-Dox (without Doxycycline); pINDUCER20 (an empty vector); and untransduced cells, which served as a negative control. **A.** LCN-2 is expressed in cell lysate**. B.** loading control (β. actin). **C.** Cell media presented a band to confirm the secretion of LCN-2 by MDA-MB-468. β.actin was used as a loading control. MW of LCN-2 is ~25 kDa and β. actin is 45 kDa.

5.3.5 Validating the Optimal Transduction of GFP Overexpression in C_2C_{12} Skeletal Muscle Cells (Myotubes) (pINDUCER20-GFP)

The transduction C_2C_{12} myotube cells was carried out using the same protocol as with MDA-MB-468 – with lentiviral stock (pINDUCER20-eGFP) – and results were validated using a fluorescence microscope. It was shown that these cells expressed GFP post-48 h, and the optimal amount of lentivirus stock was 700 µL (see Figure 5.4).

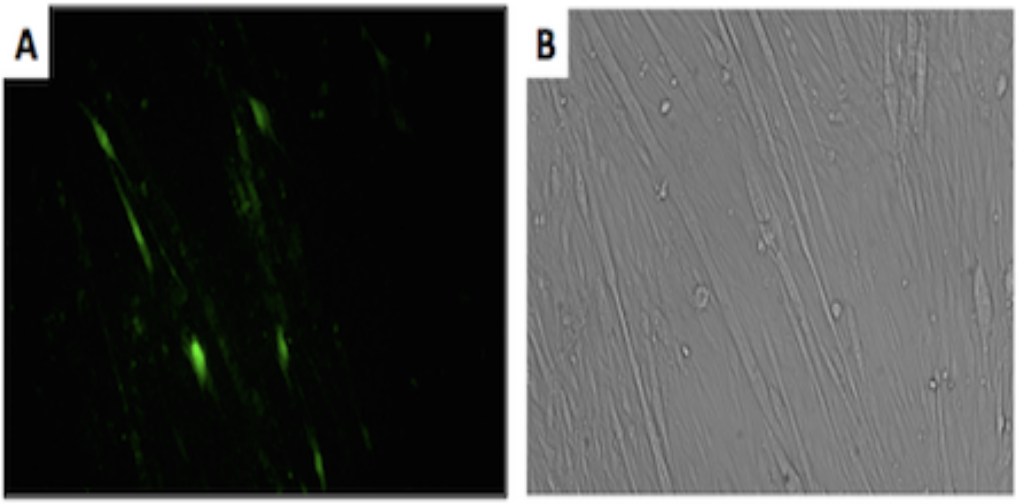

Figure 5.4. Lentiviral transduction (Infection) of GFP in C_2C_{12} murine myotubes. Monitoring of the transduction efficiency of GFP in mouse myotubes C_2C_{12} using fluorescence and light microscopy **(A, B)** respectively. Cells were transduced with different amounts of lentivirus, all expressing GFP. This image represents 700 µL used for the successful transduction of pINDUCER20-GFP post-48 h (positive control of the experiment). Images were acquired using a wide-field Zeiss 200M florescence microscope (scale bar is 100 **µ**m).

5.3.6 LCN-2 is Overexpressed and Secreted by C_2C_{12} Myotubes Using Lentiviral (pINDUCER20-LCN-2)

For LCN-2 to act as a myokine, exerting effects in an endocrine fashion, it must be secreted first by skeletal muscle cells (myotubes) into the cell media (CM). We observed lentiviral-mediated LCN-2 expression and secretion into human myotubes; its overexpression was seen in C_2C_{12} myotubes induced with 1 µg/ml of doxycycline for 48 hr following transduction of myotubes with lentivirus containing pINDUCER20-LCN-2. LCN-2 protein overexpression and secretion into C_2C_{12} myotubes was confirmed using western blotting experiments, with results showing a band in the cell lysate and cell media, confirming its overexpression and secretion by C_2C_{12} myotubes. These results demonstrate that 700 µL of lentivirus was able to secrete LCN-2 from myotubes when overexpressed.

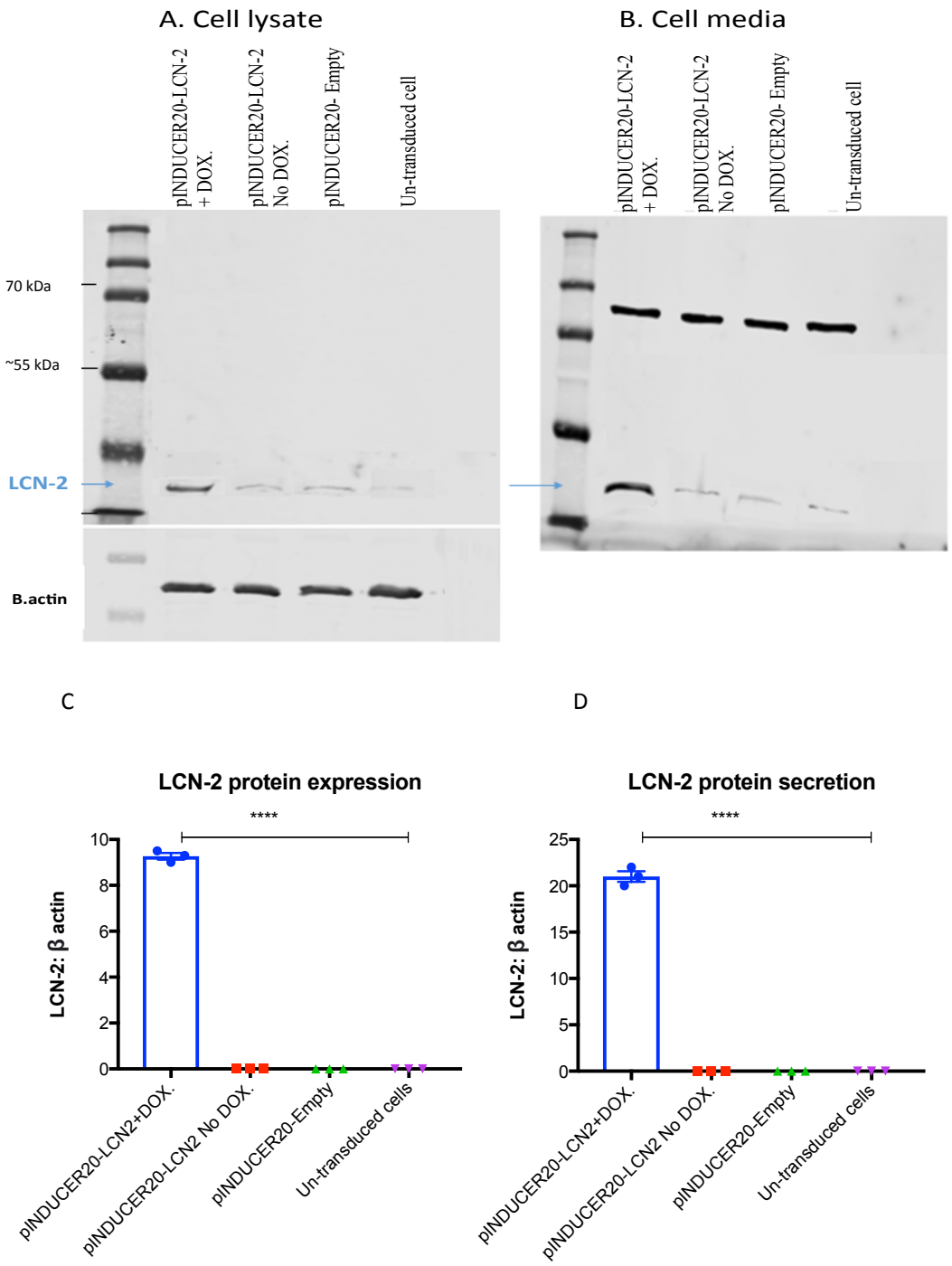

Figure 5.5. Representative blot of lentivirus transduction for the overexpression and secretion of Lipocalin-2 (LCN-2) from C_2C_{12} myotubes. Cells were transduced with pINDUCER20-LCN-2 at varied concentrations (600 µL, 1200 µL and 2400 µL). Protein samples were collected post-48 h and lysed in RIPA buffer with protease and phosphatase inhibitor. Cell culture media were collected and centrifuged for cell debris removal. Cell media were then concentrated using a Viva-spin column (MWCO 10k). **A**. Cell lysate. **B**. Cell culture media. The western blot experiment revealed overexpression and secretion of Lipocalin-2 by C_2C_{12} myotubes. Samples are pINDUCER20-LCN-2+Dox. (with the induction of Doxycycline 1 µg/ml); pINDUCER20-LCN-2-Dox (without the induction of Dox.); pINDUCER20 (empty vector); untransduced cells served as a negative control. Various concentrations were used of the lentivirus stock. All results are the same, with no difference between amount of virus that was used. MW of LCN-2 is ~25kDa and β.actin is 45 kDa. **C** and **D** represent densitometry analysis of LCN-2 expression and secretion respectively. Results are represented as mean ± SEM (****p>0.0001 n=3 independent experiments (see section 5.5.1 for more details).

5.3.7 Validating the Optimal Transduction of GFP Overexpression in Human Primary Skeletal Muscle Cells (Myotubes) (pINDUCER20-GFP)

Repeating the GFP experiment in primary myotube cells as opposed to the cell-line increased the reproducibility of the experiment. Myotube cells were infected with lentivirus containing pINDUCER20-GFP and induced with doxyxycline (DOX.) on day five for 48 hr. The cells were imaged using a wide-field Zeiss 200M florescence microscope for GFP cytoplasm overexpression (see Figure 5.6). GFP overexpression is observed by the presence of green flouresence in the cytoplasm of human myotubes.

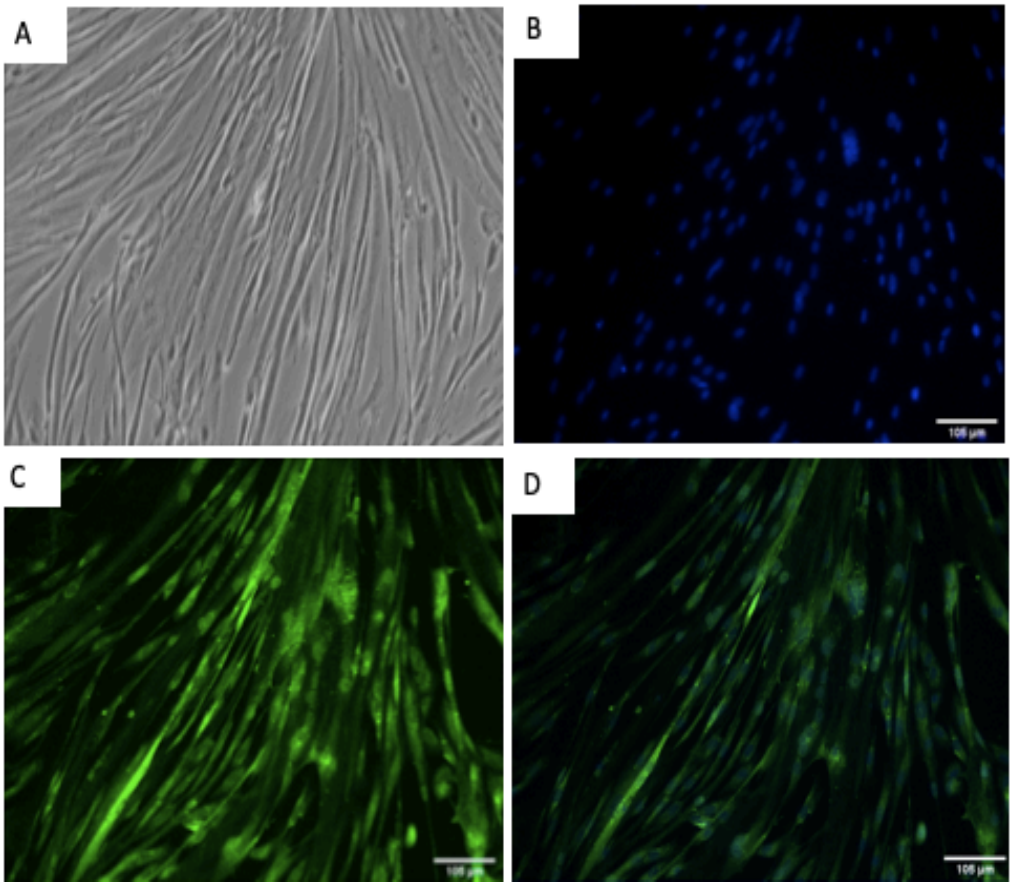

Figure 5.6. Lentiviral transduction (infection) of GFP in human skeletal muscle (myotubes). Monitoring of the transduction efficiency of GFP in human myotubes using fluorescence and light microscopy. Cells were transduced with different amount of lentivirus, all expressing GFP. This image represents 700 µL used for the successful transduction of pINDUCER20-GFP post-48 h (positive control of the experiment). Images were acquired using a wide-field Zeiss 200M florescence microscope (scale bar is 100 **µ**m). **A.** Bright field image. **B.** DAPI staining. **C.** GFP. **D.** Merged image.

5.3.8 LCN-2 mRNA Overexpression in Human Primary Skeletal Muscle Cells (Myotubes)

pINDUCER20 was used as a plasmid, a doxycycline-inducible lentiviral vector in which our chosen gene could be inserted and induced. Human skeletal muscle cells (myotubes) were infected and treated on day five with 1ug/ml DOX. (doxycycline) for 48 h. the mRNA and protein expression of LCN-2 was determined using real-time qPCR and western blotting experiments respectively. The expression of LCN-2 mRNA was detected and shown to be overexpressed by more than 6000-fold as compared to other controls.

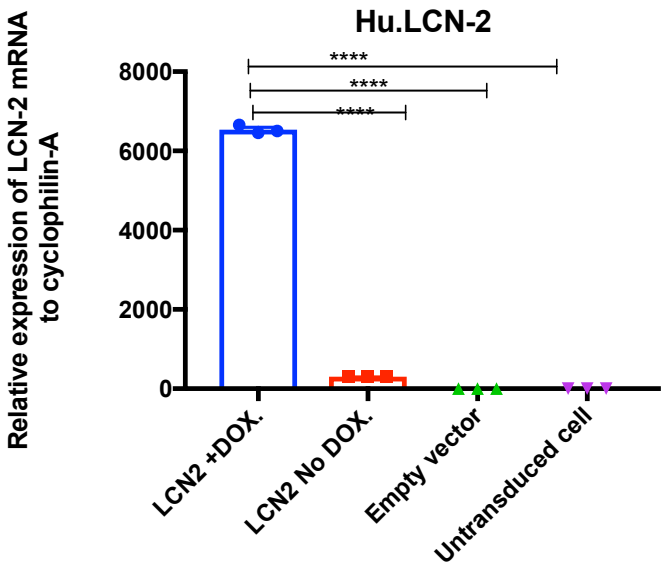

Figure 5.7. RT-PCR (qPCR) analysis following lentivirus transduction (infection) on human myotubes. Samples are pINDUCER20-LCN-2+Dox. (with the induction of Doxycycline 1 µg/ml); pINDUCER20-LCN-2-Dox (without the induction of Dox.); pINDUCER20 (empty vector); untransduced cells served as a negative control. qPCR results show the upregulation of LCN-2 mRNA expression. Cyclophilin-A was used as a normalisation gene. Data is represented as mean ± SEM (**** $p<0.0001$, n=3 independent experiments (see section 5.5.1 for more details)). Hu.LCN-2 means human Lipocalin 2.

5.3.9 LCN-2 Protein is Overexpressed and Secreted by Human Primary Skeletal Muscle Cells (Myotubes)

Human skeletal muscle cells were transduced and treated with 1ug/ml DOX. (doxycycline) for 48 h. LCN-2 mRNA and protein expression were determined using real-time qPCR and western blotting respectively. Protein expression in human skeletal muscle cells (myotubes) was detectable with 1 μg/ml (Figure 5.8). The expression was increased with a doxycycline concentration used to induce LCN-2 protein expression. To confirm that doxycycline-induced LCN-2 in human myotubes was able to secrete LCN-2 into skeletal muscle media, cell media (CM) was evaluated with western blotting, and we were able to detect the secretion level from the cell. 45 μl of cell culture media was loaded into each well. Anti-LCN-2 antibody was used to detect the protein level of LCN-2 in cell lysate and cell media. The results of western blotting demonstrated bands at a molecular weight of 25 kDa.

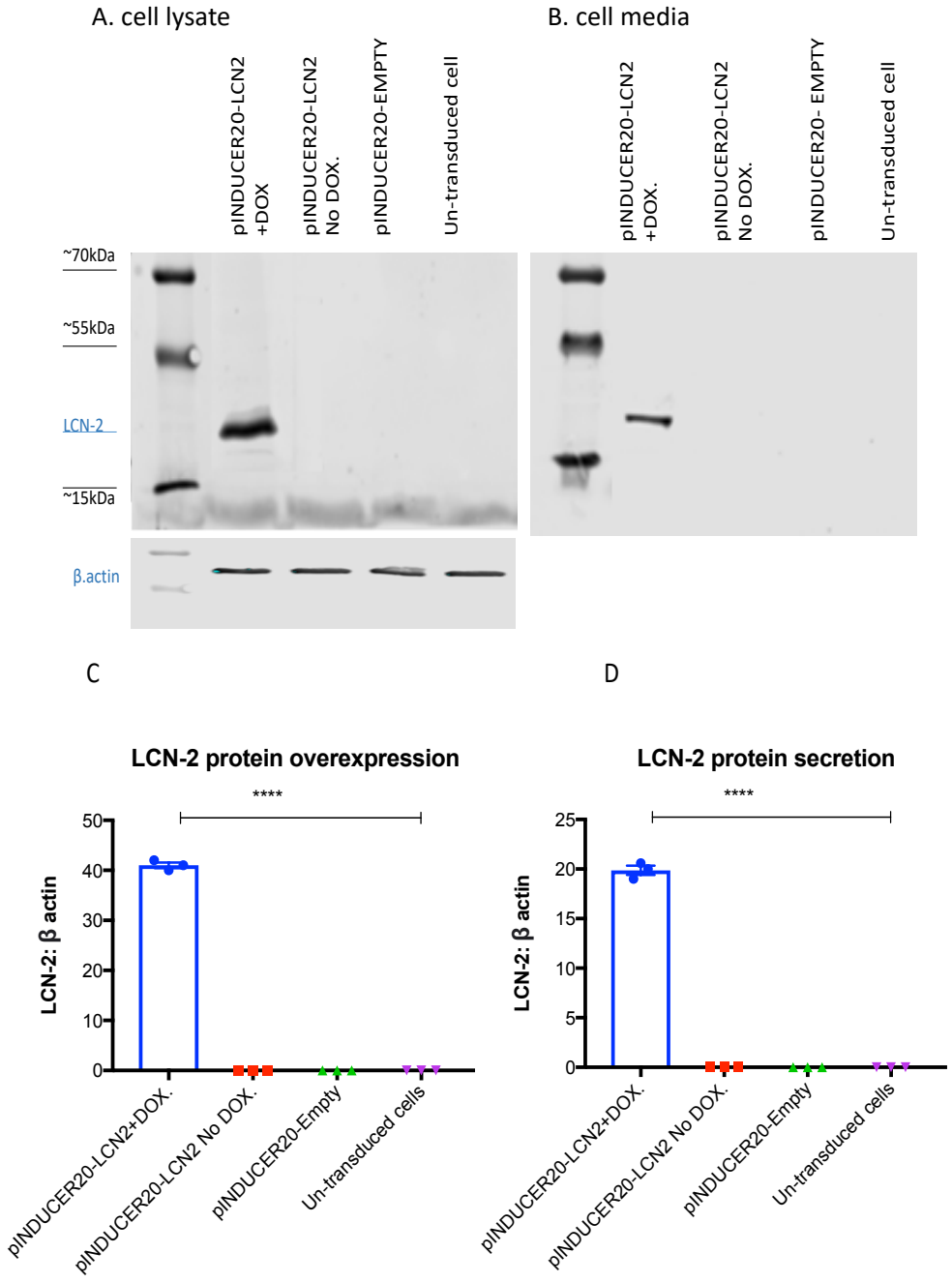

Figure 5.8. Representative blot of lentivirus transduction (infection) for the expression and secretion of Lipocalin-2 (LCN-2) from human myotubes. Cells were transduced with pINDUCER20-LCN-2+Dox. (with the induction of Doxycycline 1 µg/ml); pINDUCER20-LCN-2-Dox (without the induction of Doxycycline 1ug/ml); pINDUCER20 (empty vector), and untransfected cells served as a negative control. **A.** Cell lysate. **B.** Cell culture media. Western blot experiment was used to assess transfection efficiency in cell lysate **A** and in cell media **B** and produced 15 ml. 600 µL of the virus was used to produce more media overexpression of Lipocalin-2. Lipocalin-2 was overexpressed and secreted by human myotubes. MW of LCN-2 is ~25 kDa and β.actin is 45 kDa. **C** and **D** are densitometry analysis of LCN-2 expression and secretion respectively. Results are represented as mean ± SEM **LCN2 +DOX** sample has a P value of p<0.0001 (noted on the graph with ****), n=3 independent experiments (see section 5.5.1 for more details).

5.3.10 Successful Cloning, Construction, and Insertion of PGC1-a into an Inducible Lentiviral Vector (pINDUCER20-PGC1a)

The sample used to generate *att*B PCR product was plasmid #10974 for mammalian expression of PGC1-a, sourced from the Addgene website (**https://www.addgene.org/10974/**). PCR products were generated to create entry clones with the *PGC1-a* gene using *att*B primers flanked with PGC1-a. Sites of *att*B were incorporated into the PGC1-a PCR-product to enable the recombination with the *att*P site containing donor vector pDONR221. PGC1-a was approximately 3 Kb in length, and electrophoretic analysis of PCR products successfully provided a band at approximately ~3 Kb, which corresponds to *att*B-PGC1a (Figure 5.2 **A**).

Transformation of pDONR221-PGC1a into a suitable *rec*A *E. coli* strain was performed to allow selection of entry clones. Colony PCR amplification of entry clone inserts using M13 primers (see Chapter 2, section 2.31) was carried out to ensure that the correct PGC1a sequence was inserted into the vector (Figure 5.1 **B**). The expression clone of pINDUCER20-PGC1a was transformed into a suitable *rec*A *E. coli* strain, and the fragment of PGC1a was amplified using colony PCR (Figure 5.1 **C**) using LNCX and PIND20 primers, as explained in Chapter 2.

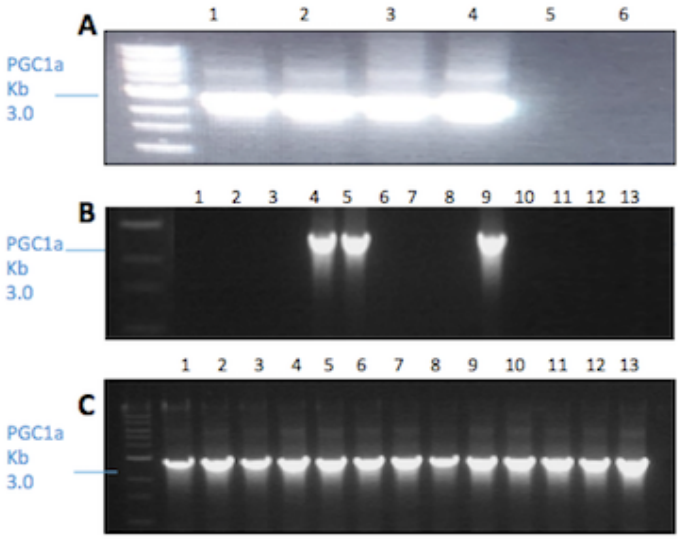

Figure 5.9. Electrophoresis analysis of lentivirus vector construct (pINDUCER20-PGC1a) **A.** Agarose gel (1%) showing PCR amplification of the *PGC1a* gene at approximately 2.5 kb using attB-primers (Lanes 1-4). **Lane 5:** No template cDNA control PCR reaction. **Lane 6:** No DNA polymerase enzyme control PCR reaction. **B.** Agarose gel (1%) showing colony PCR products resulting from transformation of TOP10 *E. coli* with entry clones generated from the BP reaction (lanes 4, 5 and 9). pDONR221-PGC1a was successfully transformed into colonies represented in lanes (4, 5 and 9). **C.** Agarose gel (1%) showing colony PCR products resulting from transformation of Stbl3 *E. coli* with pINDUCER20-PGC1a generated from the LR reaction (lanes 1-13). pINDUCER20-PGC1a was successfully transformed into the colony represented in all lanes from 1-13.

5.3.11 PGC1-a mRNA Overexpression in C_2C_{12} Skeletal Muscle Cells (Myotubes)

On day five, C_2C_{12} (myotubes) were infected and treated with 1 µg/ml DOX. (doxycycline) for 48 h (lentivirus production detailed in chapter 2, section 2.31). The mRNA and protein expression of PGC1a was determined using real-time qPCR and western blotting experiments respectively. The expression of PGC1a was detected and shown to be overexpressed by more than 1000-fold compared to other controls.

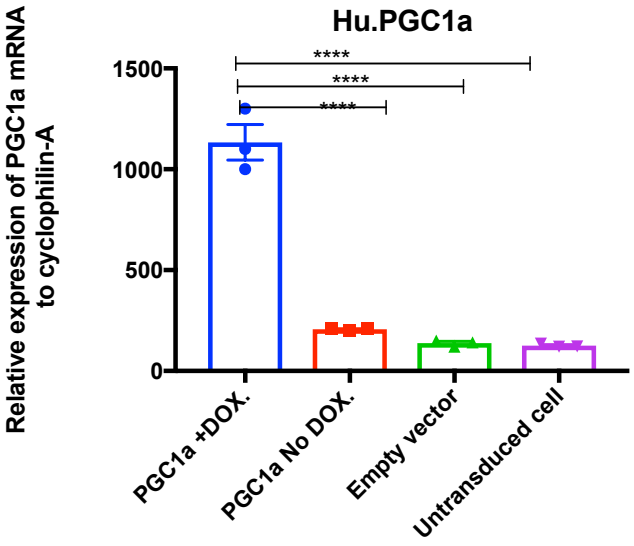

Figure 5.10. RT-PCR (qPCR) analysis following lentivirus transduction (infection) on C_2C_{12} myotubes. mRNA expression of pINDUCER20-PGC1a with DOX upregulated more than 1000-fold (**** $p<0.0001$). Data are represented as mean ±SEM. Cyclophilin-A was used as a normalisation gene.

5.3.12 PGC1-a Protein is Overexpressed by C_2C_{12} Skeletal Muscle Cells (Myotubes)

Following the transduction of human myotubes with 600 µL of pINDUCER20-PGC1a lentivirus, protein expression of PGC1a was determined by western blotting. Protein expression of PGC1a in human skeletal muscle cells (myotubes) was detectable with 1 µg/ml DOX and gave a band at the expected size (see Figure 5.11). The expression increased with the 1 µg/ml doxycycline that was used to induce and overexpress protein.

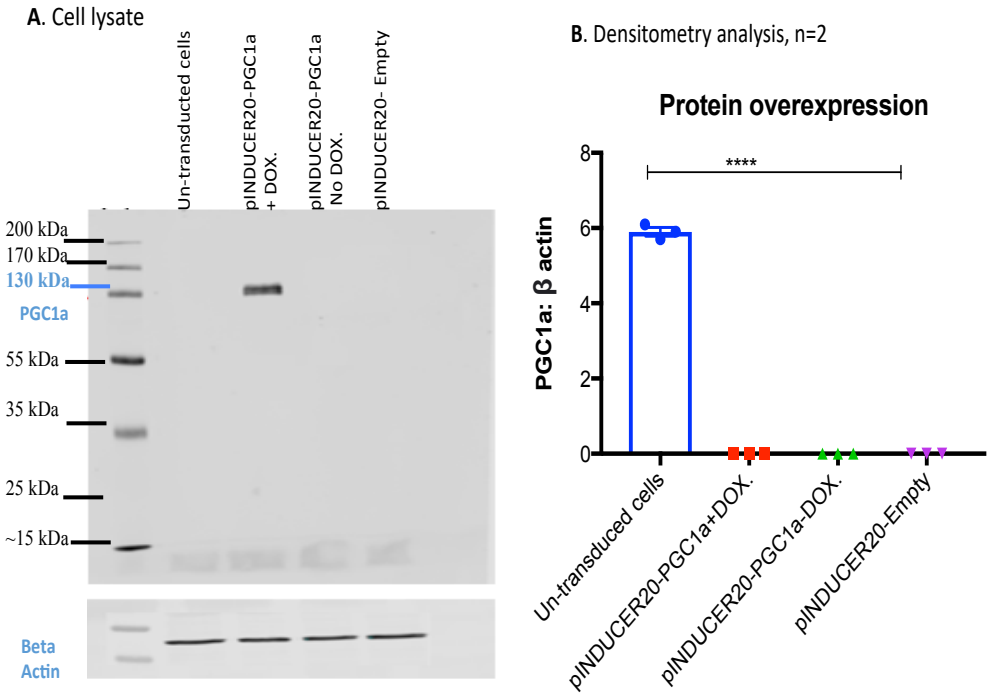

Figure 5.11. Representative blot of lentivirus transduction (infection) on C_2C_{12} myotubes for PGC1a overexpression. Cells were transduced with pINDUCER20-PGC1a+Doxycycline at 1 ug/ml); pINDUCER20-PGC1-a (without the induction of Dox.); pINDUCER20 (empty vector); and untransduced cells served as a negative control (600 µL of the viral stock were used) and samples were collected post-48 h. PGC1a was overexpressed by murine myotubes. MW of PGC1a is ~130 kDa and β.actin is 45 kDa. **B.** is densitometry analysis of PGC1a expression. Results are represented as mean ± SEM ****p<0.0001, n=3 independent experiments (see section 5.5.1 for more details).

5.3.13 LCN-2 is Secreted by C_2C_{12} Skeletal Muscle Cells (Myotubes) in Response to PGC1a Overexpression

To investigate possible LCN-2 protein secretion in cell media associated with overexpression of PGC-1α in skeletal muscle, we infected C_2C_{12} myotubes with 700 µL of pINDUCER20-PGC1a lentivirus on day five for 48 h. The effects of PGC1a overexpression upon secretion of LCN-2 in myotubes was then investigated. Western blotting results reveal that secretion levels of LCN-2 increased (as shown in Figure 5.12) compared to other controls. Results also indicated that PGC1a overexpression releases LCN-2 from skeletal muscle by 1.4-fold as compared to controls.

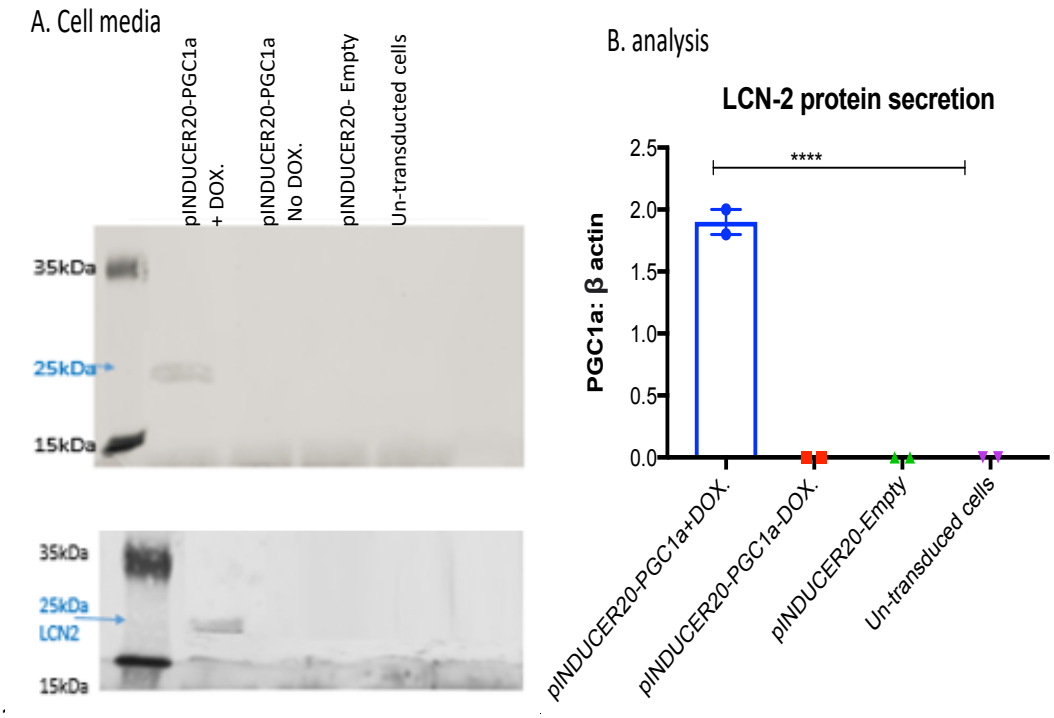

Figure 5.12. PGC-1α overexpression induces the secretion of LCN-2 into skeletal muscle cell media (C_2C_{12}) during lentiviral transduction. The protein secretion of LCN-2 was examined using western blotting. The data are presented as the mean ± SEM (****p>0.001, n = 2 independent experiments (see section 5.5.1 for more details).

5.4 DISCUSSION

Researchers have shown that LCN-2 circulation levels in serum are increased post-exercise (Nakai *et al.* 2021; Ponzetti *et al.* 2021), and in Chapter 4, we showed that LCN-2 is regulated and secreted by human skeletal muscle (myotubes) post-16 h EPS and AICAR (exercise-like effects). Following from these results, we investigated whether LCN-2 has a role in the crosstalk between muscle and adipose tissue. We aimed to assess the protein overexpression and secretion of LCN-2 and PGC1a into both cultured human and mouse (C_2C_{12}) myotubes to use this for identifying whether skeletal muscle-derived LCN-2 has effects, as other myokines do, on nearby tissue (e.g., WAT-3T3L-1), and white adipocyte specifically, in terms of lipid accumulation and lipolysis. To address the hypothesis, cloning, construction, and overexpression of PGC1-a and LCN-2 was assessed using lentiviral inducible vector; thus, MDA-MB-468 cells were used as an initial test of the study. The MDA-MB-468 cell-line was first isolated in 1977 from an elderly female patient with aggressive carcinoma of the breast (Cailleau *et al.*, 1978).

We did not determine the optimal MOI (multiplicity of infection) – defined as the ratio between number of lentiviruses and number of cells during the process of transduction – for the successful lentivirus transduction. This is because various important factors affect the optimal determination of MOI such as the nature of cells, transduction efficiency, and gene of interest. Instead, we chose several amounts of non-concentrating lentivirus in cell media of HEK293FT, using 700 µL for the MDA-MB-468 cell-line and 600 µL for both C_2C_{12} and human myotubes. Expression of green fluorescent protein (GFP), a small and stable protein (~27-kDa) that fluoresces as a monomer inside the cytoplasm of cells, was assessed in the cytoplasm of cells using various amounts of non-concentrating lentivirus-mediated expression

of LCN-2/PGC1-a and a fluorescence microscope. It is easy to detect in intact cells because of its stability, and it can be detected in amounts as small as < 10 ng of GFP per ml of culture; 5 ng of GFP per protein band on a standard SDS-PAGE gel (Drew *et al.*, 2006).

We observed a high efficiency of transduction using pINDUCER20-GFP lentivirus in the MDA-MB-468 cell-line, C_2C_{12} and human myotubes with high efficiency. Results from this investigation demonstrate that lentiviral-mediated transfection of the GFP in all cell-lines and primary human myotubes successfully induces overexpression of GFP *in vitro* (Figure 5.2; Figure 5.4; Figure 5.6). The reason for choosing the GFP as a validation step of transduction efficiency relates to its expression, which indicates the level of transduction directly without significant time demands. Moreover, GFP does not need any further enzymatic or immunoblot reactions, nor even substrate (Drew *et al.*, 2008).

We were successfully able to model the expression and secretion of LCN-2 and PGC1-a expression *in vitro* using an inducible lentiviral vector. The presence of LCN-2 in the media of infected cells with lentivirus demonstrates the secretion of LCN-2 by human muscle cells (myotubes) *in vitro*, supporting its role as a myokine (Figure 5.10). However, the difference in endocrine effects of this secreted protein may be related to the tissue-specific ligands bound to LCN-2 (Mosialou *et al.*, 2017), which in turn could determine LCN-2 action within the whole-body when secreted by specific tissues. There have been very few studies so far aimed at investigating the ligand binding of LCN-2 when secreted by tissue into circulation.

The binding pocket of lipocalins allows small hydrophobic ligands to bind and transport them for a specific job (LaLonde *et al.*, 1994), and LCN-2 has a large and more open ligand-binding pocket than other lipocalins in the family (Coles *et al.*,

1999). As such, the ability to express LCN-2 using lentiviral transduction of skeletal muscle cells enables further investigation into the possibility that a skeletal muscle-specific ligand is bound to the myokine when secreted. Duo to time constraints, we were not able to collect LCN-2 in the cell medium of myotubes infected with lentivirus to further characterise ligand binding to LCN-2 and identify whether it is endogenous; however, we were able to study its role in muscle-adipose crosstalk, as will be discussed in Chapter 6.

Myokines have previously been found to play a role in local regulation of muscle physiology, exerting benefits on whole-body metabolism and therefore preventing the risk of development metabolic diseases (Huh, 2018). Exercise-induced myokines that have been investigated recently include IL-6, irisin, FGF21, LIF, BAIBA and IL-15, all of which were found to exert either autocrine, paracrine or endocrine effects. They facilitate glucose uptake improvement, reduce fat oxidation regulation, and reduce fat accumulation in adipocytes, with most of these myokines being known as adipokines released by adipose tissue (So *et al.*, 2014; Huh, 2018).

Compared to myokines, LCN-2 can exert either autocrine, paracrine or endocrine effects in response to exercise or contractile activities. Recently, LCN-2 has been shown to regulate the function of satellite cells and enhance skeletal muscle repair though the complex formation of LCN-2 and MMP-9. This finding suggests that LCN-2 exerts a paracrine or autocrine effect on muscle physiology, as other myokines do. It is also consistent with previous reports that IL-6 has enhances the proliferation of myoblasts and helps with muscle regeneration (Tidball *et al.*, 2014; Rebalka *et al.*, 2018). It is therefore plausible to suggest that LCN-2 could have an endocrine effect on other metabolically active cells in response to its secretion by

exercise. In testing the effect of skeletal muscle-derived LCN-2 on adipocytes metabolism *in vitro*, we were able to show secretion of LCN-2 by skeletal muscle *in vitro*. We also observed that PGC1-a overexpression in muscle caused secretion of LCN-2 into skeletal muscle cell media (C_2C_{12}), as Figure 5.12 shows, supporting the hypothesis that PGC1a could be the mechanism by which LCN-2 exerts an endocrine effect. In fact, a study by Furrer in 2017 revealed that when PGC1a is overexpressed in mice, LCN-2 mRNA is upregulated significantly compared to GFP (Furrer *et al.*, 2017).

In conclusion, an inducible lentiviral vector was used to construct and enable the induction of *LCN-2* gene expression. Transduction of various cells confirmed that the LCN-2 protein was overexpressed in cells and secreted by cells into the cell media, allowing for an investigation into the role of LCN-2 as a new myokine affecting crosstalk between muscle and adipose tissue when secreted from human myotubes. To further characterise LCN-2 as a myokine, overexpression of PGC1-a in skeletal muscle was caused, and we observed the increase of LCN-2 secretion into cell media. Therefore, subsequent experiments described in the next chapter aimed to investigate the role and effect of the skeletal muscle-derived LCN-2 (myokine) on lipolysis and lipid accumulation in adipocytes.

Chapter 6: The Effects of Myotube Cell Media (CM) that Overexpresses LCN-2 on Lipolysis and Lipid Accumulation in Cultured Adipocytes

6.1 INTRODUCTION

Human skeletal muscle is known to crosstalk with adipose tissue and thus is able to influence metabolic parameters via the release of factors known as adipokines (Maury & Brichard, 2010). Myokines are factors that are released by skeletal muscle in response to physical activity and have been found to exert roles in an autocrine, paracrine or endocrine fashion on other nearby tissues such as liver, bone and adipose tissue. During physical inactivity, adipokines are released and mainly act as a pro-inflammatory to exacerbate pathological states in the body, which then leads to the onset of certain metabolic diseases such as obesity and type 2 diabetes (Iyer *et al.*, 2010). In contrast, myokines released in response of physical activity are now known to eliminate any harmful pro-inflammatory effects in the body and promote the health benefits of physical activity (Pedersen, 2011). Myokines have autocrine and paracrine effects which are involved in the regulation of muscle physiology, including muscle growth and regeneration, and even metabolism of lipids. In addition, myokines can regulate the function of bone tissue. In terms of their endocrine effects, myokines mediate whole-body metabolic changes though mechanisms that act on nearby tissue (see Figure 6.1).

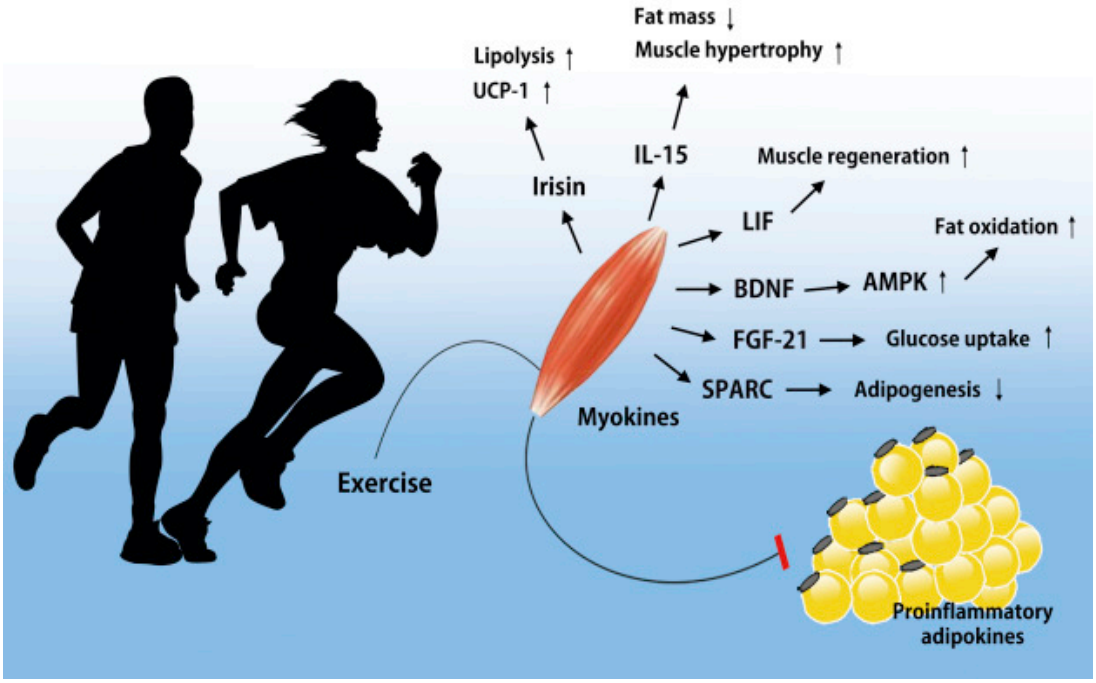

Figure 6.1. Exercise-induced myokines and their potential role. Myokines are defined as factors secreted by SkM, which subsequently exert autocrine, paracrine or endocrine effects on various organs (Pedersen, 2011).

Myokines mediate certain beneficial effects on adipose tissue, and studies have evaluated the endocrine effects of myokines on the function of adipose tissue. Interleukin 6 (IL-6), for example, is a well-known myokines that has been widely investigated (Pedersen & Febbraio, 2008). In human adipose tissue and murine-cultured adipocytes (3T3-L1), IL-6 has been shown to induce lipolysis by increasing lipolytic effects (Petersen *et al.*, 2005; Wedell-Neergaard *et al.*, 2019). Additionally, overexpression of IL-15 in skeletal muscle has been shown to inhibit adipose tissue deposition (Quinn, Anderson, Strait-Bodey, Stroud, & Argilés, 2009). Therefore, certain myokines could exert an endocrine effect and induce changes in lipolysis and lipid metabolism in adipose tissue (Tamura *et al.*, 2020).

6.1.1 Adipose Tissue Lipolysis: Key Players and Regulation

Long-term exercise, fasting and lipids are stored in the form of triglycerides (TAGs) in adipocytes, and lipolysis occurs when TAGs are completely hydrolysed into glycerol and free fatty acids (FFAs). Lipolysis is a multi-stage process, breaking down lipids in the form of TAGs and is controlled by lipases, which are specific enzymes that generate lipolytic products – one molar unit of glycerol and 3 molar units of FFAs. There are three specific lipase enzymes: Adipose triglyceride lipase (ATGL), Hormone-sensitive lipase (HSL) and Monoglyceride lipase (MGL). First, ATGL hydrolyses TAGs to DGs (Diglycerides) and the first FFA (Zimmermann *et al.*, 2004). The activity of ATGL is regulated by proteins such as comparative gene identification-58 (CGI-58) and G0/G1 switch gene (G0S2). If ATGL is bound to these proteins, its activity is inhibited; however, once these proteins are released, ATGL is active again (Lass *et al.*, 2006; Yamaguchi, 2010; Yang *et al.*, 2010). The second step is the hydrolysis of DGs to monoglycerides (MGs) and the second FFA, which is carried out by HSL. In contrast to ATGL, HSL not only hydrolyses ester bonds of DGs, but also TGs, cholesteryl, retinyl and MGs (Morak *et al.*, 2012). Finally, MGL is a selective, specific enzyme that hydrolyses MGs and therefore generates glycerol and the third FFA. Thus, lipolysis is composed of three steps in which TAGs are catalysed by three specific and different enzymes, the end lipolytic products being glycerol and FFAs (1:3 respectively) (Schweiger *et al.*, 2006) (see Figure 6.2). FFAs can bind to albumin outside adipocyte cells in the bloodstream and shuttle to nearby tissue for oxidation, such as the liver and muscles, and fatty acid molecules can convert to acetyl coenzyme A molecules to be used by the whole body as a source of energy (Ordovas & Corella, 2008).

Physiologically, lipolysis is enhanced by certain hormones and cytokines. The process of regulation that occurs via lipolysis includes the regulation of lipase mRNA expression, protein expression of lipases, other proteins involved in lipolysis, and the localisation of lipase inside cells and post-translational modifications such as protein phosphorylation (McGown, Birerdinc & Younossi, 2014). The most important mechanisms that regulate lipolysis are based on the activation of HSL and ATGL. Without stimulation, in its basal state, the CGI-58 molecule is bounded PLNP1 (perilipin-1), and HSL is located in the cytoplasm of adipocytes. Under hormonal stimulation, such as epinephine, norepinephine, or isoproterenol via β-adrenergic signalling pathway (β-ARs), adenylyl cyclase is activated (Miyoshi, Perfield, Obin, & Greenberg, 2008). The level of cyclic AMP (cAMP) is then increased in adipocytes, resulting in protein kinase A (PKA) being activated, leading to the phosphorylation of HSL and perilipin-1 on multiple serines. Thus, HSL translocates to the lipid droplet (LD), and the activation of PLNP-1 causes the release of the CGI-58 molecule, which shuttles to bind the ATGL to the LD. However, the exact mechanism by which this occurs is not yet clear. The activation of HSL and ATGL then automatically switches the lipolysis on by increasing the hydrolysis activity of TAGs (Yang & Mottillo, 2020) (see Figure 6.2).

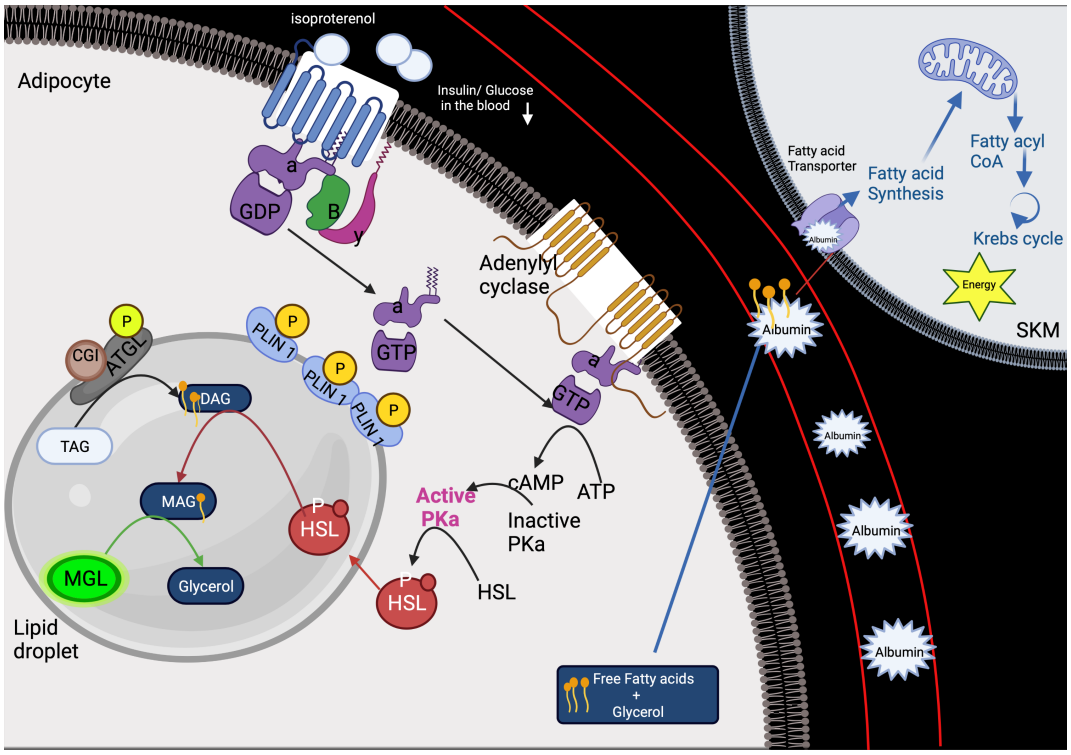

Figure 6.2. Mechanism of isoproterenol-stimulated lipolysis that regulates cultured adipocyte lipolysis of lipid droplets. Under stimulation, isoproterenol binds to β adrenergic receptors and activates adenylyl cyclase. There is then an increase in the level of cAMP (cytosolic), which stimulates protein kinase A (PKA), followed by the phosphorylation of PLIN1 and HSL at specific serines in rodents (Ser653 and Ser660). This action results in CGI-58 being released from PLNP1 and binding to ATGL for activation, and TGs convert to DGs. Following this, HSL translocates from the cytosol into LD in a phosphorylation state, resulting in DGs converting into MGs, which are further processed by MGL to release one unit of glycerol. Following the release of one unit of FFAs in each lipolytic step (a total of three units of FFAs), these lipolytic products can act as ligands for PPARα/γ, promoting the expression level of genes that could be involved in energy homeostasis. Created with Bio-render (https://biorender.com).

6.2 AIMS OF THIS CHAPTER

The aim of this chapter is to present the findings of an investigation into the endocrine effects of LCN-2 as a novel myokine secreted by skeletal muscle on llipolysis and ipid metabolism in adipocytes. The detailed objectives for this chapter and how we approached them in relation to the general aim are as follows:

- To provide an *in vitro* model of lipolysis via evaluation of the glycerol level in adipocyte cell media, protein expression level of p.HSL$^{ser\ 563}$, and total ATGL in adipocyte cell lysate for basal *vs* isoproterenol-stimulated lipolysis in cultured adipocytes post-1 h and -4 h of treatment with isoproterenol.
- To investigate the endocrine effects of myotube CM that overexpresses LCN-2 (myotube CM (LCN-2+DOX.)). Particularly, its effects on lipolysis in cultured adipocytes (3T3L-1). We aimed to measure the level of glycerol released into the cell media after treating adipocytes with 50% myotube CM (1:1) post-6 h, -24 h and -48 h treatment. Measurements were taken in nmol per mg of protein. We also evaluated changes on p.HSL^{ser563} and ATGL protein expression upon treatment post-6 h, -24 h and -48 h with 50% myotube CM (see Figure 6.3).
- To establish a good method for assessing lipid accumulation in cultured adipocytes, we differentiated 3T3 L1 cells to adipocytes cultured in 12-well plates at 4000 cells per well and stained them with Nile Red to measure the fluorescence intensity. Two approaches were used to assess the lipid accumulation with the same settings (Ex.480 nm, Em. 520 nm) for wavelength measurement (excitation and emission). The first approach measured the fluorescence intensity using a plate reader

(FLUOstar® Omega, USA), and the second measured the fluorescence intensity using a fluorescence microscope (wide-field microscope Zeiss 200M). Images were acquired using 10x magnification. The experimental plan and approaches are illustrated below in Figure 6.4.

- To investigate the endocrine effect of treatment with 50% myotube CM that overexpresses LCN-2 (myotube CM (LCN-2+DOX.)) on the lipid accumulation in adipocytes (3T3L-1) post-6 h, -24 h and -48 h using Nile Red staining to measure the fluorescence intensity, and using both a plate reader and fluorescence microscope with the same settings (Ex.480 nm, Em. 520 nm).

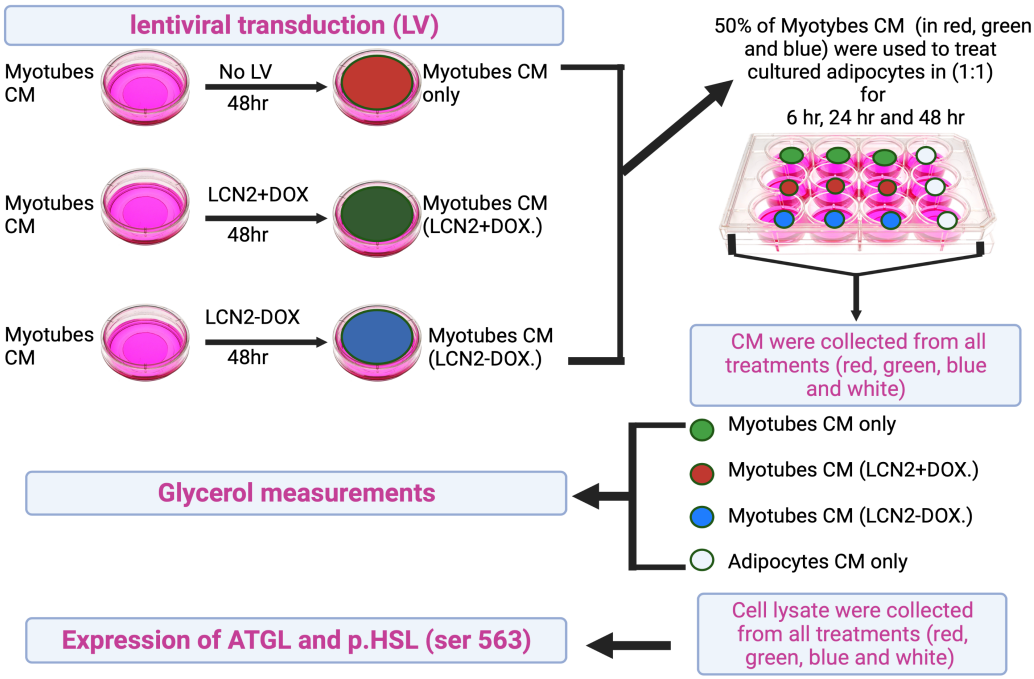

Figure 6.3. Experimental plan for treating adipocytes with 50% myotubes CM for measuring lipolysis. Human myoblast cells were plated in 50 mm dishes at a cell density of 2×10^5 cells/dish in 5 ml required media and incubated in 5% CO_2 until they reached confluence. They were then differentiated towards mature myotubes cells using the appropriate media, as indicated in Chapter 2 (Materials and Methods). On day five, lentivirus transduction of myotubes was carried out to overexpress LCN-2, and dishes without lentivirus transduction were prepared for a negative control (defined as myotubes CM only). After 48 h, the cell culture media of myotubes (myotubes CM) was collected, filtered through a 0.22 µm syringe filter, and stored at -80 °C until used. Cultured and differentiated adipocyte (3T3L-1) cells that were plated in 12-well plates at a cell density of 0.5×10^5 cells/well were placed in 1 ml of M3 ready for treatment on day six of the differentiation period. Adipocyte cell media (CM) was removed and replaced with 50% CM derived from myotubes in fresh complete media (M4). The measurement of lipolysis in cultured adipocytes was evaluated 6 h, 24 h and 48 h after treatment with myotube CM. Created with Bio-render (https://biorender.com).

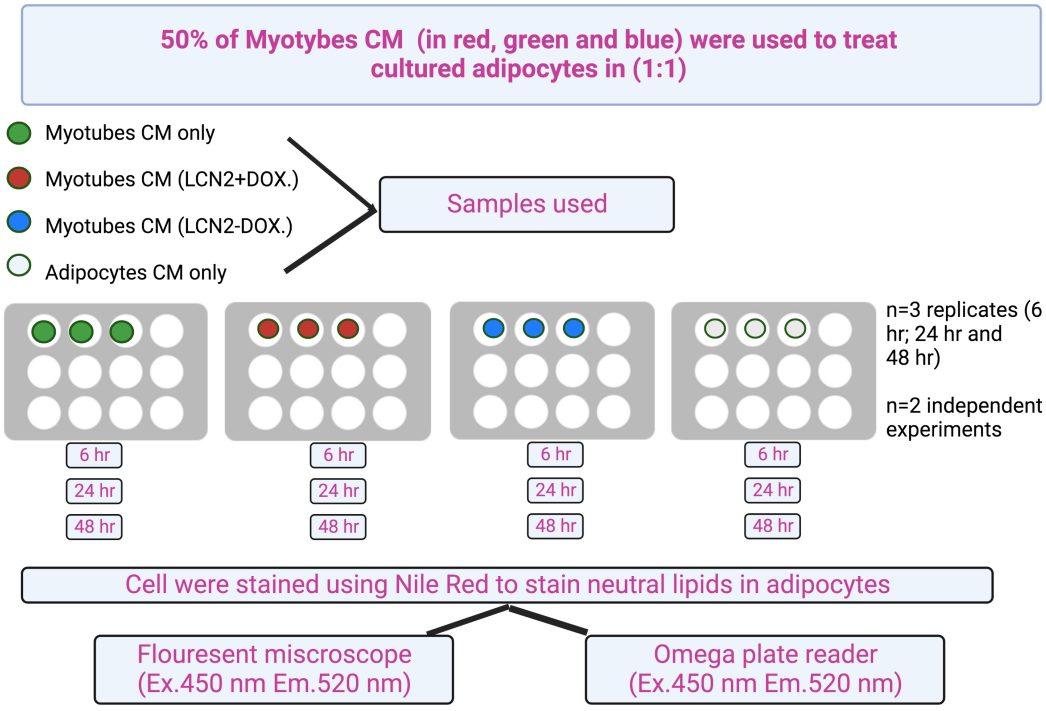

Figure 6.4. Experimental plan for treating adipocytes (3T3L-1) with 50% myotubes CM for cell staining. Human myoblast cells were plated in 50 mm dishes at a cell density of 2×10^5 cells/dish in 5 ml required media and incubated in 5% CO_2 until they reached confluence. These were then differentiated towards mature myotubes cells using the appropriate media, as indicated in Chapter 2 (Materials and Methods). On day five, lentivirus transduction of myotubes was carried out to overexpress LCN-2, and dishes without lentivirus transduction were prepared for a negative control (defined as myotubes CM only). After 48 h, cell culture media of myotubes (myotubes CM) was collected, filtered through a 0.22 µm syringe filter, and stored at -80 °C until used. Cultured and differentiated adipocyte (3T3L-1) cells that were plated in 12-well plates at a cell density of 0.5×10^5 cells/well were placed in 1 ml of M3 ready for treatment on day six of the differentiation period. Adipocyte cell media (CM) was removed and replaced with 50% CM derived from myotubes in fresh complete media (M4). Cells were fixed and stained with Nile Red (neutral lipid stain), and cells were protected from the light. After staining, cells were first used to read the fluorescence intensity using an Omega plate reader, and then images were acquired using a florescence microscope at the same setting, with the precaution of reducing the effect of lights bleaching of cells. The measurement of lipid accumulation in cultured adipocytes was evaluated post-6 h, -24 h and -48 h, and results were recorded. Created with Bio-render (https://biorender.com).

6.3 RESULTS

6.3.1 Functional Validation of Commercial Human Primary Skeletal Muscle Cells

When considering the use of commercial primary SkM myoblast cells for use in our study to investigate the role of LCN-2 in crosstalk between skeletal muscle and adipose tissue, it is important to understand the morphological changes of human SkM cells (myotubes) with serial passages and their physiological response; specifically, to insulin and palmitate treatment, which may affect the efficiency of using such commercial cells. The graphical abstract below (Figure 6.5) illustrates the experimental plan used for the validation of the use of these commercial cells (A12555). The cells were acquired from a female healthy donor.

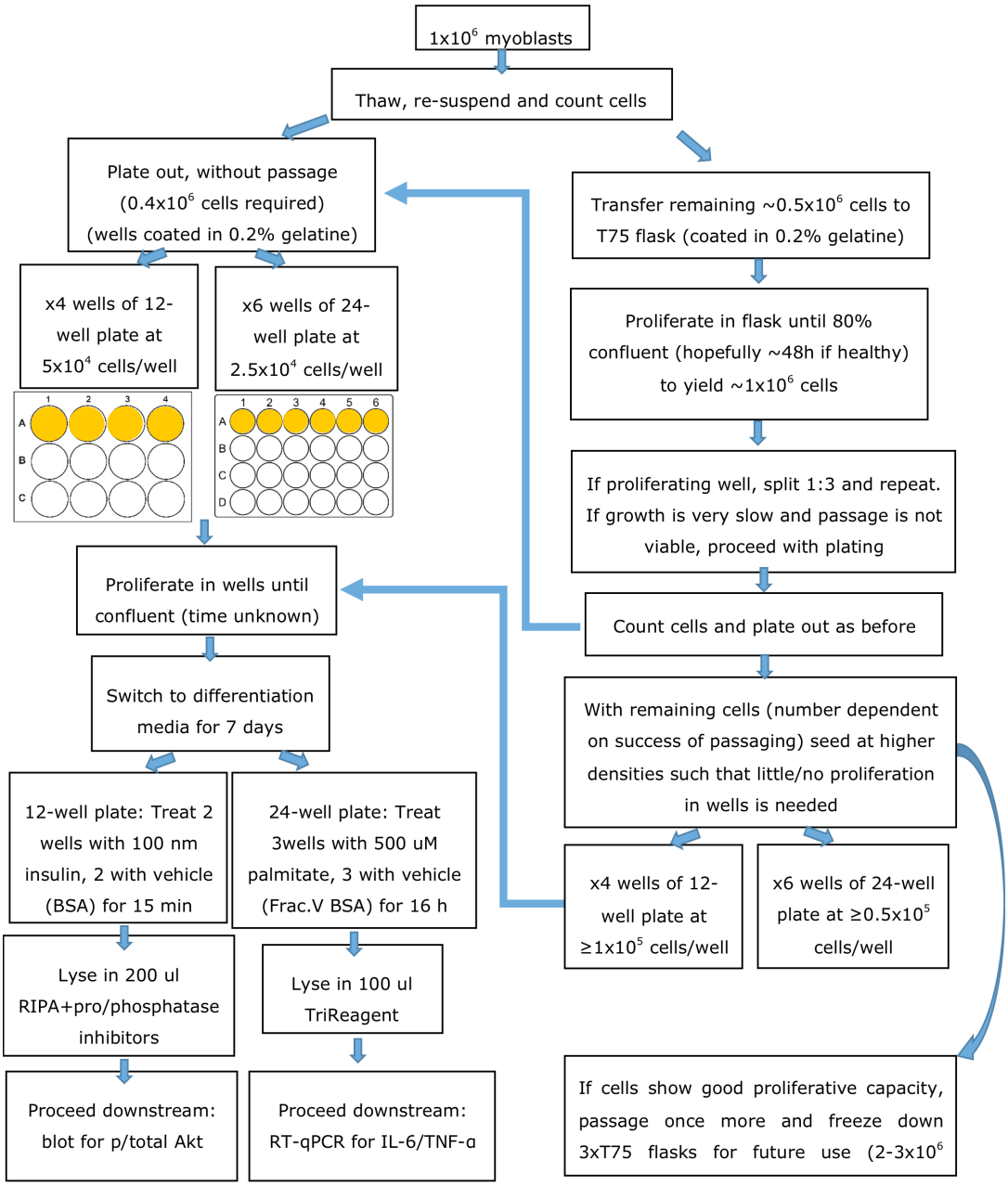

Figure 6.5. Graphical abstract of experimental plan for functional validation of commercial primary myoblasts cells differentiated towards mature myotubes.

6.3.2 Morphological Changes of Commercial Human Myotubes is Affected by Late Serial Passage Number

We aimed to determine the effects of serial cell passaging on the morphology of human myotubes derived from commercial primary skeletal muscle myoblast cells. Cell passaging is defined here as the removal of cells from the cell culture plate (12-well plate or 24-well plate) using trypsin-EDTA. Cells were then re-plated at the required cell number per well, as detailed in Figure 6.6, in a new culture plate with new cell media, as explained in Chapter 2 (Materials and Methods). Each vial contained $1x10^6$ cells, and the initial culture of cells was performed when the cell vial was removed from liquid-nitrogen. This passage was termed passage 0 (P0) and placed in either a 12- or 24-well plate with gelatine as the coating material. The other remaining cells (~$0.5x10^5$ cells of cell suspension) were used for the subsequent passages in a T75 flask. Thus, the term P0 denotes the initial culture in our study. Once the culture of skeletal muscle myoblasts had been proliferated to ~80% confluency in a T75 flask (Corning, NY). Myoblast cells were then passaged and expanded again in the flask. This culture is referred to as P1, and the same process was repeated until finished at P4. Images of differentiated myotubes were acquired on day five from P0 though to P4 at 20x magnification using phase-contrast microscopy. Five images were taken per well at each passage (P0-P4). Substantial changes were noticed in the myotubes' morphology from P2 onwards: cells switched from their normal shape (long, consistent-diameter, parallel myotubes) and became more erratic in size and arrangement. Cells from P4 became almost impossible to distinguish as myotubes since they had lost their basic structure and looked more like fibroblast cells (Figure 6.6).

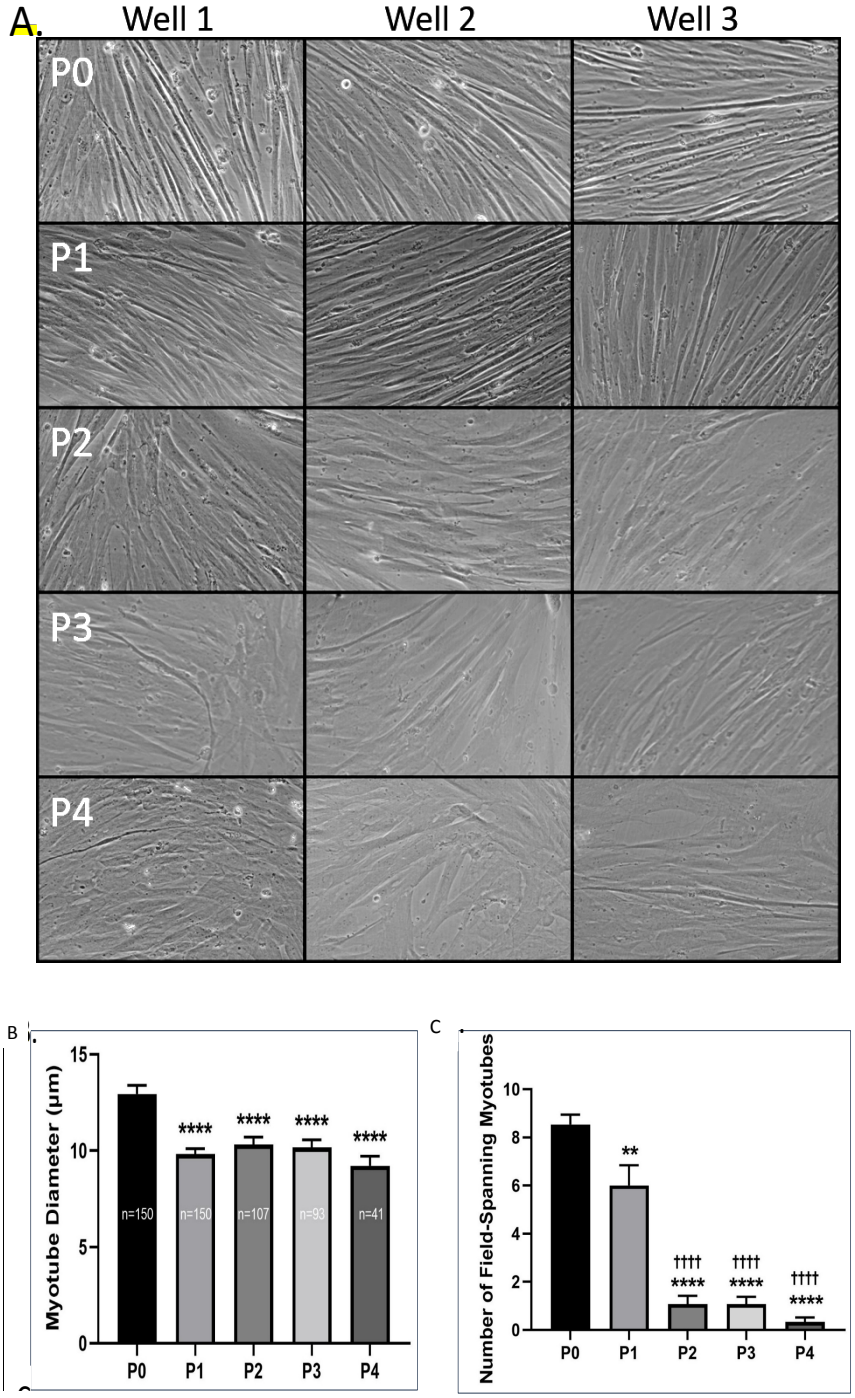

Figure 6.6. Myotube morphological changes with serial passage. **A.** Myoblasts were differentiated for 7 days before imaging on a light microscope prior to test how long we should keep passaging these commercial primary myotube cells. **B.** Mean myotube diameter (µm). Diameters of discernible myotube structures were measured in three places along their length (~25%, 50% and 75% of structure in field), and the mean was recorded. Where possible, 10 myotubes were measured per field, but fewer if less than 10 discernible myotubes were visible. Five fields were captured per well, with three wells per passage (i.e., up to 150 myotubes measured per passage). **C.** Number of myotubes per field that entirely spanned from one side of the field to its parallel side (15 fields per passage). One-way ANOVAs (analysis of variance) revealed a significant effect of passage on myotube diameter and field-spanning myotubes (both $P < 0.0001$). Post-hoc Bonferroni-corrected comparisons revealed P1 though P4 to be significantly different from P0 (** $P < 0.01$, **** $P < 0.0001$) for both diameter and field-spanning myotubes. †††† Significantly different from P1 ($P < 0.0001$). Data presented as mean ± SEM.

6.3.3 Insulin-Stimulated p.AKT-Ser473 Is Not Affected by Serial Passage Number

On day five, differentiated myotube cells were treated with 100 nM insulin or vehicle for 15 min to test their physiological response to insulin. Post-15 min, cells were lysed in RIPA buffer that contained a cocktail of protease/phosphatase inhibitors (see Chapter 2, Materials and Methods). Proteins in cell lysate of human myotubes were measured using BCA, and 30 ug of the total protein was loaded on 10% SDS-PAGE gel to evaluate the protein expression of p.AKT $^{(Ser473)}$. Results showed a strong increase in insulin-stimulated p.AKT $^{(Ser473)}$ represented by dark bands at all passages (P0-P4); however, basal pAKT declined with higher passages (Figure 6.7).

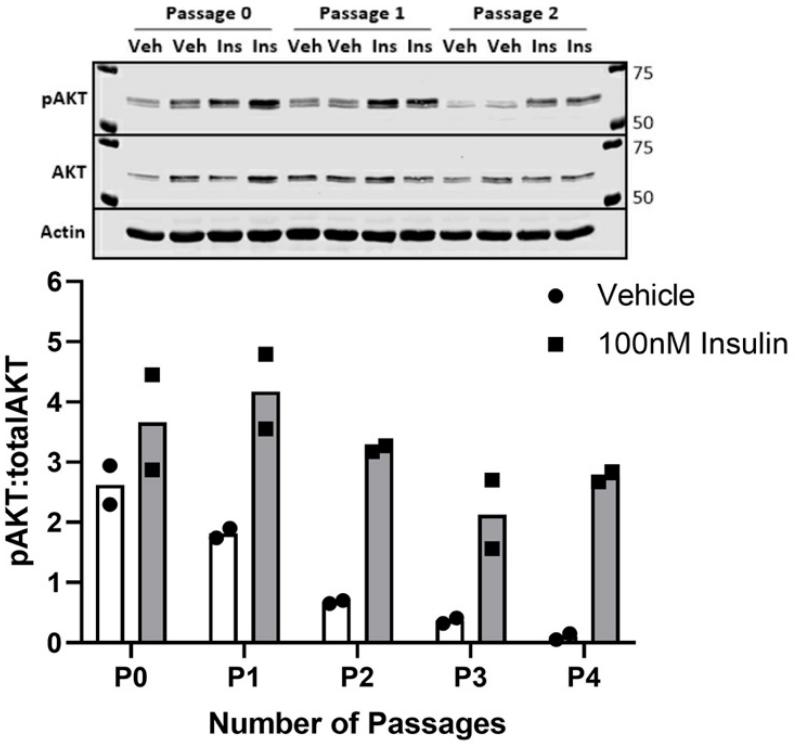

Figure 6.7. The effect of passage number of commercial human myotubes on insulin-stimulated p.AKT$^{(Ser473)}$. Representative blot of insulin-stimulated p.AKT$^{(Ser473)}$ in human myotubes that were treated with 100 nM insulin vs vehicle for 15 min on day five of differentiated myotubes. Following the treatment, cells were lysed in RIPA buffer that comprised a cocktail of protease/ phosphatase inhibitors. Protein levels were then measured using BCA, and 30 ug of the protein was loaded on 10% SDS-PAGE gel. Results indicate a strong band and thus an increase in insulin-stimulated p.AKT $^{(Ser473)}$ at all passages from P0 to P4.

6.3.4 Palmitate-Induced Inflammation Does Not Affect Inflammatory Markers in Human Myotubes with Serial Passage Number

On day five of differentiated myotubes, commercial primary human skeletal muscle (SkM) was treated with 300 μM palmitate or vehicle for 24 h. We investigated the mRNA expression of inflammatory markers (TNF-a and IL-1b). Neither 300 uM palmitate nor passage number influenced TNF-a and IL-1 β mRNA expression (Figure 6.8).

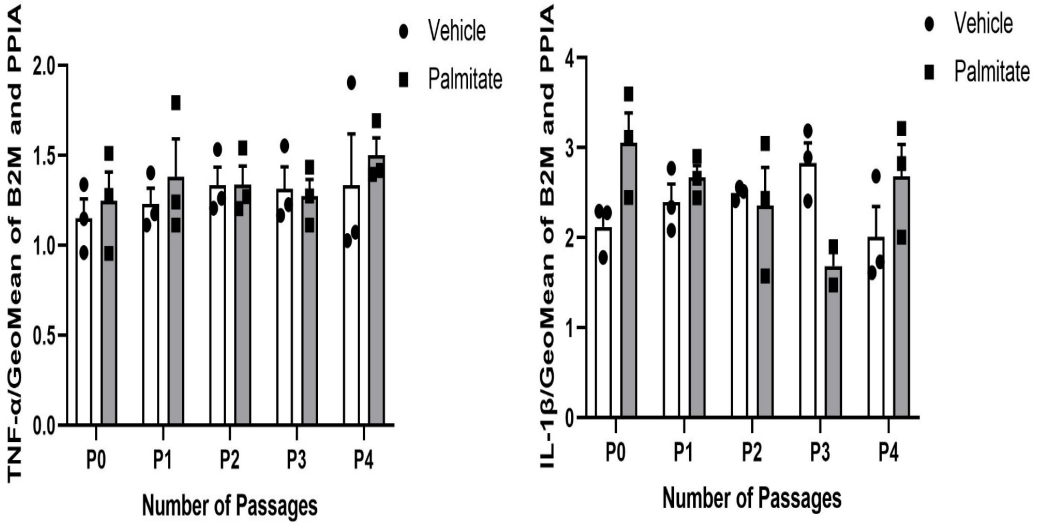

Figure 6.8. The effect of palmitate-induced inflammation on mRNA expression of primary inflammatory markers. Cultured human myotubes were treated on day five of differentiated myotubes with 300 μM palmitate vs vehicle for 24 h. Neither 300 uM palmitate nor passage number influenced TNF-a mRNA expression, but there was an effect for palmitate versus passage number for IL-1β.

6.3.5 ELISA Results Confirm the Secretion of LCN-2 into Myotube CM Post-Lentivirus Transduction Using Commercial Human Myotube Cells

In this thesis, we have identified that LCN-2 is a novel myokine secreted by murine and human skeletal muscle cells in response to 16 hr of low frequency acute exercise by EPS. The western blotting of human myotube CM and cell lysate confirms the previously reported results. In Chapter 5, the release of LCN-2 by human skeletal muscle cells in response to lentiviral transduction was confirmed, and

we generated more than 15 ml of cell media (CM) to investigate its endocrine effects as a novel myokine on nearby tissue.

One aim of this chapter is to investigate the crosstalk effects of LCN-2 on adipose tissue, and for this study, we used commercial human primary cells. To ensure the use of CM that overexpresses LCN-2, we tested successful lentivirus transduction on these commercial cells, confirming the secretion level of LCN-2 into cell media by ELISA, and so confirming that the media could be used as a treatment on cultured adipocytes. The level of LCN-2 in the myotube CM LCN-2+DOX sample was more than 1000 ng/ml while the level of LCN-2 in the myotube CM sample was less than 400 ng/ml, supporting the fact that our model of overexpression worked well and was able to release LCN-2 in high amounts.

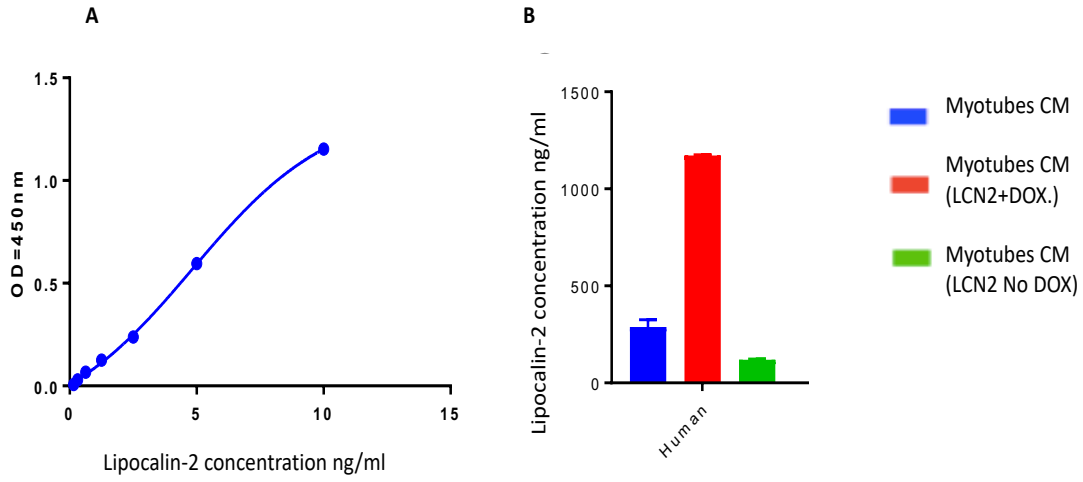

Figure 6.9. Measuring the level of Lipocalin-2 (LCN-2) in cell media derived from human myotubes by ELISA following lentivirus transduction (infection). The levels of LCN-2 in cell media were measured using ELISA in ng/ml. Cells were infected with lentivirus, overexpressing Lipocalin-2, and samples were collected post-48 h infection. The calibration curves for ELISA were assayed in duplicate and carried out according to the manual. Four parameter logistic (4PL) (sigmoidal curve) is a regression model-was used to generate the concentration of LCN-2. Human myotube CM samples are LCN-2+DOX, LCN-2-DOX and myotubes CM (uninfected cells). LCN-2+DOX significantly increased *vs* other samples, indicating that human LCN-2 was overexpressed and highly released by human myotubes cells *vs* other samples in **B**.

6.3.6 Development of an *In Vitro* Model of Lipolysis in Cultured Adipocytes Using Isoproterenol

The well-known assessment of lipolysis in cultured adipocytes *in vitro* is the assessment of lipolytic activity by measuring the release of glycerol and free fatty acids (FFAs) in the media of cultured adipocytes. There are two lipolytic states: basal and stimulated-β-adrenergic pathway. To measure the lipolytic components of cultured adipocytes, incubating cells with BSA (bovine serum albumin) is important. FAAs use BSA as a receptor since the accumulation of FFAs and glycerol extracellularly stimulates the cells to uptake FFAs and causes the re-esterification of glycerolipids. However, several FFAs and glycerols remain in the adipocyte cell media that will not all be used by cells during lipolysis. In stimulated lipolysis, the ratio of FFA and glycerol is different once it releases into media. Under the basal state, the ratio between FFA and glycerol is 1:1, but under stimulated lipolysis, the ratio is 3:1 (by β-adrenergic stimulation) (Paar *et al.*, 2012).

In our study, we aimed to develop and assess lipolysis by measuring the level of glycerol in media between basal and treatments. Here, we first validated if our differentiated adipocytes generated lipolytic products by measuring glycerol in nmol/mg of protein/h in the cell media (CM) and the expression level of total ATGL and phosphorylation expression level of HSL (p.HSL$^{(Ser\ 653)}$) using isoproterenol-stimulated lipolysis, which known to rapidly increase the level of glycerol and FFA into the incubation media within 1 hr (Langin, 2013; Baskaran & Thyagarajan, 2017). Differentiated adipocytes were pre-incubated with isoproterenol for 1 h of stimulated lipolysis, and then media were replaced with media containing 2% BSA (FA-free; Sigma-Aldrich) for glycerol measurement and the evaluation of ATGL and p.HSL protein expression. Results were obtained post 1 hr and 4 hr. An overview of

the isoproterenol-stimulated lipolysis by β-adrenergic stimulation in cultured adipocytes (general mechanism) is illustrated in Figure 6.1.

6.3.7 Isoproterenol Treatment Highly Induces the Release of Glycerol into Cell Media (CM) Post-4 h

Lipolysis is defined as the process by which triglycerides are hydrolysed into glycerol and free fatty acids (3:1). In this experiment, we aimed to assess the ability of cultured adipocytes (3T3 L1) to produce a good model of lipolysis *in vitro* by stimulating lipolysis with isoproterenol and examining the level of glycerol in media. Cells were stimulated with 10 μM isoproterenol, and lipolysis was assessed by measuring the release of glycerol into cell media of mature adipocytes due to hydrolysis of triglyceride. The 10 μM isoproterenol treatment was done on day six post differentiation of cultured adipocytes. To inhibit acyl-CoA synthetases, we incubated cultured adipocytes with 5 μM Triacsin-C (Schweiger *et al.*, 2014). Cells were treated with isoproterenol (10 uM) either with 5 μM Triacsin-C or without, and cells with no treatment (basal) served as a negative control. Stimulation of lipolysis showed an increase in the release of glycerol from 1 h to 4 h. However, post-4 h isoproterenol-stimulated lipolysis, glycerol increased rapidly by more than 60-fold compared to basal (control values) (Figure 6.10). Isoproterenol-stimulated lipolysis with 5 μM Triacsin-C showed no effect post 1 hr compared to basal, but there was a small effect on the release of glycerol by adipocytes post 4 hr (10-fold).

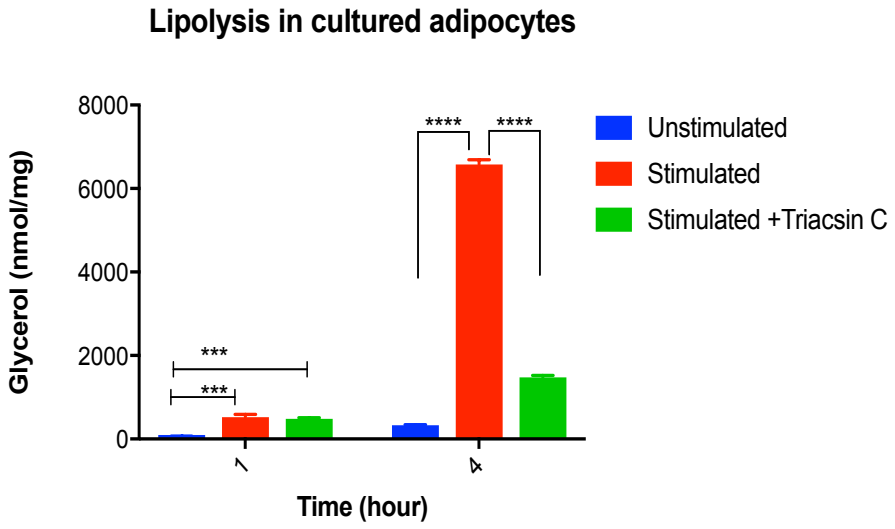

Figure 6.10. **Basal and** isoproterenol**-stimulated glycerol release in cultured adipocytes (3T3-L1).** The bar graph represents the mean ± S.E.M. of basal and isoproterenol (10 µM)-stimulated glycerol release with 5 µM Triacsin C and without 5 µM Triacsin-C. The glycerol release was measured as nmol per mg protein per hour (nmol/mg/h) in the cell media of cultured adipocytes. One-Way ANOVA statistical analysis was used and followed by post-hoc analysis for comparison. ***Represents statistical significance for p-value <0.001; **** Represents statistical significance for p-value <0.0001 for n = 2 independent experiments with 3-well replicates.

6.3.8 p.HSLSer563 is Increased with Isoproterenol Post-4 hr Treatment

We then assessed the protein expression of HSL in response to isopreternol-stimulated lipolysis (by β-adrenergic stimulation) in cultured adipocytes post 1 hr and 4 hr. Results in Figure 6.11 show that the phosphorylation level of HSL (p.HSL^{Ser563}) increased from 1 hr to 4 hr by 1.5-fold compared to basal and lipolysis stimulated with 5 µM Triacsin-C. The protein expression of total HSL is presented with light bands from 1 hr to 4 hr.

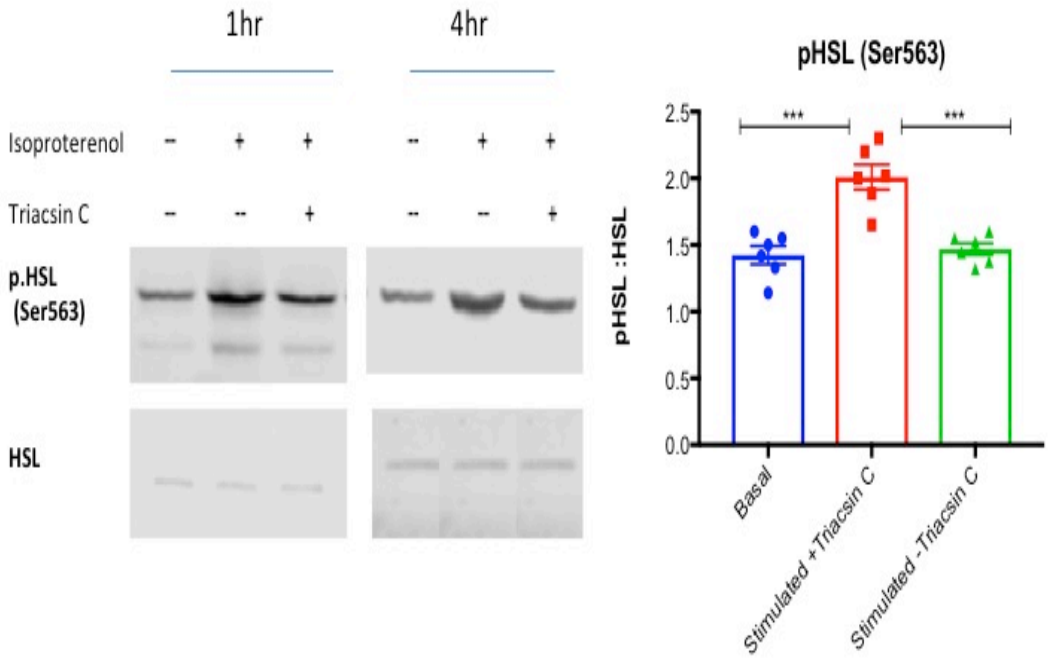

Figure 6.11. Effects of isoproterenol-stimulated lipolysis on the p.HSL (ser563) protein expression of 3T3-L1 adipocytes. On day six, differentiated 3T3-L1 to adipocytes were treated with 10 uM isoproterenol for 1 hr and 4 hr and either with or without 5uM Triacsin C. MW of p.HSL and HSL are 82kDa. One-Way ANOVA statistical analysis was used and followed by post-hoc analysis for comparison. ***Represents statistical significance for p-value <0.001 for n = 2 independent experiments with 3-well replicates.

6.3.9 The Protein Expression of ATGL Is Increased with Isoproterenol Post-4 h Treatment

We followed up on the previous experiment by measuring the protein expression of ATGL in response to isoproterenol-stimulated lipolysis (by β-adrenergic stimulation) in cultured adipocytes post 1 hr and 4 hr. Results below in Figure 6.12 show that the ATGL level increased 3-fold from 1 hr to 4 hr compared to basal and lipolysis stimulated with 5 µM Triacsin-C. The protein expression of Beta actin (b.actin) was used as a loading control of western blotting experiments.

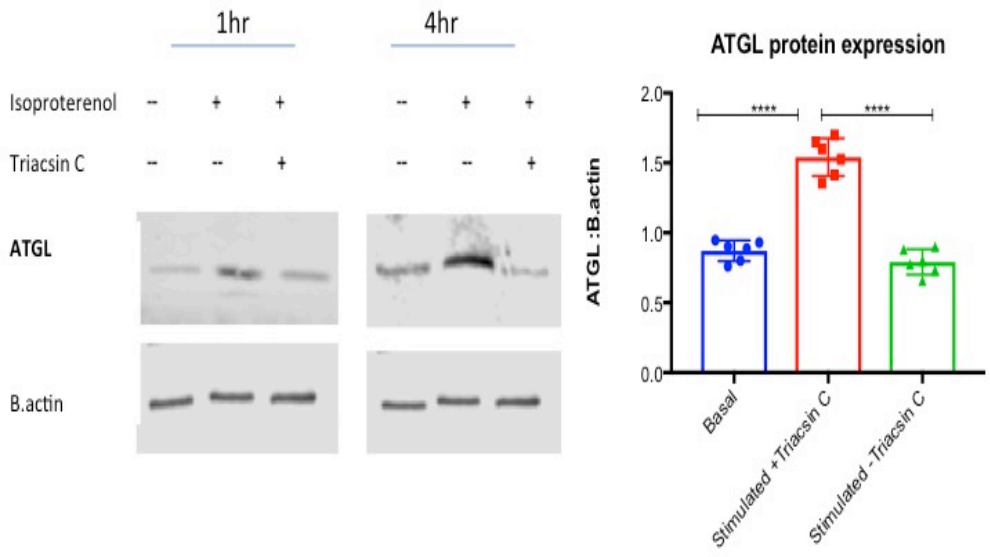

Figure 6.12. Effects of isoproterenol-stimulated lipolysis on ATGL protein expression of 3T3-L1 adipocytes. On day six, differentiated 3T3-L1 adipocytes were treated with 10 uM isoproterenol for 1 h and 4 h and either with or without 5uM Triacsin C. MW of ATGL is 56 kDa and actin is 36 kDa One-Way ANOVA statistical analysis was used and followed by post-hoc analysis for comparison. ***Represents statistical significance for p-value <0.001 for n = 2 independent experiments with 3-well replicates.

6.3.10 The Effects of Human Myotube CM Overexpression of LCN-2 Treatment on Glycerol Release in Adipocytes

Once cultured adipocytes were confirmed as releasing the glycerol into media, upregulating the expression of ATGL in cell lysate and the level of p.HSL^{Ser563} *in vitro*, we treated the adipocytes with human myotube CM. In this study, on day six, differentiated adipocytes were treated with 50% human myotube CM, as described in Figure 6.2: a mixture of adipocyte CM (media#4) and human myotube CM at a 1:1 ratio (50%) for 6 hr, 24 hr and 48 hr. Differentiated adipocyte cells *in vitro* (3T3-L1) were untreated with human myotube CM as a negative control. Human myotube CM treatments (50% on day six) were as follows: myotube CM that overexpresses LCN-2 with DOX (myotubes CM LCN-2+DOX.) using lentiviral inducible vector; myotube CM that overexpresses LCN-2 but without the addition of DOX (myotube CM LCN-2-DOX.); and myotube CM only as a control (Figure 6.13). All CMs were

collected under similar conditions following lentivirus transduction performed on human myotubes. CMs were all collected after the transduction and filtered using a 0.22 μm filter before their use on adipocytes for the treatment. Post-6 hr, -24 h and -48 h treatments, the level of glycerol in cell media was evaluated in nmol per mg of protein following the manufacturer's instructions Glycerol reagents and standards, sigma. Results show that the glycerol released into the cell media of adipocytes CM (No treatment) was 3000 nmol/mg/6 h then reduced by 1.2-fold after 24 hr and 48 hr with values of ~2500 nmol/mg and ~2000 nmol/mg respectively. Adipocyte CM was treated with 50% myotube CM (LCN-2+DOX.), and LCN-2 increased the level of glycerol significantly compared to controls, with values starting from ~3500 nmol/mg/6 h followed by ~3000 nmol/mg/24 h and 2700 nmol/mg/48 hr (see Figure 6.14). Overall, LCN-2 significantly increased the release of glycerol into cell media. However, the glycerol reduced from 6 hr to 24 hr by 1.2-fold and from 24 hr to 48 hr treatment by 1.3-fold. When we treated samples with 50% LCN-2 (myotubes CM (LCN-2+DOX.)), LCN-2 significantly increased the release of glycerol compared to other samples.

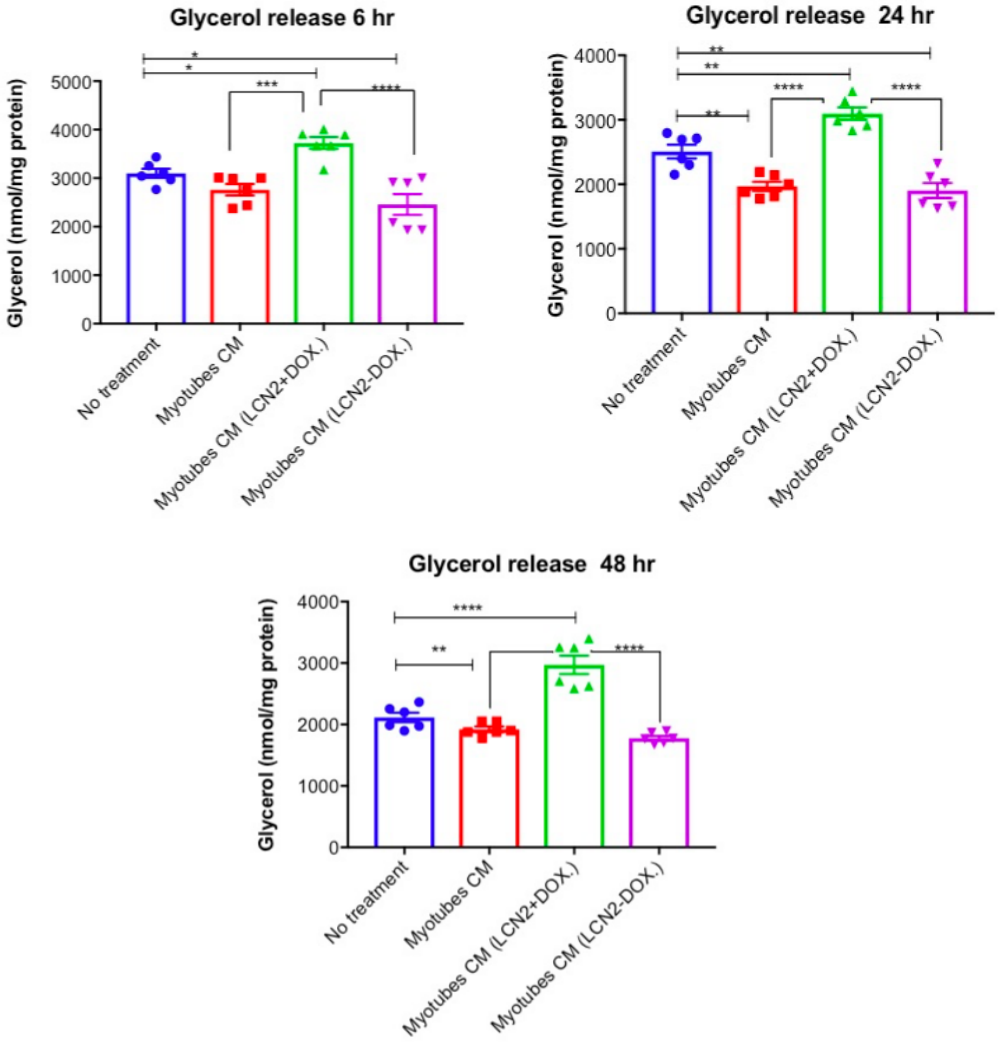

Figure 6.13. Effects of treatment with human myotube CM that overexpresses LCN-2 on lipolysis of cultured adipocytes. Post-6 hr, -24 hr and -48 hr treatment with myotube CM (from days six-eight), the levels of glycerol in the cell media of cultured adipocytes (3T3 L1) were determined, as shown above. Data are expressed as mean ± SEM, n=2 independent experiment with 3-well replicates. One-way ANOVAs were used and followed by post-hoc comparison tests (Turkey's comparisons test), *($p<0.05$); **($P<0.01$); ***($P<0.001$); ****($P<0.0001$).

6.3.11 The Effects of Treatments with Human Myotube CM that Overexpresses LCN-2 on ATGL Protein Expression in Adipocytes

The next experiment was conducted to measure the protein expression of ATGL in response to human myotube CM that overexpresses LCN-2 in cultured adipocytes post 6 hr, 24 hr and 48 hr. Results in Figure 6.14 show that the ATGL level increased from 6-48 hr when adipocyte cells were treated with 50% myotube CM (LCN-2+DOX.). No treatment samples served as a negative control and were compared to two different controls (myotube CM only and myotube CM that overexpresses LCN-2 without the induction of DOX.). We found that LCN-2 (myotube CM, LCN-2+DOX.) increased the protein expression of ATGL significantly post 48 hr by 2.3-fold compared to controls (myotube CM; myotube CM LCN-2-DOX.). However, post 6 hr and 24 hr, LCN-2 had no effect on ATGL expression compared to controls.

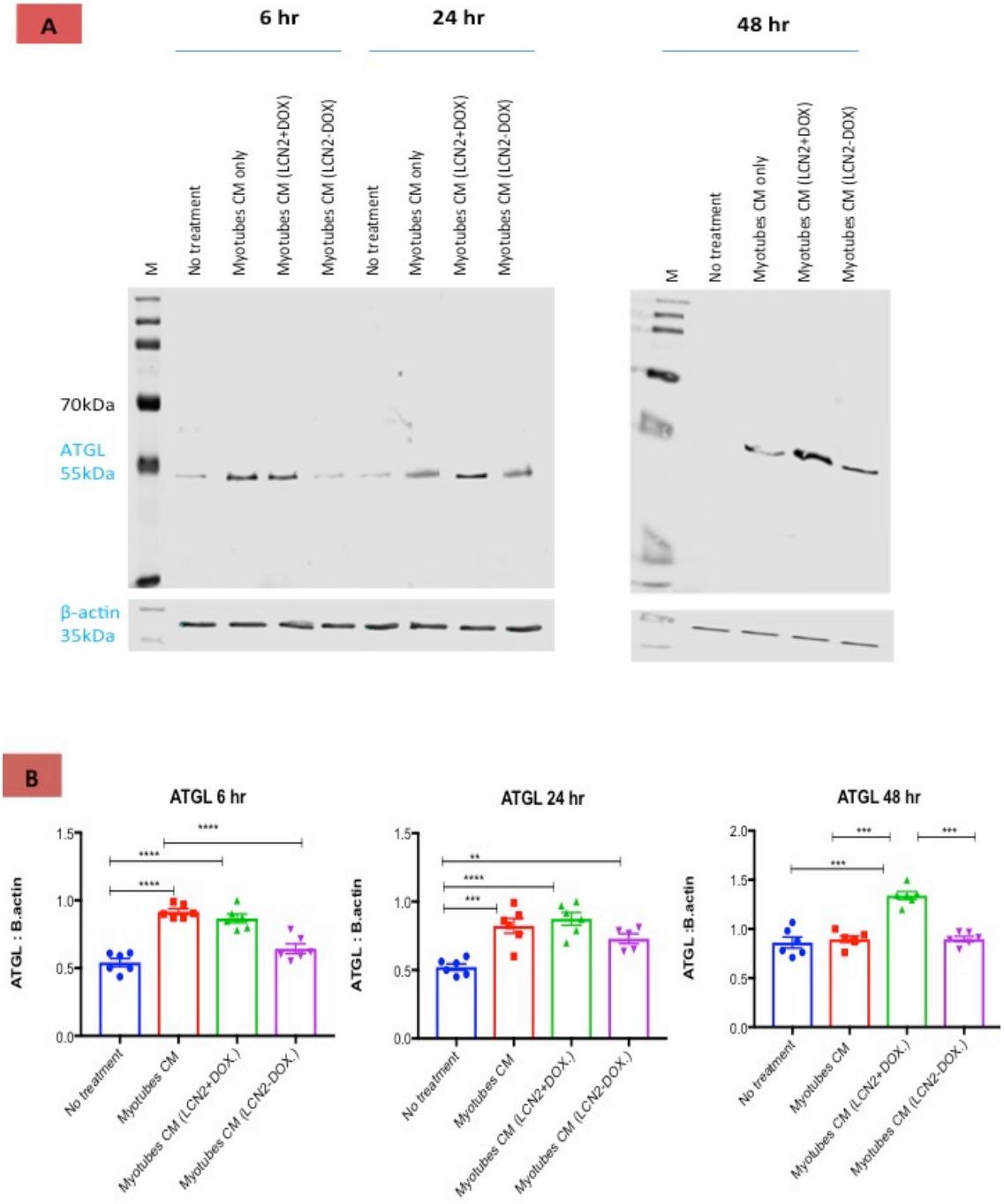

Figure 6.14. Effects of treatment with human myotube CM that overexpresses LCN-2 on lipolysis of cultured adipocytes. Following 6 hr, 24 hr and 48 hr treatment with myotube CM (from days six-eight), the protein expression of total ATGL in the cell lysate of adipocytes was evaluated via western blotting **A.** Representative blots of western blotting. **B.** Densitometry analysis using Image J, as explained in Chapter 2 (Materials and Methods). Data are expressed as mean ± SEM, n=2 independent experiments with 3-well replicates. One-way ANOVAs were used and followed by post-hoc comparison tests (Turkey's comparisons test), **(P<0.01); ***(P<0.001); ****(P<0.0001).

6.3.12 The Effects of Treatment with Myotube CM that Overexpresses LCN-2 on p.HSLser 563 in Adipocytes

The expression level of protein phosphorylation of p.HSL$^{ser\ 563}$ in response to myotube CM that overexpresses LCN-2 in cultured adipocytes post 6 hr, 24 hr and 48 hr was evaluated to determine whether LCN-2 has a role in lipolysis. Results in Figure 6.15 show that the expression level of phosphorylated protein (p.HSL$^{ser\ 563}$) increased 1-fold from 6 hr to 24 hr when adipocyte cells were treated with 50% myotube CM (LCN-2+DOX.) compared to controls. However, LCN-2 (myotube CM, LCN-2+DOX.) had no effect on phosphorylation of p.HSL$^{ser\ 563}$ post 48 hr compared to controls (myotube CM; myotube CM LCN-2-DOX.).

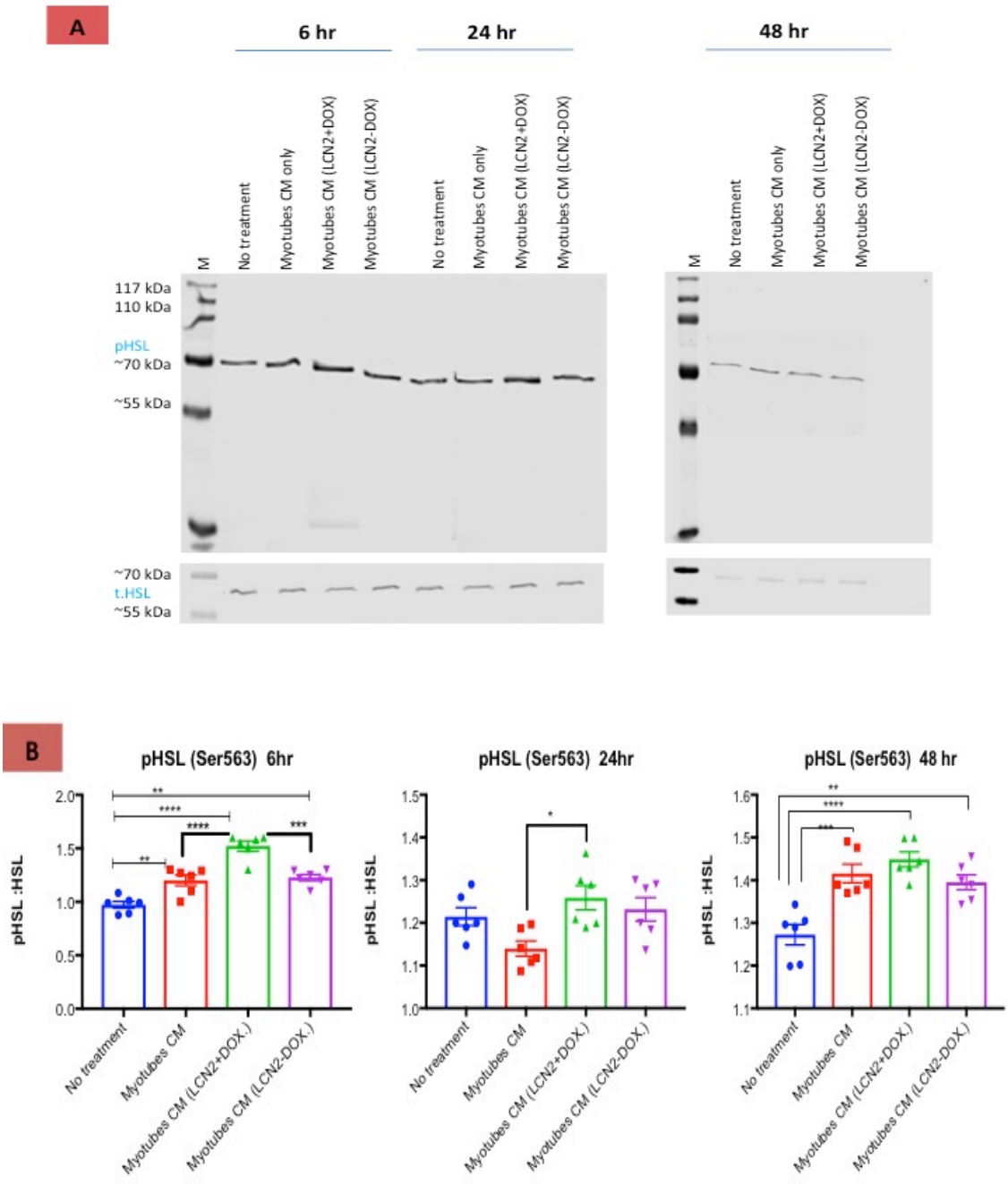

Figure 6.15. Effects of treatment with human myotube CM treatment that overexpresses LCN-2 on lipolysis of cultured adipocytes. Following 6 hr, 24 hr and 48 hr treatment with myotube CM (from days six-eight), the protein expression of p.HSL^{Ser563} in the cell lysate was evaluated via western blotting **A.** Representative blots of western blotting. **B.** Densitometry analysis using Image J, as explained in Chapter 2 (Materials and Methods). Data are expressed as mean ± SEM, n=2 independent experiments with 3-well replicates. One-way ANOVAs were used and followed by post-hoc comparison tests (Turkey's comparisons test), *(p<0.05); **(P<0.01); ***(P<0.001); ****(P<0.0001).

6.3.13 Assessment of Lipid Accumulation in Cultured Adipocytes Using Two Approaches for Measuring Fluorescence Intensity of Nile Red Staining

We used Nile Red to stain neutral lipids as it is a benzophenoxazone dye (9-diethylamino-5H-benzo[α]phenoxazine-5-one) and thus dissolves quickly in organic solvents but is insoluble in water. Nile Red was also used to stain triglycerides and cholesterol because it forms a strong colour and solubilises very well in lipids but is less soluble in solvent. It is also known to not interact with surrounding tissues and has excitation and emission wavelengths of 450-500 and 520 nm respectively (Escorcia, Ruter, Nhan, & Curran, 2018). The experimental plan and methodology used here is illustrated in Figure 6.4. 3T3 L1 cells differentiated to adipocytes were cultured in 12-well plates at 4000 cells per well and stained with Nile Red to measure the fluorescence intensity. To establish a good method for assessing lipid accumulation in cultured adipocytes, we differentiated 3T3 L1 cells to adipocytes cultured in 12-well plates at 4000 cells per well and stained them with Nile Red to measure the fluorescence intensity. Two approaches were used to assess the lipid accumulation with the same settings (Ex.480 nm, Em. 520 nm) for wavelength measurement (excitation and emission). The first approach measured the fluorescence intensity using a fluorescence microscope (wide-field microscope Zeiss 200M). Images were acquired using 10x magnification (total Nile red analysis of fluorescence images). The second approach measured the fluorescence intensity using a plate reader (FLUOstar® Omega, USA) (Orbital average analysis of the well-scan). Results post-6 h, -24 h and -48 h treatment are detailed in the following section.

6.3.14 Effects of Treatment with Myotube CM that Overexpresses LCN-2 on Lipid Accumulation in Adipocytes

Lipid accumulation (specifically triglyceride accumulation) was measured via fluorescence intensity of Nile Red staining, as shown in Figure 6.3, using both approaches (fluorescence microscope and plate reader of well scan). LCN-2 had no significant effect on the lipid accumulation in cultured, stained adipocytes post 6 hr and 24 h compared to controls (myotube CM only; myotube CM-DOX.) but did have a significant effect on triglyceride accumulation in adipocytes post-48 h treatment with 50% myotube CM that overexpresses LCN-2 (see Figures 6.16 - 6.18). We noticed that the size of lipid droplets increased in myotube CM upon treatment with cultured adipocytes only at the specific time point of post 48 hr. There is a sizeable effect of the treatment of human myotubes CM to adipocytes that could be related to other factors rather than secretion of LCN-2 in the CM derived from myotubes that affects lipolysis or the lipid metabolism, in general.

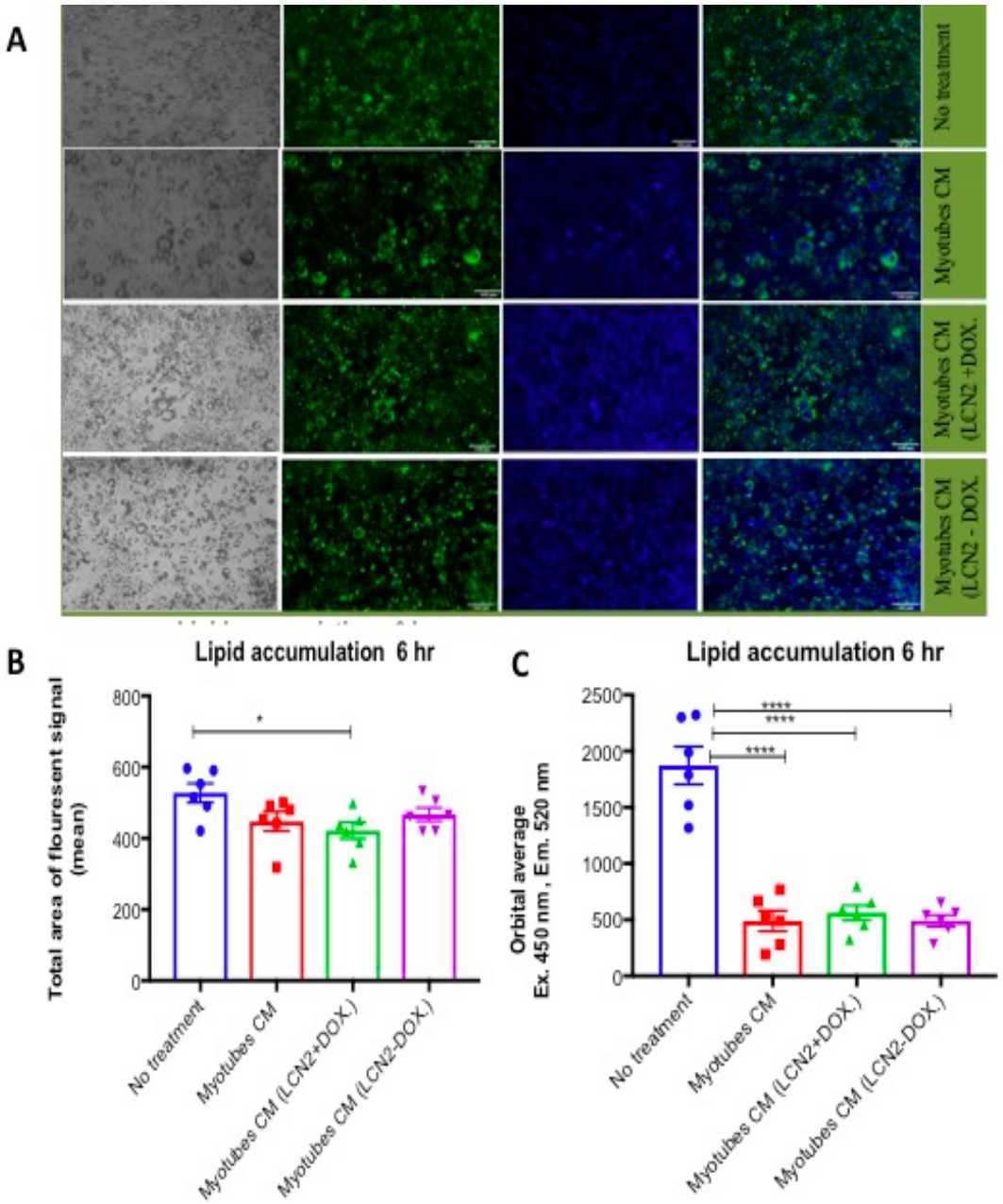

Figure 6.16. Effects of human myotube CM treatment on lipid accumulation of cultured adipocytes post-6 h. Differentiated 3T3-L1 adipocytes were incubated with 50% (1:1) myotube CM, where we overexpressed LCN-2 using lentiviral inducible vector. **A**. Representative images of adipocytes stained with Nile Red post-6 hr treatment using wide-field Zeiss 200M fluorescent microscope. **B.** Analysis of total area of fluorescent signal (Ex. 450 nm, Em. 520 nm) for all images that were acquired using a fluorescence microscope at 10x magnification ((n=2, independent experiments meaning human myotubes cultures were passaged twice with 3-well replicates within each cell passage). Methods of analysis are explained in Chapter 2 (Materials and Methods). **C.** Lipid accumulation was assessed by scanning for fluorescence signals (orbital average in each well n=3 of each treatment, n=2 independent experiments) using an Omega plate reader (Ex. 450 nm, Em. 520 nm). Statistical analysis was conducted using One-way ANOVAs, revealing significant effects when comparing treatments and no treatments ($P<0.05$; $P < 0.0001$, respectively, for **B** and **C**). Post-hoc Turkey's comparison tests were used, (**** $P < 0.0001$, * $P < 0.05$). Data are expressed as mean ± SEM. Scale bar, 100 µm.

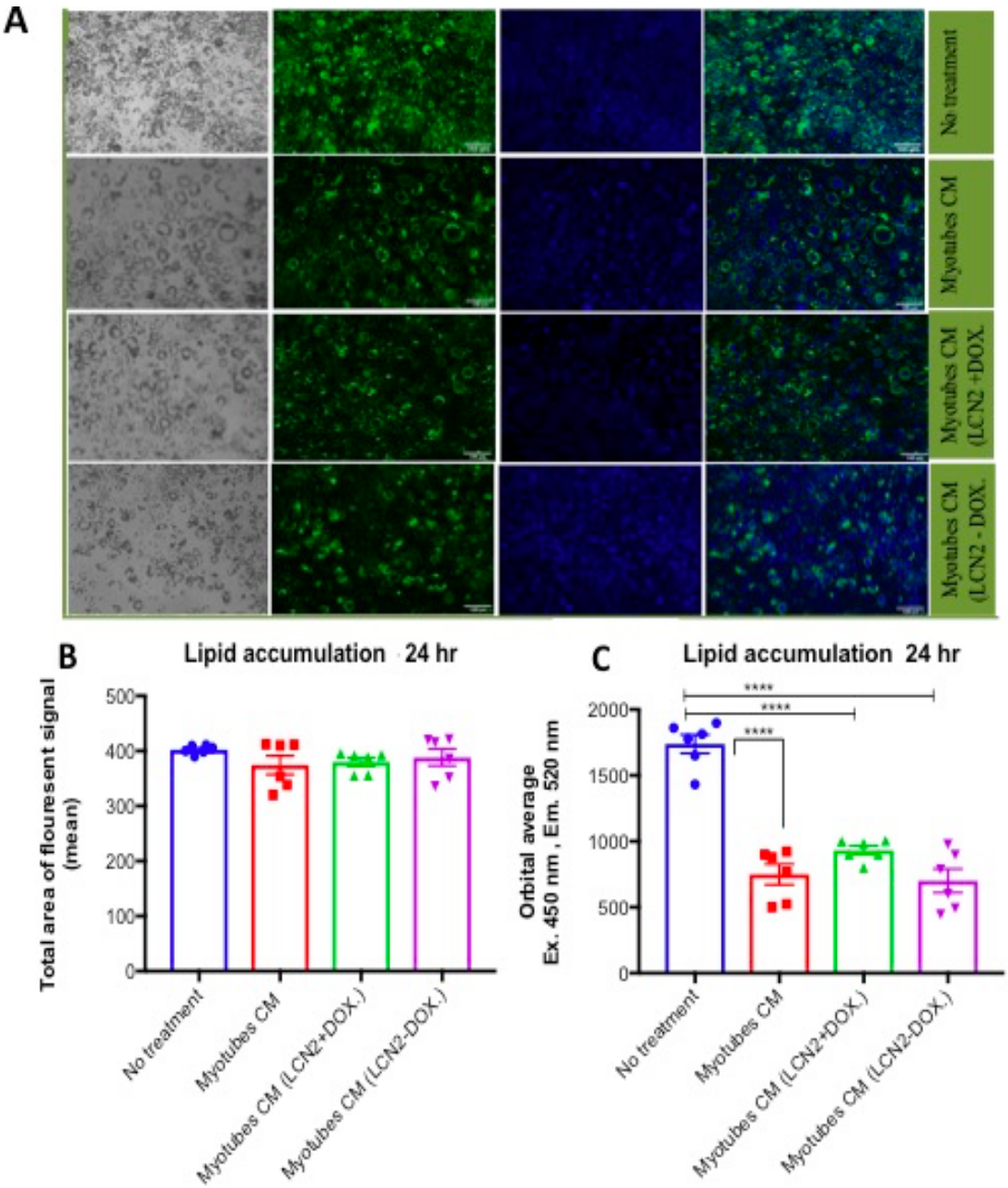

Figure 6.17. Effects of human myotube CM treatment on lipid accumulation of cultured adipocytes post-24 h. Differentiated 3T3-L1 adipocytes were incubated with 50% (1:1) myotube CM, where we overexpressed LCN-2 using lentiviral inducible vector. **A**. Representative images of adipocytes stained with Nile Red post-24 hr treatment using wide-field Zeiss 200M fluorescent microscope. **B**. Analysis of total area of fluorescent signal (Ex. 450 nm, Em. 520 nm) for all images acquired using a fluorescence microscope at 10x magnification (n=2, independent experiments meaning human myotubes cultures were passaged twice with 3-well replicates within each cell passage). Methods of analysis are explained in Chapter 2 (Materials and Methods). **C**. Lipid accumulation was assessed by scanning for fluorescence signals (orbital average in each well n=3 of each treatment, n=2 independent experiments) using an Omega plate reader (Ex. 450 nm, Em. 520 nm). Statistical analysis was conducted using One-way ANOVAs, revealing significant effects when comparing treatments and no treatments ($P<0.05$; $P < 0.0001$, respectively, for **B** and **C**). Post-hoc Turkey's comparison tests were used, (**** $P < 0.0001$, * $P < 0.05$). Data are expressed as mean ± SEM. Scale bar, 100 μm.

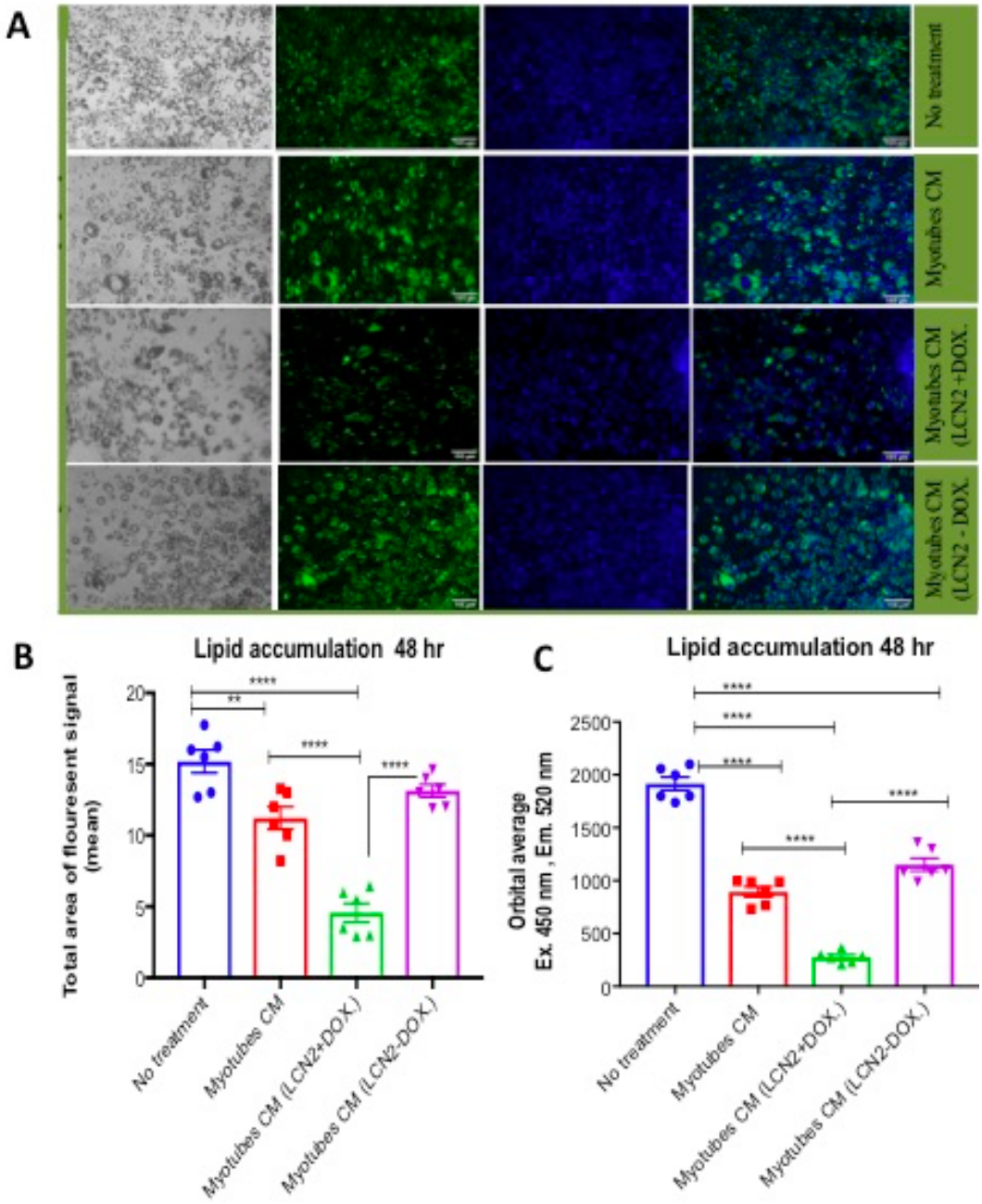

Figure 6.18. Effects of human myotube CM treatment on lipid accumulation of cultured adipocytes post-48 h. Differentiated 3T3-L1 adipocytes were incubated with 50% (1:1) human myotube CM, where we overexpressed LCN-2 using lentiviral inducible vector. **A**. Representative images of adipocytes stained with Nile Red post-48 hr treatment using wide-field Zeiss 200M fluorescent microscope. **B**. Analysis of total area of fluorescent signals (Ex. 450 nm, Em. 520 nm) for all images acquired using a fluorescence microscope at 10x magnification (n=2, independent experiments meaning human myotubes cultures were passaged twice with 3-well replicates within each cell passage). Methods of analysis were explained in Chapter 2 (Materials and Methods). **C**. Lipid accumulation was assessed by scanning for fluorescence signals (orbital average in each well n=3 of each treatment, n=2 independent experiments) using an Omega plate reader (Ex. 450 nm, Em. 520 nm). Statistical analysis was conducted using One-way ANOVAs, revealing significant effects when comparing treatments and no treatments ($P<0.05$; $P < 0.0001$, respectively, for **B** and **C**). Post-hoc Turkey's comparison tests were used (**** $P < 0.0001$, * $P < 0.05$). Data are expressed as mean ± SEM. Scale bar, 100 µm.

6.4 DISCUSSION

The general aim of this chapter was to investigate the endocrine effects of LCN-2 as an exercise-induced myokine on adipose tissue to determine whether LCN-2 exerts an endocrine effect on adipocyte metabolism. This is particularly important since we showed that LCN-2 (lipocalin-2) is released by human and murine skeletal muscle in response to EPS and AICAR – an exercise-like effect *in vitro*. Due to the COVID-19 outbreak that impacted our study by limiting our ability to recruit participants for isolating human biopsies, we instead used commercial human primary myoblasts that we differentiated towards mature human myotubes to overexpress and secrete LCN-2. Our functional validation study using commercial human primary myoblasts showed that cells preserved the structure of normal human primary skeletal muscle culture when differentiated towards the myotubes, which reflects the normal morphological *in vitro* process. However, we have shown that the cell passaging of these commercial cells (primary myotubes) does influence the morphology of myotubes. In fact, this study provides evidence for the appropriate passage number that should be used to reflect physiological responses to mimic an *in vivo* effect. Since the use of these cells showed that the cell passaging of primary commercial human myotubes does affect the cell morphology, we considered this when using human myotubes in the lab. As a result, we show for the first time that differentiated myotube cells were only used on passage 0 and 1 (P0-P1) to reduce any significant effects that may have occurred morphologically and physiologically if we had gone beyond passage 1. Thus, we treated cells on day five for a full course of seven days prior to sample collection (see Figures 6.5, 6.6 and 6.7).

The ELISA experiment confirmed the secretion of LCN-2 into cell media of human skeletal muscle (primary commercial myotube cells) in response to lentiviral

transduction using lentiviral inducible vector system. This result is in the line with our previous result obtained using primary human myotubes generated from healthy donors (participants), showing the overexpression and secretion of LCN-2 by human skeletal muscle.

3T3-L1 cells are fibroblast cells that are isolated from mice and used widely for studying adipogenesis and lipolysis, as well as any other cellular mechanism, since these cells can be differentiated towards adipocyte-like cells *in vitro* (https://www.atcc.org/products/cl-173). Our method of differentiating these cells towards adipocyte-like cells was mainly based on the use of Dexamethasone, IBMX and insulin in specific concentrations and showed good results when cells became more like adipocyte cells by day six. Many other researchers have used a combination of Dexamethasone and IBMX at different concentrations for the last several years to study adipogenesis (e.g., Camp *et al.*, 1999; Zebisch, Voigt, Wabitsch, & Brandsch, 2012; Vishwanath *et al.*, 2013).

In our study, we achieved complete differentiation of 3T3-L1 cells to adipocytes between days six and eight (see Figure 6.9). An *in vitro* model of lipolysis in cultured adipocytes (3T3-L1) was developed and validated. Isoproterenol treatment was used to stimulate TG hydrolysis *in vitro,* stimulating lipolysis in cultured adipocytes. We assessed lipolysis via two methods: the non-activity-based method and activity-based method, as summarised and illustrated by Schweiger *et al.* (2014). We measured the protein expression of ATGL and protein phosphorylation of HSL and assessed the levels of glycerol in cell media. An isoproterenol-stimulated lipolysis (10uM) model was able to release glycerol into adipocyte cell media following both 1 hr and 4 hr treatment. In addition, the combined treatment of 10 uM isoproterenol and 5 uM Triacsin-C showed a decreased level of glycerol. Our results

also showed that total ATGL protein expression was upregulated in isopreternol-stimulated lipolysis and activated the protein expression of HSL at the Ser563 site (p.HSL$^{Ser\ 563}$) after both 1 hr and 4 hr treatment. However, it was highly activated post 4 hr compared to basal and stimulated lipolysis with the addition of 5 uM Triacsin-C. Our optimised lipolysis model in this study was validated *in vitro* in cultured adipocytes and both methods of assessment were used to assess lipolysis (Schweiger *et al.*, 2014): the non-activity-based method (protein expression of lipases protein) and activity-based method (glycerol release).

To investigate the effect of LCN-2 on lipolysis, myotube CM was used to treat cultured adipocytes post 6 hr, 24 hr and 48 hr. Since we developed and validated a lipolysis model post 1 hr and 4 hr with isoproterenol-stimulated lipolysis (β-adrenergic stimulation), here using myotubes CM, we picked time points of 6 hr, 24 hr and 48 hr for the following reasons:

- Stimulation of lipolysis using isoproterenol leads to a rapid increase in the level of glycerol and FFAs into cell media within 15 min, reaching a plateau phase a few hours later (Schweiger *et al.*, 2014)
- We did not notice any change with myotube CM treatments post 1 hr and 4 hr.

We carried out lentivirus transduction experiments on human myotube-cultured cells on day five using inducible lentiviral vector system to overexpress and secrete LCN-2. We treated murine-cultured adipocytes (3T3-L1) with myotube CM in 1:1 ratio (50% treatment), and adipocyte CM only was used as a control. The different media used as a treatment on adipocytes were as follows:

- Myotube CM

- Myotube CM (LCN-2+DOX.)
- Myotube CM (LCN-2-DOX.).

Undoubtedly, lipolysis is complex, and there are many enzymes and proteins that have been shown to influence its pathway. For example, the activation or inhibition of the receptors of G protein-coupled receptors. However, we were able to demonstrate that treatment with LCN-2 (Myotubes CM LCN-2+DOX.) induced the release of glycerol into cell media following 6 h with approximately 3500 nmol/mg, 3000 nmol/mg following 24 hr, and 2700 nmol/mg following 48 hr. At each time point, LCN-2 induced glycerol released into cell media compared to all negative controls we used in this experiment.

Furthermore, we were able to identify changes that occurred to lipid metabolism intercellularly by examining the phosphorylation of HSL and ATGL since this is a critical step in the catabolism of TAGs. HSL was significantly activated on Ser563 ($p.HSL^{ser563}$) in response to the treatment of LCN-2 (myotube CM (LCN-2+DOX.)) to adipocytes post 6 hr. On the other hand, LCN-2 showed no significant activation of protein phosphorylation post 24 hr and 48 hr. It is well known that HSL has a site other than Ser563 which is linked to the activity of HSL (Krintel, Mörgelin, Logan & Holm, 2009). As a result, future investigation of other sites must be considered such as Ser660 and Ser659. Additionally, LCN-2 was able to upregulate ATGL protein expression in the cell lysate of adipocytes post-6 hr, -24 hr and -48 hr treatment compared to other controls (see Figure 6.15). However, post 48 hr, LCN-2 clearly induced the expression of ATGL by 2.3-fold. These results indicate the potential role of LCN-2 on lipolysis when secreted by human skeletal muscle. However, we should consider the differences between murine and human adipocytes regarding cell metabolism and other cellular events in response to such

treatments. For example, in animal models, an overexpression of ATGL has been shown to increase basal and stimulated lipolysis in murine adipocyte cell-lines (Meilin, Aviram, & Hayek, 2011). In addition, the KO of HSL does not show any effect on basal lipolysis but does affect stimulated lipolysis (Haemmerle *et al.*, 2006; Schweiger *et al.*, 2006). These results suggest a critical role for ATGL as a regulator of both basal and stimulated lipolysis in a murine model. Moreover, data using models of human adipocyte have shown that ATGL plays a less important role in regulating catecholamine-stimulated lipolysis in human fat cells and that there may be no similar mechanism for ATGL or HSL and the activation of lipolysis (Rydén *et al.*, 2007; Yuzbashian *et al.*, 2020). As a result, the expression of these lipase enzymes may differ in their activity and depend on the state of lipid metabolism.

Next, we examined changes regarding lipid accumulation in cultured adipocytes (3T3L-1) using Nile Red staining. We obtained lipid accumulation data using a fluorescent microscope and plate reader to measure the fluorescent signal in stained cells. We found that treatment with 50% LCN-2 (myotube CM that overexpresses LCN-2) reduced lipid accumulation significantly post 48 hr in cultured adipocytes. Indeed, prior research has shown that a mouse lacked LCN-2-accumulated excessive fats in hepatocytes (Asimakopoulou *et al.* 2014). In the same paper, it was also revealed that, in an animal model lacking LCN-2 as well as PLIN5, the formation of lipids *in vitro* and *in vivo* was not normal, which indicated the role of LCN-2 in lipid metabolism and that it could be regulated by PLIN5 in hepatocytes (Asimakopoulou *et al.* 2014). PLIN5 is a member of the perilipins family (PLIN1-PLIN5), which are involved in the formation of LD and TAGs storage. These are important in regulating lipid accumulation, inflammation and steatosis though PPARs (Sztalryd & Kimmel, 2014). In adipocytes, the role of LCN-2 is known

regarding energy metabolism and inflammation (Guo *et al.*, 2010; Zhang *et al.*, 2014; Deis *et al.*, 2019). Our results, as indicated above, show the possibility of LCN-2 to regulate cellular metabolism in adipocytes (lipid metabolism), but confirmation of these results is required to show if adipocytes take up LCN-2 inside cells. Our data shows the sizeable effect of the treatment of human myotubes CM to adipocytes that could be related to other factors rather than secretion of LCN-2 in the CM which was derived from myotubes. Analysing the CM before it is as a treatment in adipocytes is important to understand what factors affect lipid metabolism.

Additionally, the manner in which LCN-2 regulates lipid metabolism is still unclear, and further studies must be conducted to reveal this. Based on our results though, there are possible mechanisms revealed by which LCN-2 may regulate lipolysis and lipid accumulation in adipocytes as follows:

- In Chapter 3, we showed that LCN-2 and AMPK$^{(Th173)}$ is upregulated and secreted in response to AICAR and EPS (an exercise-like effect) in skeletal muscle. AMPK is an energy sensor, and it has been shown to regulate lipolysis in adipocyte though ATGL but not HSL (Jiang *et al.*, 2016). This could be the case, but more investigation is required to reveal the potential role of LCN-2 as a novel myokine in mediating the crosstalk between skeletal muscle and adipose tissue in an intermuscular fat reduction fashion (Addison, Marcus, LaStayo, & Ryan, 2014).
- In this chapter, we found that LCN-2 upregulated the expression of ATGL and reduced the accumulation of lipids following 48 hr, and thus it is possible that this is mediated by PPARγ since ATGL is PPARγ-dependant (Kershaw *et al.*, 2007).

- It has been shown that LCN-2 regulates lipid metabolism and thermogenesis in cultured adipocytes *in vitro* by mTOR (Deis, Lin, Bushman, & Chen, 2022). Studies have investigated the important role of mTORC1 in the regulation of the cAMP-PKA signalling pathway on lipid metabolism and thermogenesis *in vitro* in adipocytes by the β3-adrenergic receptor agonist (Ricoult & Manning, 2012; Liu *et al.*, 2016; Tran *et al.*, 2016). A recent study has also shown that glycerol level was reduced when LCN-2 was KO in the basal and stimulated lipolysis with isoproterenol in adipose tissue *in vivo* (Deis, Lin, Bushman & Chen, 2022), which is in line with our results in this present study.

To our knowledge, this is the first set of data indicating that LCN-2 reduces the accumulation of lipids intercellularly and enhances lipolysis by releasing glycerol (Figure 6.13), regulating key enzymes in the lipolytic pathway – including HSL and ATGL – in cultured adipocytes (3T3-L1). Whether the role of LCN-2 on lipolysis and lipid accumulation in adipocytes is a cause or effect remains unclear, and studies must be done at the molecular level to determine this. In conclusion, the 50% treatment of skeletal muscle derived LCN-2- (myotube CM (LCN-2+DOX.) induced lipolysis and reduced lipid accumulation in cultured adipocytes indicates the endocrine effects of LCN-2 as a novel myokine.

Chapter 7: General Discussion

7.1 SUMMARY OF MAIN SIGNIFICANT FINDINGS OF THE THESIS

The significant findings from studies that were carried out for the purpose of this thesis are summarised in the table below.

Table 7.1

Summary of Objectives and Significant Main Findings of this Thesis

Summary of main findings of this thesis
(Chapter 3) An *in vitro* model of exercise was developed successfully to study the upregulation and secretion of LCN-2 using electrical pulse stimulation (EPS) stimulation for 16 hr in primary human myotubes and C_2C_{12} murine myotubes: • **EPS model did not show any morphological changes to human and murine myotube cells.** • **Using this model, glucose level was reduced and lactate accumulation in cell media was higher in EPS-stimulated myotubes.** • **Using this model, stimulating myotubes with EPS for 16 hr was able to activate AMPK protein (p.AMPK ^{Th172}).** • **Using this model, PGC1-a mRNA expression was upregulated post-16 hr EPS.** • **Using this model, IL-6 mRNA expression was upregulated post-16 hr EPS.** **(Chapter 4) An *in vitro* model of exercise was used to study the upregulation and secretion of LCN-2 using electrical pulse stimulation (EPS) stimulation for 2 hr, 4 hr and 16 hr in primary human myotubes and C_2C_{12} murine myotubes:** • **The mRNA expression of ms.LCN-2 and hu.LCN-2 was upregulated in**

stimulated myotubes post-16 hr EPS.

- **The protein expression of msLCN-2 was upregulated in stimulated myotubes post 16-hr EPS but not hu.LCN-2.**
- **The level of protein secretion of both ms.LCN-2 and hu.LCN-2 was increased post 16 hr.**
- **Stimulating murine and human myotubes with EPS post 2 hr and 4 hr had no effect on the protein expression and secretion of LCN-2.**

(Chapter 4) AICAR (an exercise-like effect) was used to treat C_2C_{12} myotubes examine the expression and secretion of LCN-2:

- **LCN-2 protein expression was upregulated post-24 hr treatment but not 48 hr.**
- **LCN-2 protein secretion by myotubes was increased post 48 hr.**

(Chapter 5) An *in vitro* model of lentivirus transduction was used to overexpress hu.LCN-2 expression in cultured cells to study the endocrine effect of LCN-2 as a novel myokine:

- **GFP confirmed successful lentivirus transduction methods.**
- **Using western blot and ELISA, the level of LCN-2 protein expression and its secretion was found to be higher in cultured cells using the inducible lentivirus vectors MDA-MB468, C_2C_{12} myotubes and human primary myotubes.**

(Chapter 6) The endocrine effects of LCN-2 as a novel exercise-induced myokine:

- **Treatment with skeletal muscle-derived LCN-2 (myotube CM (LCN-2**

+DOX.)) using lentiviral transduction to overexpress and secrete LCN-2 from skeletal muscle.

- **Affected the lipid accumulation in cultured adipocytes following prolonged treatment (48 hr) compared to controls samples.**
- **Did not affect size of lipid droplets (LD), but treatment with myotube CM increased lipid droplet (LD) size compared to treatment with adipocyte CM only and myotube CM (LCN-2+DOX.)**
- **Increased the total protein expression of ATGL post 48 hr, but no effects shown post 6 hr and 24 hr.**
- **Induced the release of glycerol into media post 6 hr, 24 hr and 48 hr.**

What does this thesis add?

- **LCN-2 is a novel exercise-induced myokine.**
- **LCN-2 is released into C_2C_{12} myotube cell media in response to an exercise-like effect (AICAR).**
- **LCN-2 has powerful endocrine effects on lipolysis and lipid accumulation in cultured adipocytes.**

7.2 GENERAL DISCUSSION

Exercise is not only beneficial mentally but also physically. It has been shown to improve insulin sensitivity in muscles and the liver (Meex *et al.*, 2010) and control insulin resistance in people with T2DM (type 2 diabetics mellitus) and other metabolic diseases (Hansen *et al.*, 2016; Bhati *et al.*, 2018). A study on rats has shown good adaptation of the whole body in response to moderate exercise (Kokkinos *et al.*, 2010) on hyper-glycemia and hypertension (Richter *et al.*, 1999; Kokkinos *et al.*, 2010). Exercise has also been shown to alter various activities in skeletal muscle, such as metabolism and contractile activity, along with inducing changes on nearby tissue such as adipose, brain and liver. However, studies on the

communication between skeletal muscle and other tissues in response to exercise have failed to fully reveal the mechanisms, and so this area requires further investigation. The capacity of skeletal muscle to secrete proteins into circulation in an endocrine fashion, for example, is a mechanism for which our understanding is still developing. It is known that these proteins, when secreted by skeletal muscle in response to physical activity (exercise), are given the name 'myokines' (Raschke *et al.*, 2013), and these myokines have been shown to have positive impacts on other distant tissues in terms of metabolic diseases (Pedersen & Febbraio, 2008). When they are produced in response to physical activity by contracting myotubes (skeletal muscle), they are known to regulate metabolism and induce anti-inflammatory responses, whilst physical inactivity induces systemic inflammation (Pedersen, 2009). As a result, studying the crosstalk between muscle and nearby tissue, such as liver or adipose tissue, has become the focus of a number of recent researchers (Blair & Church, 2004). Strong and accumulative evidence has shown that myokines affect lipid metabolism and glucose uptake; however, the molecular mechanisms by which myokines are secreted in response to physical activities by skeletal muscle is poorly understood, and further studies should be undertaken to investigate this (Pedersen & Febbraio, 2008; Barra *et al.*, 2012).

Energy deficiency is defined as the condition in which the human body requires energy and consumes more oxygen, as with exercise. During low-intensity or moderate exercise, lipids are known to be a good source of energy (Schweiger *et al.*, 2006). Therefore, a process whereby adipose tissue hydrolyses triglyceride for the release of free fatty acid and glycerol is termed lipolysis, which occurs during exercise for use as energy (Berglund *et al.*, 2010). In long-duration exercise, intramuscular lipolysis and the function of adipose tissue is regulated by mechanisms

of either hormone or exercise factors that are released by skeletal muscle. The major mechanism is endocrine, an example of which is when epinephrine binds to β adrenergic receptors and thus activates both HSL and PLIN-1. Despite this knowledge, the mechanism by which lipid metabolism is regulated is not fully understood. This is, therefore, an important aspect that should be focused on to study chronic and acute responses to different types of exercise.

Since exercise induces the secretion of myokines, it increases the activity of AMP-activated protein kinase (AMPK) in skeletal muscle, and AMPK signalling pathways have been postulated to mediate a variety of metabolic consequences (Fujii *et al.*, 2006). AMPK regulates anabolic and catabolic pathways to maintain energy storage as intracellular energy, and the role of AMPK as an energy sensor is important in tissues with a high rate of energy turnover. Skeletal muscle is one of these tissues due to the dramatic variations in energy demand that occur pre and post exercise. However, in spite the concentration of myokines increasing post exercise in plasma, it not clear if these myokines are directly released by skeletal muscle cells or other cells such as blood cells and vessels (Nikolić *et al.*, 2016). Thus, in this thesis, we aimed to develop an in *vitro* model of exercise using EPS to identify novel myokines, metabolic changes and their possible secretory pathways.

LCN-2 was first noted in previous studies to be secreted by adipocytes, and since then, the role of LCN-2 as a new adipokine has been widely discussed (Aigner *et al.*, 2007; Mosialou *et al.*, 2018; Jaberi *et al.*, 2021). However, despite Lipocalin-2 protein being widely expressed in several tissues, its role has not been fully investigated in skeletal muscle, and it appears that the presence of LCN-2 is absent without stimuli (Rebalka *et al.*, 2018; Jaberi *et al.*, 2021). As a result, we focused on studying the role of LCN-2 in skeletal muscle in response to exercise since limited

studies have been conducted on the role of LCN-2 post exercise *in vivo*, and no studies have been done using an *in vitro* model. Additionally, it is helpful to understand LCN-2's role in response to exercise in an endocrine or autocrine fashion as LCN-2 levels in plasma have been shown to increase more in circulation post-acute exercise in those that are obese rather than of normal weight (Damirchi, Rahmani-Nia, & Mehabani, 2011; Ponzetti *et al.* 2021). In addition, a study by Nakai *et al.* (2021) demonstrated that the level of LCN-2 in the circulation did not change with long-term exercise over a 12-week period (Nakai *et al.*, 2021). This could indicate that the effects of LCN-2 are different depending on various factors such as type of exercise, duration and the methods of detecting LCN-2. In this thesis, we hypothesised that LCN-2 is a potential novel myokine that exerts a powerful endocrine effect post exercise. Data were provided in this thesis that support this hypothesis, and we also found that LCN-2 provides a powerful effect when secreted by skeletal muscle post exercise in an endocrine fashion (adipocytes) specifically in terms of lipid accumulation and lipolysis.

In Chapter 3, we developed an exercise model *in vitro* by using EPS, a method that has been widely used on cultured cells in various research (Aas *et al.*, 2002; Silveira, Pilegaard, Kusuhara, Curi, & Hellsten, 2006; Fujita, Nedachi, & Kanzaki, 2007; Nedachi *et al.*, 2008; Burch *et al.*, 2010; Yano *et al.*, 2011; Lambernd *et al.*, 2012; Nikolic *et al.*, 2012). In relation to previous studies, our EPS performed similarly to the protocol established by Chen *et al.* (2019), in which 1 Hz, 2 ms and 20 V for 16 h was used for identifying contraction-regulated myokines. We were able to show for the first time the upregulation of PGC1-a mRNA expression, IL-6 mRNA expression, AMPK protein and GLUT-4 using this EPS protocol in both C_2C_{12} and human-cultured myotubes. Additionally, we were able to demonstrate

lactate accumulation and a decrease in glucose concentration in the myotube cell media for both cultured C_2C_{12} and human myotubes: a significant rise of PGC1-a mRNA expression, up-regulation of IL-6 mRNA expression, AMPK activation, and recruitment of GLUT-4 via immunocytochemistry. Thus, we concluded that this model of EPS in myotubes represents a physiologically relevant *in vitro* model of exercise that can be used for future studies relating to contraction-regulated myokines.

In Chapter 4, we examined mRNA expression, protein expression and secretion of LCN-2 by applying exercise-like effects using AICAR and EPS in cultured human and murine myotubes. Studies detailed in this chapter provided the first evidence to contribute towards confirming that mRNA expression of LCN-2 is significantly upregulated post-16 hr EPS in both human and murine cultured-stimulated myotubes. However, its level was higher in murine compared to unstimulated myotubes. On the other hand, we detected the protein level in the cell lysate of murine-cultured myotubes, but it was absent in human-cultured myotubes in response to EPS. Moreover, the secretion level of LCN-2 in and by skeletal muscle (myotubes) was observed post EPS. In C_2C_{12} myotubes, the level of secretion significantly increased by 50-fold. On the other hand, human myotubes did not express LCN-2 post-2 hr, -4 hr and -16 hr EPS. The undetectable level of protein expression of LCN-2 in cell lysate of human myotubes post-2 hr and -4 hr EPS was due to the rise in mRNA level of expression not being high enough to be translated into protein. Once LCN-2 mRNA forms, synthesises and accumulates, it is transported outside the nucleus to cytoplasm and is translated into LCN-2 protein, at which point it is secreted by skeletal muscle cell to perform a specific function. Thus, all LCN-2 protein secreted by human myotube cells post 16 hr increased 3-fold compared to unstimulated

human myotubes, explaining the decline in mRNA expression of LCN-2 post-16 h of EPS but not post 2 hr or 4 hr.

This is the first time that the mRNA, protein expression and secretion of LCN-2 in skeletal muscle cells has been investigated and described post EPS stimulation. The outcomes evidenced are similar to those of other myokines, such as IL- 6, IL-8 and IL-15, which are known to be upregulated post exercise. To be specific, the level of IL-6 in circulation has been shown to rise 100-fold in response to acute exercise (Pedersen & Fischer, 2007). Other evidence indicates the role of LCN-2 in inflammation and energy homeostasis since its expression increases after LPS, TNFa and IL-1b treatment in a variety of tissues (Aigner *et al.*, 2007; Chen *et al.*, 2007; Yan *et al.*, 2007). This finding suggests the increased level of LCN-2 post exercise could be related to reduced instances of health disorders in nearby tissues. In sum, the EPS effects on LCN-2 and the up-regulation level of mRNA and protein post-exercise-like stimulus (EPS) suggest that LCN-2 is a novel myokine secreted by skeletal muscle in a time-dependent manner. In relation to the fact that researchers have noted a possible relationship between the AMPK pathway and myokine secretion or production, we noticed that our EPS model was able to activate AMPK and LCN-2 post 16 hr. On the basis that there could be a relation between the AMPK and LCN-2, AICAR treatment was used to examine the expression and secretion of LCN-2 since AICAR has been known to activate AMPK. We found that AICAR was able to express and secrete LCN-2 in a time-dependent manner, and this indicates a possible relationship between the AMPK-activation pathway and LCN-2, a finding which needs further investigation.

In Chapter 5, we aimed to assess the protein overexpression and secretion of LCN-2 and PGC1a into both cultured human and mouse (C_2C_{12}) myotubes to use this

for identifying whether skeletal muscle-derived LCN-2 has effects, as other myokines do, on nearby cells such as adipocytes (e.g., 3T3L-1 to WAT) in terms of lipid accumulation and lipolysis. To address the hypothesis, cloning for PGC1a and LCN-2 was planned carefully, constructed using a lentiviral inducible vector to overexpress the gene (Chapter 2, section 2.31), and therefore we assessed the process by using a basic cell line as a first step. MDA-MB-468 cells were used as an initial test in the study. The MDA-MB-468 cell-line was first isolated in 1977 from an elderly female patient with aggressive carcinoma of the breast (Cailleau *et al.*, 1978). We were successfully able to model the expression and secretion of LCN-2 and PGC1-a expression *in vitro* using an inducible lentiviral vector.

In this study, an inducible lentiviral vector allowing the overexpression of LCN-2 and PGC1-a was constructed to model their expression and secretion *in vitro* in skeletal muscle. Since the structure of LCN-2 comprises one N-glycosylation and one intra-chain disulfide link (Bandaranayake *et al.*, 2011), it was important for this study to mimic the expression of LCN-2 in human myotubes to retain the LCN-2 protein in its native structure with accurate post-translational modifications that are necessary for its release by myotube cells. Because myotube cells are non-proliferative, the lentiviral vector gene delivery method was chosen for this study due to its ability to infect both dividing and non-dividing cells. We observed the secretion of endogenous LCN-2 by skeletal muscle into cell media from both cultured human and murine myotubes, suggesting a role of this protein as an exercise-induced myokine. However, despite not seeing LCN-2 protein expression in cell lysate of human myotubes, we were able to see the protein expression clearly using lentiviral inducible vector.

There is evidence to suggest that PGC1a transcription factor and AMPK mediate the secretion of myokines by skeletal muscle in response to contractile activity (Karlsson *et al.*, 2020). It is therefore plausible to suggest that LCN-2 could have an endocrine effect on other metabolically active cells in response to its secretion due to exercise. Based on our data from Chapters 4 and 5, we have shown that PGC1a overexpression, EPS and AICAR secretes LCN-2 by skeletal muscle, and thus we can conclude that LCN-2 is a novel myokine and that its secretory pathway involves AMPK and PGC1a. However, this secretory pathway requires further investigation.

In Chapter 6, experiments were undertaken to investigate the endocrine effects of LCN-2 once secreted by skeletal muscle in adipocytes. We found that treatment of 50% LCN-2 ((human Myotube CM {LCN-2+DOX}) reduced lipid accumulation significantly post 48 hr in cultured adipocytes and induced ATGL expression in the cell lysate of adipocytes but not HSL (p.HSLS^{er563}). Additionally, 50% of human myotube CM (human Myotube CM {LCN-2+DOX}) was able to induce lipolysis by measuring glycerol release into cell media (CM) compared to controls. To our knowledge, this is the first set of data indicating that LCN-2 reduces the accumulation of lipids intercellularly (Figure 6:17; Figure 6.17; Figure 6:18) and enhances lipolysis by releasing glycerol (Figure 6.13). We also showed that it regulates key enzymes in the lipolytic pathway, including HSL and ATGL, in cultured adipocytes (3T3-L1). Together these data suggest plausible translation of the findings into human studies of obesity and ageing, where these effects – as well as implications of LCN-2 – should be investigated further using a novel approach (rather than of using cell lines to apply the whole subcutaneous adipose tissue secretome) which physiologically reflects the cross talk between muscle and adipose

tissue. In addition, investigating whether different compartments of adipose tissue, such as visceral and intramuscular adipose tissue, might mediate the effect of muscle LCN-2 on lipid metabolism and lipolysis is an area for future study. Previous studies have shown that anti- diabetic drugs prevent obesity-upregulated expression of LCN-2 and the circulation level in rats, T2D mice and humans dignosed with T2D ((Febbraio & Pedersen, 2020; Guo, Li, & Xiao, 2020). Additionally, it is not clear yet what effects LCN-2 has on the regulation of skeletal muscle (Wilhelmsen, Tsintzas, & Jones, 2021). Thus, it is important to study the autocrine and paracrine of LCN-2. Dysfunction of the pathway that leads to the secretion of myokines could play a role in pathogensis (e.g., T2B and sarcopenic-obesity), aging, and metabolic diseases (Severinsen & Pedersen, 2020). It has been shown that aging lowers the secretion level of some myokines, such as IGF-1, IL-15, irisin and sesterin, and effect which has been shown to be reversible using exercise (Febbraio & Pedersen, 2020; Guo, Li, & Xiao, 2020)

Whether the role of LCN-2 on lipolysis and lipid accumulation in adipocytes is a cause or effect remains unclear, and studies must be done at the molecular level to determine this. Altogether, data from this thesis indicate that LCN-2 is a novel myokine and that it has a powerful role once secreted by skeletal muscle on lipolysis and lipid metabolism in cultured adipocytes. Although LCN2 is linked to exercise-induced myokines, the specific mechanism of action is still not fully understood. More specifically, its role once secreted by skeletal muscle in response to exercise and the mechanism by which LCN-2 crosses the bloodstream (BS) to reach distant organs to perform specific functions remain areas to be studied. As a result of this knowledge gap, our proposed hypothesis, as explained in full throughout this chapter, examines how LCN-2 acts on other cells once secreted by skeletal muscle in

response to exercise. A key focus is on adipocytes that are at the ligand-binding site of LCN-2, allowing LCN-2 to bind to the cell surface receptor. As mentioned in Chapter One, the binding cavity of LCN-2 is larger and more polar compared to other lipocalin proteins. This allows the cell receptors on cell membranes to bind to LCN-2, forming a complex structure that allow the cell to perform key functions at the cellular level. This confirms the activity of LCN-2 inside cells.

A previous study was conducted using primary hepatic cells from a mice model in which the mice were fed with NAFLD (non-alcoholic fatty liver disease). Results revealed that LCN-2 acts on lipid metabolism by accumulating more intracellular lipids via PLNP-5 (Perilipin-5) (Asimakopoulou *et al.*, 2014). In addition, the same study also fed mice with methionine- and choline-deficient diets, and a lack of LCN-2 revealed increased accumulation of lipids in primary hepatic cells. In this present study, we have shown that LCN-2 reduces lipid accumulation and induces lipolysis in cultured adipocytes. Again, these data indicate that LCN-2 plays an essential role in lipid metabolism, but its mechanism must be full explored in future research, which should aim to reveal whether there are differences from tissue to tissue based on the type of ligand and cell receptor.

As previously noted, there are two known receptors of LCN-2: Megalin/LRP2 and SLC22A17. We hypothesise that LCN-2, when secreted by SkM in response to exercise, binds to the megalin receptor at the adipocyte cell surface to help facilitate the movement of LCN-2/ligand complex into cytoplasm (Figure 7.1). Lipids are the most common ligands that bind to LCN-2. These are imported by LCN-2 via megalin on the cell surface of adipocytes. Lipids can then move to the cytoplasm to activate the most common transcription factor – peroxisome proliferator-activated receptor gamma (PPARγ) – and regulate ATGL protein: the

first stage in the lipolysis pathway that occurs in adipocytes. Once LCN-2 imports its ligand via megalin, it delivers a message and then is recycled and secreted by adipose tissue (Figure 7.1).

The other cell receptor to which LCN-2 can bind is SLC22A17, and a previous study has shown that adipocytes express SLC22A17, and that LCN-2 can be taken up in and out adipocyte via this receptor to faciltate its effects (Meyers *et al.*, 2020). The mechanism of action underlying the endocrine effects of exercise-induced LCN-2 as a novel myokine is still unclear, but our results indicate that muscle LCN-2 positively regulates lipolysis and lipid metabolism via SLC22A17. Secretion of LCN-2 by skeletal muscle in response to exercise can thus cross the bloodstream to bind to the cell surface of adipose via SLC22A17 and import the effects of exercise into cells. Therefore, exercise could be responsible for increasing the conversion of AMP/ATP inside cells to stimulate the activity of AMPK and further cause lipolysis to be activated via the AMPK-ATGL pathway. Indeed, several studies have shown the involvement of AMPK in the regulation of lipolysis and in adipose tissue in response to exercise (Daval, Foufelle, & Ferré, 2006; Ahmadian *et al.*, 2011; Kim *et al.*, 2016) (Figure 7.2).

7.3 LIMITATIONS OF THE THESIS

This findings of this thesis are strengthened by the following factors. First, the careful design of experiments and use of well-defined models (i.e., an exercise model *in vitro* using human cultured myotubes of greater physiological relevance to human cell cultures that were maintained in a glucose and lactate concentration and monitored for pH and CO_2 concentration). Gene expression studies have been used widely to understand the molecular mechanism of metabolic disorders, cancers and some heart diseases (Kim *et al.*, 2010). Gene expression is known to regulate both

mRNA and protein, and their secretion levels. Studying gene expression of LCN-2 by looking at the level of mRNA and protein expression as well as their secretion into cell media is another advantage of this thesis, and therefore were able to rule out the final outcome of LCN-2 as a novel myokine in terms of its expression and secretion. It was important to examine changes at the mRNA or protein level because there is contradiction evident in findings of different studies on myokines. For instance, a study by Friedmann-Bette *et al.* (2012) showed that IL-6 is increased at the protein and mRNA level with some inflammatory markers; however, Boman, Burén, Antti and Svensson (2015) concluded that the expression level of mRNA was not changed post exercise. Therefore, we opted to base our analysis at both mRNA and protein levels and to study the level of their secretion by skeletal muscle in response to exercise.

In terms of the limitations of this thesis, first, we must acknowledge the undetectable level of LCN-2 protein in human cell lysate, perhaps due to the protein being very low in abundance and thus undetectable by western blot in the cell lysate. Therefore, the reliance on the lentivirus over-expression of LCN2 to conduct the adipocyte cross-talk studies was necessary. We have seen that over-expression of LCN2 is unlikely to have any physiological effect. Another and final limitation is the use of CM derived from human skeletal muscle (myotubes) following lentiviral transduction to overexpress mRNA and protein expression of LCN-2 (and thereby the secretion of LCN-2 by human myotubes) without measuring other factors that could be secreted by myotubes and have sizeable effects. Skeletal muscle secretes factors with and without stimuli such as the myokines MMP-2 and SPRC (Hamrick, 2012). Thus, understanding the level of secretion of these by skeletal muscle is important when treating adipocytes with myotube CM. Interestingly, IL-6 and IL-15

have not been reported to be altered due to the use of media in terms of expression and secretion under EPS *in vitro*. In a recent study, KRB buffer usage in media has been shown to be the base from which IL-6 is secreted by skeletal muscle cells (Furuichi, Manabe, Takagi, Aoki, & Fujii, 2018). Therefore, IL-6 and IL-15 are unlikely to have affected lipolysis in our study since we used DMEM media. However, measuring secreted factors in myotube CM should be considered in future work. Purification steps prior to treating adipocytes with myotube CM could be a method of validating our data on the effect of muscle-derived LCN-2 on lipolysis and lipid accumulation in adipocytes.

7.4 FUTURE WORK

Despite the effects of LCN-2 on adipose tissue and liver having been studied in some detail in recent years, it is still necessary to further characterise LCN-2 and study its pathway in different cells once it is secreted by SkM in response to exercise. Specific suggestions of future work that could be done to further understand the biology of LCN-2 are as follows. First, defining the cell receptors via which LCN-2 can act is crucial to understanding the signalling transduction pathways that LCN-2/ligands can go through to deliver messages to other cells. Second, isolation and identification of the type of ligands that bind to LCN-2 when it is secreted by skeletal muscle to perform its action on other cells is required. Third, imaging might be beneficial to determine whether LCN-2 is taken up by cells or acts only on the cell surface. This could potentially confirm the powerful effect of LCN-2 on lipolysis and lipid metabolism. Finally, it is worth investigating the comparative effects of secreted LCN-2 on multiple tissues, such as muscle, adipose and liver to uncover how LCN-2 acts on other cells.

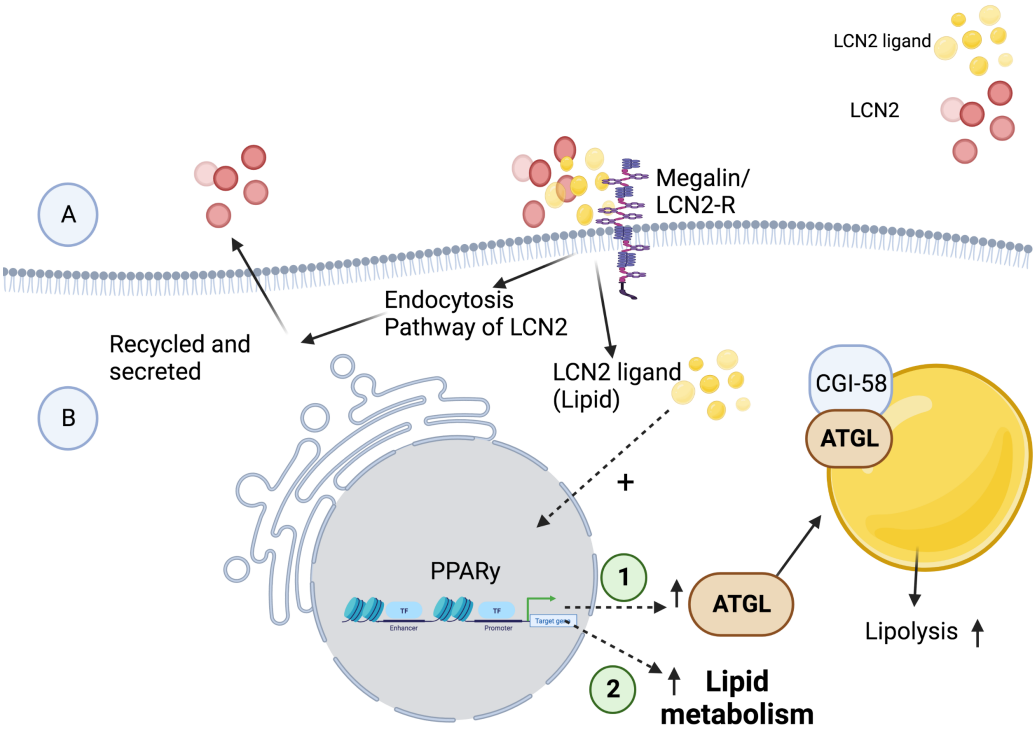

Figure 7.1. Proposed first mechanism of the effect of exercise-induced LCN-2 on adipocytes via megalin. The proposed hypothesis suggests that LCN2 plays a role in regulating lipid metabolism and lipolysis via PPARγ. **(A)** LCN-2 derived from muscle in response to exercise with its specific ligand (lipids) imported into cells via the cell surface receptor, megalin. **(B)** LCN2 imports lipids into adipocytes via the specific receptor, megalin, through endocytosis pathways. The complex of LCN2/lipid is first taken up by cells, and this causes LCN2 to release from the lipids and be recycled and secreted by adipocytes. The lipids then move into the cytoplasm, to activate the transcription factor, PPARγ. This interaction enhances lipid metabolism, resulting in decreased accumulation of lipids in adipocytes and the triggering of ATGL to enhance the lipolysis pathway inside cells. Created with Bio-Render (https://biorender.com).

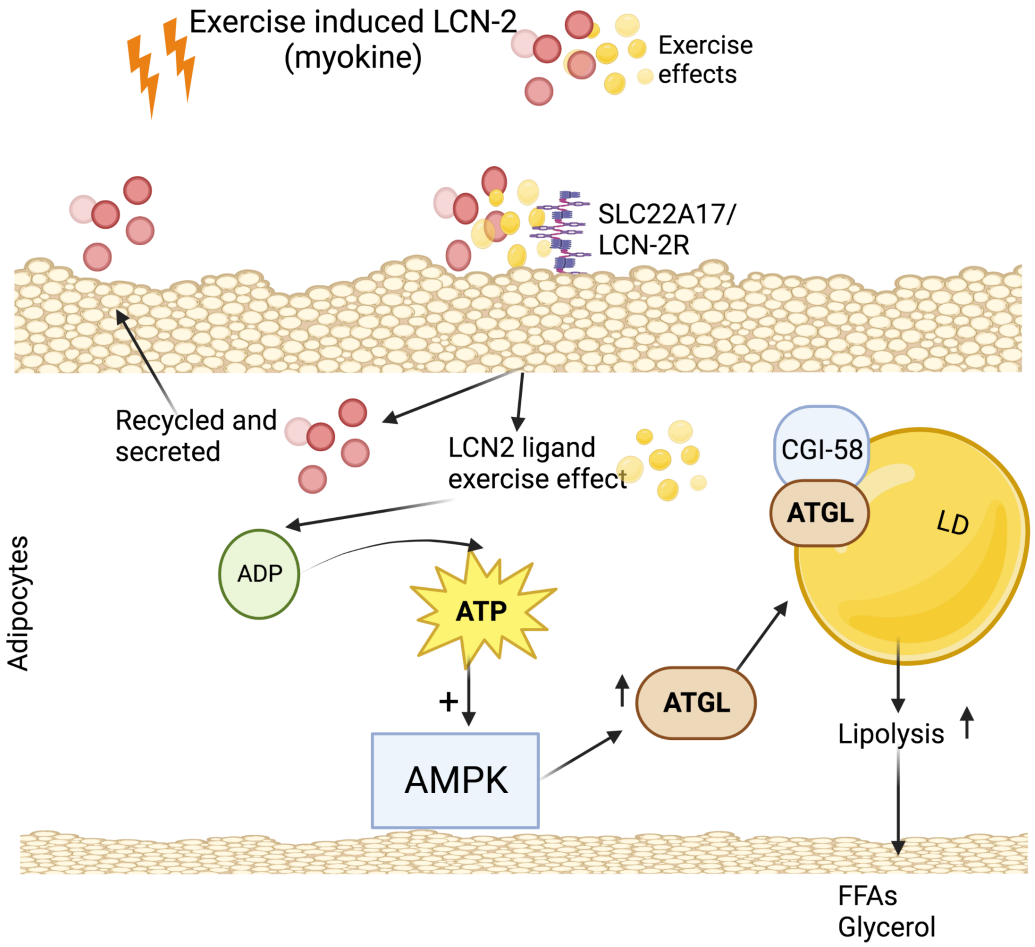

Figure 7.2. Proposed second mechanism of the effect of exercise-induced LCN-2 on adipocytes via SLC22A17. The proposed hypothesis suggests that LCN2 plays a role in regulating lipolysis via AMPK in response to exercise. (A) LCN-2 derived from muscle in response to exercise for LCN-2 to transport its effect via the cell surface receptor-SLC22A17. (B) LCN2 imports the effects of exercise-induced LCN-2 into adipocytes via the receptor, SLC22A17, by activating the conversion of ADP to ATP, a process which then stimulates AMPK. The complex of LCN2/exercise is first taken up by cells, causing LCN2 to deliver a signal before it is recycled and secreted by adipocyte. This stimulated AMPK activates ATGL to translocate from the cytoplasm into LD as the first stage of the lipolysis pathway. Created with Bio-Render (https://biorender.com).

7.5 CONCLUSION

To our knowledge, this is the first set of data indicating that LCN-2 is released by skeletal muscle in response to exercise-like effects (EPS, AICAR) (Figures 4.4 and 4.5), reduces the accumulation of lipids intercellularly (Figure 6.16; Figure 6:17; Figure 6:18) and enhances lipolysis by releasing glycerol (Figure 6.13), regulating key enzymes in the lipolytic pathway, including HSL and ATGL. Whether the role of

LCN-2 on lipolysis and lipid accumulation in adipocytes is a cause or effect remains unclear, and studies must be done at the molecular level to determine this. In conclusion, the 50% treatment of skeletal muscle-derived LCN-2- (Myotube CM (LCN-2+DOX.) induced lipolysis and reduced lipid accumulation in cultured adipocytes indicates the endocrine effects of LCN-2 as a novel myokine. Results suggest powerful communication between muscle and adipose tissue mediated by LCN-2, which induces lipolysis and could be explained as an exercise-induced reduction of intermuscular fat (Addison *et al.*, 2014).

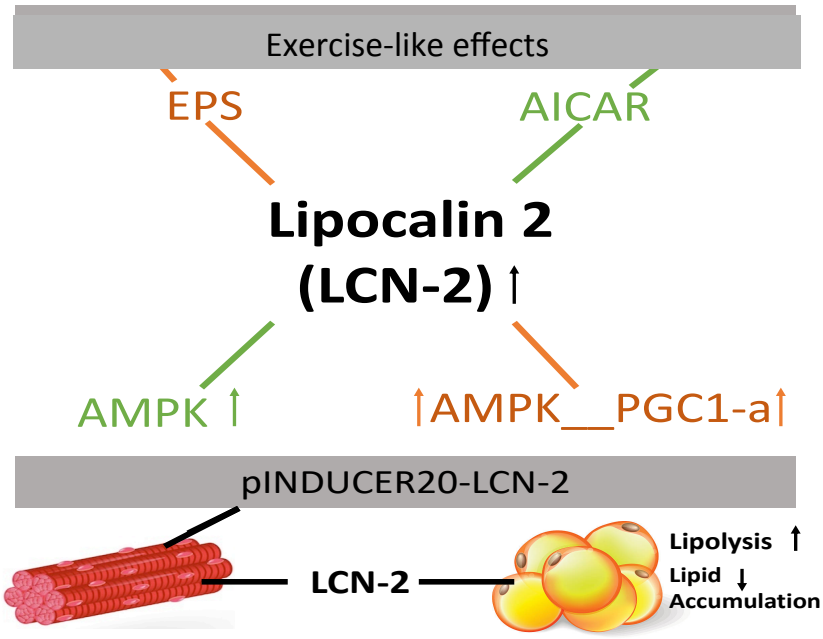

Figure 7.3. Overall proposed actions of LCN-2 following exercise-like effects *in vitro* and its endocrine effects on culture adipocytes. Created with Bio-Render (https://biorender.com).

Bibliography

Abdul-Ghani, M. A., & DeFronzo, R. A. (2010). Pathogenesis of insulin resistance in skeletal muscle. *J Biomed Biotechnol, 2010*, 476279. doi: 10.1155/2010/476279

Addison, O., Marcus, R., LaStayo, P., & Ryan, A. (2014). Intermuscular Fat: A Review of the Consequences and Causes. *International Journal Of Endocrinology*, *2014*, 1-11. doi: 10.1155/2014/309570

Ahmadian, M., Abbott, M., Tang, T., Hudak, C., Kim, Y., Bruss, M., . . . Sul, H. (2011). Desnutrin/ATGL is regulated by AMPK and is required for a brown adipose phenotype. *Cell Metabolism, 13*(6), 739-748. doi:10.1016/j.cmet.2011.05.002

Aigner, F., Maier, H., Schwelberger, H., Wallnöfer, E., Amberger, A., & Obrist, P. *et al.* (2007). Lipocalin-2 Regulates the Inflammatory Response During Ischemia and Reperfusion of the Transplanted Heart. *American Journal Of Transplantation*, *7*(4), 779-788. doi: 10.1111/j.1600-6143.2006.01723.x

Aljure, O., & Díez-Sampedro, A. (2010). Functional characterization of mouse sodium/glucose transporter type 3b. *American Journal Of Physiology-Cell Physiology*, *299*(1), C58-C65. doi: 10.1152/ajpcell.00030.2010

Asimakopoulou, A., Borkham-Kamphorst, E., Henning, M., Yagmur, E., Gassler, N., & Liedtke, C. *et al.* (2014). Lipocalin-2 (LCN2) regulates PLIN5 expression and intracellular lipid droplet formation in the liver. *Biochimica Et Biophysica Acta (BBA) - Molecular And Cell Biology Of Lipids*, *1841*(10), 1513-1524. doi: 10.1016/j.bbalip.2014.07.017

Baskaran, P., & Thyagarajan, B. (2017). Measurement of Basal and Forskolin-stimulated Lipolysis in Inguinal Adipose Fat Pads. *Journal Of Visualized Experiments*, (125). doi: 10.3791/55625

Bhati, P., Shenoy, S., & Hussain, M. (2018). Exercise training and cardiac autonomic function in type 2 diabetes mellitus: A systematic review. *Diabetes &Amp; Metabolic Syndrome: Clinical Research &Amp; Reviews*, *12*(1), 69-78. https://doi.org/10.1016/j.dsx.2017.08.015

Bhati, P., Shenoy, S., & Hussain, M. (2018). Exercise training and cardiac autonomic function in type 2 diabetes mellitus: A systematic review. *Diabetes &Amp; Metabolic Syndrome: Clinical Research &Amp; Reviews*, *12*(1), 69-78. doi: 10.1016/j.dsx.2017.08.015

Birbrair, A., Zhang, T., Wang, Z., Messi, M., Enikolopov, G., Mintz, A., & Delbono, O. (2013). Role of Pericytes in Skeletal Muscle Regeneration and Fat Accumulation. *Stem Cells And Development*, *22*(16), 2298-2314. doi: 10.1089/scd.2012.0647

Boman, N., Burén, J., Antti, H., & Svensson, M. (2015). Gene expression and fiber type variations in repeated vastus lateralis biopsies. *Muscle &Amp; Nerve*, *52*(5), 812-817. https://doi.org/10.1002/mus.24616

Brown AE, Jones DE, Walker M, Newton JL (2015) Abnormalities of AMPK activation and glucose uptake in cultured skeletal muscle cells from individuals with chronic fatigue syndrome. PLoS One 10:1–14.

Brown, A., Jones, D., Walker, M., & Newton, J. (2015). Abnormalities of AMPK Activation and Glucose Uptake in Cultured Skeletal Muscle Cells from Individuals with Chronic Fatigue Syndrome. *PLOS ONE*, *10*(4), e0122982. doi: 10.1371/journal.pone.0122982

Bryant, N., Govers, R., & James, D. (2002). Regulated transport of the glucose transporter GLUT4. *Nature Reviews Molecular Cell Biology*, *3*(4), 267-277. doi: 10.1038/nrm782

Bu, D. X., Hemdahl, A. L., Gabrielsen, A., Fuxe, J., Zhu, C., Eriksson, P., & Yan, Z. Q. (2006). Induction of neutrophil gelatinase-associated lipocalin in vascular injury via activation of nuclear factor-kappaB. *Am J Pathol, 169*(6), 2245-2253.

C2C12 | ATCC. (2022). Retrieved 27 May 2022, from https://www.atcc.org/products/crl-1772

Cabedo Martinez, A., Weinhäupl, K., Lee, W., Wolff, N. A., Storch, B., Żerko, S., . .

Cailleau, R., Olivé, M., & Cruciger, Q. (1978). Long-term human breast carcinoma cell lines of metastatic origin: Preliminary characterization. *In Vitro*, *14*(11), 911-915. doi: 10.1007/bf02616120

Camp HS, Whitton AL, Tafuri SR. PPARγ activators down-regulate the expression of PPARγ in 3T3 L1 adipocytes. *FEBS Lett.* 1999;447:186–190. doi: 10.1016/S0014-5793(99)00268-9

Cartee GD, Hepple RT, Bamman MM, Zierath JR. Exercise Promotes Healthy Aging of Skeletal Muscle. Cell Metab. 2016;23(6):1034–1047

Cartee GD. Mechanisms for greater insulin-stimulated glucose uptake in normal and insulin-resistant skeletal muscle after acute exercise. Am J Physiol Endocrinol Metab. 2015a;309(12):E949–959.

Chen HC, Bandyopadhyay G, Sajan MP, Kanoh Y, Standaert M, Farese RV, Farese RV (2002) Activation of the ERK pathway and atypical protein kinase C isoforms in exercise- and aminoimidazole-4-carboxamide- 1-β-d-riboside (AICAR)-stimulated glucose transport. J Biol Chem 277:23554–23562

Chen, H., Bandyopadhyay, G., Sajan, M., Kanoh, Y., Standaert, M., Farese, R., & Farese, R. (2002). Activation of the ERK Pathway and Atypical Protein Kinase C Isoforms in Exercise- and Aminoimidazole-4-carboxamide- 1-β-d-riboside (AICAR)-stimulated Glucose Transport. *Journal Of Biological Chemistry*, *277*(26), 23554-23562. doi: 10.1074/jbc.m201152200

Chen, W., Nyasha, M., Koide, M., Tsuchiya, M., Suzuki, N., & Hagiwara, Y. *et al.* (2019). In vitro exercise model using contractile human and mouse hybrid myotubes. *Scientific Reports*, *9*(1). doi: 10.1038/s41598-019-48316-9

Chen, X., Cushman, S. W., Pannell, L. K., & Hess, S. (2005). Quantitative proteomic analysis of the secretory proteins from rat adipose cells using a 2D liquid chromatographyMS/MS approach. J Proteome Res, 4(2), 570-577. doi: 10.1021/pr049772a

Chen, X., Cushman, S. W., Pannell, L. K., & Hess, S. (2005). Quantitative proteomic analysis of the secretory proteins from rat adipose cells using a 2D liquid chromatography- MS/MS approach. *J Proteome Res, 4*(2), 570-577. doi: 10.1021/pr049772a

Chen, Y.; Stegaev, V.; Kouri, V.P.; Sillat, T.; Chazot, P.L.; Stark, H.; Wen, J.G.; Konttinen, Y.T. Identification of histamine receptor subtypes in skeletal myogenesis. Mol. Med. Rep. 2015, 11, 2624–2630.

Choi KM, Kim TN, Yoo HJ, *et al.* Effect of exercise training on A-FABP, lipocalin-2 and RBP4 levels in obese women. *Clin Endocrinol* 2009;70:569-74.

Coudevylle, N. (2016). Biochemical and structural characterization of the interaction between the siderocalin ngal/LCN2 (neutrophil gelatinase-associated lipocalin/lipocalin 2) and the N-terminal domain of its endocytic receptor SLC22A17. *Journal of Biological Chemistry, 291*(6), 2917-2930. doi:10.1074/jbc.m115.685644

Cowland, J. and Borregaard, N. (1997). Molecular Characterization and Pattern of Tissue Expression of the Gene for Neutrophil Gelatinase-Associated Lipocalin from Humans. Genomics, 45(1), pp.17-23.

Crewe, C., An, Y., & Scherer, P. (2017). The ominous triad of adipose tissue dysfunction: inflammation, fibrosis, and impaired angiogenesis. *Journal Of Clinical Investigation*, *127*(1), 74-82. doi: 10.1172/jci88883

Damirchi, A., Rahmani-Nia, F., & Mehrabani, J. (2011). Lipocalin-2: Response to a Progressive Treadmill Protocol in Obese and Normal-weight Men. *Asian Journal Of Sports Medicine*, *2*(1). doi: 10.5812/asjsm.34821

Daval, M., Foufelle, F., & Ferré, P. (2006). Functions of AMP-activated protein kinase in adipose tissue. *The Journal of Physiology, 574*(1), 55-62. doi:10.1113/jphysiol.2006.111484

Deis, J., Guo, H., Wu, Y., Liu, C., Bernlohr, D., & Chen, X. (2019). Adipose Lipocalin 2 overexpression protects against age-related decline in thermogenic function of adipose tissue and metabolic deterioration. *Molecular Metabolism*, *24*, 18-29. doi: 10.1016/j.molmet.2019.03.007

Deis, J., Lin, T., Bushman, T., & Chen, X. (2022). Lipocalin 2 Deficiency Alters Prostaglandin Biosynthesis and mTOR Signaling Regulation of Thermogenesis and Lipid Metabolism in Adipocytes. *Cells*, *11*(9), 1535. doi: 10.3390/cells11091535

Devireddy, L., Gazin, C., Zhu, X. and Green, M. (2005). A Cell-Surface Receptor for Lipocalin 24p3 Selectively Mediates Apoptosis and Iron Uptake. Cell, 123(7), pp.1293-1305.

Drew, D., Lerch, M., Kunji, E., Slotboom, D., & de Gier, J. (2006). Optimization of membrane protein overexpression and purification using GFP fusions. *Nature Methods*, *3*(4), 303-313. doi: 10.1038/nmeth0406-303

Drew, D., Newstead, S., Sonoda, Y., Kim, H., von Heijne, G., & Iwata, S. (2008). GFP-based optimization scheme for the overexpression and purification of eukaryotic membrane proteins in Saccharomyces cerevisiae. *Nature Protocols*, *3*(5), 784-798. doi: 10.1038/nprot.2008.44

Escorcia, W., Ruter, D., Nhan, J., & Curran, S. (2018). Quantification of Lipid Abundance and Evaluation of Lipid Distribution in Caenorhabditis elegans by Nile Red and Oil Red O Staining. *Journal Of Visualized Experiments*, (133). doi: 10.3791/57352

Febbraio, M. A., & Pedersen, B. K. (2020). Who would have thought — myokines two decades on. *Nature Reviews Endocrinology*, *16*(11), 619–620. doi:10.1038/s41574-020-00408-7

Ferreira, A., Dá Mesquita, S., Sousa, J., Correia-Neves, M., Sousa, N., Palha, J. and Marques, F., 2015. From the periphery to the brain: Lipocalin-2, a friend or foe?. Progress in Neurobiology, 131, pp.120-136.

Fierbinteanu-Braticevici, C. (2010). Noninvasive investigations for non alcoholic fatty liver disease and liver fibrosis. *World Journal Of Gastroenterology*, *16*(38), 4784. doi: 10.3748/wjg.v16.i38.4784

Flower, D. (1994). The lipocalin protein family: A role in cell regulation. *FEBS Letters*, *354*(1), 7-11. doi: 10.1016/0014-5793(94)01078-1

Friedmann-Bette, B., Schwartz, F., Eckhardt, H., Billeter, R., Bonaterra, G., & Kinscherf, R. (2012). Similar changes of gene expression in human skeletal muscle after resistance exercise and multiple fine needle biopsies. *Journal Of Applied Physiology*, *112*(2), 289-295. https://doi.org/10.1152/japplphysiol.00959.2011

Friedrichsen, M., Mortensen, B., Pehmøller, C., Birk, J., & Wojtaszewski, J. (2013). Exercise-induced AMPK activity in skeletal muscle: Role in glucose uptake and insulin sensitivity. *Molecular And Cellular Endocrinology*, *366*(2), 204-214. doi: 10.1016/j.mce.2012.06.013

Fujita H, Nedachi T & Kanzaki M (2008). Accelerated de novosarcomere assembly by electric pulse stimulation in C2C12myotubes. Exp Cell Res 313, 1853–1865

Furrer, R., Eisele, P., Schmidt, A., Beer, M., & Handschin, C. (2017). Paracrine cross-talk between skeletal muscle and macrophages in exercise by PGC-1α-controlled BNP. *Scientific Reports*, *7*(1). doi: 10.1038/srep40789

Furuichi, Y., Manabe, Y., Takagi, M., Aoki, M., & Fujii, N. (2018). Evidence for acute contraction-induced myokine secretion by C2C12 myotubes. *PLOS ONE*, *13*(10), e0206146. https://doi.org/10.1371/journal.pone.0206146

Gleeson, M., Bishop, N., Stensel, D., Lindley, M., Mastana, S., & Nimmo, M. (2011). The anti-inflammatory effects of exercise: mechanisms and implications for the prevention and treatment of disease. *Nature Reviews Immunology*, *11*(9), 607-615. doi: 10.1038/nri3041

Goetz, D., Willie, S., Armen, R., Bratt, T., Borregaard, N., & Strong, R. (2000). Ligand Preference Inferred from the Structure of Neutrophil Gelatinase Associated Lipocalin. *Biochemistry*, *39*(8), 1935-1941. doi: 10.1021/bi992215v

Grøntved, A. (2013). Achievement of public health recommendations for physical activity and prevention of gains in adiposity in adults. *Obesity*, *21*(12), 2421-2421. doi: 10.1002/oby.20545

Guo, A., Li, K., & Xiao, Q. (2020). SARCOPENIC obesity: Myokines as potential diagnostic biomarkers and therapeutic targets? *Experimental Gerontology*, *139*, 111022. doi:10.1016/j.exger.2020.111022

Guo, H., Bazuine, M., Jin, D., Huang, M., Cushman, S. and Chen, X. (2013). Evidence for the Regulatory Role of Lipocalin 2 in High-Fat Diet-Induced Adipose Tissue Remodeling in Male Mice. Endocrinology, 154(10), pp.3525-3538.

Guo, H., Jin, D., Zhang, Y., Wright, W., Bazuine, M., & Brockman, D. *et al.* (2010). Lipocalin-2 Deficiency Impairs Thermogenesis and Potentiates Diet-Induced Insulin Resistance in Mice. *Diabetes*, *59*(6), 1376-1385. doi: 10.2337/db09-1735

Haemmerle, G., Lass, A., Zimmermann, R., Gorkiewicz, G., Meyer, C., & Rozman, J. *et al.* (2006). Defective Lipolysis and Altered Energy Metabolism in Mice Lacking Adipose Triglyceride Lipase. *Science*, *312*(5774), 734-737. doi: 10.1126/science.1123965

Hamrick, M. (2012). The skeletal muscle secretome: an emerging player in muscle–bone crosstalk. *Bonekey Reports*, *1*(4). https://doi.org/10.1038/bonekey.2012.60

Hansen, D., De Strijcker, D., & Calders, P. (2016). Impact of Endurance Exercise Training in the Fasted State on Muscle Biochemistry and Metabolism in Healthy Subjects: Can These Effects be of Particular Clinical Benefit to Type 2 Diabetes Mellitus and Insulin-Resistant Patients?. *Sports Medicine*, *47*(3), 415-428. https://doi.org/10.1007/s40279-016-0594-x

Hardie, D., Ross, F., & Hawley, S. (2012). AMPK: a nutrient and energy sensor that maintains energy homeostasis. *Nature Reviews Molecular Cell Biology*, *13*(4), 251-262. doi: 10.1038/nrm3311

Huang, X., Slavkovic, S., Song, E., Botta, A., Mehrazma, B., Lento, C., . . . Wilson, D. J. (2019). A unique conformational distortion mechanism drives lipocalin

2 binding to bacterial siderophores. *ACS Chemical Biology, 15*(1), 234-242. doi:10.1021/acschembio.9b00820

Huh JY (2018) The role of exercise-induced myokines in regulating metabolism. *Arch Pharm Res* 41: 1429

Hui X, Zhu W, Wang Y, Lam KS, Zhang J, Wu D, Kraegen EW, Li Y, Xu A (2009) Major urinary protein-1 increases energy expenditure and improves glucose intolerance through enhancing mitochondrial function in skeletal muscle of diabetic mice. *J Biol Chem* 284: 14050-7

Hvidberg, V., Jacobsen, C., Strong, R., Cowland, J., Moestrup, S. and Borregaard, N. (2004). The endocytic receptor megalin binds the iron transporting neutrophil-gelatinase-associated lipocalin with high affinity and mediates its cellular uptake. FEBS Letters, 579(3), pp.773-777.

I. Mosialou, S. Shikhel, J.M. Liu, A. Maurizi, N. Luo, Z. He, Y. Huang, H. Zong, R.A. Friedman, J. Barasch, P. Lanzano, L. Deng, R.L. Leibel, M. Rubin, T. Nickolas, W. Chung, L.M. Zeltser, K.W. Williams, J.E. Pessin, S. Kousteni MC4R-dependent suppression of appetite by bone-derived lipocalin 2 Nature, 543 (2017), pp. 385-390,

Jaberi, S. A., Cohen, A., D'Souza, C., Abdulrazzaq, Y. M., Ojha, S., Bastaki, S., & Adeghate, E. A. (2021). Lipocalin-2: Structure, function, distribution and role in metabolic disorders. *Biomedicine & Pharmacotherapy, 142*, 112002. doi:10.1016/j.biopha.2021.112002

Jaberi, S., Cohen, A., D'Souza, C., Abdulrazzaq, Y., Ojha, S., Bastaki, S., & Adeghate, E. (2021). Lipocalin-2: Structure, function, distribution and role in metabolic disorders. *Biomedicine &Amp; Pharmacotherapy*, *142*, 112002. doi: 10.1016/j.biopha.2021.112002

Jäger, S., Handschin, C., St.-Pierre, J., & Spiegelman, B. (2007). AMP-activated protein kinase (AMPK) action in skeletal muscle via direct phosphorylation of PGC-1α. *Proceedings Of The National Academy Of Sciences*, *104*(29), 12017-12022. doi: 10.1073/pnas.0705070104

Jiang, D., Wang, D., Zhuang, X., Wang, Z., Ni, Y., Chen, S., & Sun, F. (2016). Berberine increases adipose triglyceride lipase in 3T3-L1 adipocytes through the AMPK pathway. *Lipids In Health And Disease*, *15*(1). https://doi.org/10.1186/s12944-016-0383-4

Kamble, P., Pereira, M., Almby, K., & Eriksson, J. (2019). Estrogen interacts with glucocorticoids in the regulation of lipocalin 2 expression in human adipose tissue. Reciprocal roles of estrogen receptor α and β in insulin resistance?. *Molecular And Cellular Endocrinology*, *490*, 28-36. doi: 10.1016/j.mce.2019.04.002

Karlsson, L., González-Alvarado, M., Motalleb, R., Wang, Y., Wang, Y., & Börjesson, M. *et al.* (2020). Constitutive PGC-1α Overexpression in Skeletal Muscle Does Not Contribute to Exercise-Induced Neurogenesis. *Molecular Neurobiology*, *58*(4), 1465-1481. doi: 10.1007/s12035-020-02189-6

Kershaw, E., Schupp, M., Guan, H., Gardner, N., Lazar, M., & Flier, J. (2007). PPARγ regulates adipose triglyceride lipase in adipocytes in vitro and in vivo. *American Journal Of Physiology-Endocrinology And Metabolism*, *293*(6), E1736-E1745. https://doi.org/10.1152/ajpendo.00122.2007

Kim, K., Zakharkin, S., & Allison, D. (2010). Expectations, validity, and reality in gene expression profiling. *Journal Of Clinical Epidemiology*, *63*(9), 950-959. https://doi.org/10.1016/j.jclinepi.2010.02.018

Kjeldsen, L., Johnsen, A., Sengeløv, H., & Borregaard, N. (1993). Isolation and primary structure of NGAL, a novel protein associated with human neutrophil gelatinase. *Journal Of Biological Chemistry*, *268*(14), 10425-10432. doi: 10.1016/s0021-9258(18)82217-7

Kjobsted R, Munk-Hansen N, Birk JB, Foretz M, Viollet B, Bjornholm M, Zierath JR, Treebak JT, Wojtaszewski JF. Enhanced Muscle Insulin Sensitivity After Contraction/Exercise Is Mediated by AMPK. Diabetes. 2017;66(3):598–612.

Kjobsted R, Munk-Hansen N, Birk JB, Foretz M, Viollet B, Bjornholm M, Zierath JR, Treebak JT, Wojtaszewski JF. Enhanced Muscle Insulin Sensitivity After Contraction/Exercise Is Mediated by AMPK. Diabetes. 2017;66(3):598–612.

Kjobsted R, Pedersen AJ, Hingst JR, Sabaratnam R, Birk JB, Kristensen JM, Hojlund K, Wojtaszewski JF. Intact Regulation of the AMPK Signaling Network in Response to Exercise and Insulin in Skeletal Muscle of Male Patients With Type 2 Diabetes: Illumination of AMPK Activation in Recovery From Exercise. Diabetes. 2016;65(5):1219–1230.

Kjobsted R, Pedersen AJ, Hingst JR, Sabaratnam R, Birk JB, Kristensen JM, Hojlund K, Wojtaszewski JF. Intact Regulation of the AMPK Signaling Network in Response to Exercise and Insulin in Skeletal Muscle of Male Patients With Type 2 Diabetes: Illumination of AMPK Activation in Recovery From Exercise. Diabetes. 2016;65(5):1219–1230.

Kjobsted R, Treebak JT, Fentz J, Lantier L, Viollet B, Birk JB, Schjerling P, Bjornholm M, Zierath JR, Wojtaszewski JF. Prior AICAR stimulation increases insulin sensitivity in mouse skeletal muscle in an AMPK-dependent manner. Diabetes. 2015;64(6):2042–2055.

Kjobsted R, Treebak JT, Fentz J, Lantier L, Viollet B, Birk JB, Schjerling P, Bjornholm M, Zierath JR, Wojtaszewski JF. Prior AICAR stimulation increases insulin sensitivity in mouse skeletal muscle in an AMPK-dependent manner. Diabetes. 2015;64(6):2042–2055.

Kjøbsted, R., Munk-Hansen, N., Birk, J., Foretz, M., Viollet, B., & Björnholm, M. *et al.* (2016). Enhanced Muscle Insulin Sensitivity After Contraction/Exercise Is Mediated by AMPK. *Diabetes*, *66*(3), 598-612. doi: 10.2337/db16-0530

Klenger, F. (2016). Exercise as a Treatment for Depression: A Meta-Analysis Adjusting for Publication Bias. *Physioscience*, *12*(03), 122-123. doi: 10.1055/s-0035-1567129

Krintel, C., Mörgelin, M., Logan, D., & Holm, C. (2009). Phosphorylation of hormone-sensitive lipase by protein kinase A in vitro promotes an increase in its hydrophobic surface area. *FEBS Journal*, *276*(17), 4752-4762. doi: 10.1111/j.1742-4658.2009.07172.x

Lacham-Kaplan, O., Camera, D., & Hawley, J. (2020). Divergent Regulation of Myotube Formation and Gene Expression by E2 and EPA during In-Vitro Differentiation of C2C12 Myoblasts. *International Journal Of Molecular Sciences*, *21*(3), 745. doi: 10.3390/ijms21030745

Lambernd, S., Taube, A., Schober, A., Platzbecker, B., Görgens, S., & Schlich, R. *et al.* (2012). Contractile activity of human skeletal muscle cells prevents insulin resistance by inhibiting pro-inflammatory signalling pathways. *Diabetologia*, *55*(4), 1128-1139. doi: 10.1007/s00125-012-2454-z

Langin, D. (2013). Adipose tissue lipolysis and insulin sensitivity. *Endocrine Abstracts*. doi: 10.1530/endoabs.32.s32.3

Lass, A., Zimmermann, R., Haemmerle, G., Riederer, M., Schoiswohl, G., & Schweiger, M. *et al.* (2006). Adipose triglyceride lipase-mediated lipolysis of

cellular fat stores is activated by CGI-58 and defective in Chanarin-Dorfman Syndrome. *Cell Metabolism*, *3*(5), 309-319. doi: 10.1016/j.cmet.2006.03.005

Law, I. K., Xu, A., Lam, K. S., Berger, T., Mak, T. W., Vanhoutte, P. M., . . . Wang, Y. (2010). Lipocalin-2 deficiency attenuates insulin resistance associated with aging and obesity. *Diabetes, 59*(4), 872-882. doi: 10.2337/db09-1541

Lee-Young, R., Canny, B., Myers, D., & McConell, G. (2009). AMPK activation is fiber type specific in human skeletal muscle: effects of exercise and short-term exercise training. *Journal Of Applied Physiology*, *107*(1), 283-289. doi: 10.1152/japplphysiol.91208.2008

Lee, I., Shiroma, E., Lobelo, F., Puska, P., Blair, S., & Katzmarzyk, P. (2012). Effect of physical inactivity on major non-communicable diseases worldwide: an analysis of burden of disease and life expectancy. *The Lancet*, *380*(9838), 219-229. doi: 10.1016/s0140-6736(12)61031-9

Li Y, Yue-bai L, Yi-sheng W. Dexamethasone-induced adipogenesis in primary marrow stromal cell cultures: mechanism of steroid-induced osteonecrosis. *Chin Med J*. 2006;119(7):581–588

Li, C., & Chan, Y. R. (2011). Lipocalin 2 regulation and its complex role in inflammation and cancer. *Cytokine, 56*(2), 435-441. doi: 10.1016/j.cyto.2011.07.021

Liang, H., & Ward, W. (2006). PGC-1α: a key regulator of energy metabolism. *Advances In Physiology Education*, *30*(4), 145-151. doi: 10.1152/advan.00052.2006

Liu, D., Bordicchia, M., Zhang, C., Fang, H., Wei, W., & Li, J. *et al.* (2016). Activation of mTORC1 is essential for β-adrenergic stimulation of adipose browning. *Journal Of Clinical Investigation*, *126*(5), 1704-1716. doi: 10.1172/jci83532

Magnoni, L., Palstra, A., & Planas, J. (2014). Fueling the engine: induction of AMP-activated protein kinase in trout skeletal muscle by swimming. *Journal Of Experimental Biology*. doi: 10.1242/jeb.099192

Marcinko, K., & Steinberg, G. (2014). The role of AMPK in controlling metabolism and mitochondrial biogenesis during exercise. *Experimental Physiology*, *99*(12), 1581-1585. doi: 10.1113/expphysiol.2014.082255

McGown, C., Birerdinc, A., & Younossi, Z. (2014). Adipose Tissue as an Endocrine Organ. *Clinics In Liver Disease*, *18*(1), 41-58. doi: 10.1016/j.cld.2013.09.012

Meilin, E., Aviram, M., & Hayek, T. (2011). Insulin increases macrophage triglyceride accumulation under diabetic conditions through the down regulation of hormone sensitive lipase and adipose triglyceride lipase. *Biofactors*, *37*(2), 95-103. doi: 10.1002/biof.144

Merrill, G. F., E. J. Kurth, D. G. Hardie, and W. W. Winder. AICA riboside increases AMP-activated protein kinase, fatty acid oxidation and glucose uptake in rat muscle. Am.J.Physiol. 36: E1107-E1112, 1997.

Merrill, G., Kurth, E., Hardie, D., & Winder, W. (1997). AICA riboside increases AMP-activated protein kinase, fatty acid oxidation, and glucose uptake in rat muscle. *American Journal Of Physiology-Endocrinology And Metabolism*, *273*(6), E1107-E1112. doi: 10.1152/ajpendo.1997.273.6.e1107

Meyers, K., López, M., Ho, J., Wills, S., Rayalam, S., & Taval, S. (2020). Lipocalin-2 deficiency may predispose to the progression of spontaneous age-related adiposity in mice. *Scientific Reports, 10*(1). doi:10.1038/s41598-020-71249-7

Miller, V. L. (2014). Faculty opinions recommendation of interaction of Lipocalin 2, transferrin, and siderophores determines the replicative niche of Klebsiella

pneumoniae during pneumonia. *Faculty Opinions – Post-Publication Peer Review of the Biomedical Literature*. doi:10.3410/f.718490110.793497298

Miyoshi, H., Perfield, J., Obin, M., & Greenberg, A. (2008). Adipose triglyceride lipase regulates basal lipolysis and lipid droplet size in adipocytes. *Journal Of Cellular Biochemistry*, *105*(6), 1430-1436. doi: 10.1002/jcb.21964

Morak, M., Schmidinger, H., Riesenhuber, G., Rechberger, G., Kollroser, M., & Haemmerle, G. *et al.* (2012). Adipose Triglyceride Lipase (ATGL) and Hormone-Sensitive Lipase (HSL) Deficiencies Affect Expression of Lipolytic Activities in Mouse Adipose Tissues. *Molecular &Amp; Cellular Proteomics*, *11*(12), 1777-1789. doi: 10.1074/mcp.m111.015743

Morrison, S. and McGee, S., 2015. 3T3-L1 adipocytes display phenotypic characteristics of multiple adipocyte lineages. *Adipocyte*, 4(4), pp.295-302.

Nakai, M., Denham, J., Prestes, P., Eikelis, N., Lambert, E., & Straznicky, N. *et al.* (2021). Plasma lipocalin-2/NGAL is stable over 12 weeks and is not modulated by exercise or dieting. *Scientific Reports*, *11*(1). doi: 10.1038/s41598-021-83472-x

Narkar, V., Downes, M., Yu, R., Embler, E., Wang, Y., & Banayo, E. *et al.* (2008). AMPK and PPARδ Agonists Are Exercise Mimetics. *Cell*, *135*(1), 189. doi: 10.1016/j.cell.2008.09.014

Nikolić, N., Görgens, S., Thoresen, G., Aas, V., Eckel, J., & Eckardt, K. (2016). Electrical pulse stimulation of cultured skeletal muscle cells as a model forin vitroexercise - possibilities and limitations. *Acta Physiologica*, *220*(3), 310-331. doi: 10.1111/apha.12830

Nikolić, N., Skaret Bakke, S., Tranheim Kase, E., Rudberg, I., Flo Halle, I., & Rustan, A. *et al.* (2012). Electrical Pulse Stimulation of Cultured Human Skeletal Muscle Cells as an In Vitro Model of Exercise. *Plos ONE*, *7*(3), e33203. doi: 10.1371/journal.pone.0033203

Norrbom, J., Sundberg, C., Ameln, H., Kraus, W., Jansson, E., & Gustafsson, T. (2004). PGC-1α mRNA expression is influenced by metabolic perturbation in exercising human skeletal muscle. *Journal Of Applied Physiology*, *96*(1), 189-194. doi: 10.1152/japplphysiol.00765.2003

Ordovas, J., & Corella, D. (2008). Metabolic syndrome pathophysiology: the role of adipose tissue. *Kidney International*, *74*, S10-S14. doi: 10.1038/ki.2008.517

Paula FMM, Leite NC, Vanzela EC, Kurauti MA, Freitas-Dias R, Carneiro EM, Boschero AC, Zoppi CC (2015) Exercise increases pancreatic β-cell viability in a model of type 1 diabetes through IL-6 signaling. FASEB J 29:1805–1816.

Paula, F., Leite, N., Vanzela, E., Kurauti, M., Freitas-Dias, R., & Carneiro, E. *et al.* (2015). Exercise increases pancreatic β-cell viability in a model of type 1 diabetes through IL-6 signaling. *The FASEB Journal*, *29*(5), 1805-1816. doi: 10.1096/fj.14-264820

Pawluczyk, I. Z., Furness, P. N., & Harris, K. P. (2003). Macrophage-induced rat mesangial cell expression of the 24p3-like protein alpha-2-microglobulin-related protein. *Biochim Biophys Acta, 1645*(2), 218-227.

Pedersen, B. K. (2011a). Exercise-induced myokines and their role in chronic diseases. *Brain Behav Immun, 25*(5), 811-816. doi: 10.1016/j.bbi.2011.02.010

Pedersen, B. K. (2011b). Muscles and their myokines. *J Exp Biol, 214*(Pt 2), 337-346. doi: 10.1242/jeb.048074

Pedersen, B. K., Akerstrom, T. C., Nielsen, A. R., & Fischer, C. P. (2007). Role of myokines in exercise and metabolism. *J Appl Physiol (1985), 103*(3), 1093-1098. doi: 10.1152/japplphysiol.00080.2007

Pedersen, B., & Febbraio, M. (2008). Muscle as an Endocrine Organ: Focus on Muscle-Derived Interleukin-6. *Physiological Reviews*, *88*(4), 1379-1406. doi: 10.1152/physrev.90100.2007

Petersen, E., Carey, A., Sacchetti, M., Steinberg, G., Macaulay, S., Febbraio, M., & Pedersen, B. (2005). Acute IL-6 treatment increases fatty acid turnover in elderly humans in vivo and in tissue culture in vitro. *American Journal Of Physiology-Endocrinology And Metabolism*, *288*(1), E155-E162. doi: 10.1152/ajpendo.00257.2004

Ponzetti, M., Aielli, F., Ucci, A., Cappariello, A., Lombardi, G., Teti, A., & Rucci, N. (2021). Lipocalin 2 increases after high-intensity exercise in humans and influences muscle gene expression and differentiation in mice. *Journal Of Cellular Physiology*, *237*(1), 551-565. doi: 10.1002/jcp.30501

Quinn, L., Anderson, B., Strait-Bodey, L., Stroud, A., & Argilés, J. (2009). Oversecretion of interleukin-15 from skeletal muscle reduces adiposity. *American Journal Of Physiology-Endocrinology And Metabolism*, *296*(1), E191-E202. doi: 10.1152/ajpendo.90506.2008

Raschke S, Eckel J (2013) Adipo-myokines: two sides of the same coin--mediators of inflammation and mediators of exercise. *Mediators Inflamm* 2013: 320724

Rebalka, I., Monaco, C., Varah, N., Berger, T., D'souza, D., & Zhou, S. *et al.* (2018). Loss of the adipokine lipocalin-2 impairs satellite cell activation and skeletal muscle regeneration. *American Journal Of Physiology-Cell Physiology*, *315*(5), C714-C721. doi: 10.1152/ajpcell.00195.2017

Richter, E., & Ruderman, N. (2009). AMPK and the biochemistry of exercise: implications for human health and disease. *Biochemical Journal*, *418*(2), 261-275. doi: 10.1042/bj20082055

Ricoult, S., & Manning, B. (2012). The multifaceted role of mTORC1 in the control of lipid metabolism. *EMBO Reports*, *14*(3), 242-251. doi: 10.1038/embor.2013.5

Roberts, L., Boström, P., O'Sullivan, J., Schinzel, R., Lewis, G., & Dejam, A. *et al.* (2014). β-Aminoisobutyric Acid Induces Browning of White Fat and Hepatic β-Oxidation and Is Inversely Correlated with Cardiometabolic Risk Factors. *Cell Metabolism*, *19*(1), 96-108. doi: 10.1016/j.cmet.2013.12.003

Roca-Rivada, A., Castelao, C., Senin, L., Landrove, M., Baltar, J., & Crujeiras, A. *et al.* (2013). FNDC5/Irisin Is Not Only a Myokine but Also an Adipokine. *Plos ONE*, *8*(4), e60563. doi: 10.1371/journal.pone.0060563

Rodríguez, A., Ezquerro, S., Méndez-Giménez, L., Becerril, S., & Frühbeck, G. (2015). Revisiting the adipocyte: a model for integration of cytokine signaling in the regulation of energy metabolism. *American Journal Of Physiology-Endocrinology And Metabolism*, *309*(8), E691-E714. doi: 10.1152/ajpendo.00297.2015

Rosen, E., & Spiegelman, B. (2014). What We Talk About When We Talk About Fat. *Cell*, *156*(1-2), 20-44. doi: 10.1016/j.cell.2013.12.012

Ruth, M. (2012). A PGC1–α–dependent myokine that drives brown–fat–like development of white fat and thermogenesis. *Yearbook Of Endocrinology*, *2012*, 114-116. doi: 10.1016/j.yend.2012.04.012

Rydén, M., Jocken, J., van Harmelen, V., Dicker, A., Hoffstedt, J., & Wirén, M. *et al.* (2007). Comparative studies of the role of hormone-sensitive lipase and adipose triglyceride lipase in human fat cell lipolysis. *American Journal Of Physiology-Endocrinology And Metabolism*, *292*(6), E1847-E1855. doi: 10.1152/ajpendo.00040.2007

Sánchez, J., Nozhenko, Y., Palou, A., & Rodríguez, A. (2013). Free fatty acid effects on myokine production in combination with exercise mimetics. *Molecular Nutrition &Amp; Food Research*, *57*(8), 1456-1467. doi: 10.1002/mnfr.201300126

Schnyder, S., & Handschin, C. (2015). Skeletal muscle as an endocrine organ: PGC-1α, myokines and exercise. *Bone*, *80*, 115-125. doi: 10.1016/j.bone.2015.02.008

Schweiger, M., Schreiber, R., Haemmerle, G., Lass, A., Fledelius, C., & Jacobsen, P. *et al.* (2006). Adipose Triglyceride Lipase and Hormone-sensitive Lipase Are the Major Enzymes in Adipose Tissue Triacylglycerol Catabolism. *Journal Of Biological Chemistry*, *281*(52), 40236-40241. doi: 10.1074/jbc.m608048200

Seidell, J., & Halberstadt, J. (2015). The Global Burden of Obesity and the Challenges of Prevention. *Annals Of Nutrition And Metabolism*, *66*(Suppl. 2), 7-12. doi: 10.1159/000375143

Seldin, M., Peterson, J., Byerly, M., Wei, Z., & Wong, G. (2012). Myonectin (CTRP15), a Novel Myokine That Links Skeletal Muscle to Systemic Lipid Homeostasis. *Journal Of Biological Chemistry*, *287*(15), 11968-11980. doi: 10.1074/jbc.m111.336834

Severinsen, M., & Pedersen, B. (2020). Muscle–organ crosstalk: The emerging roles of Myokines. *Endocrine Reviews*, *41*(4), 594–609. doi:10.1210/endrev/bnaa016

Shi, H., Zeng, C., Ricome, A., Hannon, K. M., Grant, A. L., & Gerrard, D. E. (2007). Extracellular signal-regulated kinase pathway is differentially involved in beta-agonist-induced hypertrophy in slow and fast muscles. *Am J Physiol Cell Physiol, 292*(5), C1681-1689. doi: 10.1152/ajpcell.00466.2006

Silvennoinen, M., Ahtiainen, J., Hulmi, J., Pekkala, S., Taipale, R., & Nindl, B. *et al.* (2015). PGC-1 isoforms and their target genes are expressed differently in human skeletal muscle following resistance and endurance exercise. *Physiological Reports*, *3*(10), e12563. doi: 10.14814/phy2.12563

Smith, U., & Kahn, B. (2016). Adipose tissue regulates insulin sensitivity: role of adipogenesis,de novolipogenesis and novel lipids. *Journal Of Internal Medicine*, *280*(5), 465-475. doi: 10.1111/joim.12540

So, B., Kim, H., Kim, J., & Song, W. (2014). Exercise-induced myokines in health and metabolic diseases. *Integrative Medicine Research*, *3*(4), 172-179. doi: 10.1016/j.imr.2014.09.007

Spangenburg, E., Jackson, K., & Schuh, R. (2013). AICAR inhibits oxygen consumption by intact skeletal muscle cells in culture. *Journal Of Physiology And Biochemistry*, *69*(4), 909-917. doi: 10.1007/s13105-013-0269-0

Steensberg, A., Hall, G., Osada, T., Sacchetti, M., Saltin, B., & Pedersen, B. (2000). Production of interleukin-6 in contracting human skeletal muscles can account for the exercise-induced increase in plasma interleukin-6. *The Journal Of Physiology*, *529*(1), 237-242. doi: 10.1111/j.1469-7793.2000.00237.x

Strain, T., Brage, S., Sharp, S., Richards, J., Tainio, M., & Ding, D. *et al.* (2020). Use of the prevented fraction for the population to determine deaths averted by existing prevalence of physical activity: a descriptive study. *The Lancet Global Health*, *8*(7), e920-e930. doi: 10.1016/s2214-109x(20)30211-4

Sun, S., Ji, Y., Kersten, S., & Qi, L. (2012). Mechanisms of Inflammatory Responses in Obese Adipose Tissue. *Annual Review Of Nutrition*, *32*(1), 261-286. doi: 10.1146/annurev-nutr-071811-150623

Supruniuk, E., Mikłosz, A., & Chabowski, A. (2017). The Implication of PGC-1α on Fatty Acid Transport across Plasma and Mitochondrial Membranes in the

Insulin Sensitive Tissues. *Frontiers In Physiology*, *8*. doi: 10.3389/fphys.2017.00923

Sztalryd, C., & Kimmel, A. (2014). Perilipins: Lipid droplet coat proteins adapted for tissue-specific energy storage and utilization, and lipid cytoprotection. *Biochimie*, *96*, 96-101. https://doi.org/10.1016/j.biochi.2013.08.026

Tamura, K., Goto-Inoue, N., Miyata, K., Furuichi, Y., Fujii, N., & Manabe, Y. (2020). Effect of treatment with conditioned media derived from C2C12 myotube on adipogenesis and lipolysis in 3T3-L1 adipocytes. *PLOS ONE*, *15*(8), e0237095. doi: 10.1371/journal.pone.0237095

Tantiwong, P., Shanmugasundaram, K., Monroy, A., Ghosh, S., Li, M., & DeFronzo, R. *et al.* (2010). NF-κB activity in muscle from obese and type 2 diabetic subjects under basal and exercise-stimulated conditions. *American Journal Of Physiology-Endocrinology And Metabolism*, *299*(5), E794-E801. doi: 10.1152/ajpendo.00776.2009

Tran, C., Mukherjee, S., Ye, L., Frederick, D., Kissig, M., & Davis, J. *et al.* (2016). Rapamycin Blocks Induction of the Thermogenic Program in White Adipose Tissue. *Diabetes*, *65*(4), 927-941. doi: 10.2337/db15-0502

Tripp, T., Frankish, B., Lun, V., Wiley, J., Shearer, J., Murphy, R., & MacInnis, M. (2022). Time course and fibre type-dependent nature of calcium-handling protein responses to sprint interval exercise in human skeletal muscle. *The Journal Of Physiology*. doi: 10.1113/jp282739

Turner, M., Martin, N., Player, D., Ferguson, R., Wheeler, P., & Green, C. *et al.* (2020). Characterising hyperinsulinemia-induced insulin resistance in human skeletal muscle cells. *Journal Of Molecular Endocrinology*, *64*(3), 125-132. doi: 10.1530/jme-19-0169

Valero-Breton, M., Warnier, G., Castro-Sepulveda, M., Deldicque, L., & Zbinden-Foncea, H. (2020). Acute and chronic effects of high frequency electric pulse stimulation on the Akt/mTOR pathway in human primary myotubes. *Frontiers in bioengineering and biotechnology*, 1283.

Vishwanath, D., Srinivasan, H., Patil, M., Seetarama, S., Agrawal, S., Dixit, M., & Dhar, K. (2013). Novel method to differentiate 3T3 L1 cells in vitro to produce highly sensitive adipocytes for a GLUT4 mediated glucose uptake using fluorescent glucose analog. *Journal Of Cell Communication And Signaling*, *7*(2), 129-140. doi: 10.1007/s12079-012-0188-9

Wang Y, Lam KS, Kraegen EW, Sweeney G, Zhang J, Tso AW, Chow WS, Wat NM, Xu JY, Hoo RL, Xu A (2007) Lipocalin-2 is an inflammatory marker closely associated with obesity, insulin resistance, and hyperglycemia in humans. *Clin Chem* 53: 34-41

Wang, Q., Sun, J., Liu, M., Zhou, Y., Zhang, L., & Li, Y. (2021). The New Role of AMP-Activated Protein Kinase in Regulating Fat Metabolism and Energy Expenditure in Adipose Tissue. *Biomolecules*, *11*(12), 1757. doi: 10.3390/biom11121757

Wang, Y., Lam, K., Kraegen, E., Sweeney, G., Zhang, J., & Tso, A. *et al.* (2007). Lipocalin-2 Is an Inflammatory Marker Closely Associated with Obesity, Insulin Resistance, and Hyperglycemia in Humans. *Clinical Chemistry*, *53*(1), 34-41. doi: 10.1373/clinchem.2006.075614

Wang, Y., Rimm, E., Stampfer, M., Willett, W., & Hu, F. (2005). Comparison of abdominal adiposity and overall obesity in predicting risk of type 2 diabetes

among men. *The American Journal Of Clinical Nutrition*, *81*(3), 555-563. doi: 10.1093/ajcn/81.3.555

Wedell-Neergaard, A., Lang Lehrskov, L., Christensen, R., Legaard, G., Dorph, E., & Larsen, M. *et al.* (2019). Exercise-Induced Changes in Visceral Adipose Tissue Mass Are Regulated by IL-6 Signaling: A Randomized Controlled Trial. *Cell Metabolism*, *29*(4), 844-855.e3. doi: 10.1016/j.cmet.2018.12.007

Wilhelmsen, A., Tsintzas, K., & Jones, S. W. (2021). Recent advances and future avenues in understanding the role of adipose tissue cross talk in mediating skeletal muscle mass and function with ageing. *GeroScience*, *43*(1), 85–110. doi:10.1007/s11357-021-00322-4

Xie, J., Liu, H., Wandi, Y., Ge, S., Jin, Z., & Zheng, M. *et al.* (2022). Zeaxanthin Remodels Cytoplasmic Lipid Droplets via β3-Adrenergic Receptor Signaling and Enhances Perilipin 5-Mediated Lipid Droplet–Mitochondria Interactions in Adipocytes. *Food &Amp; Function*. doi: 10.1039/d2fo01094a

Xu, M., Feng, D., Wu, H., Wang, H., Chan, Y., & Kolls, J. *et al.* (2015). Liver is the major source of elevated serum lipocalin-2 levels after bacterial infection or partial hepatectomy: A critical role for IL-6/STAT3. *Hepatology*, *61*(2), 692-702. doi: 10.1002/hep.27447

Yamaguchi, T. (2010). Crucial Role of CGI-58/.ALPHA./.BETA. Hydrolase Domain-Containing Protein 5 in Lipid Metabolism. *Biological And Pharmaceutical Bulletin*, *33*(3), 342-345. doi: 10.1248/bpb.33.342

Yan QW, Yang Q, Mody N, Graham TE, Hsu CH, Xu Z, Houstis NE, Kahn BB, Rosen ED (2007) The adipokine lipocalin 2 is regulated by obesity and promotes insulin resistance. *Diabetes* 56: 2533-40

Yan, Q., Yang, Q., Mody, N., Graham, T., Hsu, C., & Xu, Z. *et al.* (2007). The Adipokine Lipocalin 2 Is Regulated by Obesity and Promotes Insulin Resistance. *Diabetes*, *56*(10), 2533-2540. doi: 10.2337/db07-0007

Yang, A., & Mottillo, E. (2020). Adipocyte lipolysis: from molecular mechanisms of regulation to disease and therapeutics. *Biochemical Journal*, *477*(5), 985-1008. doi: 10.1042/bcj20190468

Yang, X., Lu, X., Lombès, M., Rha, G., Chi, Y., & Guerin, T. *et al.* (2010). The G0/G1 Switch Gene 2 Regulates Adipose Lipolysis through Association with Adipose Triglyceride Lipase. *Cell Metabolism*, *11*(3), 194-205. doi: 10.1016/j.cmet.2010.02.003

Young, S., & Zechner, R. (2013). Biochemistry and pathophysiology of intravascular and intracellular lipolysis. *Genes &Amp; Development*, *27*(5), 459-484. doi: 10.1101/gad.209296.112

Yuzbashian, E., Asghari, G., Zarkesh, M., mirmiran, P., Hedayati, M., & Khalaj, A. (2020). Association of dietary and plasma fatty acids with adipose triglyceride lipase (ATGL) and hormone-sensitive lipase (HSL) gene expression in human adipose tissues. *Endocrine Abstracts*. doi: 10.1530/endoabs.70.yi10

Zebisch, K., Voigt, V., Wabitsch, M., & Brandsch, M. (2012). Protocol for effective differentiation of 3T3-L1 cells to adipocytes. *Analytical Biochemistry*, *425*(1), 88-90. doi: 10.1016/j.ab.2012.03.005

Zhang, Y., Foncea, R., Deis, J. A., Guo, H., Bernlohr, D. A., & Chen, X. (2014). Lipocalin 2 expression and secretion is highly regulated by metabolic stress, cytokines, and nutrients in adipocytes. PLoS One, 9(5), e96997. doi: 10.1371/journal.pone.0096997

Zhang, Y., Guo, H., Deis, J., Mashek, M., Zhao, M., & Ariyakumar, D. *et al.* (2014). Lipocalin 2 Regulates Brown Fat Activation via a Nonadrenergic Activation

Mechanism. *Journal Of Biological Chemistry*, *289*(32), 22063-22077. doi: 10.1074/jbc.m114.559104

Zimmermann, R., Strauss, J., Haemmerle, G., Schoiswohl, G., Birner-Gruenberger, R., & Riederer, M. *et al.* (2004). Fat Mobilization in Adipose Tissue Is Promoted by Adipose Triglyceride Lipase. *Science*, *306*(5700), 1383-1386. doi: 10.1126/science.1100747

Appendices

Appendix A

Solutions and Reagents

Cell-culture-work

1× Phosphate buffered saline (PBS)

Dissolve 1 phosphate buffered saline (PBS) tablet (BR0014G; Oxoid, Cheshire, UK) in 100 ml of deionized water. Sterilize solutions by autoclaving. Store the buffer at RT.

50× Tris-Acetate-Ethylene-di-amine-tetra-acid (TAE) buffer (pH 8.3)

Dissolve 242 gm of Tris-base in 700 ml of deionized water and mix well. Carefully add 57.1 ml of 100% acetic acid and 100 ml of 0.5 M ethylene-di- amine-tetra-acid (EDTA) (pH 8.0). Adjust the volume of the solution to 1 L with deionized water. The pH of this buffer is not adjusted and should be about 8.3. Store the buffer at RT. This stock solution is diluted 49:1 with deionized water to make 1× working solution. This 1× solution will contain 40 mM Tris, 20 mM acetic acid, and 1 mM EDTA.

0.5 M Ethylene-di-amine-tetra-acid (EDTA)

Dissolve 18.61 gm of EDTA in 60 ml of deionized water and mix well. Adjust pH to 8. Adjust the volume of the solution to 100 ml with deionized water. Sterilize solutions by autoclaving. Store the buffer at RT.

RNA-extraction

Diethyl pyro-carbonate (DEPC)-treated high-performance liquid chomatography (HPLC) grade water

Add 1 ml of 0.1% diethylpyrocarbonate (DEPC) to 1 L high-performance liquid chomatography (HPLC) grade water and mix well until the globules of DEPC disappear. Incubate at 37 °C overnight and then autoclave. Store at RT for up to 12 months.

3M sodium acetate (pH 5.2)

Dissolve 40.83 gm of sodium acetate in 40 ml of HPLC grade water and mix well. Allow the solution to be at RT. Adjust the pH to 5.2 with glacial acetic acid. Adjust the volume of the solution to 100 ml with HPLC grade water. Add 100 µl of 0.1% DEPC to the solution and mix well. Incubate at 37 °C overnight and then autoclave. Store the solution at RT.

Protein isolation

Radioimmunoprecipitation assay (RIPA) buffer

Mix together 2 ml of 1.5 M sodium chloride, 500 µl of 1 M Tris-hydrochloride (pH 7.6), 2 ml of 10% Triton X-100, 2 ml of 10% sodium deoxycholate, 200 µl of 10% sodium dodecyl sulfate (SDS) and 13.3 ml deionized water. Aliquot and store at -20 °C. Before using RIPA buffer, add 40 µl of 25× Complete Protease Inhibitor Cocktail stock solution (11697498001; Roche, Penzberg, Germany) in 1 ml of RIPA buffer.

1.5 M sodium chloride (NaCl)

Dissolve 8.766 gm of NaCl in 80 ml of deionized water and mixed well. Adjust the volume of the solution to 100 ml with deionized water. Sterilize solutions by autoclaving. Store the buffer at RT.

1 M Tris-hydrochloride (pH 7.6)

Dissolve 12.11 gm of Tris-base in 80 ml of deionized water and mix well. Adjust pH to 7.6. Allow the solution to be at RT. Final adjust the pH to 7.6. Adjust the volume of the solution to 100 ml with deionized water. Sterilize solutions by autoclaving. Store the buffer at RT.

10% Triton X-100

Mix together Triton X-100 10 ml and 90 ml deionized water. Store the solution at 4 °C.

10% sodium deoxycholate (Na deoxycholate)

Dissolve 1 gm of Na deoxycholate in 5 ml of deionized water and mixed well. Adjust the volume of the solution to 10 ml with deionized water. Protect the solution from light and store at RT.

10% sodium dodecyl sulfate (SDS)

Dissolve 10 gm of SDS in 70 ml of deionized water and mixed well. Leave the solution at RT to allow bubbles to disappear. Adjust the volume of the solution to 100 ml with deionized water. Store the solution at RT.

Western blotting

2× Laemmli buffer

Mix together 1 ml of 1 M Tris-hydrochloride (pH 6.8), 4 ml of 10% SDS, 0.31 gm of dithiotheitol (DTT), 2 ml of glycerol, 20 µl of 0.5M EDTA and 2 mg of

bromophenol blue. Adjust the volume of the buffer to 10 ml with deionized water. Aliquot and store at -20 °C.

6× Laemmli buffer

Mix together 4.5 ml of 1 M Tris-hydrochloride (pH 6.8), 1.8 gm of SDS, 1.39 gm of DTT, 9 ml of glycerol and 9 mg of bromophenol blue. Adjust the volume of the buffer to 15 ml with deionized water. Aliquot and store at -20 °C.

1 M Tris-hydrochloride (pH 6.8)

Dissolve 12.1 gm of Tris-base in 80 ml of deionized water and mix well. Adjust pH to 6.8. Adjust the volume of the solution to 100 ml with deionized water. Store the buffer at RT.

10× Running buffer

Dissolve 75.7 gm of Tris-base, 360.5 gm of glycine, and 25 gm of SDS in 1.5 L of deionized water and mix well. Adjust the volume of the solution to 2.5 L with deionized water. Store the stock buffer at RT and dilute to 1× before use.

10× Transfer buffer

Dissolve 75.7 gm of Tris-base and 360.5 gm of glycine in 1.5 L of deionized water and mix well. Adjust the volume of the solution to 2.5 L with deionized water. Store the stock buffer at RT. To make 1× transfer buffer, mix 100 ml of 10× transfer buffer, 200 ml of methanol and 700 ml of deionized water per litre.

10× Tris-buffered saline (TBS)

Dissolve 75 gm of Tris-base, 200 gm of sodium chloride and 5 gm of potassium chloride in 1.5 L of deionized water and mix well. Adjust pH to 7.6.

Adjust the volume of the solution to 2.5 L with deionized water. Store the stock buffer at RT.

Tris-buffered saline and 0.1% Tween 20 (TBST)

Mix 100 ml of 10× TBS with 900 ml of deionized water. Add 1 ml of Tween 20 and mix well.

Phosphate buffered saline with Triton X-100 (PBST)

Add 18 gm of sodium chloride and 3 ml of Triton X-100 to 1 L of 0.2 M PB and 1 L of deionized water and mixed well. Store the buffer at RT.